University Library

A gateway to Melbourne's research publications

Minerva Access is the Institutional Repository of The University of Melbourne

Author/s:
Chandran, Yogeswari

Title:
Characterisation of the putative cysteine protease effectors OspD2 and OspD3 from Shigella species

Date:
2020

Persistent Link:
https://hdl.handle.net/11343/238864

Terms and Conditions:
Terms and Conditions: Copyright in works deposited in Minerva Access is retained by the copyright owner. The work may not be altered without permission from the copyright owner. Readers may only download, print and save electronic copies of whole works for their own personal non-commercial use. Any use that exceeds these limits requires permission from the copyright owner. Attribution is essential when quoting or paraphrasing from these works.

Characterisation of the putative cysteine protease effectors OspD2 and OspD3 from *Shigella* species.

by

Yogeswari Chandran

ORCiD: 0000-0001-8949-1974

Submitted in total fulfilment of the requirements of the degree of Doctor of Philosophy

January 2020

Department of Microbiology and Immunology

The University of Melbourne

at the Peter Doherty Institute for Infection and Immunity

ABSTRACT

Diarrheal disease caused by bacterial pathogens continues to be a major public health concern worldwide due to significant increases in mortality annually. Members of the *Shigella* genus contribute significantly to bacterial diarrheal incidences worldwide. *Shigella* is a Gram-negative facultative anaerobe that belongs to the family *Enterobacteriaceae*. They are considered highly infectious as only 10-100 organisms are required to cause disease. Like many other Gram-negative gut pathogens, *Shigella* utilizes a type III secretion system (T3SS) during infection to translocate bacterial effector proteins into host cells which interfere with host signaling pathways to benefit their survival. The exact function of many T3 effector proteins remains unknown. However recently, the T3SS effector EspL from enteropathogenic *Escherichia coli* (EPEC), was shown to contain a cysteine protease catalytic motif that targets and degrades the host RHIM domain containing proteins, RIPK1, RIPK3, TRIF and DAI, hence blocking inflammation and necroptotic cell death during infection. Homologues of EspL are also found in *Shigella*, namely: OspD2 and OspD3. Although previously labelled as *Shigella* toxins, the exact function of these effectors is yet to be elucidated. The primary aim of my study is to characterize the role of OspD2 and OspD3 and to determine their host cell targets. Overexpression experiments with OspD2 or OspD3 and the RHIM family of proteins suggest that OspD3, but not OspD2 targets and cleaves the RHIM family of proteins. We also showed OspD3 blocking both inflammation and necroptotic cell death in NF-κB dependent luciferase assays and cell viability assays respectively. However, this was not seen upon infection of HeLa 299s with wildtype and mutant *Shigella* strains. This therefore led to further investigations for the identification of other host cell targets of OspD2 and OspD3 via mass spectrometry. Several unique host cell targets for OspD2 and OspD3 were identified from mass spectrometry and an enrichment analysis of the hits, suggest the involvement of these proteins in anti-viral defense, particularly the Type I IFN signaling pathway. Elucidating the roles of these effectors in the interferon signaling pathways will be important in understanding the roles between bacteria pathogens and interferon as unlike viral infections, these are severely understudied.

Further analysis via overexpression studies showed that OspD2 and OspD3 may be working cooperatively in cleaving IRF3/IRF7 and IRF9 during Type I IFN signaling and hence blocking the pathway. Furthermore, we also demonstrated by infection of HeLa 299s that OspD2 cleaves IRF3, however cleavage of IRF9 by OspD3 was not seen.

In summary, we have performed characterization of two cysteine protease effectors of *Shigella* and their host cell targets. This work creates the platform for understanding how these effectors function and how this knowledge may be used as valuable tools for subsequent investigation of host cell defense mechanism.

DECLARATION

This is to certify that:

i. The thesis comprises only my original work towards the Doctor of Philosophy except where indicated in the preface,
ii. Due acknowledgement has been made in the text to all other material used,
iii. The thesis is fewer than 100 000 words in length, exclusive of tables, maps, bibliographies, and appendices.

……

Yogeswari Chandran,

Department of Microbiology and Immunology,

The University of Melbourne,

at the Peter Doherty Institute for Infection and Immunity,

and Hudson Institute of Medical Research

PREFACE

In accordance with the regulations of The University of Melbourne, I acknowledge that some of the work presented in this thesis was collaborative. Specifically:

In chapter 3, the GST-tagged OspD3 and OspD3$_{C64S}$ recombinant proteins were made by James Murphy and Emma Petrie. 3xFlag-OspD2 and 3xFlag-OspD3 were made by Sabrina Mühlen. Doxycycline inducible 3xFlag-WT EspL in HT-29 cells were made by Georgina Pollock.

In chapter 4, the PROTOMAP analysis was carried out by Nichollas Scott. HA-IRF1, HA-IRF5, HA-IRF7 were cloned into pCDNA3 vectors with the assistance of Jiyao Gan.

The remainder of this thesis comprises only my original work.

ACKNOWLEGEMENTS

Firstly, I would like to thank my supervisor, Liz, for giving me the opportunity to carry out my PhD in her laboratory. I really appreciate, her for replying to my first ever mail and having the confidence in me to carry out my PhD in her laboratory. Thank you, Liz for allowing me to work on a very challenging and exciting project and for having the patience in me, to carry out my work efficiently throughout the years. One important lesson from you which I would take with me forever, will be to remain humble and kind, regardless of how successful you become in your career. I am also extremely grateful to you for encouraging me and welcoming me back to work after a difficult phase in my life. I greatly admire the passion you have for science, and your enthusiasm for the topic, have motivated to me to learn so much from you these past few years.

Next, I would also like to thank Jac for your supervision during my initial phase of PhD. You were extremely patient in guiding me when I first started my PhD at the Hartland lab, and never hesitated to clear any of my doubts. You taught me how to remain positive throughout and to appreciate negative results as progress as well. Meeting me twice a week, just to make sure that I am on track with my project, despite your busy schedule is really appreciated. Also, thank you for always having your door open for me whenever I just needed to have a chat with you, besides science.

I would also like to thank Cristina for all of your help and guidance. You had been a big support for me during these past few years, not just with work. You are extremely intelligent and meticulous with your experiments and you have made sure that my work reflects the same. You always welcomed me in your office when I am with any doubts, and have tried your best to make me feel better. Thank you also for always making sure that I am feeling well and for all those text messages, checking on me when I fall sick. It means a lot to me, especially when you are away from home. Biggest thanks to you as well for looking through my thesis at an amazing fast pace, you are simply incredible!

I would also like to express my thanks to rest of the Hartland members past and present, for all your scientific advices and friendship these past few years. You guys have made lab life more fun and enjoyable. Thank you to Cristina, Kitty, Gina, Shivani, Ying, Raissa, Pengfei, Jiyao, Max and Linda, you guys have made lab life more fun and enjoyable. I will always enjoy our weekly Thursday morning teas and trivia we had at Dr Dax when we were still in PDI. Special thanks also go to, Raissa, Pengfei, Linda and Jiyao for becoming great friends over the years.

You guys have been a big part in relieving those PhD stress and I have always looked forward to our occasional dinner/ potlucks and organ attack game nights. I would also like to thank Ying, for not only being an amazing lab manger but also for being the sweetest and driving me back home from Hudson whenever possible.

Next, I would also like to thank my "adopted" lab, the Rogerson lab, especially to Janavi and Amaya. Thank you, guys, for giving me a space to sit and work in your lab. You guys are super fun and have always included me in all of your lab events. All the hugs, laughs, words of encouragements and coffee breaks will never be forgotten.

I would like to extend my thanks to Nick for being very patient and helping me with PROTOMAP screen. You are one of the reasons I had something exciting to work with during my PhD. Thank you, Nick, for answering all my emails and questions throughout the years. Thank you also to Hayley and Jason who were part of my PhD committee and having provided me with useful suggestions and guidance over the years.

I am grateful to my dearest friends, Padma, Kanmani, Janavi, Bhavna, Lekha, Rama, Amaya, Karthik and Sateesh. Thank you all for all the love and emotional support throughout the years. I am happy to know that we have each other's back.

Last but not the least, I would love to express a huge thank to my amazing family, Appa, Amma, Akka, Chetan and Vihaan kutty. You guys, are simply wonderful, and thank you so much for all the words of encouragement, and motivation during my PhD. Appa, thank you so much for all your morning motivational calls, which I now miss a lot, to remind me to take each day with a smile. I now know that there's a heaven past the sky with my very own angel watching over me. Thank you to Amma for being the strong person you are, and for making me believe in myself and for encouraging me to do this PhD. Akka, thank you for always being there to encourage me when I am down, for being the person I can call at any time of the day and for putting up with all my emotional dramas. I know I can always count on you for anything! And finally, I would like to thank my dearest Vihaan, for all your smiles, kisses and cuddles, one of the main reasons for keeping me going during those tough days.

ABBREVIATION

%	Percentage
°C	Degree Celsius
2-DGE	Two-dimensional gel electrophoresis
ACN	Acetonitrile
Amp	Ampicillin
AMPs	Antimicrobial peptides
APOB	Apolipoprotein B
ASC	Apoptosis-associated speck-like protein
BBB	Blood brain barrier
BI-1	Bax inhibitor-1
BIR	Baculovirus inhibitor of apoptosis protein repeat
BSA	Bovine serum albumin
CARD	Caspase-activation and recruitment domain
cFLIPL	Cellular FLICE-like inhibitory protein
CLRs	C-type lectin receptors
Cm	Chloramphenicol
CVB	Coxsackievirus B3
DAMPs	Damage-associated molecular pattern molecules
DBD	DNA-binding domain
DC	Dendritic cell
DD	Death domain
DMEM	Dulbecco's Modified Eagle Media
DMSO	Dimethyl sulfoxide
dsRNA	Double stranded RNA
DTT	Dithiothreitol
EAEC	Enteroaggregative *E. coli*
EHEC	Enterohaemorrhagic *E. coli*
EIEC	Enteroinvasive *E. coli*
EPEC	Enteropathogenic *E. coli*

EspG	*E. coli* secreted protein G
ETEC	Enterotoxigenic *E. coli*
F	Forward
FAE	Follicle-associated epithelium
FBS	Fetal Bovine Serum
g	Gram
GAS	γ activated sequence
GBPs	*GTPase family of guanylate-binding proteins*
GBPs	Guanylate-binding proteins
gDNA	Genomic deoxyribonucleic acid
GEMS	Global Enteric Multicenter Study
GFP	Green fluorescent protein
GI	Gastrointestinal
Gln100	Glutamine residue at position 100
GSDMD	Gasdermin D
GST	Glutathione S-transferase
GTPases	Guanosine triphosphatases
h	Hours
HRP	Horseradish peroxidase
HRV C3	Human Rhinovirus 3C protease
IAD	IRF association domain
IE6	Integrative element 6
IFN	Interferon
IKK	IκB kinase
IL	Interleukin
Ipa	Invasion plasmid antigen
IRAK	IL-1R-associated kinase
ISD	Interferon stimulatory DNA
ISGF3	Interferon-stimulated gene factor 3
ISGs	Interferon-stimulated genes

ISRE	Interferon-stimulated response elements
JAK	Janus kinase
JAKMIP3	Janus kinase and microtubule-interacting protein
JH	Janus homology domains
Kan	Kanamycin
LA	Luria Agar
LB	Luria-Bertani
LCMV	Lymphocytic choriomemingitis virus
LD	Linker domain
LDS	Lithium dodecyl sulfate
LPS	Lipopolysaccharide
LRRs	Leucine-rich repeat
LUBAC	Linear chain assemble complex
M cells	Membranous epithelial cells
MAP4	Microtubule associated protein 4
MAPK	Mitogen-activated protein kinases
MAVS	Mitochondrial antiviral signalling protein
MD2	Myeloid differentiation factor 2
MEV	Multiple experiment viewer
MHV	Mouse hepatitis virus
mins	Minutes
mL	Milligram
MLKL	Mixed lineage kinase domain-like protein
mm	Millimetre
mM	Millimolar
mRNA	Messenger ribonucleic acid
MS	Mass spectrometry
MX2	*MX dynamin like GTPase 2*
MyD88	Myeloid differentiation primary response protein 88
NEMO	NF-κB essential modulator

NES	Nuclear export signal
NF-κB	Nuclear factor-κB
ng	nanogram
NLE	Non-LEE encoded
NLR	NOD-like receptor
NLS	Nuclear localization signal
nM	nanometre
NOD	Nucleotide-binding oligomerisation domain
N-WASP	Neural Wiskott-Aldrich syndrome protein
ORF	Open reading frame
Osp	Outer *Shigella* proteins
PAI	Pathogenicity islands
PAMPs	Pathogen associated molecular patterns
PBS	Phosphate buffer saline
pDCs	Plasmacytoid dendritic cells
PFA	Paraformaldehyde
PMN	Polymorphonuclear leukocytes
poly I:C	Polyinosine-deoxycytidylic acid
ppm	Parts-per-million
PROTOMAP	Protein Topography and migration analysis platform
PRRs	Pattern recognition receptors
PtdIns(4,5)P_2	Phosphatidylinositol 4,5-bisphosphate
PtdIns(5)P	Phosphatidylinositol 5-monophosphate
pY	Tyrosine-phosphorylation site
PYD	Pyrin domain
R	Reverse
RHD	Rel homology domain
RHIM	(RIP) homotypic interaction motifs
Rho GTPase	Rho guanosine triphosphatase
RIG-I	Retinoic acid-inducible

RIP	Receptor-interacting serine/threonine-protein
RIPK1	Receptor interacting serine/threonine-protein kinase 1
RIPK3	Receptor interacting serine/threonine-protein kinase 3
RLRs	RIG-I gene-like receptors
RNA	Ribonucleic acid
rpm	Revolution per minutes
RPMI	Roswell Park Memorial Institute
RSV	Respiratory syncytial virus
S. boydii	*Shigella boydii*
S. dysenteriae	*Shigella dysenteriae*
S. flexneri	*Shigella flexneri*
S. sonnei	*Shigella sonnei*
SAM	S-adenosyl-L-methionine
SCF-TrCP	Stem cell factor-TrCP complex
SDS	Sodium dodecyl sulphate
SH2	Src homolgy 2 domain
ShET1	*Shigella* enterotoxin 1
ShET2	*Shigella* enterotoxin 2
SILAC	Stable isotope labelling with amino acids in cell culture
SOB	Super optimal broth
SOC	Super optimal broth with catabolite repression
SPATA2	Spermatogenesis-associated 2
SRL	*Shigella* resistance locus
ssRNA	Single stranded RNA
Stx	Shiga toxins
T3SS	Type III secretion system
TAD	Transcriptional activation domain
TAK1	Transforming growth factor- β-activated kinase 1
TBC	Tre-2/Bub2/Cdc16 domains
Tet	Tetracycline

TFA	Trifluoroacetic acid
TLRs	Toll-like receptors
TMB	Tetramethylbenzidine
TNFR1	TNF receptor 1
TRAF6	TNFR-associated factor 6
TRIF	TIR-domain-containing adapter-inducing interferon-β
TSA	Tryptic soy agar plates
Tyk2	Tyrosine kinase 2
v/v	Volume by volume
VBSs	Vinculin binding sites
VSV	Vesicular stomatitis virus
w/v	Weight by volume
WN	West nile virus
WT	Wild type
Z-VAD	z-VAD-FMK
μg	microgram
μL	Microlitre
μM	Micrometre

TABLE OF CONTENTS

LIST OF FIGURES

LIST OF TABLES

Chapter One:

Literature Review

CHAPTER 1: Literature review

1.1 Introduction

Diarrhoeal disease, which can be a symptom of gastrointestinal infection, is a major public health concern worldwide [1]. It is the second leading cause of mortality in children under 5 years old, with an estimated 1.7 billion cases of diarrhoeal disease in children annually, especially in developing countries in Africa, Central America and some parts of Asia. Almost all incidences of diarrhoeal disease in developing countries occur due to poor hygiene practices and limited or lack of access to clean drinking water. In addition, the absence of sufficient, modern up-to-date medical treatments, public health efforts, a lack of education and malnutrition contribute to the increased occurrence of diarrhoeal disease in these countries [2].

A diverse range of pathogens including viruses, parasites and bacteria are capable of causing diarrhoea. Infection is often transmitted from human to human via the stools of an infected individual indirectly to the mouth of another individual due to poor hygiene or sanitation, termed the faecal oral route of disease [3, 4]. Species of *Shigella*, *Salmonella*, *Escherichia coli*, *Campylobacter*, *Aeromonas hydrophila* and *Plesiomonas shigelloides* are some of the most common bacterial enteric pathogens responsible for diarrhoeal diseases worldwide [5]. These pathogens vary in their mechanism of pathogenesis and in the number of organisms required to cause disease. For instance, different serotypes of *Salmonella* species infect humans or animals respectively and *Vibrio cholera* has a high infectious dose of millions of organisms required to cause disease [3]. Amongst these pathogens, a 2013 study conducted by Global Enteric Multicenter Study (GEMS), on severe to moderate diarrhoea in children below the age of 5 in Asia and Africa, ranked *Shigella* spp, as one of the most common causes of diarrhoea [6, 7].

1.2 *Shigella* epidemiology

1.2.1. Discovery and nomenclature of *Shigella*

Shigella is a primate specific, non-motile, non-sporulating, small (1-3 μM), rod shaped facultative anaerobe that belongs to the family *Enterobacteriaceae* [8] . It was first discovered by Japanese scientist Dr Kiyoshi Shiga in 1896 while investigating an epidemic of dysentery in Japan [9]. Dr Shiga developed straightforward and simple techniques to isolate the organism which had previously eluded many researchers. He identified a Gram-negative bacillus from stools that was negative for indole and fermented dextrose but did not form acid from mannitol.

He initially named the bacterium *Bacillus dysenterie*. He also described the production of toxins, in particular the Shiga toxin from the isolated organism. Immediately after Dr Shiga's discovery, many other researchers described the identification of a similar organism, resulting in many changes in nomenclature. The genus was eventually named *Shigella* in the 1930 edition of Bergey's Manual of Determinative Bacteriology [10].

1.2.2. Infectious dose of *Shigella* and global burden

Shigella species give rise to acute gastrointestinal infections termed shigellosis. They do so by invading the mucosa and producing toxins which result in local inflammation that is occasionally associated with extra-intestinal manifestations [11, 12] . *Shigella* is resistant to low pH and able to invade and survive in the acidic pH of the human gastrointestinal tract. The ability to survive in such low pH is a critical pathogenic feature of *Shigella*, which contributes towards the low infectious dose required for infection of humans, as little as 10 microorganisms [13-15]. When infected, the symptoms of shigellosis can differ from mild watery diarrhoea to more serious bacillary dysentery with fever, severe abdominal cramps and mucus and blood-containing stools. There is also a risk of patients with shigellosis being susceptible to other complications such as haemolytic uremic syndrome, encephalopathy and septicaemia in the absence of efficient treatments [4].

The past 30 years have seen a decline in the number of *Shigella*-induced diarrhoeal episodes. This is due to an increased availability of antibiotics, oral rehydration with micronutrients and a decrease in malnutrition [16]. However, *Shigella* was still ranked second as a leading cause of diarrhoeal-associated deaths in 2015, by the Global Burden of Disease Consortium, especially in children less than 5 years old [1]. As mentioned earlier, almost 70% of reported *Shigella* cases annually occur in children [2, 17]. Children aged between 1 – 4 years old are the most susceptible to *Shigella* infection with those between 5 and 9 years old the next highest risk group [18]. *Shigella*-induced diarrhoea is also prevalent in military deployed to endemic regions. In addition, travellers visiting these endemic countries are also susceptible to these infections. *Shigella*-induced traveller's diarrhoea has been labelled as a more disabling form of diarrhoea compared to infections by enterotoxigenic *E. coli*, which is currently the leading causative agent of Traveller's diarrhoea [19, 20]. In developing countries, *Shigella* infections are reported all year round, however an increase in incidences is noted during rainy seasons. [21]. Outbreaks of shigellosis are also reported in industrialised countries, especially amongst homosexual men [2, 22].

Shigellosis is usually self-limiting and can be treated with either oral rehydration to restore the electrolyte loss or by administration of antimicrobial agents/antibiotics. The incubation period after infection is typically 12 – 48 hours but may sometimes be up to one week. Adults mostly get mild infections and may experience watery stools for a few days with minimal onset of fever. However, the clinical presentation is more severe in children with a whole range of symptoms including abdominal cramps, high fever, malaise, vomiting and bloody dysentery [18, 23]. Despite initially being susceptible to most antibiotics including ampicillin, tetracycline, sulfonamides and trimethoxazole, *Shigella* is rapidly developing and acquiring resistance to these more common and cheaper antimicrobial agents, which were considered first-line therapies [22, 24]. This resulted in *Shigella* being declared a serious threat by international disease control programmes, requiring novel disease interventions including an active vaccine [16]. Moreover, given the fact that *Shigella* is primate specific, an effective vaccine may eventually result in eradication or significant reduction in *Shigella* infection worldwide. However, there are no effective *Shigella* vaccines currently available [2, 25].

1.3 Evolution of *Shigella* species

Shigella species are members of the Enterobacteriaceae family with *E. coli*. *E. coli* comprises the pathotypes enteropathogenic *E. coli* (EPEC), enterotoxigenic *E. coli* (ETEC), enterohaemorrhagic *E. coli* (EHEC), enteroaggregative *E. coli* (EAEC), enteroinvasive *E. coli* (EIEC) and diffusely adherent *E. coli* [26, 27]. Despite sharing the same family, *Shigella* is unique from these other pathogens in its mechanism of pathogenesis and its evolutionary history. Amongst all the different *E. coli* pathotypes, EIEC is the only organism that shows similar biochemical and pathogenic features identical to *Shigella*. Both *Shigella* and EIEC are non-motile, contain a virulence plasmid and do not utilise lysine as a source of carbon for growth. It was predicted that these pathogens evolved independently on many occasions from the commensal *E. coli*, with *Shigella* evolving as early as 50 000 to 270 000 years ago [28, 29].

After the initial identification of *Shigella dysenteriae (S. dysenteriae)*, the genus expanded further with the finding of *Shigella flexneri (S. flexneri)* in the year 1899, *Shigella sonnei (S. sonnei)* in the year 1906 and lastly *Shigella boydii (S. boydii)* in the year 1921. This eventually led the genus of *Shigella* to be traditionally divided into these four species [30]. Although *S. dysenteriae* was the first identified *Shigella* species, it is rarely isolated from patients today. *S. sonnei* is the most common cause of shigellosis in developed countries in North America and

Europe whereas *S. flexneri* is the most common pathogen in developing countries in parts of Africa and Asia [31].

1.3.1. Clustering of *Shigella* species

Initially, when genomics research was just beginning, a comparison of 8 chromosomal housekeeping genes of *Shigella* revealed that the genus *Shigella* can be categorized into 3 main clusters, C1, C2 and C3. A few outliers were identified beyond these clusters but nevertheless, they were still enclosed within the lineages of *E. coli* [28] . Subsequently, due to advances in technology within the field of genomics, a comparison of a further 23 chromosomal genes revealed similar results with a better resolution obtained. These more recent findings therefore subdivided Cluster C1 into 3 further subclasses, SC1, SC2 and SC3 [28, 32, 33].

The subdivision of *Shigella* into serotypes was based on their O-antigens and biochemical properties and it was noted that almost all serotypes of *Shigella* except *S. sonnei* shared their lipopolysaccharide (LPS) O antigen with *E. coli* [34]. *S. sonnei* was an outlier in the clusters, as its phylogenetic relationship with the other species of *Shigella* is still not clear. *S. sonnei* is thought to have evolved more recently compared to the other serotypes and species of *Shigella* [35]. It also contains only one O antigen which is also present in *Plesimonas shigelloides* which is a genetically distant Gram negative bacterium [35]. *S. dysenteriae* and *S. boydii* have similar O antigens to *E. coli* and these isolates display a well characterised set of O antigens [34]. All *S. flexneri* strains except serotype strain 6 contain a common polysaccharide backbone made up of linear tetrasaccharide. Differences in these serotypes are due to O-acetylation and/or glucosylation at various positions of the backbone [36]. This complexity in *Shigella* species serotyping was therefore reported by Ewing in 1986 as being based "partly on biochemistry, partly on serology and partly on tradition." [37-39].

Among these different species of *Shigella*, *S. flexneri* has been used as the most common cellular models of infections for the study of host-pathogen interactions [40]. As such, the majority of this thesis will focus on findings with this particular species of *Shigella*.

1.4 Life cycle of *Shigella*

Shigella is transmitted to humans via the faecal oral route typically via ingestion of food or water contaminated with the bacteria. The bacteria then pass through the stomach and reach the large intestine where an infection is established (Figure 1.1). At the gut, *Shigella* comes into contact with almost 1000 different species of micro-organism [41]. Despite this, *Shigella*

ensures its survival amongst the gut microbiota through the secretion of a protein termed colicin which acts as an inhibitory protein, targeting phylogenetically similar microorganisms [42].

The first step of *Shigella* pathogenesis is the invasion of the epithelial barrier. *Shigella* is initially transcytosed across the epithelial barrier via two distinct pathways. In the intestinal epithelium are lymph nodes/follicles (also known as the Peyer's patches) and above these follicles sits the follicle-associated epithelium (FAE) which contains numerous endocytic M cells (membranous epithelial cells). These cells function by constantly translocating particles, microorganisms and antigens from the gut lumen to the mucosal lymphoid tissue layer [43-45]. The mucosal lymphoid tissue layer is an intraepithelial pocket enriched with immune cells such as macrophages and lymphocytes, that trigger an immune response by phagocytosing and degrading foreign particles [46]. In the alternative pathway, *Shigella* interacts directly with the apical side of the epithelial cells via tiny protrusions termed filopodia. These protrusions capture *Shigella* and retract the bacteria towards the cell body for invasion to take place [47]. Grassart and colleagues have also recently reported, using bioengineered organ on chip models, that *Shigella* initially also directly infects the apical surface of the epithelial cells by taking advantage of the intestinal microarchitecture and the intestinal mechanical forces [48]. Once across the intestinal epithelium, *Shigella* is engulfed by resident immune cells such as macrophages. However, *Shigella* escapes into the host cytoplasm and induces cell death in the macrophages. Macrophages undergoing cell death release proinflammatory cytokines such as interleukin 1 and 18 (IL-1 and IL-18). This process is caspase-1 dependent whereby caspase-1 targets and cleaves IL-1β and IL-18, releasing their biologically active forms into the cytoplasm. IL-1β is necessary for initiating early onset inflammation and both IL-1β and IL-18 are responsible for the massive infiltration of polymorphonuclear leukocytes (PMN) to the site of *Shigella* infection [49]. This massive influx of PMN cells destroys the integrity of the epithelium through tissue destruction and hence making it possible for more bacteria to cross the intestinal epithelium without the need of M cells [50]. *Shigella* then multiplies and survives intracellularly via the help of virulence factors inducing a type III secretion system (T3SS), see section 1.5.3, as well as actin-based polymerisation for cell to cell spread [51]. The mode of entry, pathogenicity and virulence factors involved during *Shigella* infections as well as host immune responses activated during *Shigella* infections will be discussed further in detail below.

1.5 Virulence of *Shigella*

1.5.1. Pathogenicity islands of *Shigella*

Evolution of the bacterial genome by either gene deletions or horizontal gene transfer between microorganisms is a very dynamic process [50]. Pathogenicity islands (PAI) are chromosomal insertions of large mobile genetic regions containing virulence associated genes. Gain of these PAIs is vital for the evolution of pathogenic bacteria [52]. PAIs are characterised by the presence of a mosaic-like structure instead of homogeneous regions of acquired DNA and comprise genomic segments around 10 to 200kb. In addition to this, there is a tendency for some PAIs to lose their virulence features at high frequency, making them genetically unstable [53]. To date, five PAIs have been identified in *Shigella* species but their exact involvement in pathogenesis is not clearly defined. These are SHI-O, SHI-1, SHI-2, SHI-3 and the *Shigella resistance* locus (SRL) (Figure 1.2) [54].

SHI-O contains genes that define the structure of the O antigen of the bacterial lipopolysaccharide, which is important for determining the *Shigella* serotype. The acquired immune response which is triggered upon *Shigella* infection is largely O antigen-dependent, meaning immunity is not effective against other serotypes of *Shigella* with different O antigens. The presence of this PAI enables *Shigella* to alter its O-antigen during infection using glycosyltransferases to alter sugar composition as a mechanism of immune evasion [55].

The SHI-1 contains several genes including *pic, sigA, set1A* and *set1B*. SigA is a serine protease autotransporter that was reported to be an enterotoxin which contributes to fluid accumulation in rabbit ileal loop model of *Shigella* infection [56, 57]. It also alters the cytoskeleton of epithelial cells by cleaving intracellular alpha-fodrin [58]. Pic is an extracellular serine protease involved in the degradation of mucin and hemagglutination during *Shigella* infection [59]. set1A and set1B encode the enterotoxin ShET1 which contributes to accumulation of fluid in the intestines and subsequent formation of watery diarrhea during *Shigella* infection in the rabbit ileal loop model [60].

Shiga toxins (Stx) are also commonly produced during *S. dysenteriae* infections and during infection with certain serotypes of EHEC infections [51]. The toxins have also been reported to be present in other *Shigella* species such as *S. flexneri* [61]. These toxins are extremely potent and Stx activity results in fluid accumulation in rabbit ileal loops. The Stx function as ribotoxins which inhibit protein synthesis in the host cells, giving rise to apoptotic cell death. These toxins can also induce altered gene or protein expression in the host cells [51]. They are

also toxic against many different cell types and can give rise to vascular lesions in the central nervous system, kidney and colon [51].

SHI-2 comprises of genes including *iucA- iucD, shiD* and *shiA*. This PAI is necessary for the bacteria to survive in stressful environments. *iucA- iucD* encode aerobactins which allow the bacteria to survive in low iron conditions where they need must compete with other bacteria for survival and growth [62]. ShiD is involved in immunity to colicin I and V which are bacteriocidal toxins produced by other bacteria [63]. ShiA is a membrane protein involved in down regulating inflammation by suppressing innate T cell signaling [64].

Of the remaining PAIs, SHI-3 is found only in *S. boydii* and similarly to SHI-2, is required for iron acquisition in low iron environments [65]. SRL contains genes that are necessary for resistance against antibiotics such as tetracycline (*tetA to tetD, tetR),* ampicilin (*oxa-1),* streptomycin (*aadA1)* and chloramphenicol (*cat)* [66].

Shigella virulence is also further enhanced by the loss of numerous genes by either gene deletion or inactivation with an estimate of more than 726 genes lost and 200 new pseudogenes acquired as compared to its ancestor *E. coli*. This acquisition and loss or reduction of genes was important for *Shigella* to adapt to an intracellular lifestyle [51, 67].

1.5.2. The *Shigella* virulence plasmid

The molecular machinery that is critical for *Shigella* invasion and subsequent intracellular survival is encoded on a large virulence plasmid. The *Shigella* virulence plasmid is approximately 220 kb in size, encoding nearly 100 genes [68]. The plasmid contains a core 31 kb cluster of genes termed the entry region which encodes genes essential for invasion and actin-based motility including regulation and assembly of the T3SS, and molecular chaperones. This entry region is necessary for virulence and is highly conserved among all *Shigella* species [67] .

The genes encoded within the entry region can be broadly clustered into four groups based on their function (Figure 1.3). Group one contains effectors that are secreted by the T3SS. These effectors are required for manipulating host cell processes to support bacterial survival. The invasion plasmid antigen genes (*ipaA-D*) fall in this group and are necessary for host cell invasion and bacterial survival and for the secretion and translocation of additional effectors into the host cell [69-71]. Group two contains the membrane expressed *mxi* genes and the surface expressed *spa* genes [72, 73]. This mxi-spa locus encodes all the components required for the function and assembly of the T3SS and, collectively with the Ipa proteins, allows

translocation of effector proteins into the host cell. Group three contains *virB* and *mxiE* which encode transcriptional activators. They function by regulating the T3SS associated genes located throughout the virulence plasmid. VirB is particularly required for transcription of *mxi*, *spa* and *ipa* genes [74-77]. Lastly, group four contains *ipgA*, *ipgC*, *ipgE* and *spa15* which encode chaperones necessary to stabilise substrates of the T3SS present in the cytoplasm. IpgC in particular is required for the stability of IpaB and IpaC, while IpgE is required for the stability of IpgD. IpgC and Spa15 also control the transcriptional regulation of other T3SS effectors present beyond the core 31kb region of the virulence plasmid [77-79]. Besides these genes, there are also genes present outside of the 31kb core region of the virulence plasmid which are required for post invasion virulence functions. They include the outer *Shigella* proteins (Osp) which manipulate host cell responses to ensure the survival of the bacteria [80]. These proteins are effectors and include OspB, OspC2, OspD1-3, OspE1-2, OspF, OspG, OspDI and OspZ [81]. There are also other genes on the plasmid which are required for the regulation of actin polymerisation that is typical of *Shigella* infections, namely *icsA/virG, sopA/iscP* and *phoN2* [51, 82].

The expression of virulence genes is usually very tightly regulated as permanent expression would require excess energy. Upon entry of the bacteria into the host, differences in temperature initiate the expression of these virulence proteins [75, 83]. An increase in the temperature to 37°C after the intake of bacteria is one of the main factors for expression of genes from the virulence plasmid entry region. Moreover, other triggers such as changes in iron concentration, osmolarity and pH are also capable of inducing expression of these genes [84-86].

The key regulators which are required to respond to these changes in the environment and control the expression of the genes are encoded on the bacterial chromosome [83, 87]. One such gene, *virF* which is a transcriptional activator, becomes activated at 37°C and in turn activates *virB* and *icsA* expression. This activates transcription of genes including those from the entry region to allow the invasion of the bacteria into the host cells [88].

1.5.3. The type three secretion system

The T3SS is a complex machinery which is made up of around 25 proteins (Figure 1.4). It was first identified in *Yersinia* species in 1994 by Rosqvist and colleagues who characterised a unique molecular apparatus that was able to release bacterial proteins into the extra-bacterial supernatant [89]. T3SS from diverse bacteria are closely related to and share a common ancestral origin with the bacterial flagellum. This is supported by the fact that the basal bodies

of both T3SS and flagella are highly similar in structure. Several proteins share high amino acid similarity and exhibit several functional similarities [90, 91]. The T3SS has been identified in a wide range of gram negative bacteria such as *Salmonella* species, *Burkholderia* species, EPEC and EHEC [92].

1.5.4. Architecture of the T3SS apparatus

The TT3S apparatus spans 3 membranes (the outer and inner membrane of the bacteria and the host cell plasma membrane) and connects the host and bacterial cytoplasm. Structurally the T3SS can be divided into 3 main components; the seven ringed basal body (around 32 nm in length), a C-ringed body, and a hollow needle-like structure (around 60 nm in length) that projects from the outer bacterial membrane and penetrates into the host cell membrane [93]. The needle length is genetically controlled and changes according to the size of molecules present at the surfaces of the bacteria and host cell [94]. The needle also contains a channel in the centre which is around 3 nm wide which restricts protein translocation. Fully folded proteins do not fit in the narrow channel and hence are not translocated unless they are unfolded.

The initial step for the assembly of the Mxi-Spa T3SS of *Shigella* is the formation of the basal body. The basal body extends from the inner membrane of the bacteria, and spans the periplasm, the peptidoglycan layer and the outer membrane. MxiG which is a membrane protein and MxiJ, a lipoprotein are required to make up the inner membrane and periplasmic rings of the T3SS respectively [95, 96]. In addition to this, several Spa proteins such as Spa9, 24, 29 and 40 and the MxiA protein are also involved in the formation of the inner membrane ring [97, 98]. MxiD, a secretin protein, is the main component of the outer membrane ring. It is initially secreted to the periplasm via a Sec-dependent pathway and is subsequently inserted and stabilised in the outer membrane by another lipoprotein MxiM [99-101].

The next step in the assembly of the T3SS is the formation of the T3SS needle. The needle is made up of two subunits, a minor MxiI subunit and a major MxiH subunit. These two components form a helix-like structure which extends and protrudes into the extracellular space. Cytoplasmic proteins which are a part of the inner membrane ring of the basal body tightly regulate the formation of the T3SS needle. The length of the needle is further regulated by the Spa32 protein [93, 102, 103].

1.5.5. Recognition of substrates by the T3SS and insertion into the host cell

Spa47, a c-ring ATPase plays a crucial role in assembly of the T3SS and the secretion of effectors. This ATPase hydrolyses ATP and generates the transmembrane proton motive force. The energy generated from this is required for transmembrane transport of the proteins, a process that is typically not thermodynamic in nature. Furthermore, the energy generated is also needed for chaperon release and for T3SS substrate unfolding [104, 105].

Once the assembly of the T3SS apparatus is completed, translocator proteins such as IpaB and IpaC (which are hydrophobic) and IpaD (which is hydrophilic) are translocated to the T3SS needle tip. This is to mediate the secretion of effector proteins into the host cell [71, 106]. These Ipa proteins are initially stored in the cytoplasm and are associated with chaperones in order to avoid premature secretion of effectors. The IpgC chaperone, associates with IpaB and IpaC while IpaD is able to remain inactive and chaperone itself [107, 108]. Studies have revealed that IpaD retains a fixed position and shape at the tip of the needle and associates with IpaB to keep it inside the needle and inhibit the release of effectors. However, in the presence of a host cell and activation of the T3SS, IpaD undergoes a conformational transformation. This in turn releases IpaB from the locked position and gives way to its interaction with IpaC and insertion into the membrane to form a multimeric translocation opening [109, 110]. It has also been postulated that MxiH might also go through slight changes in its shape and moves through the needle in order to prime and open the needle pore for the movement of other effectors [111].

1.5.6. Initial adherence and bacterial entry into host cells

Upon T3SS induction, *Shigella* triggers the accumulation and aggregation of lipid raft markers at the entry regions into the host [67, 112]. Cholesterol or lipids are generally present in most eukaryotic membranes and are typically unevenly distributed between the two bilayers of the membrane. They have unique biophysical characteristics and together with sphingolipids, form lipid rafts or microdomains in the membranes. These lipid rafts have numerous functions in regulating various signalling pathways. They include vesicle trafficking within cells, endocytosis, apoptosis and activation of immune responses [113, 114]. Importantly, these lipid rafts are also where the first interaction between *Shigella* and host cells occur. Aggregation of lipid rafts by *Shigella* then attracts many putative signalling molecules and receptors to the entry site that aid entry of *Shigella* into the host cell. *Shigella* associates with two host receptors, CD44 (hyaluronan receptor) and α5β1 integrin. Interaction with CD44 happens via IpaB while interaction with the α5β1 integrin occurs by the IpaB, IpaC and IpaD multimeric complex.

Association with these receptors then initiates actin cytoskeletal rearrangement and induces *Shigella* invasion into the host cell [112].

Actin cytoskeletal rearrangements are important for the uptake of *Shigella* into host cells. *Shigella* induces actin cytoskeleton polymerization by manipulating small GTPases and tyrosine kinases which play an important role in governing the host cytoskeleton reorganization. The T3SS effectors IpgB1/IpgB2 exploit the small GTPase RhoG/ELMO/Dock180 pathway to induce the formation of membrane ruffles in the host. IpgB1 functions by mimicking the activity of the host small GTPase Rho and regulating the association of the ELMO/Dock180 complex to the host cell membrane. This in turn activates Rac1 to induce the formation of membrane ruffles at the entry sites [115]. The formation of these ruffles is further amplified by another T3SS effector, IpgD. IpgD functions by activating Arf6 which is involved in actin organization and endocytosis [116, 117].

Another T3SS effector VirA was suggested to induce microtubule destabilisation as well as formation of membrane ruffles, however the function of VirA has been controversial [118, 119] . Dong and colleagues have also reported that VirA has Tre-2/Bub2/Cdc16 domains (TBC)-like dual finger motifs which targets and inactivates Rab GTPases and facilitates the escape of *Shigella* from autophagy-mediated host response [120].

Phosphoinositides have been shown to have a pivotal role in regulating actin cytoskeleton organization. Dephosphorylation of phosphatidylinositol 4,5-bisphosphate [PtdIns(4,5)P_2] into phosphatidylinositol 5-monophosphate [PtdIns(5)P] results in reduction in the membrane tethering force, resulting in remodelling of the actin filaments and membrane blebbing. The *Shigella* T3SS effector, IpgD plays a central role in the dephosphorylation of PtdIns(4,5)P_2 to form PtdIns(5)P. This then aids in the dissociation of the plasma membrane from the cytoskeleton which promotes membrane ruffle formation [121].

IpaA, a T3SS effector then associates with actin filaments via binding to vinculin. This process leads to actin depolymerization and hence results in a decrease in adhesion between the extracellular matrix and cells and subsequent anchoring of the bacteria to the membrane ruffles [122]. This process also aids in closing the *Shigella* vacuole and completes the invasion process [123]. However recently Valencia-Gallardo and colleagues reported that IpaA contains three vinculin binding sites (VBSs) which are required for bacteria invasion [124]. They reported that IpaA VBS3 can directly bind to talin (a cytoskeletal linker), which is essential for filopodial adhesions and subsequent capture of *Shigella* [124].

1.5.7. Phagosomal escape, intracellular replication and cell-to-cell spread

After internalization, *Shigella* rapidly induces lysis of the phagosome and escapes from the vacuole in less than 15 minutes. Although the process via which this happens in not very clear, it is though that IpaB and IpaC may be directly creating holes in the vacuole, resulting in the lysis [69, 125, 126] [127]. Another recent study also reported that IpgD, recruits Rab11 to the *Shigella* containing vacuole, inducing its rapture, in a mechanism which is still not yet defined [128].

Once *Shigella* escapes the phagocytic vacuole, the bacteria reside and multiply in the cytoplasm of the host cell. In one way, residing in the cytoplasm, is beneficial for the bacteria as it not exposed to extracellular host immune defences. However, the bacteria must still avoid intracellular host immune defence mechanisms. One-way *Shigella* does this is via intercellular spread to new host cells by directed actin tail polymerisation [67]. The bacterial outer membrane protein IcsA/VirG plays a vital role in mediating actin polymerisation. VirG is an autotransporter and contains 3 distinctive domains, a β-core in the C-terminus, a middle α-domain and a secretion signal domain in its N terminus [67]. IcsA is unipolar meaning it is expressed at one pole of the bacterial cell surface [67]. This asymmetric localisation of the protein is necessary for the actin based movement of the bacteria and localisation is mediated by the outer membrane serine protease, SopA/IcsP, which cleaves VirG [67]. The activity of VirG results in the recruitment and activation of host proteins such as vinculin and N-WASP (neural Wiskott-Aldrich syndrome protein). Activated N-WASP then binds to the Arp2/Arp3 complex and initiates actin polymerisation. This complex promotes actin nucleation and elongation of the actin filaments, enabling *Shigella* to be propelled through the host cytoplasm [129].

In order to survive in the cytoplasm, *Shigella* must evade host responses to infection such as autophagy. Autophagy is an intracellular degradation process utilised by the host to get rid of unwanted or dysfunctional cellular components, including microorganisms [130]. Autophagy can be initiated upon nutrient starvation which is induced upon rupture of the phagocytic vacuole by *Shigella* [131]. The lysed phagocytic vacuole of *Shigella* becomes ubiquitinated which are recognised by the autophagy receptors p62 and NDP52. This will result in the recruitment of the autophagy protein LC3, for autophagosome biogenesis [132]. In the cytosol, the *Shigella* autotransporter IcsA can be recognised by the autophagy protein Atg5 [133]. However, *Shigella* secretes another bacterial protein, IcsB, to inhibit the host autophagy

process and prevent bacterial engulfment by autophagic vacuoles. IcsB functions by associating with IcsA to mask the autophagy-inducing site and prevent its interaction with Atg5 [133].

1.6 Immune responses to infection

The intracellular lifestyle of *Shigella* enables the pathogen to evade many immune responses triggered in the sub epithelial environment. However, bacterial components of *Shigella* can be still sensed by host internal surveillance systems which can cause the activation of an immune response against the bacteria. *Shigella* is able to promote its survival inside the host through the secretion of T3SS effectors to hinder immune responses.

The mammalian immune system encompasses a first line, non-specific innate immune defence and a subsequent adaptive immune defence or acquired immune response which aim to eliminate pathogens. The innate immune system becomes activated immediately but in a non-specific manner upon encountering a pathogen and includes barriers to prevent entry of these pathogens into the host tissues [134, 135]. Some examples of physical barriers and defence mechanisms employed by the innate immune system includes the mucus layer that is secreted in the respiratory, genitourinary and gastrointestinal (GI) tract, cilia which aid in clearing the mucus layer, skin, sweat, tears and gastric acids. The adaptive immune response is far more specific and includes cells such as B and T lymphocytes which are able to elicit highly specific immune responses against pathogens. The important feature of this defence mechanism is immune memory, where subsequent infection by the same pathogen will be countered immediately with a rapid, specific and strong response [136]. Despite the fact that immune responses are necessary to eliminate pathogens, an excessive inflammation response in particular can often be detrimental to the host. This occurs during activation of the innate immune response where there are often significant increases in inflammatory cells recruited to the site of infection, inducing excessive inflammation. Therefore, there should be a balanced response where the immune reach is robust and efficient as well as being self-limiting [137].

1.6.1. Innate immune responses to infection

The innate immune system utilises germline-encoded pattern recognition receptors (PRRs) to identify viral and bacterial pathogens. These PRRs recognize pathogen associated molecular patterns (PAMPs) which are evolutionarily conserved elements present in microbes. Examples of PAMPs include lipopolysaccharide (LPS) and porins found on the outer membranes of gram

negative bacteria as well as, bacterial lipopeptides and lipoproteins, peptidoglycan and lipoteichoic acids found on cell walls of gram positive bacteria, flagellin present in the flagella of bacteria, bacterial nucleic acid and single stranded RNA (ssRNA) and double stranded RNA (dsRNA) from viruses [138]. There are distinct PRRs which interact with specific PAMPs, resulting in the activation of precise signalling pathways. In addition to PAMPs, PRRs can also recognize the host endogenous damage-associated molecular pattern molecules (DAMPs) to elicit an immune response. Currently, PRRs can be grouped into five different families. They are transmembrane proteins such as C-type lectin receptors (CLRs) and Toll-like receptors (TLRs) and cytoplasmic receptors such as the NOD-like receptors (NLRs), dsDNA cytosolic receptors and the retinoic acid-inducible (RIG-I) gene-like receptors (RLRs) [139].

The consequences of the signalling pathways triggered by these PRRs and PAMPs/DAMPs are inflammation and host cell death. A key regulator of both these processes is the NF-κB transcriptional activator. Host cell death plays a vital role in the clearing of damaged cells, in confining inflammation and tissue damage locally, as well as eliminating pathogens and activating adaptive immune responses. Programmed host cell death as a result of bacterial damage can be grouped into three categories: pyroptosis, necroptosis and apoptosis [140].

Pyroptosis is defined as a proinflammatory type of programmed cell death which depends on the activation of the inflammatory proteases, caspase 1 or caspase 4/11, formation of the inflammasome and subsequent production of mature IL-18 and IL-1β. Apoptosis is defined as a non-inflammatory form of regulated cell death induced extrinsically by death receptors or intrinsically through a mitochondria-dependent pathway. This eventually results in activation of executioner caspases, shrinkage of the cell, chromatin condensation, blebbing of the plasma membrane and apoptotic body formation. Lastly necroptosis is defined as an inflammatory cell death which gives rise to swelling of cell, intracellular leakage and membrane rupture and is caspase independent [117, 140, 141].

1.6.2. RHIM protein-dependent signalling to initiate inflammatory and cell death pathways

Several different host signalling pathways result in the activation of inflammation and cell death signalling. Many involve the receptor-interacting serine/threonine-protein (RIP) homotypic interaction motifs (RHIM) domain containing proteins, RIPK1, RIPK3, TRIF and DAI. RIPK1 is the main regulator of both inflammation and cell death signalling pathways in response to TNF signalling and upon the availability of adaptor molecules. RIPK1 activator can give rise to either NF-κB activation, apoptosis or necroptosis [141].

Ligation of the TNF receptor 1 (TNFR1) by TNF results in the formation of a short-lived signalling complex termed complex I or TNF-RSC. This complex is an important checkpoint for necroptosis and cell survival. It involves association of the death domain (DD) of TNFR1 with the DD or RIPK1 and TRADD [142]. This is followed by TRADD recruiting adaptor proteins such as TRAF2/5 as well as the E3 ubiquitin ligases cIAP1/2, for the catalysis of the K63 ubiquitin modifications on RIPK1 [143]. K63 ubiquitination then mediates TAB2/3 recruitment in order to activate transforming growth factor- β-activated kinase 1 (TAK1). It also mediates the addition of linear ubiquitination (M1-Ubi) assembly complex (LUBAC) to the complex. In addition to this, the deubiqitinating enzyme CYLD and the adaptor protein spermatogenesis-associated 2 (SPATA2) are also recruited to the complex. [144-147]. SPATA2 functions by disassembling M1-Ubi. Thus, recruitment of both M1-Ubi and the deubiqitinating enzymes regulates both the addition and removal of RIPK1 and TNFR1 within complex I. TAK1 activation also results in pro-survival signalling induction by complex I through NF-κB and MAPK pathways, which also induce an inflammatory response [148]. The pro-survival activity of NF-κB is regulated by cIAP1/2 as well as cellular FLICE-like inhibitory protein (cFLIPL) [149]. Phosphorylation of RIPK1 by NF-κB components IKKα and IKKβ, prevents the formation of another complex termed complex II or the pro-cell death complex. Complex II comprises IIa and IIb based on proteins and composition of complex II [142, 150]. Both these complexes can induce both apoptosis and necroptosis depending on the presence and activity of caspase 8 [141].

Complex IIa is formed when TRADD dissociates from TNFR1 and this is followed by FADD and caspase 8 being recruited into the complex [142, 151]. Activation of caspase 8 and induction of apoptosis by this complex is independent of the kinase activity of RIPK1 [141, 151]. Subsequently, complex IIb is formed when cIAPs, TAK1, IKKα/β *or TRADD* are inactive or absent. In this complex, the kinase activity of RIPK1 is necessary for the activation of caspase 8 and apoptosis [151, 152].

The formation of necrosome is then initiated when caspase 8 is absent or inactivated. RIPK1 will then recruit and activate RIPK3 via RHIM-RHIM interactions. The necrosome from complex IIa includes TRADD, RIPK1, RIPK3 and FADD while TRADD is absent in the necrosome resulting from complex IIb [153-155]. Upon formation of the necrosome RIPK3 becomes autoactivated and phosphorylates MLKL (mixed lineage kinase domain-like protein) which then oligomerises and translocates to the plasma membrane and induces membrane rupture [156].

As such, inactive RIPK1 is initially held in a closed conformation at the TNFR1, making its RHIM and DD domains inaccessible for the pro-cell death complexes to be formed. Subsequent de-ubiquitylation then frees RIPK1 and allows the formation of these pro-cell death complexes [157]. Apoptosis and necroptosis are then initiated depending on the availability of caspase 8 which cleaves and inactivates RIPK1 which would otherwise associate with RIPK3 in complex II [158].

Other RHIM containing proteins such as TRIF and DAI can also form a necrosome, termed the non-classical necrosome, involving RHIM interactions with RIPK3 [159]. For example CMV viral infections of 3T3-SA or primary MEF cells result in RIPK1-independent but RIPK3-dependent necroptosis which also requires ZBP1/DAI [160]. Similarly, upon TLR3 stimulation in endothelial cells and fibroblasts, RIPK3-dependent necroptosis depends on the activity of TRIF but not RIPK1 [161].

1.6.3. NF-κB and MAPK signalling

Nuclear factor-κB (NF-κB) proteins are group of transcription factors which regulate numerous cellular processes such as development and function of the immune system, cell survival, differentiation and proliferation [162]. There are five members in this family, namely: RelA/p65, RelB, c-Rel, NF-κB1/p50 and NF-κB2/p52. They are all structurally related and contain a 300 amino acid region at the N-terminus termed the Rel homology domain (RHD). This region includes the DNA-binding, dimerization and nuclear localization domains [163]. Members of the Rel family (p65, RelB and c-Rel) also contain a transactivation domain in their C-terminus. The NF-κB proteins (p50 and p52) on the other hand have multiple auto-inhibitory ankyrin repeats in their C-terminus [164]. These repeats are proteolytically removed to form active p50 and p52 proteins during signalling. The NF-κB proteins regulate the transcription of genes by forming homo- or hetero-dimers with either κB enhancer or specific DNA segments. This association can affect the target gene transcription both negatively and positively [165]. The most commonly expressed form of the NF- κB proteins in mammalian cells is the heterodimer formed by p65 with p50.

Canonical signalling in the NF- κB pathway consists of an upstream regulatory step, which includes the activation of the multi-subunit IκB kinase (IKK) complex. This complex consists of a NF-κB essential modulator (NEMO) which acts as a scaffold. It also contains the catalytic kinase subunits, (IKKα and/or IKKβ) [166]. This pathway is activated upon exposure to a range of stimuli such as PRRs, the T cell and B cell receptor and members of the TNF receptor

(TNFR) superfamily [167]. In the canonical pathway, IκBα is targeted for degradation via IKK mediated phosphorylation [168]. Once activated, the IKK complex phosphorylates IκBα at two specific serine residues at the N-terminal, particularly, serine 32 and serine 36 [169]. This then triggers lysine polyubiquitination of IκBα and subsequent degradation by the proteasome. p65:p50 heterodimers are then free to translocate into the nucleus where they bind to κB consensus sites located on the promoters of various genes such as the IL-8 gene, promoting transcription of relevant genes in response to infection such as proinflammatory cytokine genes [170, 171].

The mitogen-activated protein kinases (MAPK) are kinases which phosphorylate serine and threonine residues to regulate crucial cellular processes including cell death pathways and the immune defence [172] . The three important and well-studied MAPK pathways are the p38 pathway, the ERK1/2 pathway and the c-JUN pathway [172].

Pathogens can also target MAPK pathways in order to inhibit an immune response in the host cells [173]. Proinflammatory cytokines such as TNF, IL-1, IL-10 and IL-12 are induced as a consequence of MAPK pathways [174-176]. IL-10 and IL-12 are produced by dendritic cells and macrophages, resulting in these cytokines promoting a Th2 and Th1 immune response respectively in order to protect the host against both extracellular and intracellular pathogens [176]. IL-10 production is regulated by the ERK1/2 pathway which then induces Th cell differentiation into Th2. Th2 cells regulate the humoral response to induce the production of anti-inflammatory cytokines such as IL-4-5, IL-9 and IL-13. IL-10 also has a role in preventing tissue damage and down-regulating inflammation [177]. IL-12 production is regulated by p38 pathway to induce a Th1 response [175, 178]. This then induces the production of pro-inflammatory cytokines such as IL-2, IFNγ and TNF which aid is inducing an immune response against intracellular pathogens [176].

1.6.4. Toll-like receptors (TLRs)

Another manner through which host cells induce inflammation and cell death signalling pathways in response to microbial pathogens is via the action of TLRs. TLRs are the most studied and well characterised PRRs which were first reported in the fruit fly, *Drosophila melanogaster* [179]. These PRRs are required for sensing extracellular pathogens and intracellular pathogens present in lysosomes and endosomes [180]. TLRs are not only limited to and present in immune cells such as macrophages and dendritic cells (DCs) but can also be expressed in epithelial cells and fibroblasts. The classical TLRs are type I transmembrane

proteins which comprise three different structural motifs, an N-terminal leucine-rich repeat (LRRs) domain, a middle transmembrane domain and a cytoplasmic Toll/IL-1R homology (TIR) domain [181]. These domains are required for different functions where the LRR are needed for PAMP recognition and the TIR domain is necessary for signal transduction. A total of 13 and 10 TLRs have been identified in mice (TLR1 to TLR13) and humans (TLR1 to TLR10) respectively. They can be divided into two main categories based on their localisation, as either intracellular TLRs (TLR1, 2, 4, 5, 6 and 10 or intracellular TLRs (TLR3, 7, 8, 9, 11, 12 and 13) [182, 183].

1.6.5. TLR ligand recognition

The different TLRs recognise and interact with different PAMPs and DAMPs and these interactions have been summarised according to the microorganisms they detect in the table below (Table 1.1). Many TLRs play important roles in initiating an innate immune response during bacterial infection. TLR2, which forms a heterodimer with either TLR1 or TLR6, senses various bacterial components such as peptidoglycans and lipoproteins from both gram-negative and gram-positive bacteria. It also specifically detects lipoteichoic acid from gram positive bacteria, glycolipids from *Treponema maltophilum* (a gram negative bacteria which causes in chronic periodontitis) and phenol-soluble modulin from *Staphylococcus aureus* (a gram positive bacteria) [181, 184]. TLR2 also recognises atypical LPS which is structurally dissimilar to typical LPS and is present on non-enterobacteria including *Helicobacter pylori*, *Porphyromonas gingivalis* and *Leptospira interrogans* [185].

TLR4 is essential for recognising lipopolysaccharide (LPS) which is a component of the cell wall of Gram-negative bacteria. LPS is composed of an O-antigen, a core oligosaccharide and an endotoxin, Lipid A, and it is Lipid A that is recognized by TLR4. TLR4 on its own is not responsive to LPS and forms a complex with myeloid differentiation factor 2 (MD2) on the cell surface in order to recognise LPS [186].

Another TLR which plays a role in host defence during bacterial infection is TLR5. The protein flagellin is an essential component of bacterial flagella, which are required for some bacterial adhesion and invasion of host cells. Flagellin is detected by TLR5 to elicit an immune response in cells [187]. TLR5 is located on the basolateral surface of intestinal epithelial cells and thus recognises bacteria upon invasion across the intestinal epithelium [188].

Unmethylated CpG motifs in bacterial DNA are important for stimulating an inflammatory response, resulting in a strong T-helper 1 like immune response upon detection [189]. In

contrast, mammalian DNA is mostly methylated and does not induce an immune response [162]. Studies have shown that TLR9 deficient mice do not respond to unmethylated CpG DNA illustrating the role of TLR9 in recognizing unmethylated bacterial CpG DNA, distinguishing self-DNA from bacterial DNA [190]. CpG DNA motifs are also present in certain DNA viruses including Herpes Simplex virus, and TLR9 is able to sense this CpG DNA to illicit an immune response [191].

TLR11 which is expressed only in macrophages and kidney, liver and bladder epithelial cells is important for mounting an immune response to uropathogenic bacteria. Kidney cells of mice deficient in TLR11 are highly vulnerable to infection by uropathogenic bacteria [192]. However, humans do not express full-length TLR11, due to the presence of a stop codon in the open reading frame (ORF) of the TLR11 gene [192]. Hence TLR11 is dispensable for immune defence in humans.

TLRs have also been implicated and well-studied in viral, fungal and protozoan infections. TLR4 and TLR2 recognize viral envelope proteins from respiratory syncytial virus (RSV), human cytomegalovirus and measles virus to name a few [193-196]. In addition, TLR3 is required for the sensing of double stranded RNA (dsRNA), which is produced by some viruses and it's synthetic analog, the polyinosine-deoxycytidylic acid (poly I:C) [197]. Contrary to the role of TLRs in eliciting a protective immune response against microbial pathogens, it has also been reported that mice deficient in TLR3 are more resistant to West Nile virus infection because the immune response triggered via TLR3 results in blood brain barrier (BBB) disruption and subsequent infection of the brain [198].

1.6.6. TLR signalling

TLR signalling can occur through pathways into two, myeloid differentiation primary response protein 88 (MyD88)-dependent pathway and the TIR domain-containing adaptor-inducing IFNβ (TRIF)-dependent pathway.

1.6.7. MyD88 dependent pathway

All TLRs utilises MyD88 as a signalling adaptor. MyD88 is made up of two main domains, the death domain (DD) and the TIR domain. Upon stimulation with the appropriate ligands, MyD88 interacts with a serine/ threonine kinase termed the IL-1R-associated kinase (IRAK)-4 which contains a DD at the N terminus. This leads to the activation of IRAK-1 and IRAK-2 and their phosphorylation. The IRAKs then dissociate from MyD88 to interact with an E3 ubiquitin protein ligase, the TNFR-associated factor 6 (TRAF6). TRAF6 engages with an E2

ubiquitin-conjugating enzyme complex to eventually activate the MAP kinases (p38 and JNK) as well trigger activation of the NF-κB pathway [180].

Aside from the activation of these pathways, TLR7 and TLR9 signalling can also cause the activation of type I interferon (IFN) production in plasmacytoid dendritic cells (pDCs) [199]. In these specialised cells, a complex comprising of MyD88, IRAK-1, TRAF3, TRAF6, IKKα and IRF7 is formed, resulting in the phosphorylation and translocation of IRF7 into the nucleus where it activates type I IFN gene expression [200].

1.6.8. TRIF dependent pathway

TRIF harbours an N-terminal domain which contains consensus TRAF-6 binding sites, a middle TIR domain and a C-terminal RHIM domain. TRIF signaling can give rise to either IRF3 activation or NF-κB activation depending on the interaction of different proteins with different regions of TRIF [201].

Upon signalling via TLR4 or TLR3, the TIR domain of TRIF interacts with the TIR domain of TRAM and TLR3 respectively. The C terminus RHIM domain is then responsible for the activation of NF-κB and subsequent initiation of apoptosis or necroptosis depending on the inhibition of caspase 8 [202-204]. The TIR domain is also important for mediating the formation of a signalling complex comprising TLRs as well as TRAM and TRIF, whereas the N-terminal domain is involved in downstream events by interacting with TRAF6 [205, 206]. TRIF signalling then gives rise to the activation of transcription factors such as NF-κB, AP-1 and IRF3. This eventually results in the expression of cytokines, including type I IFN [204].

1.6.9. Interferon signalling pathway

One outcome of TRIF signalling is the production of IFNβ and subsequent type I IFN response [207]. Interferons belong to a family of cytokines which are involved in regulating numerous cellular and biological responses including mediating cell survival, resistance against viral infections, promotion of anti-tumor events and modulation of immune responses [208]. The three most well characterised IFNs are IFNα, IFNβ and IFNγ. Interferons can be classified based on the receptor through which they signal; type I IFN, type II IFN and type III IFN [209]. Type I IFN comprise13 subtypes of IFNα, IFNβ, IFNω, IFNε and IFNκ. Type II IFN consists only of IFNγ and type III IFNs are made up of IFNλ1, IFNλ2, IFNλ3 and IFNλ4 [210-212].

Type 1 IFNs are produced by all cell types with exceptionally high amounts produced by plasmacytoid dendritic cells (pDC) in response to stimulus by microbial agents [213, 214].

Upon reaching a target cell, IFNα/β bind to the type I IFN transmembrane surface receptors consisting of the subunits IFNAR1 and IFNAR2. This in turn activates the Janus kinase (JAK-STAT) signaling pathway (Figure 1.5). The JAKs are protein tyrosine kinases consisting of JAK1-3 and Tyk2 (tyrosine kinase 2). These kinases consist of 7 homologous domains (Janus homology domains (JH)) which are needed for subsequent interactions with STATs [215]. STATs are transcription factors which consist of 7 functionally and structurally conserved domains including a transcriptional activation domain (TAD), tyrosine-phosphorylation site (pY), Src homolgy 2 domain (SH2), DNA-binding domain (DBD), linker domain (LD), coiled-coil domain and an N-terminal domain [216]. In the canonical signalling pathway, dimerisation of the receptors IFNAR1 and IFNAR2 initiates their association with JAK1 and TYK2. These proteins then cross-phosphorylate to create docking sites for binding of STATs. STAT1 then becomes phosphorylated on Tyr701 and STAT2 becomes phosphorylated on Tyr690, resulting in their hetero-dimerisation and association with IRF9.

The STAT1:STAT2:IRF9 complex that is formed (termed the interferon-stimulated gene factor 3 (ISGF3)) translocates into the nucleus where it binds to specific promoter regions of interferon-stimulated genes (ISGs) to induce their transcription. These regions are called the interferon-stimulated response elements (ISRE) regions and they are present in the promoters of almost 300 genes [217, 218]. In the ISGF3 complex, STAT1 is necessary to provide stability for the binding of ISGF3 to the promoter region, and the TAD region of STAT2 is required for the transcriptional activity of the complex [219-221]. IRF9 is crucial for binding to the ISRE and provides DNA-protein interaction sites for STAT1 and STAT2 [215, 222-224]. IRF9, on its own, exhibits only a weak affinity to ISREs and is not capable of transcriptional activity. However, this is overcome upon efficient association with STAT1 and STAT2 where in addition to the 9 nucleotide core region within the ISRE which IRF9 binds to, STAT1 and STAT2 provide additional contact to the DNA for efficient association with ISREs [222, 225, 226]. IRF9 also includes a bipartite basic nuclear localization signal (NLS) which is present within its DNA binding domain. This signal is necessary for interaction with importin-α adapter family members such as importins-α3, −α5, and −α7 [227].

Upon association of STAT2 with the C-terminus of IRF9, recognition of the NLS signal within IRF9 by the importin-α: importin-β1 complex enables the translocation of STAT2 into the nucleus [227]. In the absence of a stimulus, unphosphorylated STAT2 remains associated with IRF9. The NLS signal from IRF9 and the nuclear export signal (NES) within the C-terminus of STAT2, results in the complex shuttling in and out of the nucleus constitutively. However,

upon activation and phosphorylation as a result of IFN signalling, STAT2 and STAT1 dimerise which results in a conformational change that masks the NES signal of STAT2 which then results in import of the complex into the nucleus. In addition to this, the NES signal in STAT2 also shuttles the ISGF3 complex back into the cytoplasm following dephosphorylation and dissociation of STAT2 from STAT1 in the nucleus [227].

In addition to the canonical signalling pathway, type I IFN can also engage in non-canonical signalling via IRF9 and STAT2. STAT2 can form heterodimers with STAT1, STAT3 and STAT6 without the presence of IRF9 to bind to γ activated sequence (GAS) regions to induce the transcription of target genes [228-230]. IRF9 can interact with phosphorylated STAT2 homodimers without the presence of STAT1 to bind to ISRE elements for the transcription of ISGs [231]. This was seen when investigation in U3A cells that were deficient in STAT1 were still able to form STAT2 homodimers to give rise to IFIT3 (an ISG). However, it was noted that IFIT3 was not typically produced during the canonical ISGF3 signalling [232]. It was also noted that the expression of several ISGs (ISG15, PKR and APOBEC3G) were only affected upon STAT2 and IRF9 siRNA knockdown human hepatocytes but not during STAT1 siRNA knockdown [233]. In addition to these studies, mice that were deficient for STAT1 also exhibited a STAT2-dependent protection against dengue infections [234]. Although the biological significance of forming these non-canonical complexes are not well understood, these complexes may form as a background option in the absence of STAT1. Furthermore, it was reported that these non-canonical complexes can also be cell type-specific, especially in the case of B cells where IRF9 complexes with phosphorylated STAT6 and STAT2 to form an ISGF3-like complex [230]. Therefore, the diversity in type I IFN signalling with the many complexes formed with or without IRF9, suggests that there are broad effects contributed by type I IFN signalling via the transcription of numerous ISGs involved in both innate and adaptive immune responses.

1.6.10. NOD-like receptor signalling

Host cells can trigger inflammation and cell death signalling also via NLR signalling. NLR signalling is important for sensing microbial invasion into host cells. In terms of structure, NLRs have a central oligomerization and nucleotide-binding (NOD or NACHT) domain, C-terminal leucine-rich repeats (LRR) and an N-terminal protein interaction effector domain [235]. As the name suggests, the N-terminal domain is required for interactions with other proteins for effector functions. The most common effector domains are the pyrin domain (PYD) and the caspase-activation and recruitment domain (CARD). The C-terminal LRR

domain is needed for ligand sensing and binding and the central domain, which comprises several distinct motifs, is needed for oligomerization and dNTPase activity [236]. The NLRs can be divided into 4 subfamilies based on their N-terminal domains. These are NLRA, which contain the acidic transactivation domain, NLRB, which contain a baculovirus inhibitor of apoptosis protein repeat (BIR), NLRC which contain the CARD domain and NLRP which contain the PYD domain PYD. The NLRA and NLRB subfamilies contain one member each, the MHC-II transactivator (CIITA) and the NAIP respectively. There are 6 members in the NLRC subfamily, including NOD1 (NLRC1), NOD2 (NLRC2), NLRC3-5 and NLRX1. There are 14 members present in the NLRP subfamily, NLRP1-14 [237, 238]. NLRs have four main functions, they can be involved in the formation of inflammasomes, in the activation of gene transcription, in autophagy or in inflammatory signal transduction.

1.6.11. Inflammasome formation

The inflammasome is defined as a multiprotein oligomeric complex which plays a role in the activation of caspase-1. Caspase-1 plays a crucial role in the maturation and activation of the precursors of the proinflammatory cytokines, IL-1β and IL-18, resulting in pyroptosis and subsequent induction of inflammation [238, 239].

Gasdermin D (GSDMD) has a role of mediating pyroptosis downstream of caspase 1 and 11[240, 241]. GSDMD, a substrate if caspase 1, is cleaved by the caspases to yield two fragments, a 31 kDa N terminus and 22 kDa C terminus fragments. The 31 kDa cleaved GSDMD is essential to induce pyroptosis, although the mechanism is still unclear [240].

The canonical inflammasome consists of an NLR (except AIM2 and IFI6), an inactive zymogen, pro-caspase 1 and an adaptor protein termed the apoptosis-associated speck-like protein (ASC) which contains two domains, a CARD domain and a pyrin domain [242].The domains of the ASC aid in acting as a bridge for the interaction of some NLRs which lack the CARD domains with pro-caspase 1 [243]. Based on the ability of the NLRs to form inflammasomes, they can be divided into two groups, the canonical caspase-1 dependent inflammasome forming NLRs and the non-canonical NLRs which do not act through caspase-1 but instead activate caspase-11 in mice and caspase 4 and 5 in humans [243]. NLRP3 is an NLR that can exhibit both canonical and non-canonical inflammasome formation depending on both the type of tissue and stimulus present [243].

Inflammasome activation has been studied extensively during *Shigella* infection, in particular the NLRC4 inflammasome by binding directly with caspase 1. NLRC4 inflammasome formation is activated via PAMPs released from *Shigella*, such as the bacterial T3SS system [243]. It was also reported that the NLRP1B inflammasome is activated during *Shigella* infection [244]. NLRP1B is activated in cells which are undergoing metabolic stress as a result of host cell damage or nutrient depletion that may have arisen due to *Shigella* infection [244]. The NAIPs from human have also been reported to recognise the flagellin and T3SS needle components, the rod and needle [245]. NAIP then partners with NLRC4 to initiate the formation of NAIP/NLRC4 inflammation, in order to activate procaspase 1[245].

Caspase 4, GSDMD and NLRP3 inflammasomes are also activated by LPS, particularly by the EHEC *E. coli* which initiates the Stx2-LPS complex, in human THP1 cells [246]. It was reported that non canonical caspase 4 inflammation formation and cleaved GSDMD triggers mitochondrial ROS formation and Stx2-LPS complex formation and subsequent NLRP3 inflammation formation to initiate cytokine maturation and pyroptosis [246].

Lastly, the pyrin inflammasome are activated when they sense Rho guanosine triphosphatase (Rho GTPase) which are induced by bacterial toxin, resulting in the activation of caspase -1 and IL-18 and IL-1β secretion [247].

1.7 Innate immune responses to *Shigella*.

The host employs several strategies to sense *Shigella* during invasion. The presence of mucus in the gut is considered the first line of nonspecific defence against microbial infections of the gut. This mucus contains antimicrobial peptides (AMPs) which are important to maintain intestinal homeostasis as well as to protect against these microbial pathogens [248, 249]. The production of several AMPs such as human b-defensins 1 and 3 and LL-31 are down-regulated during *Shigella* and EIEC infections [250, 251]. Transcription of the mucin gene MUC5AC is also affected during *Shigella* infection of mucin-producing epithelial cells, resulting in creation of only a thin layer at the apical surface of the cells, hence increasing infection rate of the bacteria [252].

Typically, *Shigella* invade the intestinal epithelium from either the apical side or, upon translocation across M cells, the basolateral side of the epithelium before infecting resident macrophages [48, 253]. *Shigella* T3SS effector proteins, target important signalling pathways

of both macrophages and enterocytes, resulting in modulation of crucial host cell functions, although the epithelial cell model is better studied. The T3SS Ipa proteins are crucial for infection of both the epithelial cells and macrophages [109, 254, 255]. In macrophages, IpaB mediates the escape of *Shigella* from the phagosome into the cytoplasm. This results in the activation of caspase-1, which results in the generation of mature IL-1β and IL-18. This is accompanied by pyroptotic cell death and the recruitment of PMN leukocytes to the site of infection [256]. Invasion of epithelial cells by *Shigella* on the other hand, does not result in pyroptotic cell death, despite requirement of the Ipa proteins for *Shigella* escape into the cytoplasm [253]. Other differences between cell types were examined by Lucchini *et al* who constructed cDNA microarrays to determine *Shigella* genes which exhibited transcriptional adaptation during infection of macrophages (U937 cells) and epithelial cells (HeLa epithelial cells) [253]. Both U937 cells and HeLa cells, despite being distinct at the cell biological level, had comparable cytosolic environments due to the similar patterns of *S. flexneri* gene expression in these cells. However, some obvious differences between the two cell types were the YdeO and EvgA regulons which were induced highly in U937 cells compared to HeLa cells. These regulons play a role in acid resistance of *E. coli* [257] and an explanation for this could be acidification of the macrophage cytosol as a consequence of *Shigella* infection. Genes within the *ipa-mxi-spa* region as well as genes that encode proteins linked to energy generation (such as succinate dehydrogenase, cytochrome bo3 and NDH-1) also showed a delayed response in HeLa cells compared to U937 cells, suggesting that the epithelial cell cytosol is more favourable than the macrophage cytosol for bacterial replication at early stages of infection [253]. Given these differences, it is important to study *Shigella* infection dynamics in both cell types.

During infection, inflammasome activation as well as binding of LPS from extracellular *Shigella* to TLR4 and binding of cell wall peptidoglycan from intracellular *Shigella* to NOD1 and NOD2 induces a pro-inflammatory response, resulting in the production of proinflammatory cytokines and chemokines to stimulate the immune response [258, 259].

After crossing the intestinal epithelium, *Shigella* is phagocytosed by macrophages and induces pyroptosis upon recognition of MxiI and MxiH (T3SS needle components) by NAIP1 and NAIP2. This results in activation of NLRC4-dependent inflammasome and induces pyroptotic macrophage cell death [260]. IpaB also contributes to macrophage pyroptosis by forming ion channels to allow potassium ion influx, which is sensed by the NLRC4 inflammasomes for pyroptosis [261]. In addition to these mechanisms, the effector IpaH7.8 also activates NLRC3

and NLRC4 inflammasome formation by mediating macrophage cell death in a IpaH7.8 E3 ligase- dependent mechanism through targeting the host glomulin/ FAP68 (GLMN) [262].

Dying macrophages also results in pyroptosis-mediated recruitment of neutrophil to the site of infection. It has been reported that *Shigella* acts to inhibit neutrophil recruitment and activation by several mechanisms. The ShiA virulence PI from *Shigella* prevents the recuitment of neutrophil in an unknown mechanism [263]. *Shigella* also modifies and decreases its LPS acetylation levels. This subseqently reduces inflammasome activation, IL-Ib secretion and neutrophil activation [264].

Controversially, neutrophil recruitment during the initial stages of *Shigella* infection, enables the bacteria to reach and baso-lateral side of the epithelial cells [265]. However, these neutrophils also undergo T3SS-dependent necroptosis during *Shigella* infection [266]. As such the role of neutrophil recruitment during *Shigella* infection is still not well understood.

1.8 Evasion of the host innate immune response

Shigella has utilised many strategies to overcome host surveillance and establish an infection. Importantly, *Shigella* T3SS effectors have evolved mechanisms to ensure the survival of the bacterial within the host by interfering with these responses at different levels including the inhibition of inflammatory signalling and protein secretion [51]. The functions of some of these T3SS effectors in evading the host defence response are discussed below.

The T3SS effector OspI is a glutamine deamidase which functions by deaminating a glutamine residue at position 100 (Gln100) to a glutamic acid residue in a E2 ligase UBC13. By doing this, OspI is able to inhibit TRAF6 polyubuquitination. TRAF6 polyubuquitination is necessary for the diacylglycerol– CBM (CARD–BCL10–MALT1) complex–TRAF6–NF-κB signalling pathway [95]. Further studies on the OspI structure have revealed the presence of a putative catalytic triad (cysteine–histidine–aspartic acid) which is needed for this deamination and subsequent inhibition of immune responses during infection [267, 268].

OspG is a serine/threonine protein kinase that inhibits NF-κB signalling by targeting the host ubiquitin-conjugating enzyme, UbcH5 [269], a member of the stem cell factor-TrCP complex (SCF-TrCP). UbcH5 is involved in the ubiquitination and degradation of phospho-IκBα [169] and the prevention of ubiquitination of phospho-IκBα therefore inhibits activation of the NF-κB pathway [269].

The T3SS effector, OspF, affects MAPK signalling. In early studies, transient expression of OspF in HEK 293T cells revealed the ability of OspF to inhibit MAPK (Erkl/2, JNK, and p38 kinases) activation but not NF-κB signalling [80]. Further studies revealed the phosphothreonine lyase activity of OspF, which dephosphorylates MAPKs by targeting the phosphothreonine of the pT-X-pY motif present in phospho-MAPKs. By doing this, OspF is able to abrogate the MAPK signalling pathways [270, 271].

Another T3SS effector which modulates the host immune response is IpaH9.8. IpaH9.8 belongs to the family of E3 ligases involved in ubiquitination [272]. During *Shigella* infection, the bacteria present in the cytosol are coated by interferon induced guanylate-binding proteins (GBPs), which restrict bacterial movement and spread. However, IpaH9.8 ubiquitylates GBP1, resulting in its proteasomal degradation and thereby facilitating bacterial motility and cell to cell spread [273, 274].

The IpaH4.5 is also invovled in inhibiting NF-κB activation, by interacting directing via poly ubiquitinylation of the p65 subunit of NF-κB [275]. This T3SS effector also plays a role in negatively regulating the type I IFN signalling [276]. Specifically, TBK1, which activates IRF3 for type I IFN response is targeted by IpaH4.5, which subjects it to proteosomal degradation via Lys48-linked poly- ubiquitinylation.

The T3SS effectors IpaH1.4 and IpaH2.5 have a role in dampening NF-κB signalling [277]. They target the E3 ubiquitin ligase complex, linear chain assemble complex (LUBAC) subunits HOIL-1 and HOIP for proteosomal degradation. LUBAC is needed to catalyse the production of Met1-linked ubiquitn chains and rapid activation of NF-κB [278, 279].

Another mechanism via which *Shigella* interfere with pro inflammatory responses initiated by the host cells is via the T3SS effector OspC3. OspC3 prevents activation of the non-canonical caspase 4 dependent inflammasome by specifically interacting with the p19 subunit of caspase 4, thus inhibiting heterodimerisation with the p10 subunit of caspase 4. By inhibiting caspase-4 activity, OspC3 is able to prevent pyroptotic host cell death which benefits *Shigella* replication and cell spread [280].

The Golgi apparatus plays a critical role in cytokine secretion and cell surface receptor expression in host cells. The T3SS effectors, IpaJ, VirA and IpaB can disrupt the Golgi

apparatus upon *Shigella* infection [51]. IpaJ is a cysteine protease which targets and cleaves the N-myristoylated glycine from ARF1, which is important for adhering to the Golgi membrane. ARF1 thus gets released and disrupted, which eventually results in inhibition of the trafficking of the host cytosolic sensor, STING during *S. flexneri* infection. This curtails the type 1 IFN response as well as the secretion of cytokines such as CXCL10 [281-283]. VirA functions by targeting and catalysing GTP hydrolysis in Rab1, thereby acting as a RabGAP. By doing this, VirA inactivates Rab1 and prevents the localisation of Rab1 containing vesicles from ER to the Golgi, thus disrupting the Golgi apparatus [120] . IpaB on the other hand, binds to cholesterol from the inner membrane and redirects it to the *Shigella* entry site at the plasma membrane, resulting in the disruption of the Golgi [284]. The T3SS effector IpgD also reduces inflammatory responses by producing PtdIns(5)P which functions by blocking hemichannels and preventing the release of the danger signal, ATP. Released ATP promotes inflammation in the gut by binding to purinergic receptors and resulting in the activation of the NLRP3 inflammasome formation [285, 286].

As such, *Shigella* has evolved several mechanisms to manipulate the host immune response and establish a replicative niche in host cells, mostly via T3SS effector dependent interference of host signalling pathways. The strategies discussed above are likely not the only strategies employed by *Shigella* to evade the host immune response and there are many more which remain to be explored. Some of these are not unique to *Shigella* but also shared by other bacterial pathogens.

1.8.1. Effectors modulating innate immune responses from related bacterial pathogens

Similar to *Shigella*, several EPEC effectors modulate host innate immune responses. *Shigella* and EPEC belong to the same Enterobacteriaceae family and both utilise a T3SS to deliver effectors into host cells to alter host cell physiology during infection [287]. Despite their different modes of pathogenesis, several T3SS effectors secreted by these pathogens share amino acid sequence homology, and hence, may have similar functions. However, it is also possible that these effectors have differing or additional roles in addition to the functions shared with their homologues.

EspG (*E. coli* secreted protein G) and EspG2 are EPEC T3SS effectors that are homologous to VirA from *Shigella* and have similar host cell functions. VirA has two well defined functions, one is the RhoGAP activity that leads ot activation of the GTPase Rac 1 resulting in membrane ruffling that facilitates the entry of *Shigella* into the host cell. The other is to disrupt the host cytoskeletal microtubule network in order to allow the bacteria to move along, following

uptake into the cell. Similar to VirA, EspG and EspG2 play a role in inhibiting and destabilising microtubule polymerisation in the host cells [288]. Furthermore, it was previously reported that EspG and VirA localise to the Golgi and interact with the Golgi matrix protein GM130, resulting in disruption and inhibition of the Golgi function [289].

The non-LEE encoded effector NleE is another T3SS effector from EPEC which is involved in repressing innate immune signalling [290]. NleE inhibits NF-κB activation by inhibiting TAK1 activation. NleE was identified as a novel S-adenosyl-L-methionine (SAM) dependent cysteine methyltransferase that modulates TAB2 and TAB3 [291]. TAB2 and TAB3 are ubiquitin sensory proteins which have a role in NF-κB signalling by detecting ubiquitinated TRAF proteins. NleE specifically modifies the cysteine present within the Npl4 zinc finger in domains of TAB2/3 thereby blocking the ability of TAB2/3 to bind ubiquitinated TRAF and hence repressing NF-κB activation [292]. OspZ from *Shigella* is homologous to NleE and also interacts with and modifies TAB3 resulting in the inhibition of host NF-κB signalling and decreased IL-8 transcription [291].

NleH is another T3SS effector from EPEC which is homologous to OspG of *Shigella*. NleH1 and NleH2 have 80% sequence identify with each other and the C terminus of NleH1 and NleH2 exhibit high degree amino acid similarity with OspG (30% to 27% identity to OspG) [269]. Despite the high sequence identity between NleH1 and NleH2, a 10 amino-acid between residues 127-136 in NleH2 is not present in NleH [293]. In addition to this, the 95 amino acid fragments at the N terminus of NleH are not present in OspG. OspG and the NleHs all contain a minimal kinase domain and exhibit kinase activity of OspG. The major difference between the NleHs and OspG is that OspG has ubiquitin binding capacity and binds ubiquitin-loaded E2 conjugating enzymes [294].

NleH1 and NleH2 have a reported role in dampening inflammation by inhibiting apoptosis and suppressing NF-κB activation when there is an overexpression of IκB [294]. They have been beed reported to function by attenuating TNF induced, phospho-IκB degradation by inhibiting ubiquitination [294]. Furthermore, during EPEC and *C. rodentium* infections NleH was reported to inhibit caspase activation, thereby modulating apoptosis [178]. Both NleH1 and NleH2 inhibited the activation of caspase-3 in response to staurosporine treatment. However, this was not seen in the case of OspG [293]. It was found that NleH could bind Bax inhibitor-1 (BI-1). BI-1, present in the ER membrane, which may explain the inhibition of apoptosis [295].

EspL is a T3SS effector from EPEC that is located upstream of NleB1 and NleE in the integrative element 6 (IE6) genomic island [296]. EspL is homologous to OspD2 and OspD3 from *Shigella* and functions as a cysteine protease to specifically target host cell RHIM-containing proteins for degradation to limit epithelial cell death and inflammation during EPEC infection [296]. OspD3 and OspD2 are encoded on the virulence plasmid by the *senA* and *senB* genes and are 568 amino acids and 533 amino acids in length respectively. Both these proteins have a molecular weight of 63 kDa and share 38% similarity at the amino acid level [297].

OspD3 (also known as SenA, ShET2 or ShET2-1) was initially detected in enteroinvasive *E.coli* (EIEC), called the EIEC enterotoxin and was reported to have iron regulated enterotoxin activity [297]. It was also found to alter electrolyte and fluid secretion in rabbit intestinal models both *in vivo* and *in vitro* [298]. Despite an initial report that OspD3 transcription requires the presence a promoter upstream of *ospC1* (another T3SS effector gene), and that these genes were co-transcribed [68, 88], subsequent studies showed that *ospD3* does not require *ospC1* to be expressed [299]. OspD3 has also been shown to target IL-8 secretion. Farhan *et al* reported that *S. flexneri* 2a strain 2457T lacking *ospD3* induced less IL-8 production in T84 and Hep-2 epithelial cell lines tested [297]. However, it was not known if this reduction in IL-8 secretion affected PMN infiltration which is characteristic of *Shigella* infections [297]. In contrast to this finding, another group reported that Δ*ospD3* mutants induced more IL-8 secretion and they verified their findings by testing three different human epithelial cells, HT-29 cells, HCT-8 cells and T84 cells [299]. They also hypothesised from their findings that OspD3 may be targeting a eukaryotic protein to reduce IL-8 secretion, as a mechanism to regulate PMN infiltration. However, further work is required in this area and despite being labelled as an enterotoxin, the specific function of OspD3 is yet to be elucidated.

Sequencing of the *Shigella* virulence plasmid has also revealed the presence of a ShET2 paralog which was named ShET2-2 (also known as OspD2 or SenB) [300]. For many years OspD2 was described as a protein with unknown function but recently it was reported that OspD2 regulated T3SS activity [301]. A mT3_*E. coli* laboratory strain which contains a functional *Shigella* T3SS was used in these experiments [302, 303]. This laboratory strain contains the 31 kb entry portion of the *Shigella* virulence plasmid and a plasmid encoding VirB which is IPTG-inducible [304]. This strain is able to produce a fully assembled and functional T3SS and also secretes 4 effectors (IpaA, IpgB1, IscB and IpgD), enabling the strain to efficiently invade host cells [302]. Each of the *Shigella* effectors was then introduced into this

strain individually and screened for bacterial-induced cytotoxicity and found OspD2 was found to prevent cell death. Hence it appeared that OspD2 had an overall role of inhibiting translocation of effectors after invasion to preserve the replicative niche of *Shigella*, which is in the cytoplasm.

Despite the work on OspD2 by this group, the primary role of OspD2 during *Shigella* infection was still not clear. There was also lack of work to identify host targets of OspD2. The potential cysteine protease activity of OspD2 was also investigated by this group [301]. However, it was found that over expression of both OspD2 and its catalytically inactive mutant $OspD2_{C79A}$ in epithelial cells, contributed to a similar reduction in bacterially-induced cell death. It was thus concluded by this group that OspD2 is not a cysteine protease and did not degrade any bacterial or mammalian proteins [301]. However, this was not verified experimentally.

The *Shigella* virulence plasmid encodes four transcriptional regulators, VirF, VirB, MxiE and Orf81 [305]. VirB is needed for the transcription of genes at the entry region and VirF regulates the transcription of VirB. MxiE is required for the secretion of several effectors whose expression is induced under conditions of secretion. Using macroarray analysis, Le Gall *et al*, reported that T3SS substrates can be categorised into three groups according to their regulation. These are firstly, those which are under the control of VirB, secondly, those which are under the control of MxiE and lastly those under the control of both VirB and MxiE. These differential expression patterns of the T3SS effectors suggested that the effectors are required at different times after *Shigella* interaction with the host cell. This study reported that OspD2 was expressed under the control of VirB whereas OspD3 was expressed in a MxiE-dependent manner. It was also reported that homologous effectors do not necessarily belong to the same expression class, such as in the case of OspD2 and OspD3. It was also noted that effectors under the control of VirB are expressed, regardless of an active T3SS apparatus and hence OspD2 may be expressed and stored in the cytoplasm until the protein is transported via the T3SS into the host cell. Since OspD3 is regulated by MxiE, OspD3 is expressed in the second wave of effectors that are required at a later stage during infection [305]. However, *Faherty* et al, reported that OspD3 and OspC1 are not co transcribed and since MxiE binds to the promoter of OspC1 to induce expression of OspC1, this contradicts with the earlier study that OspD3 is regulated by MxiE. As such, more investigation is required in this area [299].

1.9 Aims

Significant research has been conducted in recent years to understand the mechanisms of action and functions of *Shigella* T3SS effectors. Despite some effectors having now well-defined roles during infections, there is still a lack of understanding of the roles and host targets of many other effectors. When this study began, the role of the EPEC T3SS effector EspL was recently determined by our laboratory. Despite being homologues of EspL, the roles of OspD2 and OspD3 had yet to be fully elucidated. In particular, identification of the enzymatic activities and host targets of OspD2 and OspD3 as T3SS effectors will aid in determining their function during *Shigella* infection which may provide valuable insights into the molecular basis of *Shigella* infection. Thus, the broad aim of this study was to characterise and investigate the functions of the *Shigella* effectors OspD2 and OspD3.

The specific aims of this study were:

1) To investigate whether OspD2 and OspD3 are cysteine proteases that cleave RHIM proteins, similar to EspL
2) To screen for additional host targets of OspD2 and OspD3 via SILAC based mass spectrometry screens, and further characterise these targets

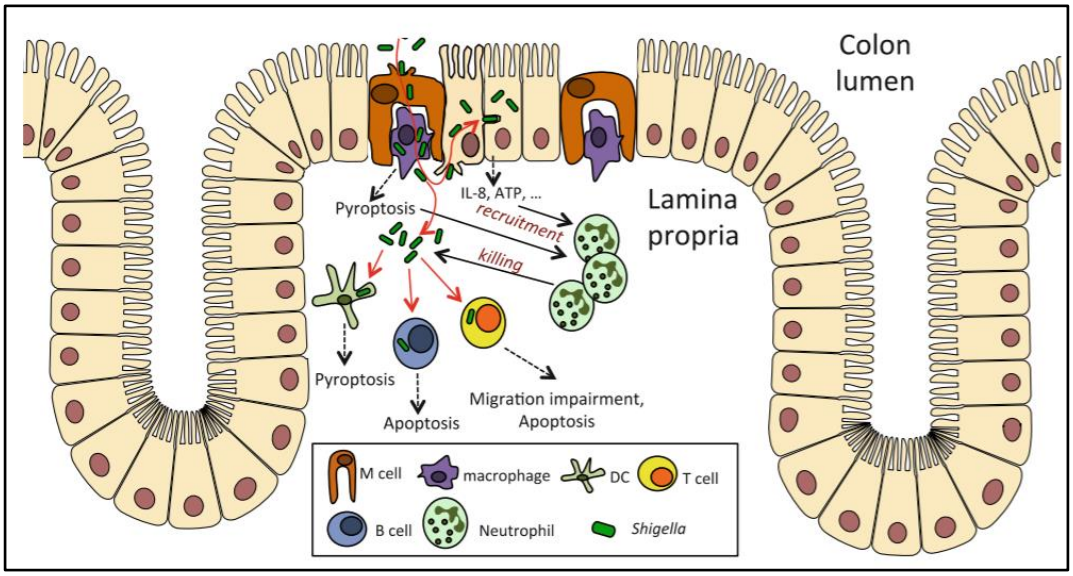

Figure 1. 1: Schematic view of *Shigella* cellular pathogenesis.

Shigella invades the intestinal epithelium through M cells and is phagocytised by underlying macrophages. *Shigella* induce macrophage cell death and are released into the extracellular space where they enter surrounding cells via directed actin polymerisation. Dying macrophages then release cytokines which recruit PMNs to the site of infection. PMNs cause destruction to the intestinal epithelium which facilitates more bacterial entry into the epithelium without the need of M cells. Eventually PMNs present will entrap and kill the bacteria, reducing the infection. Sourced from [51].

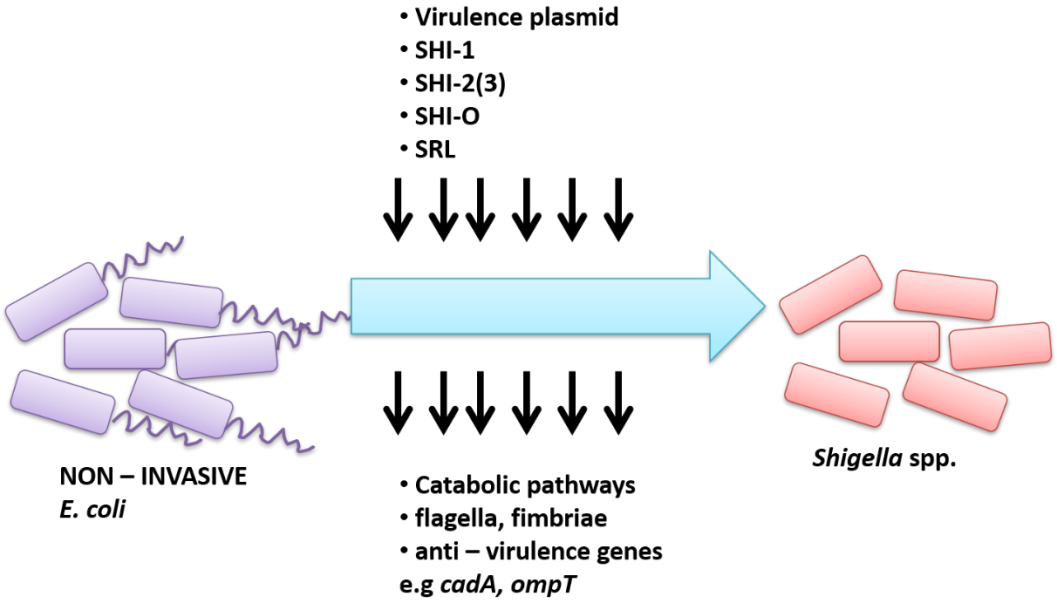

Figure 1. 2: Evolution of *Shigella* from their ancestor *E. coli*.

Shigella has gained a virulence plasmid and several PAIs as well as losing several anti-virulence genes and its flagella to gain virulence. Adapted from [50].

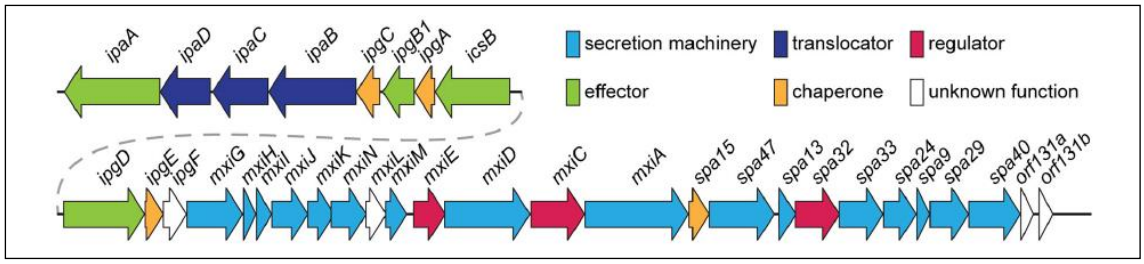

Figure 1. 3: Summary of the gene organization of the entry region of the *Shigella* virulence plasmid.

The genes are grouped in two operons, *ipa/ipg* and the *mxi/spa*. The genes are color coded according to their protein function. The secretion machinery incorporates genes required for the assembly of the T3SS. The translocators include components which make up the translocon, necessary for effector translocation. The regulators modulate the expression and function of T3SS. The chaperones help in stabilizing the effectors before secretion. Sourced from [306].

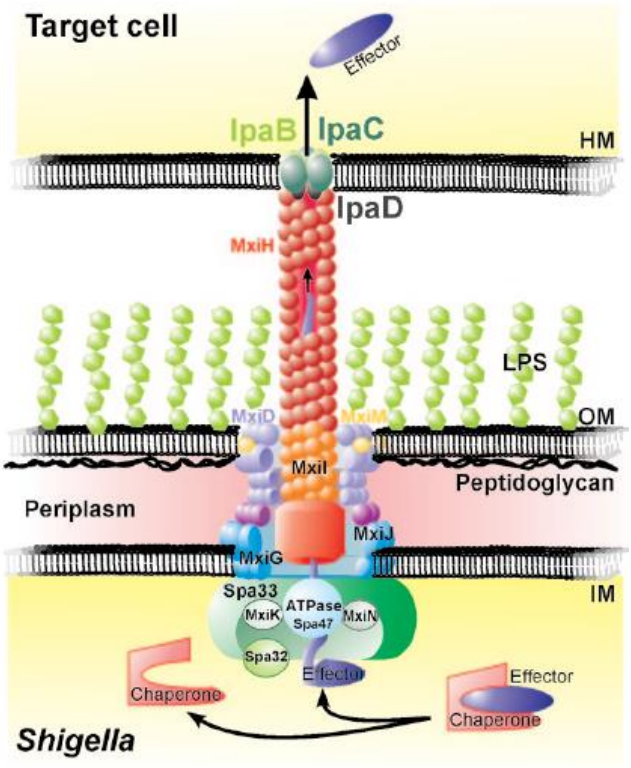

Figure 1. 4: Structure of the T3SS apparatus.

The T3SS spans 3 membranes (outer and inner bacterial membrane and host plasma membrane). A syringe-like hollow structure arises from the outer bacterial membrane and connects to the host cell membrane through which translocators transport effectors directly into the host cell. Sourced from [67].

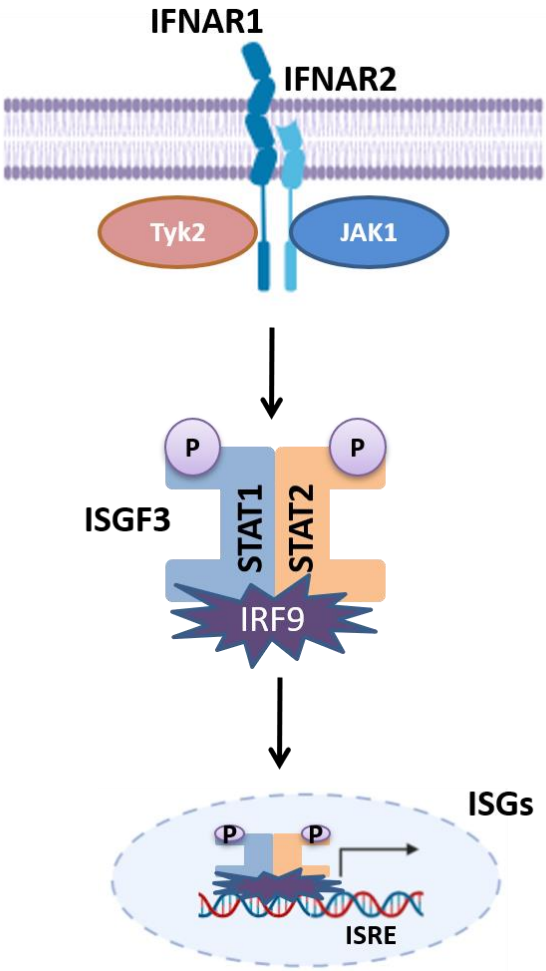

Figure 1. 5: Schematic view of type I IFN signalling.

Type I IFN signalling is initiated when IFNα/β bind to the cell surface receptors IFNAR1 and IFNAR2. Binding to the IFNAR receptors will then recruit JAK1 and Tyk2 proteins to induce signalling via the ISGF3 complex consisting of STAT1, STAT2 and IRF9. This complex will then translocate to the nucleus to bind to the ISRE elements present on the promotors of ISGs, in order to mediate transcription of ISGs.

Table 1. 1: TLR and their respective ligands

TLR	Localization	Pathogens and ligands
TLR1	Plasma membrane	Bacteria - Triacyl lipoprotein
TLR2	Plasma membrane	Bacteria and Viruses – Lipoprotein/ peptidoglycans/ Envelope proteins
TLR3	Endolysosome	Viruses – dsRNA, poly I:C
TLR4	Plasma membrane	Bacteria and Viruses – LPS, Envelope proteins
TLR5	Plasma membrane	Bacteria – Flagellin
TLR6	Plasma membrane	Bacteria and Viruses – Diacyl lipoprotein
TLR7	Endolysosome	Viruses- ssRNA, Imidazoquinoline
TLR8	Endolysosome	Bacteria and Viruses- ssRNA, Imidazoquinoline
TLR9	Endolysosome	Bacteria and Viruses – CpG DNA
TLR11	Plasma membrane	Uropathogenic bacteria

Chapter Two:

Materials and methods

CHAPTER 2: Materials and methods

2.1 Bacterial strains, media and growth conditions

The bacterial strains and media used in this study are listed in Tables 2.1 and 2.2 respectively. *E. coli* were grown in Luria-Bertani (LB) broth or Luria Agar (LA) at 37 °C in the presence of the antibiotics when required. The antibiotics used were ampicillin (100μg/ml) (Astral Scientific), kanamycin (100 μg/ ml) (Amresco) and chloramphenicol (25 μg/ ml) (Boehringer). The *Shigella* strains were plated onto Tryptic soy agar plates (TSA) with 2 % Congo Red (Sigma-Aldrich). *Shigella* strains were inoculated in LB broth and grown overnight at 37 °C prior to infection. The necessary antibiotics were added when necessary.

2.2 DNA isolation, purification and manipulation

2.2.1. Purification of Plasmid DNA

Plasmid DNA expressing *E. coli* were grown in LB at 37 °C incubator in the presence of antibiotics when required with aeration for 16 hours. Grown bacteria were pelleted at 4000 rpm for 10 mins. Plasmid DNA was extracted using the QIAprep® Spin Miniprep kit (QIAGEN, California, USA) according to the manufacturer's instructions.

2.2.2. Purification of Genomic DNA

Bacteria was grown in LB at 37 °C in the presence of the necessary antibiotics with aeration for 16 hours. Bacteria was pelleted at 4000 rpm for 10 mins. Genomic DNA was isolated using the Quick-gDNA^{TM} MiniPrep Kit (ZymoResearch) according to the manufacturer's instructions.

2.2.3. Purification of PCR products

DNA was purified from either an agarose gel or in solution using the Wizard® SV gel and PCR Clean-Up System (Promega). For purification of DNA from agarose gels, the PCR products were excised from the gels using a sterile scalpel blade and purified according to the manufacturer's protocol.

2.2.4. Restriction enzyme digestion

All restriction digests were carried out using buffers and enzymes supplied from NEB and Roche, according to the manufacturer's protocol.

2.2.5. DNA Ligation

DNA ligation was carried out using T4 DNA ligase (Promega). DNA fragments were ligated into the desired plasmids (Table 2.3) at an insert to vector ratio of 3:1. Ligation was carried out at 4 °C overnight.

2.2.6. DNA sequencing and analysis

The ABI PRISM Big Dye Terminator v3.1 Cycle Sequencing kit was used for sequencing. Capillary electrophoresis was performed by Micromon DNA Sequencing Facility (Monash University, Victoria, Australia) DNA sequences obtained were analysed using Sequencher® version 5.0 sequence analysis software (Gene Codes Corporation).

2.2.7. Oligonucleotides

Synthetic oligonucleotides (Sigma Aldrich) used in PCR and sequencing and bacterial mutant construction are listed in Table 2.4.

2.3 Site directed mutagenesis

Site-directed mutagenesis was carried out using the Stratagene QuikChange II Site-Directed Mutagenesis kit (Agilent Technologies) according to the manufacturer's instructions. p3xFLAG-OspD3 and pF3xFLAG-OspD2 were used as templates and the conserved cysteine was substituted with serine. After amplification the DNA plasmid was digested with *DpnI* at 37 °C overnight. The sample was transformed into XL1-Blue chemically competent cells and selected onto the appropriate antibiotic LB plates.

2.4 Agarose Gel Electrophoresis

DNA fragments were run and analysed on 1-2 % (w/v) agarose gels made up in TAE buffer 40 mM Tris, 0.114 % (v/v) glacial acetic acid, 1 mM EDTA (pH 8.3). 1 x SYBR®Safe DNA Gel Stain (Invitrogen, California, USA) were added to the gel before gel casting. 6 x gel loading dye (NEB) was mixed with DNA prior to gel loading. Either 100bp or 1kb DNA ladders (NEB) were used to determine the size of the DNA loaded. The gels were visualized by a UV transilluminator, Amersham Imager (GE Healthcare).

2.5 Polymerase Chain Reaction

2.5.1. PCR amplifications

Amplification of DNA was carried out using either AmpliTaq Gold® DNA (Life Technologies) polymerase or Phusion® High-Fidelity DNA polymerase (NEB). Briefly, PCR

reactions were performed in a 50 µL volume containing a final concentration of 200 ng DNA template, 0.7 µM of each dNTP, 0.2 µM or each primer and 1 unit of DNA polymerase. The GS482 G-STORM thermal cycler (G-STORM) was used to carry out PCR amplifications. PCR cycling conditions generally used were an initial heat start at 95 °C for 5 min, followed by 35 cycles of denaturation at 95 °C for 30 sec, annealing at 55-65 °C for 30 sec (this depends on the melting temperature of the primer used) and extension at 72 °C for 1 min per 1kb of expected PCR product and lastly a final extension for 5 min at 72 °C. Oligonucleotides/ primers (Sigma Aldrich) used are listed in Table 2.4.

2.5.2. Colony PCR

Colonies to be screened were picked using sterile toothpicks or tips. Colony PCR was carried out in a 20 µL reaction with a final concentration of 1x GoTaq® Green Master Mix and 0.1 µM of each primer. PCR cycling conditions used were a denaturation step at 95 °C for 2 mins, 30 cycles of 95 °C for 30 sec, 50-65 °C for 30 sec (temperature depends on melting temperature of primer) and 72 °C for 1 min per kb of expected PCR product size.

2.6 Construction of expression vectors

2.6.1. Construction of pFTRE3G vectors expressing the putative wild type and catalytic mutant OspD2 and OspD3

OspD2 and OspD3 were amplified from p3xFLAG-OspD2 and p3xFLAG-OspD3 using the primer pairs, pLenti3xFlag F with either pFTRE3G OspD2 R or pFTRE3G OspD3 R. The PCR amplification consist of a hot start at 95 °C for 5 mins followed by 35 cycles of 95 °C for 30 sec, 55 °C for 30 sec and 72 °C for 2 min and a final extension at 72 °C for 5 mins. $OspD2_{C79S}$ and $OspD3_{C64S}$ catalytically inactive mutants were created using the Stratagene QuikChange II Site-Directed Mutagenesis kit (Agilent Technologies) according to the manufacturer's instructions, using the primer pairs $OspD2_{C79S}$F/$OspD2_{C79S}$R and $OspD3_{C64S}$F/$OspD3_{C64S}$R respectively. The resultant PCR products were ligated with pFTRE3G at an insert:vector molar ratio of 3:1. The ligation products were transformed using XL-1 Blue cells colony PCR and sequencing reaction was carried out on the positive colonies.

2.6.2. Construction of pCDNA3 vectors expressing HA-IRF1 – HA-IRF9

Human HA-IRF2, HA-IRF8 and HA-IRF9 were purchased from Sino Biology and Addgene respectively. The remaining human IRFs were Flag-tagged and were kind gifts from Paul Hertzog (IRF6) and Prof Shunbin Ning (IRF1,3,4,5,7) laboratories. They were cloned into HA-pCDNA3 vectors using the following primers. For IRF1, primer pairs HA-IRF1 F/ HA-IRF1

R were used HA-IRF1 F/ HA-IRF1 R. For IRF3, primer pairs HA-IRF3 F/ HA-IRF3 R were used. For IRF4, primer pairs HA-IRF4 F/ HA-IRF4 R were used. For IRF5, primer pairs HA-IRF5 F/ HA-IRF5 R were used. For IRF6, primer pairs HA-IRF6 F/ HA-IRF6 R were used and for IRF7, primer pairs HA-IRF7 F/ HA-IRF7 R were used. The PCR amplification consists of a hot start at 95 °C for 5 mins followed by 35 cycles of 95 °C for 30 sec, 55 °C for 30 sec and 72 °C for 2 min and a final extension at 72°C for 5 mins. The resultant PCR products were digested with BamH1 and EcoR1 for HA-IRF1,4 and 5, HindIII and EcoR1 for HA-IRF3 and Kpn1 and Not1 for HA-IRF6-7 and ligated into pCDNA3 at an insert:vector molar ratio of 3:1. The ligation products were transformed into XL-1 Blue chemically-competent cells. Colony PCR was performed using primer pairs T7 F and pCDNA3 R and sequencing reaction were carried out using to confirm positive colonies.

2.6.3. Construction of pCDNA3 vectors expressing IRF9$_{9\text{-}213aa}$-HA and IRF9$_{117\text{-}393aa}$-HA

IRF9$_{9\text{-}213aa}$-HA and IRF9$_{117\text{-}393aa}$-HA were cloned into HA-pCDNA3 vectors using the following primers pairs, HA IRF9$_{DNAdomain}$ F/ HA IRF9$_{linkerdomain}$ R and HA IRF9$_{linkerdomain}$F/ IRF9 IRF9$_{IAD1domain}$ R respectively. The PCR amplification consists of a hot start at 95 °C for 5 mins followed by 35 cycles of 95 °C for 30 sec, 55 °C for 30 sec and 72 °C for 2 min and a final extension at 72 °C for 5 mins. The resultant PCR products were digested with BamH1 and EcoR1. The ligation products were transformed into XL-1 Blue chemically-competent cells. Colony PCR was performed using primer pairs T7 F and pCDNA3 R and sequencing reaction were carried out using to confirm positive colonies.

2.7 Transformation

2.7.1. Preparation of chemically competent cells

Two different strains of chemically competent E. coli were used, the XL1-Blue and DH5α. Bacteria were grown overnight with agitation at 37 °C. The overnight culture was sub-inoculated into super optimal broth (SOB) at a ratio of 1:100 and growth at 16 °C until an OD600 of 0.4-0.8 was achieved. Bacteria were pelleted at 4 °C for 15 min at 2500 rpm and washed in chilled transformation buffer supplemented with 10 mM PIPES, 15 mM $CaCl_2.2H_2O$ and 250 mM KCl. 50 µL aliquots of chemically competent cells were generated by snap freezing in a dry ice and ethanol bath and subsequently stored at -80 °C.

2.7.2. Chemical transformation

Chemically competent E. coli cells were thawed on ice before the addition of 100 ng of plasmid DNA or DNA ligation products and incubation on ice for 30 min. The cells were heat shocked at 42 °C for 90 secs, followed by incubation on ice for an additional 2 mins. The transformed cells were recovered in 1 mL of super optimal broth with catabolite repression (SOC) with agitation at 37 °C for 90 mins. Cells were then plated onto LB plates with the necessary antibiotics.

2.7.3. Preparation of electrically competent *Shigella*

A colony of *Shigella* from congo red supplemented TSA plates was inoculated into LB and grown overnight at 37 °C with agitation. The overnight culture was sub-cultured into LB at a ratio of 1:50 and grown at 37 °C until the OD600 reached 0.6-0.8. Bacteria were placed on ice for 10 mins and harvested at 4000 rpm for 10 mins, before washing twice with ice-cold distilled water and centrifugation at 4 °C for 10 min at 4000 rpm. Cells were washed and resuspended finally with ice-cold 10 % glycerol (v/v) diluted in sterile water and 20 µL aliquots were generated by snap freezing in a dry ice and ethanol bath and subsequently stored at -80 °C.

2.7.4. Electroporation transformation

Electrocompetent *Shigella* was thawed on ice and 100 ng of plasmid DNA was added to the cells. 0.1 cm gap electroporation cuvette (Cell Projects) were chilled on ice before addition of electrocompetent *Shigella* mixed with the plasmid DNA. The Micropuler electroporator (Bio-Rad) was used to electroporate the plasmid DNA into *Shigella* with an electric pulse of 2.3 kV at 200 Ω and 25 µF. 1 mL of SOC were added to the cells, before recover for 90 min at 37 °C with agitation. The cells were then plated onto TSA plates with congo red and the necessary antibiotics.

2.8 Western blot

Cells were lysed in ice-cold lysis buffer (50 mM Tris-HCl pH 7.4, 150 mM NaCl, 1 mM EDTA, 1% Triton X-100, 10 mM NaF, 1 mM PMSF, 2 mM Na_3VO_4 with 1 x EDTA-free Complete Protease Inhibitor Cocktail (Roche)). Cell lysates were spun down 13,000 rpm for 10 mins in a 4 °C microcentrifuge. Supernatant was added to 1 x Bolt® lithium dodecyl sulfate (LDS) sample buffer (Life Technologies) and dithiothreitol (DTT) (Astral Scientific) to a final concentration of 50 mM. The samples were then boiled at 70 °C for 10 mins before loading onto 4-12 % Bis-Tris gels (Life Technologies). MES or MOPS (Thermo Fisher scientific) buffer was used depending on the expected sizes of the proteins. SeeBlue® pre-stained protein

standard (Life Technologies) was used as a ladder and proteins were separated using XCell SureLock™ Mini-Cell system (Life Technologies). Proteins were transferred onto nitrocellulose membranes via the iBlot2 Dry Blotting System (Life Technologies) for 5 mins at 23 V. Membranes were blocked in 5% skimmed milk in TBS containing 0.1 % Tween 20 for 1 hour, washed, and probed with the necessary primary antibody made up in TBS containing 5 % bovine serum albumin (BSA; Sigma-Aldrich) and 0.1 % Tween 20 overnight with agitation at 4 °C. Horseradish peroxidase (HRP)-conjugated anti-rabbit or anti-mouse (PerkinElmer) diluted at 1:3000 in TBS supplemented with 5 % BSA and 0.1 % Tween 20 were used as secondary antibodies. Antibodies used for immunoblotting are listed in Table 2.5. The immunoblots were washed and developed using Amersham ECL™ Western Blotting Detection Reagents (GE Healthcare) and detection was carried out using the Amersham Imager (GE Healthcare).

2.9 Alignment of protein sequences

Proteins sequences were aligned using Clustal Omega (https://www.ebi.ac.uk/Tools/msa/clustalo/). The results were represented using Easy Sequencing in PostScript (ESPript) version 3.0 (http://espript.ibcp.fr/ESPript/ESPript/).

2.10 Mammalian tissue culture

Cell lines used, HeLa 229s, HT-29 and HEK 293T were growth in Dulbecco's Modified Eagle Media (DMEM) or Roswell Park Memorial Institute (RPMI) with GlutaMax™ culture media (Gibco, Life Technologies) supplemented with 10 % (v/v) heat-inactivated Fetal Bovine Serum (FBS) (Thermo Fisher Scientific). Cells were maintained in a 37 °C, 5 % CO_2 incubator.

2.11 Transfection

HEK 293T cells were transfected using FuGENE®6 transfection reagent (Promega) according to manufacturer's instructions. HEK 293T cells were seeded at $1X10^5$ cells/ mL and incubated at 37 °C, 5 % CO2 for 24 hours. FuGENE®6 transfection reagent was mixed with Opti-MEM®I (1X) + GlutaMAX™-I (Life Technologies) for 5 mins before the addition of the required DNA plasmid. The ratio of Fugene to DNA used was 3:1. This mixture was incubated for 20 min and added to the HEK 293T monolayers and incubated for 16 hours.

2.12 Luciferase reporter assay

HEK 293T at seeded at 2 X 10^4 cells/ mL onto 24 well trays. After 16 hours, the cells were co-transfected with 0.2 μg of pNF-κB-Luc (Clontech) or 0.2 μg pISRE (Clontech) and 0.05 μg of pRL-TK (Promega) and derivatives of p3xFlag-*Myc*-CMV-24 (0.4 μg). 24 hours after transfection, the cells were stimulated with either 20 ng/ mL TNF (eBioscience) and incubated for another 16 hours or stimulated with 25 ng/ mL IFNα (Sigma-Aldrich) for 3 hours in 5 % CO_2 at 37 °C. The assay was performed using a dual-luciferase reporter assay (Promega Part# TM040) on the HEK 293T cell lysates according to the manufacturer's protocol. Luminance was measured on a ClarioSTAR microplate reader (BMG Labtech).

2.13 Construction of Doxycycline inducible stable cell lines

Doxycycline inducible stable cell lines were created in HT-29 cells. To produce lentivirus, HEK 293T cells were seeded at 2X10^5 cells/ mL in 10 cm culture dishes allowed to grow overnight. The cells were co transfected with 10 μg of pFTRE3G-Flag-EspL, pFTRE3G-Flag-$EspL_{C47S}$, pFTRE3G-Flag-OspD2, pFTRE3G-Flag-$OspD2_{C79S}$, pFTRE3G-Flag-OspD3 or pFTRE3G-Flag-$OspD3_{C64S}$ with 2 μg of pCMV8.2 and 0.8 μg of pVSV-G, using FuGENE®6 Transfection Reagent (Roche) according to manufacturer's protocol. 24 hours later, the culture media was replaced with fresh media, and left for an additional 48 hours for virus production. 5 μg/ mL polybrene (Sigma Aldrich) was added to the virus-containing supernatant which was harvested and passed through a 0.45 μM filter. Virus was added to HT-29 cell monolayers and incubated at 37 °C, 5 % CO2 for 24 hours. Infected cells were selected by treating with 5 μg/ mL polybrene for at least one week. Expression of FLAG tagged proteins were tested by adding 100 ng/ mL of doxycycline at varying time points and by immunoblotting with anti-Flag antibody.

2.14 Examining cysteine protease activity in HT-29 stable cell lines by immunoblot

Doxycycline inducible HT-29 stable cells were seeded at 1X10^5 cells / mL and incubated at 37 °C, 5 % CO2 for 24 hours. Cells were induced with 100 ng/ mL doxycycline for 0.5, 2, 6, 8, 16 and 24 hours. When looking for IRF3 and IRF9 expression, 25 ng/ mL IFNα was also added together with doxycycline for the indicated timepoint. After which, cells were lysed in ice-cold lysis buffer ((50 mM Tris-HCl pH 7.4, 150 mM NaCl, 1 mM EDTA, 1 % Triton x-100, 10 mM NaF, 1 mM PMSF, 2 mM Na_3VO_4 with 1 x EDTA-free Complete Protease Inhibitor Cocktail (Roche)). Cell lysates were spun down 13,000 rpm for 10 min in a 4 °C microcentrifuge. Samples were processed for western blot as indicated in section 2.8.

2.15 Preparation of HT-29 cell lysates for incubation with GST-tagged OspD3 and GST-tagged OspD3$_{C64S}$ recombinant proteins

HT-29 cells were seeded at 1 X 10^5 cells / mL and incubated at 37 °C, 5 % CO2 for 24 hours. After which, cells were lysed in ice-cold PBS containing 10 mM NaF, 1 mM PMSF, 2 mM Na_3VO_4 with 1 x EDTA-free Complete Protease Inhibitor Cocktail (Roche). Cell lysates were spun down 13,000 rpm for 10 min in a 4 °C microcentrifuge. Recombinant GST tagged OspD3 and OspD3$_{C64S}$ were incubated with the cell lysates at 37 °C for 2 hours before sample preparation for immunoblotting.

2.16 Cell viability (MTT) assay

Doxycycline inducible HT-29 cells expressing either WT or the catalytically inactive OspD2, OspD3, or EspL were seeded in 24 well tissue culture plates overnight to settle and adhere to well bottom. 100 ng/ mL doxycycline was added to induce the expression of the proteins. After 6 hours, the cells were treated with 20 ng/ mL. TNF (Calbiochem), 500 nM Birinapant and 25 μM z-VAD-FMK (Abcam) for another 18 hours. After washing with PBS, DMEM containing 0.1 μg/ mL 3-(4,5-Dimethylthiazol-2-yl)-2,5- diphenyltetrazolium bromide (MTT) (Sigma) was added for 1 hour, followed by the addition of 100 μL of dimethyl sulfoxide (DMSO) (Sigma) to the wells for 1 min with shaking. The absorbance at 540 nm was measured using the CLARIOstar microplate reader (BMG Labtech).

2.17 Construction of bacterial mutants

Shigella mutants were generated via lambda red recombination. Kanamycin or chloramphenicol cassettes from pkD3 and pkD4 respectively were used to replace the genes of interest. Single mutants were generated by replacement of the gene of interest with kanamycin cassette and double mutants were generated using kanamycin and chloramphenicol cassettes. The pKD3-4F and pKD3-4 R primers were used to amplify the cassettes. 500 kb flanking OspD2, OspD3 and MxiD were amplified using OspD2$_{down}$F/R, OspD2$_{up}$F/R, OspD3$_{down}$F/R, OspD3$_{up}$F/R and MxiD$_{down}$F/R, MxiD$_{up}$F/R primer pairs. Overlap PCR was carried out to ligate the flanks with the cassettes. The first step of overlapping PCR was carried out in 50 μL reaction. Briefly 1 x Phusion® High-Fidelity buffer, 1 unit of Phusion® High-Fidelity DNA polymerase (NEB), 0.2 mM dNTPs, 100 ng of Kanamycin or Chloramphenicol cassette, 100 ng of "up" and "down" flanks each and 1.5 μL DMSO were added per reaction. PCR cycling conditions used were a denaturation step at 98 °C for 30 sec, 10 cycles of 98 °C for 10 sec, 52 °C for 30 sec and 72 °C for 30 sec. The second step of overlapping PCR includes, a 50 μL

reaction of 1 x Phusion® High-Fidelity buffer, 1 unit of Phusion® High-Fidelity DNA polymerase (NEB), 0.2 mM dNTPs, 1 μM "up" flank and "down" flank primers and 1.5 μL DMSO. PCR cycling conditions used in the second step were a denaturation step at 98 °C for 10 sec, 35 cycles of 98 °C for 10 sec, 65 °C for 30 sec and 72 °C for 45 sec and lastly a final extension for 5 min at 72 °C. The PCR was run on 1% agarose gels and DNA purification of PCR products were carried out. Temperature sensitive pKD46 lambda red recombinase was electroporated into *Shigella* electrocompetent cells and transformants which grown at 30 °C were selected. pKD46 harbouring *Shigella* electrocompetent cells were generated and overlap PCR products were electroporated into these cells. The cells were then grown on selective antibiotic plates. The transformants were grown overnight on LB and gDNA was prepared. Deleted regions were amplified using primer pairs $OspD2_{down}$F/R, $OspD2_{up}$F/R, $OspD3_{down}$F/R, $OspD3_{up}$F/R and $MxiD_{down}$F/R, $MxiD_{up}$F/R and sent for sequencing using primers pairs $OspD2_{mutant}$seq F/ R, $OspD3_{mutant}$seq F/ R and $MxiD_{mutant}$seq F/ R. To create the double mutants, the Δ*ospD2* strains were used as template and OspD3 was replaced using chloramphenicol cassette

2.18 *Shigella* infections of HeLa 229 cells

Wildtype and mutant *Shigella* strains were streaked on TSA plates supplemented with 2% congo red and antibiotics and incubated at 37 °C incubator overnight. A single red colony of *Shigella* was picked using sterile disposable loops and inoculated into LB and grown at 37 °C overnight with agitation. The bacteria were sub-cultured 1:50 in LB and grown at 37 °C until OD600 reached 0.6-0.8. HeLa 229s were seeded onto 24 well plates at 1 X 10^5 cells/ mL and left to adhere at 37 °C, 5 % CO2 overnight. Before infection, HeLa 229s were washed to remove any residual FBS and were infected with *Shigella* at a MOI of 100. The infection was synchronized by centrifugation at 700g for 10 min and incubated at 37 °C, 5 % CO_2 for 1 hour. The infected cells were then washed with PBS, and 100 μg/ mL of gentamicin (Pharmacia) was added till the appropriate time-points.

2.19 Microscopy

HeLa 229 cells were seeded at 1 X 10^5 cells/ mL onto 24 well trays with coverslips and infected with GFP-tagged *Shigella flexneri* strains. At the required time points, the cells were fixed with 4 % (wt/vol) paraformaldehyde (Sigma) PFA for 12 mins. Alexa Fluor 647 Phalloidin (Life Technologies) diluted 1: 4000 in PBS and Hoechst staining solution (Sigma Aldrich) diluted

1: 4000 in PBS for 30 min. The cells were washed for 3 times with PBS and mounted onto microscope slides using Prolong Gold mounting medium (Life Technologies) and images were acquired using a Zeiss confocal laser scanning microscope.

2.20 Human IP-10 ELISA

Human IP-10 ELISA was performed on *Shigella* infected cells or doxycycline inducible HT-29 cells treated with 100 ng/ mL of doxycycline for 24 hours followed by addition of interferon stimulatory DNA (ISD) for another 24 hours. Human IP-10 ELISA was carried out using OptEIA™ (BD Biosciences) kit according to the manufacturer's protocol. Briefly, 96 well plate (Thermo Fisher Scientific) were coated with coating antibody diluted in sodium bicarbonate and sodium carbonate at 4 °C, overnight. The next day, the wells were washed using washing buffer containing 10% phosphate buffer saline (PBS) dissolved in MilliQ water and 0.05% Tween 20. Blocking was carried out for 1 hour at room temperature using blocking buffer containing 10% PBS and 10% FBS dissolved in MilliQ water. Human IP-10 standards serial dilutions were carried out in blocking buffer, ranging from 2000 pg/ mL to 62.5 pg/ mL. 60 µL of standards and samples were added to wells and incubated for 2 hours with agitation at room temperature. Detection buffer, containing 1:1200 detection antibody and 1:500 detection enzyme dissolved in blocking buffer were added to wells or 1 hour and incubated with shaking at room temperature. 3,3′,5,5′ Tetramethylbenzidine (TMB) (Sigma Aldrich) was used as substrate and added to the wells for 5 mins. Finally, stopping solution consisting of 0.5M Sulphuric acid (BDH) was added to the well. Absorbance was measured using the FLUOstar Optima (BMG Labtech).

2.21 PROTOMAP Mass spectrometry

2.21.1 Generation of PROTOMAP samples

1 X 10^5 cells/ mL of doxycycline inducible OspD2, $OspD2_{C79S}$, OspD3 and $OspD3_{C64S}$ were seeded in 10cm tissue culture plates. The cells were labelled with heavy SILAC amino acids Arg4/ Lys6 for the wildtype proteins and Arg0/ Lys0 for the catalytically inactive proteins and incubated for three cell passages. Following which, the cells were treated with 100 ng/ mL of doxycycline for 6 hours before lysis using the GdmCl lysis buffer (6M GdmCl, 100 mM Tris pH 8.5, 10 mM TCEP, 40mM CAA supplemented 1 x EDTA-free Complete Protease Inhibitor Cocktail. The samples were quantified by BCA assay and the wildtype and catalytically inactive proteins for each OspD2 and OspD3 were mixed at a ratio of 1:1 (200µg light and

heavy protein) and separated using SDS-PAGE. The resulting gels were fixed and visualized with Coomassie G-250 according to protocol of Kang *et al* [307]. 25 evenly spaced contiguous bands, ranging in size from 198 kDa to 6 kDa, were excised and de-stained in a 50:50 solution of 50 mM NH_4HCO_3 / 100 % ethanol for 20 mins at room temperature with shaking at 750 rpm. De-stained samples were then washed with 100 % ethanol, vacuum-dried for 20 mins and rehydrated in 10 mM DTT in 50 mM NH_4HCO_3. Reduction was carried out for 60 mins at 56 °C with shaking. The reducing buffer was then removed and the gel bands washed twice in 100% ethanol for 10 mins to remove residual DTT. Reduced ethanol washed samples were sequentially alkylated with 55 mM Iodoacetamide in 50 mM NH_4HCO_3 in the dark for 45 mins at RT. Alkylated samples were then washed with 2 rounds of 100% ethanol and vacuum-dried. Alkylated samples were then rehydrated with 12 ng/ µl trypsin (Promega, Madison WI) in 40 mM NH_4HCO_3 at 4°C for 1 hour. Excess trypsin was removed, gel pieces were covered in 40 mM NH_4HCO_3 and incubated overnight at 37 °C. Peptides were concentrated and desalted using C_{18} stage tips before analysis by LC-MS [308, 309].

2.21.2. LC-MS

C_{18} stage tips purified peptides were resuspend in Buffer A* (2 % Acetonitrile (ACN), 0.1 % Trifluoroacetic acid (TFA)) and loaded onto an in-house packaged 35 cm, 75 µm inner diameter, 360 µM outer diameter, 1.7 µM 130 Å CSH C_{18} (Waters, Manchester, UK) reverse phase analytical column with an integrated HF etched nESI tip. Samples were loaded directly onto the column using a ACQUITY UPLC M-Class System (Waters) at 400 nL /min for 35 minutes with Buffer A (0.1 % formic acid) and eluted at 300 nL/ min using a gradient altering the concentration of Buffer B (99.9 % ACN, 0.1 % FA) from 0 % to 32 % B over 100 min, then from 32 % to 40 % B in the next 10 min, then increased to 80% B over 8 min period, held at 100 % B for 2 min, and then dropped to 0 % B for another 20 min. RP separated peptides were infused into a Q-Exactive (Thermo Scientific, San Jose CA) mass spectrometer and data acquired using data dependent acquisition. One full precursor scan (resolution 70,000; 350-2,000 m/z, AGC target of 3×10^6) followed by 10 data-dependent HCD MS-MS events (resolution 17.5 k AGC target of 1×10^5 with a maximum injection time of 200 ms, NCE 28 with 20% stepping) were allowed with 35 s dynamic exclusion enabled. The resulting mass spectrometry proteomics datasets for this work have been deposited to the ProteomeXchange Consortium via the PRIDE partner repository with the dataset identifier [310].

2.21.3. Mass spectrometry data analysis

MaxQuant (v1.5.3.1) [311] was used for identification and quantification of the resulting experiments, with the resulting biological replicates searched together to ensure a global false discovery rate of less than 1% in accordance with the work of Schaab *et al* [312]. Database searching was carried out against the UniProt/Swiss-Prot human database (downloaded 24/10/2013, 84,843 entries) supplemented with the OspD3/2 fasta files (Q2TH43 and Q6XW09 respectively, downloaded 07/10/2016 from UniProt) with the following search parameters: carbamidomethylation of cysteine as a fixed modification; oxidation of methionine, acetylation of protein N-termini, trypsin/P cleavage with a maximum of two missed cleavages. A multiplicity of two was used, with each multiplicity denoting one of the SILAC amino acid combinations (light and heavy respectively). The precursor mass tolerance was set to 50 parts-per-million (ppm) and for the first search and 10 ppm for main search, with a maximum false discovery rate of 1.0 % set for protein identifications. To enhance the identification of peptides between fractions and replicates, the Match between Runs option was enabled with a precursor match window set to 2 min and an alignment window of 10 min. The resulting protein group output was processed within the Perseus (v1.4.0.6) [313] analysis environment to remove reverse matches and common proteins contaminates prior to analysis with Matlab R2016a (http://www.mathworks.com) for proteomap mapping according to the approach of Stoehr G *et al* [314]. Enrichment analysis was performed within Perseus, utilizing UniProt derived GO terms, GSEA, KEGG and Pfam assignments.

Table 2. 1: List of Media used in study

Media	**Components**
Luria-Bertani (LB) broth	1 % (w/v) tryptone, 0.5 % (w/v) yeast extract, 171 mM NaCl, pH 7.2
SOB medium	2 % (w/v) tryptone, 0.5 % (w/v) yeast extract, 10 mM NaCl, 2.5 mM KCl, 10 mM MgCl2 and 10 mM MgSO4
SOC medium	SOB supplemented with 20 mM glucose
RPMI with GlutaMax™	RPMI supplemented with 10 % FBS
DMEM with GlutaMax™	DMEM supplemented with 10 % FBS

Table 2. 2: List of bacterial strains used in study

Strains	Characteristics	Source/reference
DH5α	*E. coli K-12 endA1 hsdR17* (rk- mk+) *supE44 thi-1 recA1gyrA* (NalR) *relA* Δ(*lacIZYA-argF*)U169 deo*R* (Φ80*d*lacΔ[*lacZ*]M15)	[315]
XL-1 Blue	*E. coli recA1 endA1 gyrA96 thi-1 hsdR17 supE44 relA1 lac[F'proAB lacIqZΔM15 Tn10* (Tetr)]	Stratagene
Shigella flexneri 2457T	Wild type *Shigella* flexneri 2a strain	[316]
Δ*mxiD, Shigella flexneri* 2457T	2457T Δ*MxiD*::Kan (Kan^R)	This study
Δ*ospD2, Shigella flexneri* 2457T	2457T Δ*OspD2*::Kan (Kan^R)	This study
Δ*ospD3, Shigella flexneri* 2457T	2457T Δ*OspD3*::Kan (Kan^R)	This study
Δ*ospD2*Δ*ospD3, Shigella flexneri* 2457T	2457T Δ*OspD2*Δ*OspD3*::Cm/Kan (Cm^RKan^R)	This study

Table 2. 3: List of plasmids used in study

Plasmids	Characteristics	Resistance	Source/Reference
pGEM®-T-Easy	High copy number cloning vector	Amp^R	Promega
p3xFLAG-Myc-CMV-24	N-terminal Met-3XFlag and Cterminal *c-myc* expression vector	Amp^R	Sigma Aldrich
pEGFP-C2	N-terminal Green fluorescent protein (GFP) expression vector	Amp^R	Clontech
pRL-TK	Renilla luciferase expression vector	Amp^R	Promega
pNF-κB-Luc	NF-κB dependent luciferase expression vector	Amp^R	Clontech
pISRE-Luc	IFNα dependent luciferase expression vector	Amp^R	Promega
pFTRE-puro	Inducible lentiviral expression vector	Amp^R	WEHI
p3xFLAG - OspD2	Full length codon optimized OspD2 in p3xFLAG-Myc-CMV-24	Amp^R	Sabrina Mühlen
p3xFLAG - $OspD2_{C79S}$	Full length codon optimized $OspD2_{C79S}$ in p3xFLAG-Myc-CMV-24	Amp^R	This study
p3xFLAG - OspD3	Full length codon optimized OspD3 in p3xFLAG-Myc-CMV-24	Amp^R	Sabrina Mühlen
p3xFLAG - $OspD3_{C64S}$	Full length codon optimized $OspD3_{C64S}$ in p3xFLAG-Myc-CMV-24	Amp^R	This study
p3xFLAG - EspL	Full length codon optimized EspL in p3xFLAG-Myc-CMV-24	Amp^R	[296]
p3xFLAG - $EspL_{C47S}$	Full length codon optimized $EspL_{C42S}$ in p3xFLAG-Myc-CMV-24	Amp^R	This study
p3xFLAG-IRF1	Full length human IRF1 in pCDNA3 with N terminal 4X HA tag	Amp^R	Shunbin Ning
pHA-IRF2	Full length human IRF2 in pCMV3 with N terminal 1X HA tag	Kan^R	Sino Biological
p3xFLAG-IRF3	Full length human IRF3 in pCDNA3 with N terminal 4X HA tag	Amp^R	Kathleen McCaffrey
p3xFLAG-IRF4	Full length human IRF4 in pCDNA3 with N terminal 4X HA tag	Amp^R	Shunbin Ning

p3xFLAG-IRF5	Full length human IRF5 in pCDNA3 with N terminal 4X HA tag	Amp^R	Shunbin Ning
pHA-IRF6	Full length human IRF6 in pCDNA3 with N terminal 4X HA tag	Amp^R	Paul Hertzog
p3xFLAG-IRF7	Full length human IRF7 in pCDNA3 with N terminal 4X HA tag	Amp^R	Shunbin Ning
pHA-IRF8	Full length human IRF8 in pCMV3 with N terminal 1X HA tag	Kan^R	Sino Biological
pHA-IRF9	Full length human IRF9 in pCDNA3 with N terminal 1X HA tag	Amp^R	Addgene
pHA-$IRF9_{9-213aa}$	human $IRF9_{9-213}$ motif in pCDNA3 with N terminal 4X HA tag	Amp^R	This study
pHA-$IRF9_{117-393aa}$	human $IRF9_{117-393}$ motif in pCDNA3 with N terminal 4X HA tag	Amp^R	This study
pGFF-C2-RIPK1	human RIPK1 in p…. with N terminal GFP tag	Amp^R	John Silke
pGFP-C1-RIPK3	human RIPK3 in p…. with N terminal GFP tag	Amp^R	John Silke
pHA-TRIF	Full length TRIF with C terminal HA tag	Amp^R	Ash Mansell

Table 2. 4: List of oligonucleotides used in study

Name	Primer sequences 5' -3'
$OspD2_{(C79S)}$ F	GGGCGCCAAATCGTGTCTCGGCATCTGGCCAGC
$OspD2_{(C79S)}$ R	GCTGGCCAGATGCCGAGACACGATTTGGCGCCC
$OspD3_{(C64S)}$ F	GCAGACTGATCGTGTCCAGACACCTGGCCAG
$OspD3_{(C64S)}$ R	CTGGCCAGGTGTCTGGACACGATCAGTCTGC
p3xFLAG F	AATGTCGTAATAACCCCGCCCCGTTGACGC
p3xFLAG R	TATTAGGACAAGGCTGGTGGGCAC
pLenti 3xFlag F	CAGGATCCATGGACTACAAAGACCATGACGGTG
pFTRE3G OspD2 R	GGGGCTAGCCTAGAGGAAGTGGTTAAACC
pFTRE3G OspD3 R	CCCGCTAGCTCAGCTCTTGATGTTCTTC
OspD2 seq F	GCGCGTGCAGGAGTCG
OspD2 seq R	CCCGAACATGCGGATGG
OspD2 seq R	GGAGAAGTATGGGGCCGTC
OspD3 seq F	CGTGCCCGCCATCATC
OspD3 seq R	GTACTCGATGTTGATGG
OspD3 seq R	GGCAGTTCAGGTTC
pKD3-4 F	TGT GTA GGC TGG AGC TGC TTC
pKD3-4 R	CAT ATG AAT ATC CTC CTT AG
$OspD2_{up}$F	TAATGAACTACGAAGCGATCGAG
$OspD2_{up}$R	GAAGCAGCTCCAGCCTACACATAACGGCATAGAAG ACAACCATAG
$OspD2_{down}$F	CTAAGGAGGATATTCATATGTTTTTATGAGACTGTA ATTTAAA
$OspD2_{down}$R	TTGTTTTCTGTCTGAGGGTTCAT
$MxiD_{up}$F	TCTTGCTTTTTGGGACTATTTCA
$MxiD_{up}$R	GAAGCAGCTCCAGCCTACACATTTTTTCATTTATTTT TTTCAC
$MxiD_{down}$F	CTAAGGAGGATATTCATATGAATTACTAACTATAAA GTAGGTG
$MxiD_{down}$R	AGCTGTGGTTCAAGTTTCATTTT
$OspD3_{up}$F	TTAGCGCTCATAATTCAAGCTGT
$OspD3_{up}$R	GAAGCAGCTCCAGCCTACACATGATGGCATATGTAT ATATTCCT
$OspD3_{down}$F	CTAAGGAGGATATTCATATGAAAAGCTGAATATTAT CTCGTG
$OspD3_{down}$R	GGTGATAAAGTCTGCAAATACGG
$OspD2_{mutant}$seq F	AGGATTCCAGATTGTGAACCATAG
$OspD2_{mutant}$seq R	CTGGCTCCTGAGCGCCATAAACA
$OspD3_{mutant}$seq F	TGCTATGGAAAAAATCTTGCCCCTG
$OspD3_{mutant}$seq R	GCGTGTCCGGCAGGGTGAAGACCA
$MxiD_{mutant}$seq F	TTAATTCGAGGGATATAATTGTATTG
$MxiD_{mutant}$seq R	TCACTTGGATATTGAAAAATATATAA
T7 F	AATACGACTCACTATAGG
pCDNA3 R	ATGCGATGCAATTTCCTC
IRF9 seq F	GAGAGGGGCCGCATGGATG
IRF9 seq R	GGATGGGGCAAAGGCGCTGCAC
IRF6 seq R	ATTTAGCTGGGTCAGGGTCATC

IRF6 seq R	CTGGCCATTCTTCCCCAAAGC
IRF6 seq F	CAGTCGCAGCACCATGTTCCC
IRF6 seq F	CATCTTGGTTCAGGTCATTCCAG
IRF1 seq F	GCCTGTTTGTTCCGGAGC
IRF1 seq F	CGTGGATGGGAAGGGGTACC
IRF1 seq R	CCACGTCTTGGGATCTGGCTC
IRF1 seq R	CAGATCACTGGTGCTGTCCGGC
IRF7 seq F	CGCGCGCAAGGACCTGAGCG
IRF7 seq F	CCCGGACCAGAAGCAGCTGCGC
IRF7 seq R	GTGGTGGGACAGCTGCGGGGGCC
IRF7 seq R	GGTGCACTCGGCACAGCCAGG
HA $IRF9_{DNAdomain}$ F	GGATCC GAC ATG GCC TAC CCA TAC GAT GTT CCA GAT TAC GCT TAC CCA TAC GAT GTT CCA GAT TAC GCT ACCCGAAAACTCCGGAAC
HA $IRF9_{linkerdomain}$ F	GGATCC GAC ATG GCC TAC CCA TAC GAT GTT CCA GAT TAC GCT TAC CCA TAC GAT GTT CCA GAT TAC GCT CCAGGAATCGTCTCTGGCC
IRF9 $IRF9_{IAD1domain}$ R	GAATTC CTACACCAGGGACAGAATGGC
HA $IRF9_{linkerdomain}$ R	GCC GAATTC TCAAGGAAGCAGAAACTCCAGG
HA IRF1 F	GCC GGATCC ATG GCC TAC CCA TAC GAT GTT CCA GAT TAC GCT TAC CCA TAC GAT GTT CCA GAT TAC GCT ATGCCCATCACTCGGATGC
HA IRF1 R	GCC GAATTC CTACGGTGCACAGGGAAT
HA IRF2 F	GCC GGATCC ATG GCC TAC CCA TAC GAT GTT CCA GAT TAC GCT TAC CCA TAC GAT GTT CCA GAT TAC GCT ATGCCGGTGGAAAGGATGC
HA IRF2 R	GCC GCGGCCGC TTAACAGCTCTTGACGCGG
HA IRF3 F	GCC AAGCTT ATG GCC TAC CCA TAC GAT GTT CCA GAT TAC GCT TAC CCA TAC GAT GTT CCA GAT TAC GCT ATGGGAACCCCAAAGCCAC
HA IRF3 R	GCC GAATTC TCAGCTCTCCCCAGGGCC
HA IRF4 F	GCC GGATCC ATG GCC TAC CCA TAC GAT GTT CCA GAT TAC GCT TAC CCA TAC GAT GTT CCA GAT TAC GCT ATGAACCTGGAGGGCGG
HA IRF4 R	GCC GAATTC TCATTCTTGAATAGAGGAATGGC
HA IRF5 F	GCC GGATCC ATG GCC TAC CCA TAC GAT GTT CCA GAT TAC GCT TAC CCA TAC GAT GTT CCA GAT TAC GCT ATGAACCAGTCCATCCCAG
HA IRF5 R	GCC GAATTC TTATTGCATGCCAGCTGGG
HA IRF6 F	GCC AAGCTT ATG GCC TAC CCA TAC GAT GTT CCA GAT TAC GCT TAC CCA TAC GAT GTT CCA GAT TAC GCT ATGGCCCTCCACCCCC
HA IRF6 R	GCC GCGGCCGC TTACTGGGGAGGCAGGGC
HA IRF7 F	GCC GGATCC ATG GCC TAC CCA TAC GAT GTT CCA GAT TAC GCT TAC CCA TAC GAT GTT CCA GAT TAC GCT ATGGCCTTGGCTCCTGAGAG
HA IRF7 R	GCC GCGGCCGC CTAGGCGGGCTGCTCCA

Table 2. 5: List of Antibodies used for immunoblotting

Antibodies	Dilutions	Source
β-Actin, monoclonal	1: 5000	Sigma Aldrich
Flag M2, monoclonal	1: 1000	Sigma Aldrich
GFP, monoclonal	1: 2000	Roche Applied Science
HA-Tag (C29F4), monoclonal	1: 1000	Cell Signalling
IRF3, monoclonal	1: 1000	Cell Signalling
IRF9, monoclonal	1: 1000	Biolegend
IRF9, monoclonal	1: 1000	Santa Cruz Biotechnology
Mouse IgG, HRP conjugate	1: 3000	Perkin Elmer
Rabbit IgG (H+L), HRP conjugate	1: 3000	Perkin Elmer
RIP, monoclonal	1: 1000	BD Transduction Lab
RIP3 (human) monoclonal	1: 1000	Cell Signalling

Chapter Three:

Investigation of the RHIM protein cleavage by OspD2 and OspD3

CHAPTER 3: Investigation of RHIM protein cleavage by OspD2 and OspD3

3.1 Introduction

Shigella is an intracellular pathogen which uses a type III secretion system (T3SS) to transport bacterial proteins termed effectors into host cells during infection. These effectors have been extensively studied and it is now known that several of them have roles in suppressing the host innate immune response [40, 306]. Homologues of several *Shigella* T3SS effectors are also found in other T3SS bacterial pathogens including EPEC and EHEC. For example, the *Shigella* T3SS effectors OspD2 and OspD3 are homologous to the EPEC T3SS effector EspL, which was recently identified as a novel cysteine protease [296].

Proteases are proteolytic enzymes also known as peptidases or proteinases [317]. They act as molecular knives to cleave amino acid sequences into smaller fragments and are necessary for both non-specific hydrolysis of proteins and for cleavage of specific protein substrates in a process which is highly selective, efficient and limited. The latter usually results in irreversible changes and impact a range of biological processes such as tissue morphogenesis and remodelling, angiogenesis, fertilisation, inflammation and immunity, necrosis, apoptosis, autophagy and cell proliferation and differentiation. Proteases are considered important drug targets because of their roles in pathological conditions, such as neurodegenerative disorders, cancer and inflammatory diseases [318]. Initially, proteases were classified based on the position at which they hydrolysed the target peptide bonds of their substrate proteins. They were known as aminopeptidases, which cleave at the N-terminus of their substrates, carboxypeptidases which cleave at the C-terminus of their substrates or endopeptidases which cleave in the middle of the molecule. After extensive research in the field, proteases were re-classified into the aspartic, metallo, glutamic, cysteine, threonine and serine protease families based on their different catalytic approaches [319, 320]. The cysteine proteases contain catalytic Cys residues in the active site, which serve as nucelophiles that attack the peptide bonds of the substrate. Cysteine proteases possess also additional catalytic residues, a His and Asn which form a catalytic triad with Cys within the active site. The histidine residue in this triad serves as a proton donor to increase the nucleophilicity of the cysteine residue. The cysteine residue then contributes to the formation of the initial tetrahedral thioester intermediate by attacking the carbon of the reactive peptide bond. Stability of the intermediate is then contributed by hydrogen bonding between a highly conserved glutamine residue and the substrate oxyanion [321].

Bacterial proteases are an extensive group of enzymes that play an important role in virulence for many bacterial pathogens. The roles of bacterial proteases include degradation of host cell physical barriers for efficient penetration and dissemination within the host [322] or by colonizing the host defense mechanisms [323]. There are many and diverse examples of bacterial effector proteins that function as proteases. For example, the T3SS effector, AvrRpt2, is a cysteine protease from the plant bacterial pathogen, *Pseudomonas syringae*, that contributes to a hypersensitive response in *Arabidopsis thaliana* plants [324]. AvrRpt2 functions by cleaving the Arabidopsis protein RIN4. This then negatively regulates resistance by interacting with the plant resistance protein RPS2 and activating RPS2 [325, 326]. AvrRpt2 is initially delivered into plant cells in an inactive form [327], but the plant cyclophilin triggers autoproteolytic cleavage of the AvrPphB precursor as well as a controlled degradation of RIN4 [327].

Other T3SS effector cysteine proteases include YopT from *Yersinia* species and GtgE from *Salmonella*. YopT recognizes post translationally modified RhoA GTPases and releases them from cell membranes by proteolytic cleavage at the C terminus. This then results in the disruption of the host cell actin cytoskeleton [328]. GtgE specifically modifies the Rab32 subfamily of proteins by cleaving the regulatory switch I region. This then results in the manipulation of vesicular trafficking at the *Salmonella*- containing vacuole (SCV). Inactivation of Rab32 also appears to be important for SCV maturation [329]. However, more investigation is required to understand how GtgE mediated Rab32 cleavage contributes to the infection process.

GtgA, GogA and PipA are all novel zinc metalloprotease T3SS effector proteins from *Salmonella* species [330]. All suppress the host innate immune response by dampening the activation of NF-κB signalling pathway. All three effectors cleave the N terminal domain of the p65 subunit of NF-κB between residues Gly-40 and Arg-41 as well as cleaving RelB [331].

Alignment of EspL with homologues from other bacterial pathogens such as *Shigella*, *Yersinia* and *Salmonella* revealed conserved residues Cys47, His131 and Asp153 hence revealing a putative cysteine protease motif. Furthermore, EspL showed similarity within its N terminus to the CA clan of papin-like cysteine proteases such as YopT from Yersinia spp during analysis of secondary structure predictions using Phyre [296].

EspL blocks necroptosis and inflammatory signalling in the host cell during EPEC infection [296]. EspL specifically targets and cleaves host proteins that contain a receptor-interacting protein kinase homotypic interaction motif (RHIM). These proteins include the receptor interacting serine/threonine-protein kinase 1 and 3 (RIPK1) and (RIPK3), TIR-domain-containing adapter-inducing interferon-β (TRIF) and Z-DNA-binding protein 1/DNA-dependent activator of IFN-regulatory factors (ZBP1/DAI) [296]. These RHIM containing proteins have important roles in inflammatory and apoptotic/necroptotic cell death signalling pathways [141]. RIPK1 is the main player in regulating NF-κB signalling in response to interaction between TNF and its receptor TNFR1 to induce an inflammatory response in the cells. Alternatively, RIPK1 may also induce apoptosis in the cells when its forms a cytosolic complex together with TRADD, FADD and caspase 8. When the activity of caspase 8 is inhibited, RIPK1 can also interact with RIPK3 through their RHIM domains, to give rise to necroptosis [296].

RHIM containing proteins therefore have an important role in innate immune signalling and/or cell death signalling. By cleaving RHIM proteins, EspL is able to dampen inflammation and prevent cell death. Previous work by the Hartland laboratory revealed that RIPK1 was degraded upon infection with wild type (WT) EPEC [296]. In contrast, this was not observed during infection with the EPEC T3SS mutant. Infection with derivatives of EPEC lacking different genomic islands including ΔPP4 or ΔPP4-IE6 as well as single effector gene mutants, revealed that EspL was necessary for RIPK1 degradation during infection. Treatment with proteasome or caspase inhibitors such as MG132 or z-VAD-FMK (Z-VAD) failed to inhibit EspL-dependent RIPK1 loss, suggesting that EspL directly targeted RIPK1 and that EspL may have proteolytic activity [296].

In this chapter we aimed to determine if the EspL homologues OspD2 and OspD3, were cysteine proteases and to determine whether they cleave host RHIM proteins, similarly to EspL. For many years OspD2 had no known function, however it was recently reported that OspD2 is involved in inhibiting T3SS effector translocation during infection [301]. However, the potential cysteine protease activity of OspD2 was not required for this phenotype, and cleavage of RHIM proteins was not examined by this group. In addition to this, the proteolytic host targets of OspD3 have also not been investigated. OspD3 was only previously reported to be an enterotoxin which promotes IL-8 secretion [297, 298] . Understanding whether OspD2 and OspD3 cleave host RHIM proteins may help define the host cell targets and functions of these

effectors, especially in regulating cell death and inflammatory signaling pathways during *Shigella* infection.

3.2 Results

3.1 Alignment of full length EspL, OspD2 and OspD3 revealed a conserved cysteine protease catalytic triad.

To gain insight into OspD2 and OspD3 function, their protein sequences were aligned with their EPEC homologue EspL. Alignment was carried out using Clustal Omega and the results were represented using ESPript3. We identified a conserved cysteine protease motif in all three effectors, where the cysteine 64 (C_{64}), histidine 148 (H_{148}) and aspartate 171 (D_{171}) of OspD3 and cysteine 79 (C_{79}), histidine 163 (H_{163}) and aspartate 186 (D_{186}) of OspD2 were aligned with the previously characterised motif of cysteine 47 (C_{47}), histidine 131 (H_{131}) and aspartate 153 (D_{153}) within EspL (Fig 3.1A). These proteins also revealed a similarity of almost 40% at their amino acid level (Fig 3.1A).

Previous work from our group showed that mutation of the catalytic residue C_{47} to serine abolished the cysteine protease activity of EspL [296]. Thus, to investigate the potential cysteine protease activities of OspD2 and OspD3, we mutated C_{79} and C_{64} to serine in OspD2 and OspD3 respectively. Plasmid constructs that were codon optimised for mammalian cell expression of N-terminal 3xFlag-epitope-tagged OspD2 and OspD3 were used for the site-directed mutagenesis. These constructs alongside constructs that express EspL and $EspL_{C47S}$ (also with an N terminal 3xFlag-epitope tag) were transfected into HEK 293T cells for immunoblotting (Fig 3.1B).

Both wild type and catalytically inactive OspD2 were well-expressed in HEK 293T cells. However, both Flag-tagged wild type OspD3 and wild type EspL were not strongly detected in comparison to their catalytic mutants (Fig 3.1B). One reason for this could be that both Flag-OspD3 and Flag-EspL were not well-expressed in this cell line. However, it was previously observed that despite Flag-EspL having a low detection levels in mammalian cell lines, cleavage of its host cell targets, the RHIM-containing proteins were still detected [296]. We therefore presumed that Flag-EspL was expressed but not well detected, possibly because the N-terminal Flag tag was targeted for cleavage by the active cysteine protease itself. Similarly, low detection of Flag-OspD3 could also be due to self-processing.

3.2 Cleavage of human RHIM containing proteins, RIPK1 and RIPK3 upon ectopic co-expression with OspD2, OspD3 and EspL in HEK 293T cells.

As mentioned previously, EspL cleaves the host RHIM family of proteins, RIPK1 and RIPK3, by directly targeting the RHIM in these proteins [296]. Since OspD2 and OspD3 also contain

a potential cysteine protease motif and are 40% similar to EspL, we next wanted to examine if RHIM proteins were cleaved by OspD2 and OspD3. We co-transfected 3xFlag-tagged OspD2, $OspD2_{C79S}$, OspD3, $OspD3_{C64S}$, EspL or $EspL_{C47S}$ into HEK 293T cells with either pEGFP-C2:RIPK1 or pEGFP-C2:RIPK3. p3xFlag-Myc-CMV-24 was used as a control. We then lysed the cells and detected cleavage of the RHIM proteins by immunoblotting (Figure 3.2). We noted that whenever GFP tagged proteins were expressed, we detected a band almost the size of GFP (28 kDa) using GFP antibodies. This band was present even when GFP-RIPK1 or GFP-RIPK3 were expressed with the control vector. We presume that this was a breakdown product of the GFP- fusion protein, possibly reflecting the occurrence of an unstable site likely to be targeted for degradation by the host cell. In the presence of Flag-OspD2 we detected a substantial reduction in GFP-RIPK1, however it was completely degraded in the presence of both Flag-OspD3 and Flag-EspL (Figure 3.2A). We also detected a band smaller in size to RIPK1 at around 80kDa in samples co-expressed with Flag-OspD3 and Flag-EspL. We presumed this was an OspD3 or EspL-induced cleavage product of GFP-RIPK1. Based on the size of the cleaved fragment, we predicted this cleavage to take place in the C terminus of RIPK1, where the RHIM is located [332]. Since EspL targets and cleaves the RHIM domain in these proteins, we predicted that OspD2 and OspD3 would cleave these regions as well. No cleavage of GFP-RIPK1 was detected by Flag-$OspD2_{C79S}$, Flag-$OspD3_{C64S}$ or Flag-$EspL_{C47S}$, supporting the importance of these cysteine residues in the catalytic activity of OspD2 and OspD3.

When GFP-RIPK3 was over-expressed in HEK 293T cells, we did not detect cleavage by Flag-OspD2, however we detected slight cleavage by Flag-OspD3 and complete cleavage by Flag-EspL (Figure 3.2B). A band smaller in size to RIPK3 was also noted in samples co-expressing Flag-EspL, likely a cleavage product GFP-RIPK3. A very faint band, smaller in size to RIPK3 was also detected in the presence of Flag-OspD3, likely to be an OspD3-induced cleavage product. Levels of this breakdown product were much lower than in cells with EspL co-expression. This could potentially reflect that OspD3 did not cleave GFP-RIPK3 as efficiently as EspL.

From these results, we can summarize that the residues C_{79} and C_{64} of OspD2 and OspD3 respectively are required for cysteine protease catalytic activity. However, OspD2 and OspD3 did not target host RHIM proteins as efficiently as EspL. Cleavage of the RHIM proteins by OspD2 was extremely weak. OspD3 on the other hand, showed complete cleavage of some RHIM proteins but not the others. In addition to this, the targets RIPK1 and RIPK3 were

overexpressed in this experiment. Hence, we next wanted to investigate the cleavage of RHIM proteins when expressed endogenously by host cells.

3.3 Cleavage of endogenous RHIM proteins in doxycycline-inducible HT-29 cell lines expressing OspD3 and EspL but not OspD2.

To further examine cleavage of endogenously expressed RIPK1 and RIPK3 by OspD2 and OspD3, we utilised a lentiviral transduction system to generate HT-29 cell lines which stably express 3xFlag-tagged OspD2, $OspD2_{C79S}$, OspD3, $OspD3_{C64S}$, EspL and Esp_{C47S} under the control of a doxycycline-dependent promoter. The expression of the Flag-fusion proteins by these cell lines was detected by immunoblotting after induction with doxycycline over a period of 24 hours (Figure 3.3). Robust doxycycline induction of the Flag fusion proteins was detected, with the exception of Flag-EspL and Flag-OspD3, similar to the transfection of HEK 293T cells (Figure 3.1B and 3.3). As expected, we saw a loss of RIPK1 and RIPK3 in EspL-expressing cells from 2 hours of doxycycline induction (Figure 3.3A). In contrast, the levels of RIPK1 and RIPK3 were unaffected in the presence of $EspL_{C47S}$. Likewise, when OspD3 was expressed, we observed loss of endogenous RIPK1 and RIPK3 from 2 hours of doxycycline induction. There was no impact on RHIM protein levels in the presence of $OspD3_{C64S}$ (Figure 3.3B). This was consistent with the co-transfections of Flag-OspD3 with GFP-RIPK1 and GFP-RIPK3 (Figure 3.2). However, when OspD2 or $OspD2_{C79S}$ was expressed, there was no impact on amounts of endogenous RIPK1 and RIPK3 in HT-29 cells (Figure 3.3C).

3.4 Purified OspD3 cleaves endogenous RIPK1 and RIPK3 in HT29 cell lysates

To further examine OspD3 cleavage of RIPK1 and RIPK3 in HT-29 cells, we tested the ability of purified recombinant WT OspD3 and $OspD3_{C64S}$ to cleave RIPK1 and RIPK3 in HT-29 cell lysates (Figure 3.4). Purified and soluble GST-tagged OspD3 and $OspD3_{C64S}$ were used for the experiment. Upon incubation of purified WT OspD3 with HT-29 cell lysates, we detected cleavage of both RIPK1 and RIPK3. Cleavage of RIPK1 and RIPK3 was not detected upon incubation with $OspD3_{C64S}$.

3.5 OspD3 and EspL inhibit NF-κB-dependent gene transcription of a luciferase reporter

Given that RIPK1 complexes with other adaptor proteins for canonical NF-κB signalling, and that OspD2, OspD3 and EspL cleave RIPK1 with different efficiencies, we next wanted to investigate the role of these proteases in NF-κB signalling [333]. We therefore tested their

ability to inhibit TNF-induced NF-κB dependent gene transcription of a luciferase reporter. Upon stimulation with TNF, NF-κB activation was evident in HEK 293T cells transfected with the empty vector p3xFlag-*Myc*-CMV-24 compared to unstimulated cells, corresponding to an increase in luciferase activity (Figure 3.5). Overexpression of Flag-OspD2 and Flag-OspD2$_{C79S}$ did not inhibit NF-κB signalling upon stimulation with TNF; likely due to RIPK1 being unaffected in these cells. In contrast, overexpression of Flag-OspD3 inhibited NF-κB dependent luciferase activity. Surprisingly OspD3$_{C64S}$ also slightly inhibited NF-κB activation in comparison to p3xFlag-*Myc*-CMV-24 expressing cells. We speculated this could be due to OspD3$_{C64S}$ binding to RIPK1 to some extent, although this was not seen for Flag-EspL, which was able to inhibit the activity of RIPK1 slightly. As expected, Flag-EspL inhibited NF-κB activity. Hence OspD3 and EspL inhibited NF-κB-dependent luciferase activity, consistent with cleavage of RIPK1.

3.6 OspD3 inhibits TNF-induced necroptosis in HT-29 cell lines

RHIM domain interactions are critical for necroptotic signalling. Our laboratory previously found that EspL inhibited TNF-induced necroptosis by cleaving RIPK1 and RIPK3 [296]. Therefore, we investigated if OspD2 and OspD3 could also inhibit necroptosis, given the observed cleavage of RIPK1 and RIPK3 (Figure 3.2 and Figure 3.3). We used the HT-29 cell lines which stably express 3xFlag-tagged OspD2, OspD2$_{C79S}$, OspD3, OspD3$_{C64S}$, EspL and EspL$_{C47S}$ and induced the cells with doxycycline for 24 hours. Following this, the stable cell lines were treated with TNF, z-VAD (a caspase inhibitor) and birinapant (an inhibitor of NF-κB) for 24 hours to induce necroptosis, before cell viability was detected by measuring MTT reduction (Figure 3.6) [334]. Treating the cells with TNF induces signalling via the RHIM proteins in the HT29 cell lines to initiate either inflammation, apoptosis or necroptosis. Inhibition of caspase activity by the addition of z-VAD and inhibition of NF- κB activation by the addition of birinapant will then inhibit inflammation and apoptosis, steering the cell lines towards death by necroptotic signalling.

As expected, cells expressing EspL were protected from necroptotic cell death (Figure 3.6A). In contrast, cells expressing the catalytically inactive EspL$_{C47S}$ were not protected from necroptotic cell death. Consistent with EspL, cells expressing OspD3 were also protected from necroptotic cell death, while those expressing OspD3$_{C64S}$ were not (Figure 3.6B). In contrast, cells expressing either OspD2 or OspD2$_{C79S}$, were not viable upon treatment with necroptotic stimuli. This supports the previous findings that OspD2 does not cleave RIPK1 and RIPK3 in

the stable cell lines and hence cannot inhibit necroptosis (Figure 3.6C). Interestingly, we observed that the OspD3 stable cell line was protected from necroptotic cell death even in the absence of doxycycline treatment to induce OspD3 expression. We presumed this may be because there is some OspD3 expressed even without induction with doxycycline. Therefore, we tested for "leaky" expression of OspD3 in these cell lines. For this, HT-29 cell lines which stably express 3xFlag-tagged OspD2, OspD2$_{C79S}$, OspD3, OspD3$_{C64S}$, EspL and Esp$_{C47S}$ under the control of a doxycycline-dependent promoter were both induced and left uninduced with doxycycline for 24 hours (Figure 3.6D). The loss of endogenous RIPK1 was measured to determine if uninduced cells expressed OspD3 which could cleave RIPK1. Degradation of RIPK1 was observed in cells expressing OspD3 but without induction with doxycycline in comparison to cells expressing OspD3$_{C64S}$, confirming leaky expression of OspD3.

3.7 No cleavage of RIPK1 in HeLa 229 cells upon infection with wildtype *S. flexneri 2a*, strain 2457T

We next investigated OspD2 and OspD3 mediated cleavage of RIPK1 and RIPK3 during infection with *Shigella* in HeLa 229 cells. HeLa 229s do not express RIPK3 and hence only the expression of RIPK1 was determined in this experiment [335]. Infections were carried out using wildtype *S. flexneri 2a*, strain 2457T from Renato Morona [316], a non-invasive T3SS mutant (Δ*mxiD* strain), Δo*spD2*, Δ*ospD3* strain and Δo*spD2ospD3* double mutant strains constructed here. The presence of OspD2 and OspD3 genes in this wild type strain was confirmed via nucleotide sequencing. The mutants were constructed via lambda red combination and the genes were replaced with either a kanamycin or chloramphenicol cassette. The deletion of gene was then confirmed via sequencing of amplified target regions. However, despite the findings in our overexpression studies, we did not detect any major differences in RIPK1 levels at the time points tested. At 8 h post infection, there was a slight decrease in the levels of RIPK1 expression in the WT and OspD2 and OspD3 single and double strains, and we presume this may be due to cell loss as the amount of actin was also less in these samples. Overall, these results called into question whether RIPK1 or RHIM proteins generally were bona fide targets of OspD2 and OspD3.

3.3 Discussion

Gram negative bacteria such as *Shigella* and EPEC have evolved mechanisms to manipulate host cell signalling and subvert immune responses to facilitate their survival. They primarily do this through their T3SS effector proteins. In recent years tremendous efforts have been made in studying these effectors [336]. Some effectors are homologous across these bacterial species, possibly performing similar cellular functions. For example, EspL, a T3SS from EPEC has homologues in *Shigella*, which are termed OspD2 and OspD3 [296]. EspL was identified to be a cysteine protease which cleaves the host RHIM proteins, RIPK1 and RIPK3 and inhibits necroptosis. EspL, OspD2 and OspD3 were all found to be almost 40% percent identical to one another. As such, it was hypothesised that OspD2 and OspD3 may also function as cysteine proteases that target host RHIM proteins.

Prior studies on OspD3 identified it to have enterotoxin activity. This was validated when grown in iron-depleted environment, OspD3 contributed to fluid accumulation in isolated rabbit ileal loops as well as an increase in short circuit and potential difference in Ussing chambers. [60, 298, 337]. OspD3 has also been reported to have a contrasting role in increasing and reducing IL-8 secretions in epithelial cell lines by two different groups [297, 337]. One hallmark of *Shigella* infection is the induction of a massive PMN infiltration upon infection [67]. PMN infiltration is initiated due to IL-8 secretion produced as a result of NF-κB signalling triggered by intracellular replication of *Shigella* [338, 339]. However, there was no investigation of whether the reduction or increase in IL-8 secretion had a direct impact on PMN infiltration or if this occurred independently of the enterotoxin role of OspD3. OspD2 is another T3SS effector of *Shigella* which for a long time had no known function. However, Mou *et al.* recently published that OspD2 is involved in the inhibition of effector translocation during infection [301]. Mou *et al.* also reported that the cysteine protease activity of OspD2 was not required for this function as they observed $OspD2_{C79A}$ mutants reduced cell death to the same levels as wild type OspD2. However, cleavage of RHIM proteins by OspD2 was not investigated by this group [296].

In order to understand the functions of OspD2 and OspD3, we first aimed to confirm their cysteine protease activities and examine their potential to cleave RHIM proteins based on their similarity to EspL. For this we created catalytically inactive mutants of OspD2 and OspD3, mutating the conserved cysteine residues C_{79} and C_{64} respectively, to serine. We observed variable expression of OspD2 and OspD3 and their catalytic mutants by transient transfection. We suggest that the first possible explanation for this could be there being a low transfection

efficiency of these two Flag-fusion proteins in the cells. However, previous work from our group showed that despite Flag-EspL having a low detectable expression in mammalian cell lines, cleavage of its host cell targets, the RHIM-containing proteins was still evident [296]. Previous studies of cysteine proteases reported that they are capable of auto-activation [321, 340]. This happens when the pro-domain of the protease is cleaved in order to activate the protease, under the influence of pH change [340]. It was also reported that auto activation of the cysteine protease can occur in a wide pH range of 4.3-7.3, and that an acidic pH can increase the rate of the auto-activation process by many folds [341]. As such, we presume that the expression of Flag-OspD3 and Flag-EspL in HEK 293T cells could have possibly exposed these Flag fusion proteins to an environment with a difference in pH in comparison to that in bacteria. This could have resulted in these proteins becoming auto-activated and cleaving their tags. As the Flag tags are located at the N-terminus of these proteins, re-cloning Flag-OspD3 and Flag-EspL with a C terminal Flag tag may improve detection of these proteins. The expression of Flag-OspD2 however, was not affected, perhaps indicating that OspD2 does not undergo self-processing similar to EspL and OspD3.

Despite this, Flag fusion proteins were used to investigate the cleavage of GFP-RIPK1 and GFP-RIPK3, which are known to be cleaved by EspL. We found Flag-OspD3 also cleaved GFP-RIPK1 and GFP-RIPK3 (Figure 3.2). In contrast, Flag-OspD2 showed only weak cleavage of GFP-RIPK1 and no cleavage of GFP-RIPK3 (Figure 3.2). Expression of proteins during transfection results in increased protein expression in comparison to their normal cellular levels. Furthermore, there is the possibility that the recombinant proteins expressed upon transfection may undergo post translational modifications which are not present when natively expressed. As such, over-expression studies are a quick method of investigating predicted functions of proteins, but it is important to keep in mind that the phenotype we observed may be an artefact of over-expression. It was thus necessary to determine whether endogenous RHIM proteins were cleaved by OspD2 and OspD3.

We tested cleavage of endogenous RIPK1 and RIPK3 in HT-29 cell lines stably expressing the effectors and their catalytically inactive mutants. OspD3 efficiently cleaved both RIPK1 and RIPK3 in the stable cell line as opposed to OspD2 (Figure 3.3B/C). Our combined results from both the over expression and stable cell line experiments suggested that OspD3 was indeed a cysteine protease that was able to cleave the RHIM proteins, RIPK1 and RIPK3 but that OspD2 likely had a different substrate range.

Cleavage of RIPK1 and RIPK3 during infection is not only limited to bacterial infection. Wagner *et al* also recently reported that the HIV-1 protease, PR, is able to cleave RIPK1 and another RIP kinase, RIPK2, during HIV infection [342]. However, instead of targeting the RHIM domain, PR cleaves between residues 436-462 within RIPK1. These residues are located in the intermediate domain just between the kinase domain and RHIM domain in RIPK1. By employing a mammalian 2-hybrid system, they also found that cleavage of RIPK1 at these sites affected interaction with RIPK3 and inhibit necroptosis. They then concluded that PR targets RIPK proteins so HIV-1 can establish a persistent infection and suppress the innate immune response [342]. Croft *et al* also reported that the Human Rhinovirus 3C protease (HRV C3) cleaved RIPK1 during human rhinovirus infection, which infects the upper respiratory tract. They showed via HRV16 infection of cells, together with chemical inhibitors and induces of apoptosis (Actinomycin D and z-vad-FMK) that the HRV16 3C protease cleaves RIPK1. This cleavage of RIPK1 was concurrent with cleavage of RIPK1 by caspase 8 during apoptosis. The RIPK1 cleavage product by caspase 8 is pro-apoptotic and subsequent cleavage of this processed form of RIPK1 by HRV 3C may therefore be a mechanism by which HRV alters apoptosis to create a cellular environment which favours viral replication [343]. In addition to this, Harris *et al* also reported that RIPK3 is cleaved by a cysteine protease $3C^{pro}$ during coxsackievirus B3 (CVB) infections. This cleavage directly interferes with necroptotic cell death signalling during CVB infection [344]. Likewise, we assume that OspD3 cleaves RIPK1 and RIPK3 in order to block downstream RHIM protein signalling. Since TNF signalling can activate both cell-death and cell survival pathways simultaneously, we tested the ability for these cysteine proteases to inhibit NF-κB signalling as well as necroptosis [158, 345]. Upon TNF activation, RIPK1 forms a complex with other adaptor proteins to initiate NF-κB signalling [333]. We predicted OspD3 would inhibit NF-κB signalling as it cleaves RIPK1. Consistent with loss of RIPK1, ectopic expression of OspD3 but not $OspD3_{C64S}$, inhibited TNF-induced expression of an NF-κB dependent luciferase reporter (Figure 3.5). Also consistent with our immunoblot findings, ectopic expression of OspD2 did not inhibit TNF-induced NF-κB-dependent gene transcription. One outcome of NF-κB signalling is the secretion of IL-8 during *Shigella* infections [67]. Since we saw OspD3 inhibition of NF-κB-dependent gene transcription, we assume downstream responses such as IL-8 secretion were also affected or reduced. This was further supported by a previous report where OspD3 was shown to decrease IL-8 secretion, particularly a *Shigella* ospD3 mutant showed significantly reduced IL-8 secretion into the basolateral regions during infection of epithelial cells such as Hep-2 and T84 [297]. However, another group subsequently reported that an Δ*ospD3* mutant instead induced

IL-8 secretion significantly in three different human epithelial cells, HT-29 cells, HCT-8 cells and T84 cells tested compared to WT *Shigella* infection[299]. These contrasting findings by two different groups, calls for further investigation to determine the role of OspD3 in IL-8 secretion and the host cell targets identified to be directly targeted by OspD3 for this phenotype.

EspL also cleaves RIPK1 and RIPK3, hence preventing RIPK1/RIPK3-dependent necroptosis [296]. Given that RIPK1 and RIPK3 are also cleaved by OspD3, we predicted that OspD3 would prevent RIPK1/RIPK3-dependent necroptosis. We treated cells with TNF, v-ZAD and birinapant to induce necroptosis [334]. The Biindole-based Smac–mimetic birinapant inhibits NF-κB signalling and promotes apoptosis by behaving as an IAP antagonist and mimics the binding of Smac to cIAP1/2 and XIAP, to prevent caspase inhibition [346-349]. v-ZAD is a caspase inhibitor which was also added to the cells to block apoptosis and promote necroptosis [350]. An MTT assay was carried out to quantify the number of viable cells upon treatment of these compounds. OspD2 did not protect the cells from necroptosis, supporting our finding that OspD2 does not target RHIM proteins. As predicted, OspD3 protected the cells from necroptotic cell death and this depended on its catalytic activity. This once again supports the role of OspD3 as a cysteine protease that cleaves RHIM proteins.

We next tested the ability for these cysteine proteases to cleave RIPK1 and RIPK3 during *Shigella* infection. We carried out the infections in HeLa 229 cells as this cell type showed (~70%) infection rate using a GFP-tagged WT *Shigella* strain. However, the HeLa 229 cell line does not express RIPK3 and therefore we only tested for cleavage of RIPK1[335]. Since the cysteine protease effectors were previously reported as either early or late expressed effectors, infections were carried out at 2 hours, 8 hours and 24 hours, in order to include an early, intermediate and late timepoint to assess RIPK1 levels [306]. Although there was a slight decrease in RIPK1 expression in cells infected with WT *Shigella* and Δ*ospD2*, Δ*ospD3* and Δ*ospD2ospD3* mutants at 8 hours of infection, there were no significant differences in RIPK1 levels during the three timepoints of infection tested. This slight decrease in RIPK1 levels were not consistent with the significant RIPK1 cleavage observed during EPEC infections [296]. We presume that even though it may appear that there was less RIPK1 in these samples, the loading control suggested that there were less cells in these samples, hence reflecting an increased cell death. As such, we assume that the RHIM proteins may not be the preferred targets of OspD2 and OspD3 during *Shigella* infections, although infection of a cell line expressing RIPK3 is needed to fully support this conclusion.

In summary, we concluded that OspD3 is a cysteine protease which cleaves host RHIM proteins. We demonstrated OspD3 cleavage of RIPK1 and RIPK3 and inhibition of downstream signalling such as necroptosis and NF-κB transcription when OspD3 was expressed in mammalian cells. OspD2 on the other hand, was unable to cleave the RHIM proteins and did not protect cells from necroptosis even upon overexpression. OspD2 also did not prevent NF-κB signalling upon stimulation with TNF. Unfortunately, we did not see any major changes in RIPK1 levels during *Shigella* infection between the wildtype and that mutant *Shigella* strains. As such, we hypothesise that OspD2 and OspD3 may preferentially cleave other cellular targets during infections. Thus, the goal of the following chapter was to examine other potential host targets of these two effectors, OspD2 and OspD3, using an unbiased proteomics-based approach.

A

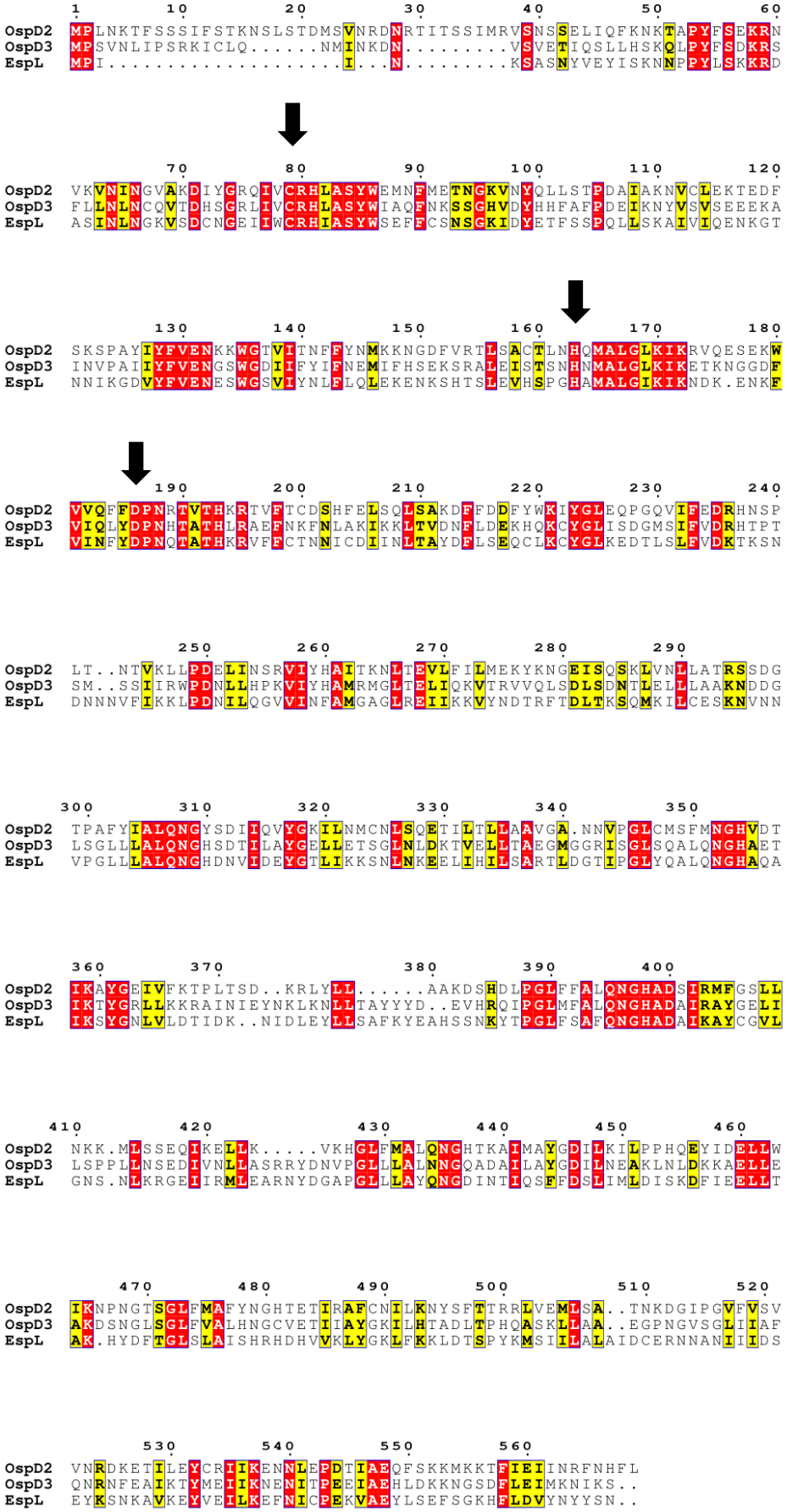
1 10 20 30 40 50 60
OspD2 MPLNKTFSSSIFSTKNSLSTDMSVNRDNRTITSSIMRVSNSSELIQFKNKTAPYFSEKRN
OspD3 MPSVNLIPSRKICLQ.....NMINKDN.........VSVETIQSLLHSKQLPYFSDKRS
EspL MPI.....I...N.........KSASNYVEYISKNNPPYLSKKRD
70 80 90 100 110 120
OspD2 VKVNINGVAKDIYGRQIVCRHLASYWEMNFMETNGKVNYQLLSTPDAIAKNVCLEKTEDF
OspD3 FLLNLNCQVTDHSGRLIVCRHLASYWIAQFNKSSGHVDYHHFAFPDEIKNYVSVSEEEKA
EspL ASINLNGKVSDCNGEIIWCRHIASYWSEFFCSNSGKIDYETFSSPQLLSKAIVIQENKGT
130 140 150 160 170 180
OspD2 SKSPAYIYFVENKKWGTVITNFFYNMKKNGDFVRTLSACTLNHQMALGLKIKRVQESEKW
OspD3 INVPAIIYFVENGSWGDIIFYIFNEMIFHSEKSRALEISTSNHNMALGLKIKETKNGGDF
EspL NNIKGDVYFVENESWGSVIYNLFLQLEKENKSHTSLEVHSPGHAMALGIKIKNDK.ENKF
190 200 210 220 230 240
OspD2 VVQFFDPNRTVTHKRTVFTCDSHFELSQLSAKDFFDDFYWKIYGLEQPGQVIFEDRHNSP
OspD3 VIQLYDPNHTATHLRAEFNKFNLAKIKKLTVDNFLDEKHQKCYGLISDGMSIFVDRHTPT
EspL VINFYDPNQTATHKRVFFCTNNICDIINLTAYDFLSEQCLKCYGLKEDTLSLFVDKTKSN
250 260 270 280 290
OspD2 LT..NTVKLLPDELINSRVIYHAITKNLTEVLFILMEKYKNGEISQSKLVNLLATRSSDG
OspD3 SM..SSIIRWPDNLLHPKVIYHAMRMGLTELIQKVTRVVQLSDLSDNTLELLLAAKNDDG
EspL DNNNVFIKKLPDNILQGVVINFAMGAGLREIIKKVYNDTRFTDLTKSQMKILCESKNVNN
300 310 320 330 340 350
OspD2 TPAFYIALQNGYSDIIQVYGKILNMCNLSQETILTLLAAVGA.NNVPGLCMSFMNGHVDT
OspD3 LSGLLLALQNGHSDTILAYGELLETSGLNLDKTVELLTAEGMGGRISGLSQALQNGHAET
EspL VPGLLLALQNGHDNVIDEYGTLIKKSNLNKEELIHILSARTLDGTIPGLYQALQNGHAQA
360 370 380 390 400
OspD2 IKAYGEIVFKTPLTSD..KRLYLL......AAKDSHDLPGLFFALQNGHADSIRMFGSLL
OspD3 IKTYGRLLKKRAINIEYNKLKNLLTAYYYD..EVHRQIPGLMFALQNGHADAIRAYGELI
EspL IKSYGNLVLDTIDK..NIDLEYLLSAFKYEAHSSNKYTPGLFSAFQNGHADAIKAYCGVL
410 420 430 440 450 460
OspD2 NKK.MLSSEQIKELLK.....VKHGLFMALQNGHTKAIMAYGDILKILPPHQEYIDELLW
OspD3 LSPPLLNSEDIVNLLASRRYDNVPGLLLALNNGQADAILAYGDILNEAKLNLDKKAELLE
EspL GNS.NLKRGEIIRMLEARNYDGAPGLLLAYQNGDINTIQSFFDSLIMLDISKDFIEELLT
470 480 490 500 510 520
OspD2 IKNPNGTSGLFMAFYNGHTETIRAFCNILKNYSFTTRRLVEMLSA..TNKDGIPGVFVSV
OspD3 AKDSNGLSGLFVALHNGCVETIIAYGKILHTADLTPHQASKLLAA..EGPNGVSGLIIAF
EspL AK.HYDFTGLSLAISHRHDHVVKLYGKLFKKLDTSPYKMSIILALAIDCERNNANIIIDS
530 540 550 560
OspD2 VNRDKETILEYCRIIKENNLEPDTIAEQFSKKMKKTFIEIINRFNHFL
OspD3 QNRNFEAIKTYMEIIKNENITPEEIAEHLDKKNGSDFLEIMKNIKS..
EspL EYKSNKAVKEYVEILKEFNICPEKVAEYLSEFSGKHFLDVYNYYSN..

B

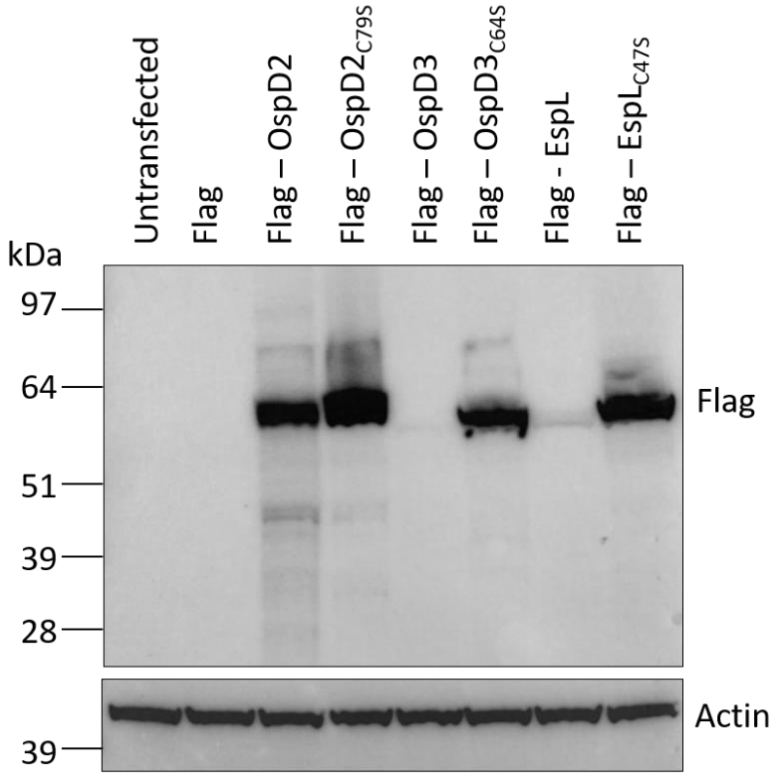

Figure 3. 1: Ectopic expression of wild type and site-directed, catalytically inactive OspD2, OspD3 and EspL in HEK 293T cells.

(A) Alignment of EspL from EPEC E2348/69 and its homologues OspD2 and OspD3 from *Shigella flexneri 2a 2457T*.

Conserved cysteine protease residues in the catalytic triad (Cys, His and Asp) of EspL, OspD2 and OspD3 are indicated by arrows. Alignment was performed using Clustal Omega and representation of alignment was performed using ESPript3. The red highlight indicates residues which are identical between OspD2, OspD3 and EspL while the yellow highlight shows residues which are similar among OspD2, OspD3 and EspL

(B) Immunoblot of ectopically expressed OspD2, OspD3 and EspL and site-directed, catalytically inactive $OspD2_{C79S}$, $OspD3_{C64S}$ and $EspL_{C47S}$ mutants.

p3xFlag-myc-cmv-24, Flag-OspD2, Flag-$OspD2_{C79S}$, Flag-OspD3, Flag-$OspD3_{C64S}$ Flag-EspL and Flag-$EspL_{C42S}$ were expressed in HEK 293T cells. Cells were harvested for immunoblotting and expression was detected using anti-Flag antibodies. Antibodies to β-actin were used as a loading control. Immunoblot is representative of at least three independent experiments.

A

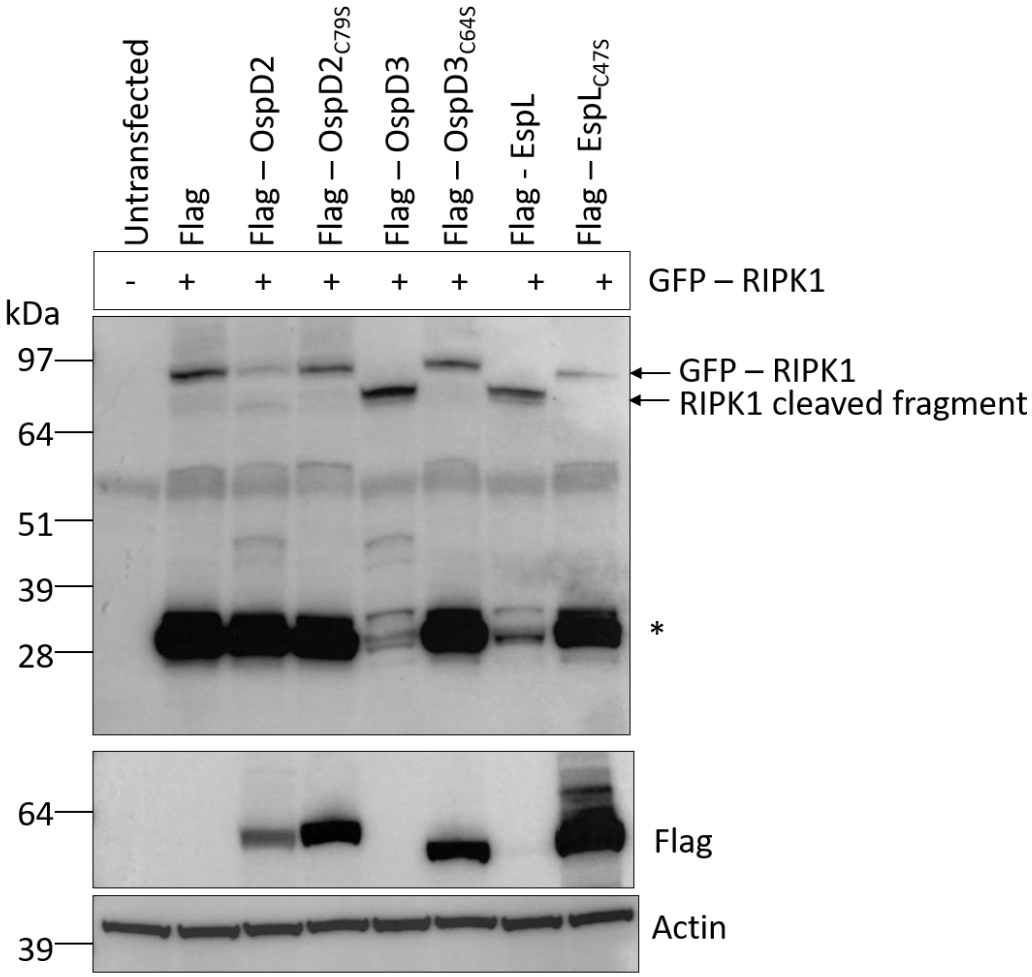
Untransfected
Flag
Flag – OspD2
Flag – OspD2C79S
Flag – OspD3
Flag – OspD3C64S
Flag - EspL
Flag – EspLC47S
- + + + + + + +
GFP – RIPK1
kDa
97
64
51
39
28
GFP – RIPK1
RIPK1 cleaved fragment
*
64
Flag
39
Actin

B

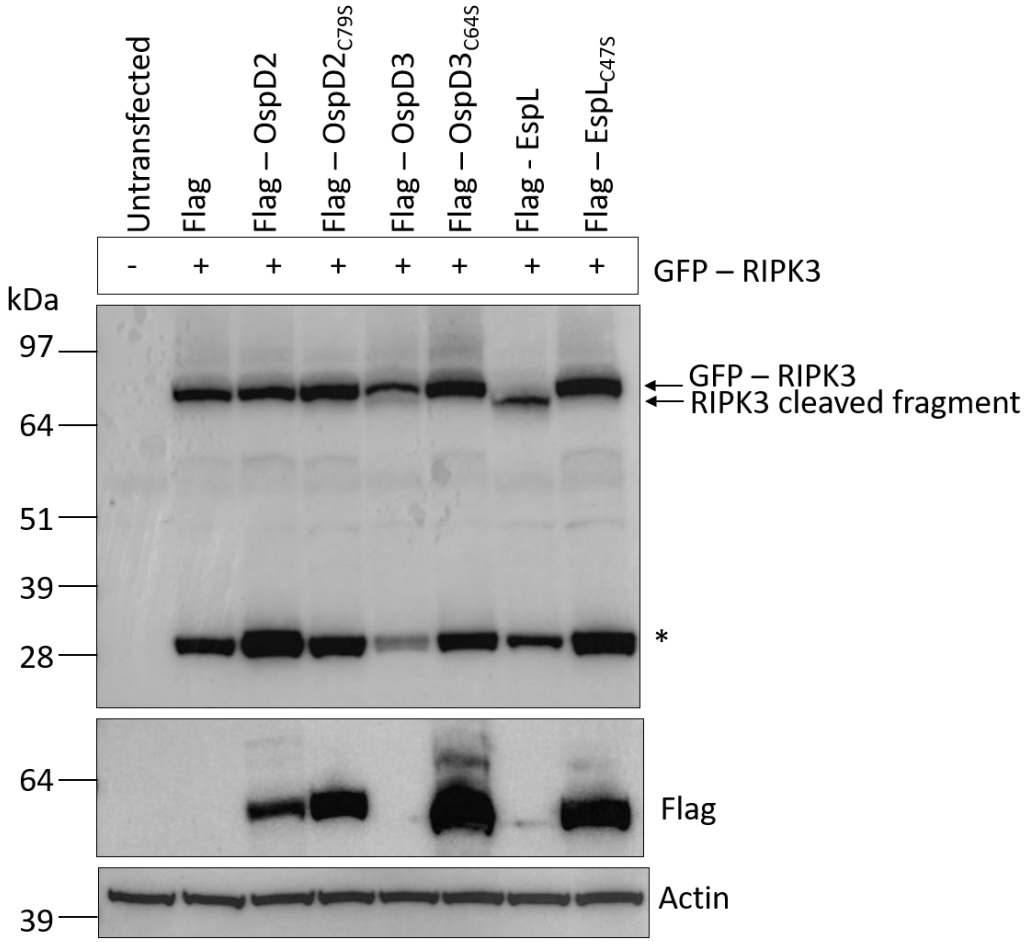

Figure 3. 2: Ectopic co-expression of wild type and catalytically inactive OspD2, OspD3 and EspL with human RHIM containing proteins, RIPK1, RIPK3 or TRIF in HEK 293T cells.

Immunoblots of HEK 293T cells transfected to express wild type and catalytically inactive Flag-tagged OspD2, OspD3 and EspL and either GFP-RIPK1 (A) or GFP-RIPK3 (B). Cells were harvested for immunoblotting and protein expression was detected using anti-Flag, anti-GFP or anti-HA antibodies. Antibodies to β-actin were used as a loading control. Top arrows indicate full length GFP-RIPK1 and GFP-RIPK3. Bottom arrow indicates the presence of any cleaved fragments. * indicates the presence of a cell-induced GFP tag degradation product (A, B). Immunoblot is representative of at least three independent experiments.

A

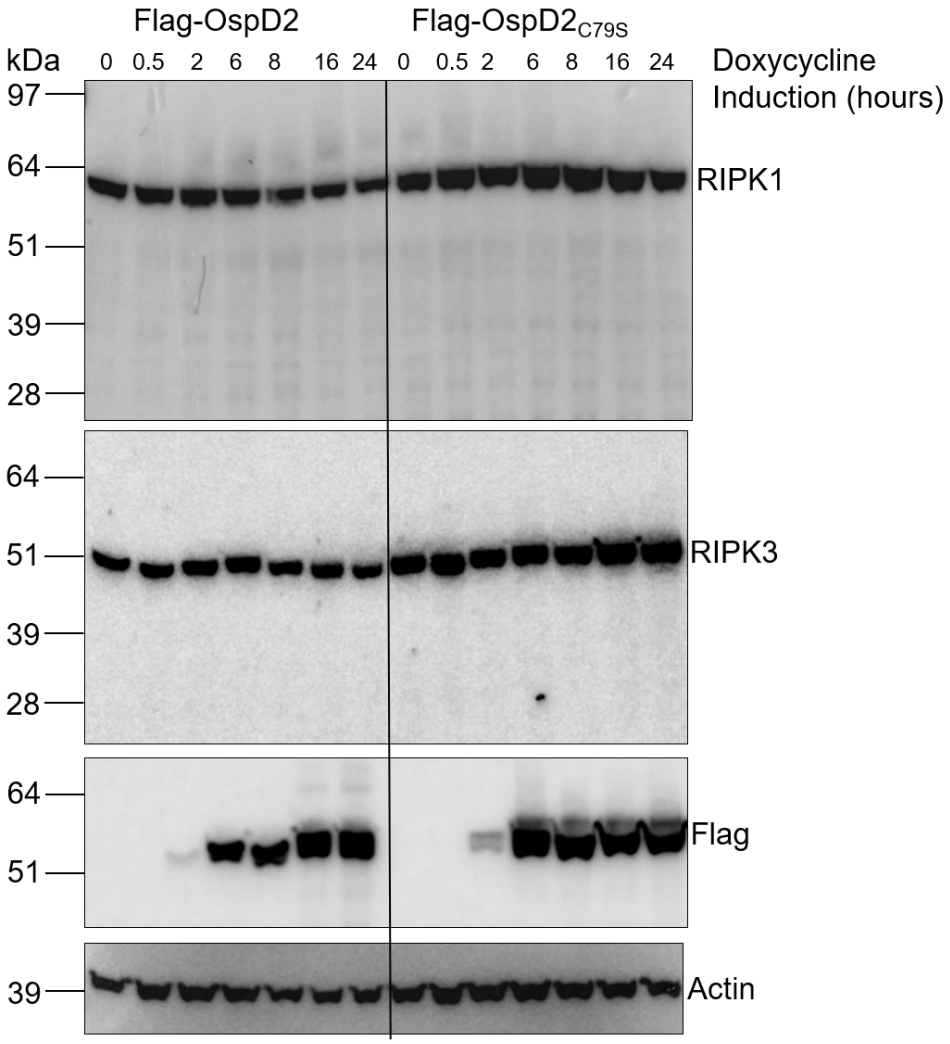
Flag-OspD2
Flag-OspD2C79S
kDa
0 0.5 2 6 8 16 24 0 0.5 2 6 8 16 24
Doxycycline Induction (hours)
97
64
51
39
28
RIPK1
64
51
39
28
RIPK3
64
51
Flag
39
Actin

B

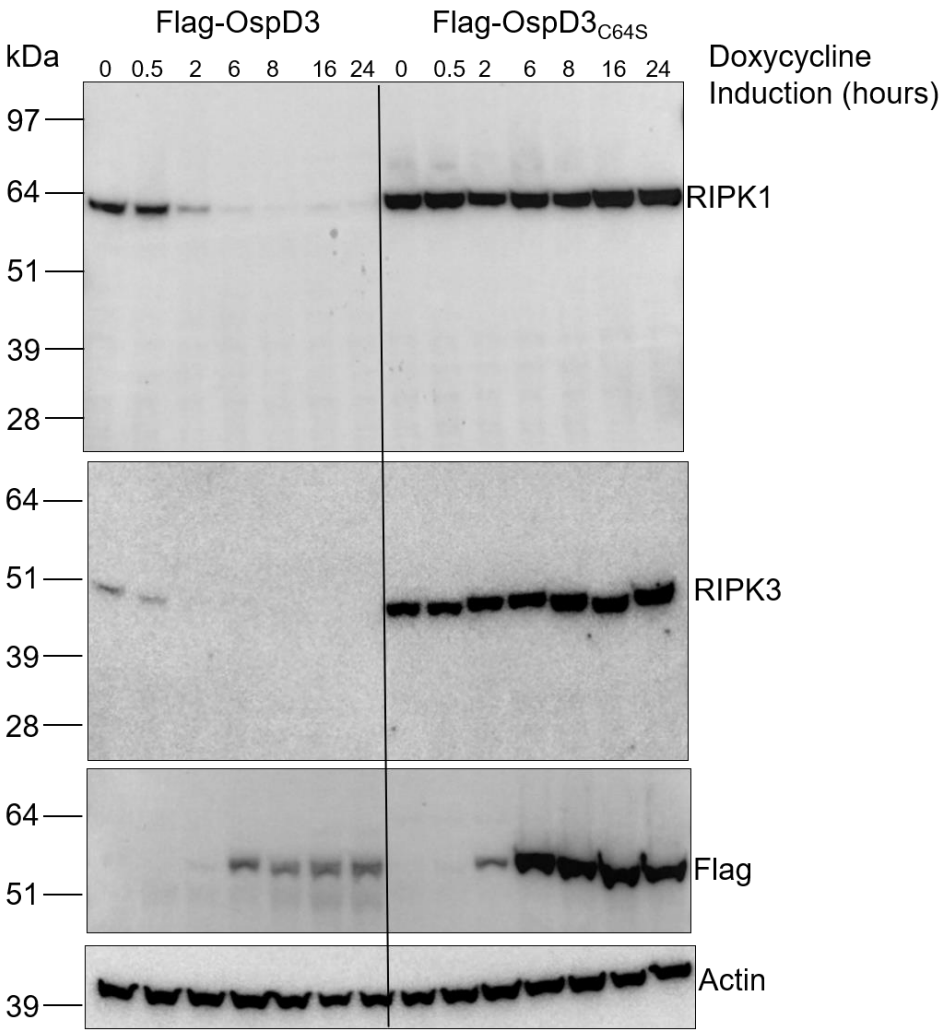
Flag-OspD3
Flag-OspD3C64S
kDa
0 0.5 2 6 8 16 24 0 0.5 2 6 8 16 24
Doxycycline
Induction (hours)
97
64
51
39
28
RIPK1
64
51
39
28
RIPK3
64
51
Flag
39
Actin

C

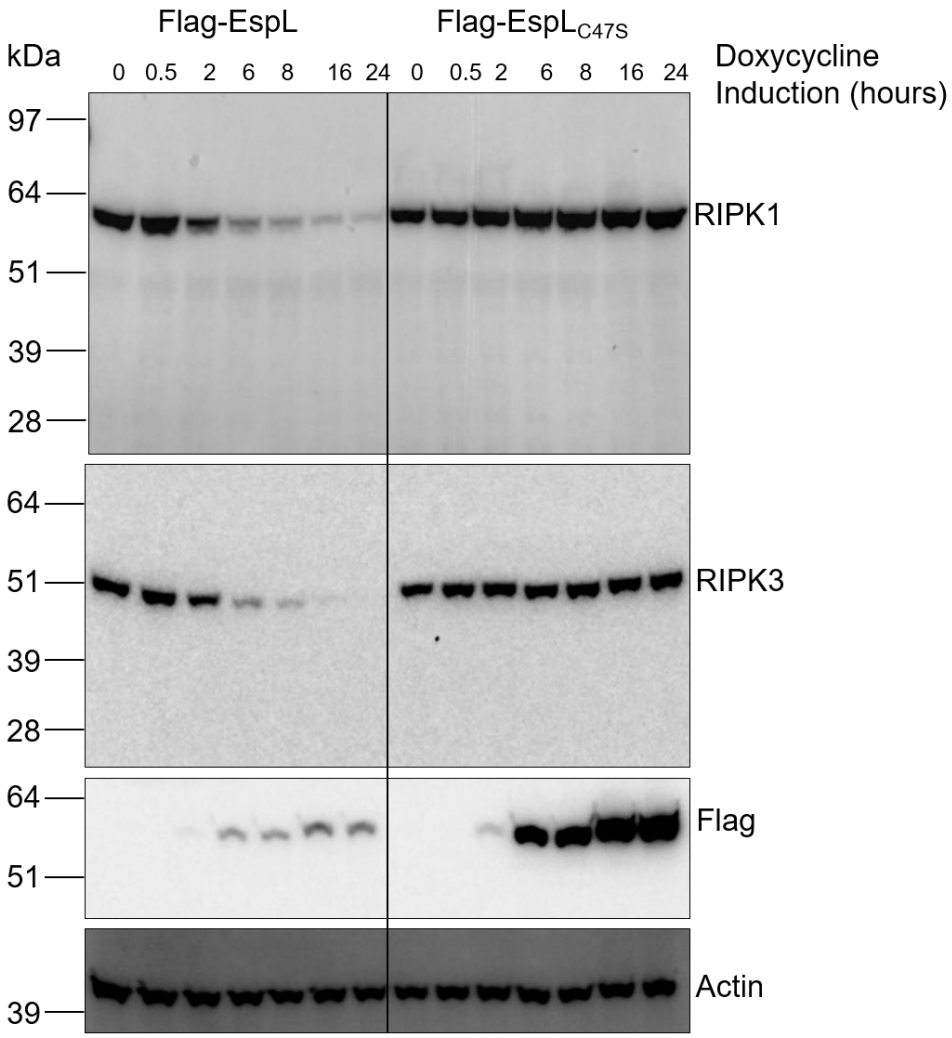

Figure 3. 3: **Cleavage of endogenous RHIM proteins in doxycycline inducible HT-29 cells expressing wild type and catalytically inactive OspD2, OspD3 and EspL.**

Immunoblots showing levels of RIPK1 and RIPK3 in doxycycline inducible HT-29 cell lines expressing Flag-EspL or Flag-EspL$_{C47S}$ (A), Flag-OspD3 or Flag-OspD3$_{C64S}$ (B) or Flag-OspD2 or Flag-OspD2$_{C79S}$ (C) which were induced with doxycycline for various timepoints as indicated. Expression of endogenous RIPK1 and RIPK3 were detected using anti-RIPK1 and anti-RIPK3 antibodies. Expression of wild type and catalytically active Flag-OspD2, Flag-OspD3 and Flag-EspL were detected using anti-Flag antibodies. Antibodies to β-actin were used as a loading control. Immunoblots are representative of at least three independent experiments.

A

B

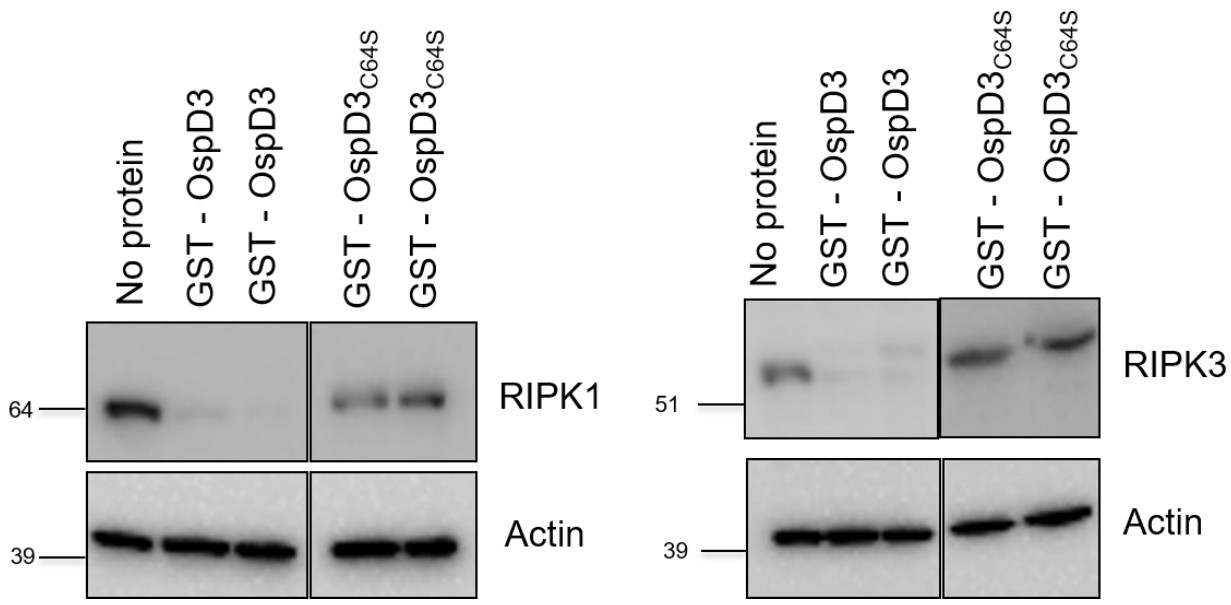

Figure 3. 4: Purified OspD3 cleaves endogenous RIPK1 and RIPK3 in HT-29 cell lysates

Immunoblots showing cleavage of RIPK1 (A) and RIPK3 (B) by purified OspD3 in HT-29 cell lysates. Expression of endogenous RIPK1 and RIPK3 were detected using anti-RIPK1 and anti-RIPK3 antibodies. Antibodies to β-actin were used as a loading control. Immunoblots are representative of at least three independent experiments.

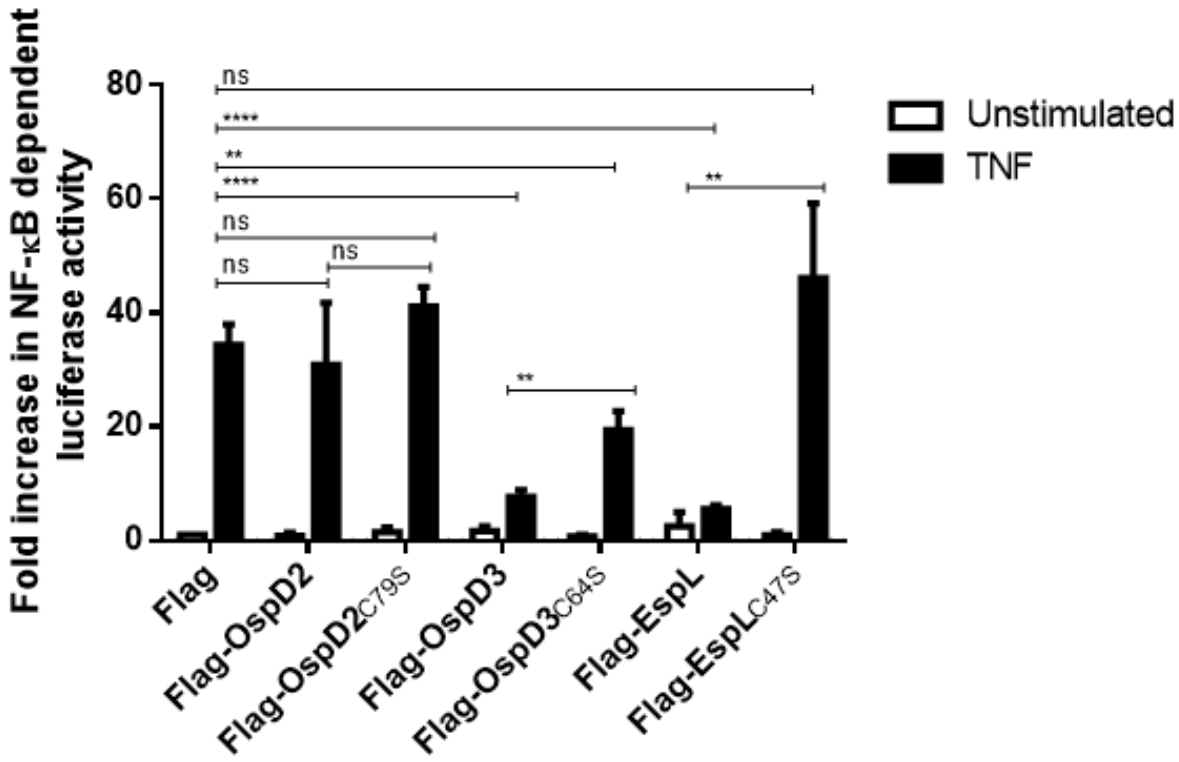

Figure 3. 5: **OspD3 and EspL inhibit NF-κB dependent gene transcription of a luciferase reporter.**

Fold increase in NF-κB-dependent luciferase activity in HEK 293T cells transfected with p3xFlag-*Myc*-CMV-24 (Flag), pFlag-OspD2, pFlag-OspD2$_{C79S}$, pFlagOspD3, pFlagOspD3$_{C64S}$, pFlag-EspL or pFlag-EspL$_{C47S.}$ Cells were left unstimulated or stimulated with TNF for 3 hours where indicated. NF-κB activation was measured as a fold change initially normalised to *Renilla* luciferase and then to unstimulated Flag-expressing cells. Results are the mean ±SEM of three independent experiments carried out in duplicate. (Significantly different to p3xFlag-*Myc*-CMV-24-transfected HEK 293T cells stimulated with TNF.) *p< 0.05, **p< 0.01, ***p< 0.001, ****p<0.0001, two-tailed unpaired T test.

A

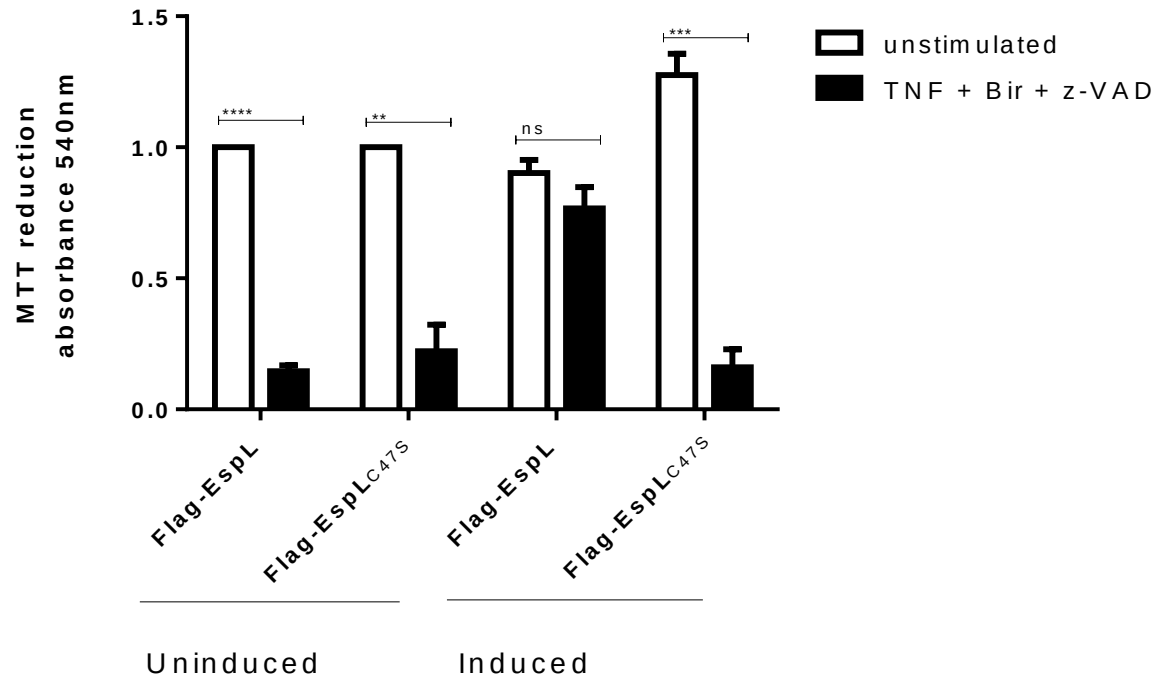
MTT reduction
absorbance 540nm
1.5
1.0
0.5
0.0
****
**
ns
***
unstimulated
TNF + Bir + z-VAD
Flag-EspL
Flag-EspLC47S
Flag-EspL
Flag-EspLC47S
Uninduced
Induced

B

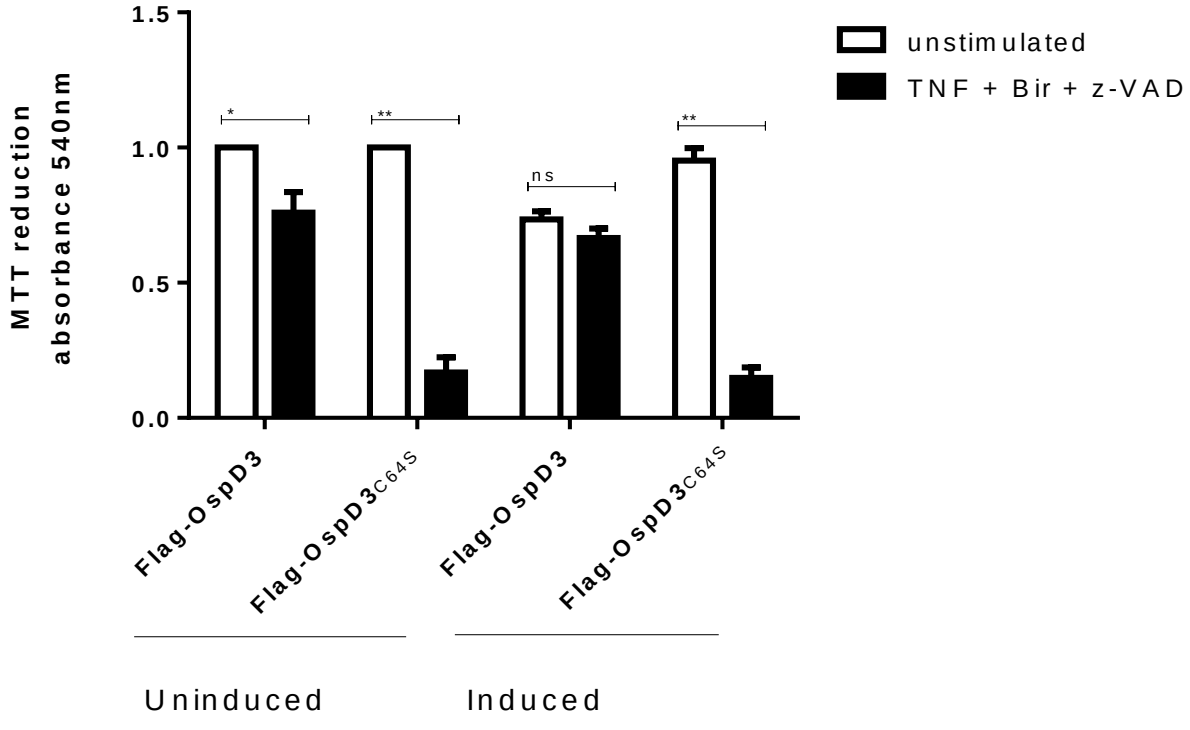
MTT reduction
absorbance 540nm
1.5
1.0
0.5
0.0
*
**
ns
**
unstimulated
TNF + Bir + z-VAD
Flag-OspD3
Flag-OspD3C64S
Flag-OspD3
Flag-OspD3C64S
Uninduced
Induced

C

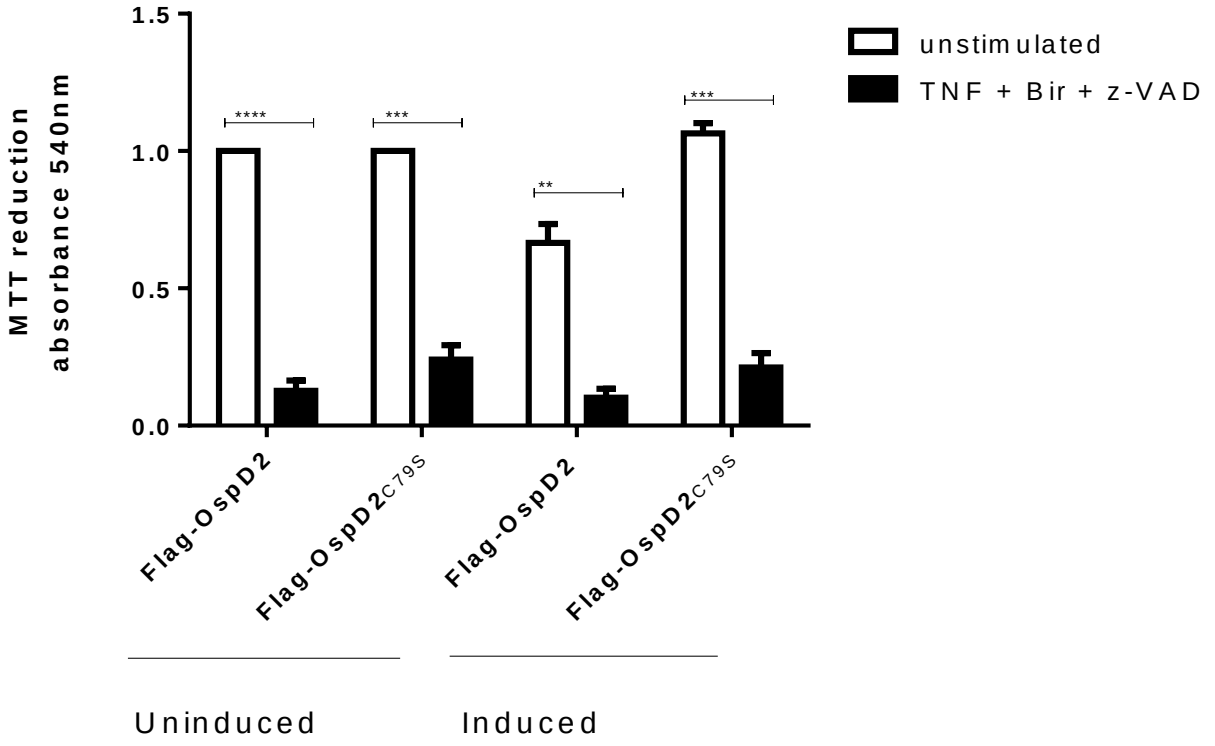
MTT reduction absorbance 540nm
1.5
1.0
0.5
0.0
unstimulated
TNF + Bir + z-VAD
****
***
**
***
Flag-OspD2
Flag-OspD2C79S
Flag-OspD2
Flag-OspD2C79S
Uninduced
Induced

D

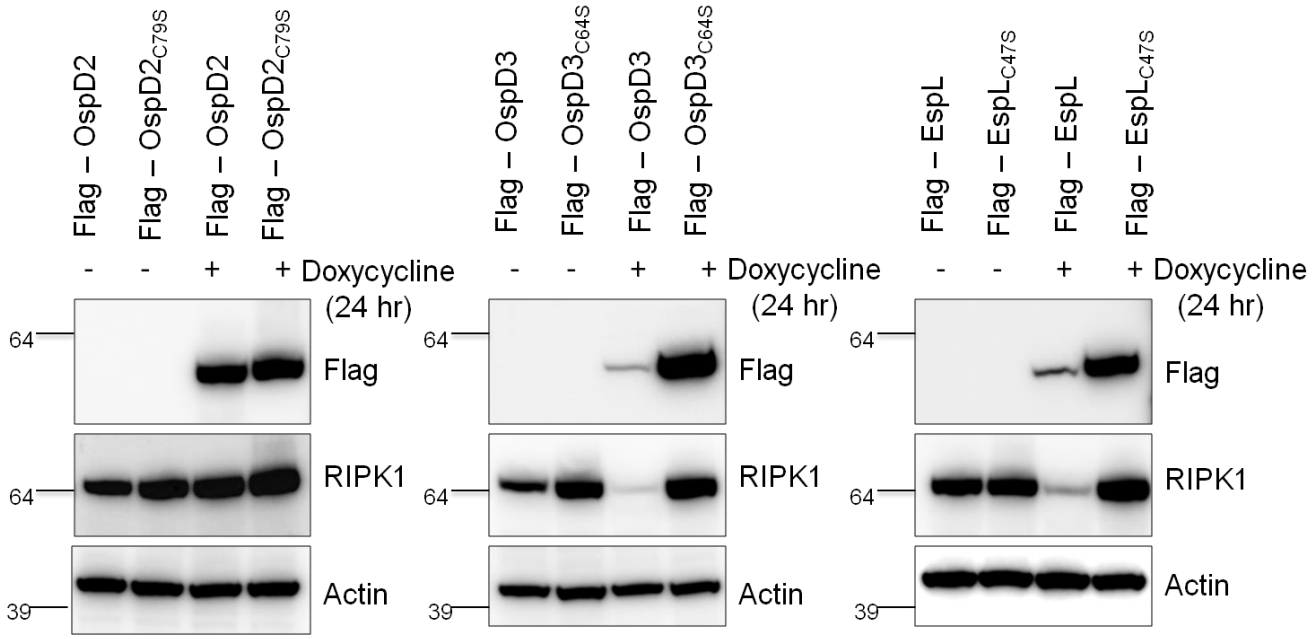
Flag – OspD2
Flag – OspD2C79S
Flag – OspD2
Flag – OspD2C79S
- - + + Doxycycline (24 hr)
Flag – OspD3
Flag – OspD3C64S
Flag – OspD3
Flag – OspD3C64S
- - + + Doxycycline (24 hr)
Flag – EspL
Flag – EspLC47S
Flag – EspL
Flag – EspLC47S
- - + + Doxycycline (24 hr)
64
Flag
64
RIPK1
39
Actin

Figure 3. 6: **OspD3, like EspL, inhibits TNF-induced necroptosis**

MTT reduction in doxycycline-inducible HT-29 cells stably expressing (A) Flag-EspL, Flag-$EspL_{C47S}$, (B) Flag-OspD3, Flag-$OspD3_{C64S}$, (C) Flag-OspD2 and Flag-$OspD2_{C79S}$ and treated with TNF, z-VAD and birinapant for 24 hours. Results are the mean ±SEM of absorbance at 540 nm from three independent experiments carried out in duplicate, and normalised to unstimulated, uninduced Flag-EspL, Flag-OspD2 or Flag-OspD3 cell lines. (Significantly different to induced cells left unstimulated and stimulated with TNF, z-VAD and birinapant). *p< 0.05, **p< 0.01, ***p< 0.001, ****p<0.0001, two-tailed unpaired T test. (D) Immunoblot showing levels of levels of RIPK1 in doxycycline inducible HT-29 cell lines expressing Flag-EspL and Flag-$EspL_{C47S}$, Flag-OspD3 and Flag-$OspD3_{C64S}$ or Flag-OspD2 and Flag-$OspD2_{C79S}$ with and without doxycycline induction. Expression of RIPK1 was detected using anti-RIPK1 antibodies. Expression of wild type and catalytically active Flag-OspD2, Flag-OspD3 and Flag-EspL were detected using anti-Flag antibodies. Antibodies to β-actin were used as a loading control.

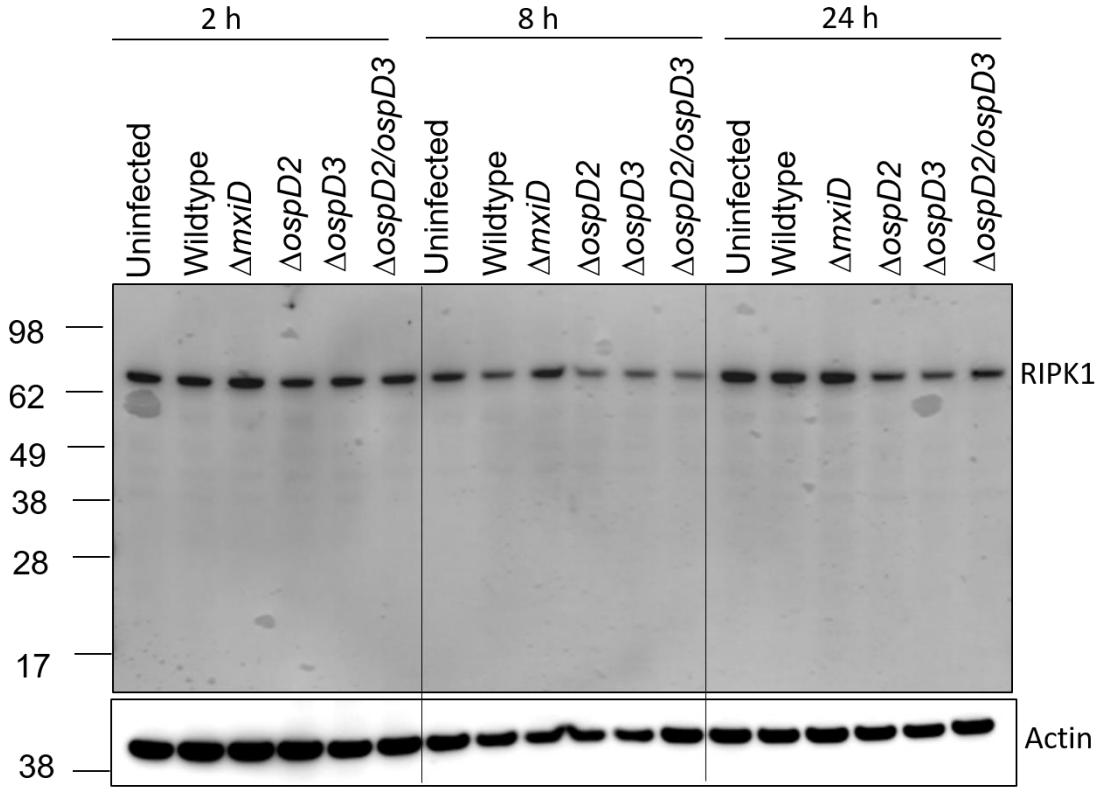

Figure 3. 7: **No cleavage of RIPK1 in HeLa 229 cells upon infection with wildtype and mutant *S. flexneri* 2a, 2457T strains.**

Immunoblot showing RIPK1 expression in HeLa 229 cells either left uninfected, or infected with WT *S. flexneri* 2a, 2457T, Δ*mxiD*, Δ*ospD2*, Δ*ospD3* and Δ*ospD2ospD3*. Infections were carried out at three timepoints of 2 h, 8 h and 24 h. RIPK1 expression was detected using anti-RIPK1 antibodies. Antibodies to β-actin were used as a loading control. Representative immunoblots of at least three independent experiments.

Chapter Four:

Identification and characterisation of host targets of OspD2 and OspD3 using SILAC-based PROTOMAP

CHAPTER 4: Identification and characterisation of host targets of OspD2 and OspD3 using SILAC-based PROTOMAP

4.1 Introduction

Proteins are macromolecules with multiple domains and a diverse range of functions. Here, we hypothesised that the *Shigella* effectors, OspD2 and OspD3 may have multiple functions in host cells, with several host targets. Findings from our previous chapter showed that, similar to EspL from EPEC, OspD3 may be involved in cleaving the RHIM proteins, RIPK1 and RIPK3. However, unlike EPEC, this was not seen during *Shigella* infection for RIPK1. Thus, we concluded OspD2 and OspD3 may be targeting additional host proteins during *Shigella* infections. To test this, we utilised an unbiased approach to determine the range of host cell targets of OspD2 and OspD3. We used a proteomics approach for identifying host targets, rather than traditional protein-interaction approaches such as co-immunoprecipitation and yeast-two-hybrid screens.

In order to identify proteins cleaved by OspD2 and OspD3, and to better understand the protease-substrate relationships on a global level, stable isotope labelling with amino acids in cell culture (SILAC) was coupled with a proteomics approach, termed PROTOMAP (Protein Topography and migration analysis platform) [351, 352]. This approach distinguishes proteolytic events in the cells by identifying shifts in protein migration using a combination of proteomics and SDS-PAGE [352]. Furthermore, by coupling this approach with stable isotope labelling, it was possible to introduce a difference in mass between the two proteomes being studied (cells expressing active versus inactive enzyme) [353, 354]. A major advantage of this approach is that due to the differentially labelled peptides, the two proteomes can be analysed simultaneously. Also by combining these differently labelled peptides at the initial steps of the workflow, we can avoid any variation obtained as a result of sample processing including differences in protein separation or non-specific proteolysis, in order to achieve a higher degree of accuracy during quantification [355]. By labelling cells expressing the wild type and catalytically inactive OspD2 and OspD3 with isotopically heavy and light amino acids respectively, we can identify any changes in the host cell proteins as a result of these effectors.

Using the stable cell lines designed in Chapter 3, we undertook a target screen using PROTOMAP. From this, we identified proteins to be involved in anti-viral defences as possible proteolytic targets of OspD2 and OspD3. A main component of the host anti-viral defence is type I IFN signalling. Compared to type II and III IFNs, type I IFNs (IFNα/β) are expressed

broadly in almost all cell types [356]. They signal via the heterodimeric IFNAR receptors to activate JAK/STAT signalling which ultimately forms the ISGF3 complex, comprised of phosphorylated STAT1, STAT2 and IRF9. This complex then translocates to the nucleus to induce the transcription of almost 300 ISGs [207, 356]. ISGs exhibit various roles during infection by either inhibiting crucial steps in pathogenesis, inducing host cell death or activating the innate and/or adaptive immune response [357, 358].

Since the initial discovery of type I IFN in 1957, IFNα and β has been well studied with established roles in antiviral responses [359]. The type I IFN response is usually beneficial to the host by inhibiting viral replication [207, 360]. Deletion of IFNAR1 or other downstream components of type I IFN signalling in animal models of viral infections, results in an increase in viral replication and spread and subsequent lethality [361]. This has been reported during infections with vesicular stomatitis virus (VSV), lymphocytic choriomemingitis virus (LCMV) and west nile virus (WNV) which resulted in an increased mortality of mice upon IFNAR1 deletion [362]. Furthermore, it was seen that type I IFN production during mouse hepatitis virus (MHV) and coronavirus infection was necessary to limit viral replication [363].

In contrast, the interaction between bacterial pathogens and type I IFN signalling/production and ISGs is not well understood. It has been reported that type I IFN signalling can both positively and negatively regulate bacterial infection. For instance, type I IFN signalling has a detrimental effect on the host during infections with bacteria such as *Listeria monocytogenes*, *Francisella tularensis*, *Salmonella*, and *Staphylococcus aureus*. Alternatively, type I IFN signalling is protective to the host during infections with bacteria such as *Legionella*, *Streptococcus pyogenes* and *Helicobacter pylori* [207]. This disparate effect of type I IFN signalling depends on a few factors, such as the host cell type, the duration and timing of the response as well as the magnitude of the response [207]. Hence, since our screen for host targets of OspD2 and OspD3 revealed proteins involved in type I IFN signalling, we investigated this interaction during *Shigella* infection. This work provides new insights into the different signalling pathways targeted by bacterial effector proteins.

4.2 Results

4.1 SILAC based PROTOMAP screen

We wanted to employ an unbiased approach to determine the host cell targets of OspD2 and OspD3. For this, we carried out a SILAC-based PROTOMAP screen, where doxycycline inducible HT-29 cell lines expressing wild type Flag-OspD2 and Flag-OspD3 were labelled with "heavy" (Arg4/Lys6) amino acids and their respective catalytic mutants with "light" (Arg0/Lys0) amino acids (Figure 4.1). The expression of the cysteine proteases was then induced with doxycycline for 6 hours before the cells were lysed. Protein amounts were quantified so that an equal quantity of both wild type and catalytically inactive protease-expressing cell lysates could be mixed at a ratio of 1:1 before separation by SDS-PAGE. The resulting gels were fixed and stained with Coomassie G-250 according to protocol of Kang *et al.*[307]. 25 evenly spaced contiguous bands, ranging in size from 198kDa to 6KDa, were excised and subjected to tryptic in gel digestion before analysis of peptides by mass spectrometry. Peptides were searched against the UniProt/Swiss-Prot human database supplemented with the sequence of OspD2 and OspD3. A peptide protein ratio was calculated by identifying a peptide and comparing the intensity of the identified peptide to its isotopologue. The overall SILAC ratio was then calculated by comparing the ratio of isotopologues for each peptide and this was summed up to give a protein level ratio which is represented on volcano plots (Figure 4.2A and C). Proteins observed to consistently and significantly change in abundance (with a $p<0.05$) and with a $\log_2$ average fold change of more than 1 or -1 were of interest for further analysis. Detailed information of the proteins identified is represented in tables 4.2B and D, which includes the fold change (SILAC ratio) and statistical significance across the 3 replicates. From the OspD2 PROTOMAP analysis we identified JAKMIP3 (Janus kinase and microtubule-interacting protein), MX2 (interferon induced GFP-binding protein), APOB (Apolipoprotein B) and MAP4 (microtubule associated protein 4) to have the highest fold change values, being less abundant when wild type OspD2 was present. However, no changes in the abundance of RHIM containing proteins were identified. This was in agreement with our previous findings that OspD2 did not cleave the RHIM proteins RIPK1 and RIPK3.

From the OspD3 PROTOMAP analysis, we identified RIPK1 as a hit with a fold change of -3.22 (Figure 4.2C and D). This was also consistent with our previous findings that OspD3 cleaved RIPK1. However, we did not detect RIPK3 as a significant hit from the screen. This

could be due to the duration of induction of the HT-29 stable cell lines with doxycycline of 6 hours, although our previous immunoblotting suggested cleavage of the RHIM proteins at 6 hours induction with doxycycline. Perhaps a longer induction time would result in detectable cleavage of RIPK3 in this PROTOMAP screen. We also identified several anti-microbial proteins such as MX2, OAS2, OAS1, IFIT1, ISG15 and IRF9 as hits in the OspD3 PROTOMAP screen.

In order to associate the significant protein hits according to their functions, we carried out an enrichment analysis (Figure 4.3A and 4.3B). The enrichment analysis was carried out using a Fisher exact test within the Perseus software. The Fisher exact test is a statistical test which is routinely used to identify the occurrence of non-random association between proteins or variables [364]. Using the results from the Fisher exact test, a heat map was generated via Multiple experiment viewer (MEV) where keyword enrichment terms were plotted against the enrichment factor calculated. From this we saw both screens were enriched for protein involved in antiviral defence and innate immunity.

4.2 OspD2, OspD3 and EspL inhibit ISRE-dependent gene transcription of a luciferase reporter.

Since we identified anti-viral and interferon-related proteins as targets in both the OspD2 and OspD3 PROTOMAP screens, we chose this pathway for further investigation, in particular the effect of OspD2, OspD3 on type I IFN signalling. We also used EspL as a control in this assay, where we tested the ability of OspD2, OspD3 and EspL to inhibit type I IFN induced ISRE-dependent gene transcription of a luciferase reporter. Upon stimulation with IFNα, ISRE-dependent transcription was evident in HEK 293T cells transfected with the empty vector p3xFlag-*Myc*-CMV-24 in comparison to unstimulated cells (Figure 4.4). Overexpression of wild type Flag-OspD2, Flag-OspD3 and Flag-EspL all inhibited ISRE-dependent transcription. In contrast, the catalytically inactive Flag-OspD2$_{C79S}$, Flag-OspD3$_{C64S}$ and Flag-EspL$_{C47S}$ further activated ISRE gene transcription in the presence of IFNα. This result supported our initial hypothesis that both OspD2 and OspD3 may inhibit type I IFN signalling, and that this was dependent on their cysteine protease activity.

4.3 OspD3 cleaves IRF9 in co-transfected HEK 293T cells

Type I IFN signalling is initiated when IFNα/β bind to the IFNAR receptors. IRF9 is integral to the type I IFN signalling pathway and upon activation, complexes with phospho-STAT1 and phospho-STAT2 to form the transcriptionally active ISGF3 complex. ISGF3 translocates into

the nucleus to bind to ISRE elements present in the promoter of ISGs and induces their expression [365]. Since we observed OspD2 and OspD3 inhibited IFN-induced ISRE-dependent transcription, we deduced that one or more proteins in this pathway were targeted for cleavage by OspD2 or OspD3.

One particular protein of interest that was identified as a potential target in the OspD3 screen was IRF9. Formation of the ISGF3 complex which includes IRF9 is central to type I IFN signalling [366], and since the role of type I IFN during bacterial infections is severely unstudied, we presumed IRF9 was a good choice for further analysis [359]. IRF9 had SILAC ratio of -1.88 in the presence of active OspD3. In addition to this, we also identified several ISGs (IFIT1, MX2, OAS1, ISG15 and IFIH1) as hits in the OspD3 PROTOMAP screen. We assume these ISGs identified may be either direct or indirect targets as a consequence of IRF9 cleavage by OspD3.

It is known that STAT2-IRF9 can form a complex without the need for any stimulus or subsequent signalling by the type I IFN receptors to produce the basal expression of many ISGs [367]. We therefore next wanted to confirm the expression levels of IRF9 in HT-29 cell lines without the presence of any stimulus. This would then support the identification of IRF9 as a target protein in the OspD3 PROTOMAP screen, which was carried out without the presence of any stimulus. As a positive control, we treated HT-29 cells with either IFNα or IFNγ over 24 hours to induce IRF9 expression. Samples were lysed and tested for IRF9 expression by immunoblotting. As suspected, we detected the presence of IRF9 without any stimulation with IFNα and IFNγ (Figure 4.5A and 4.5B). However, stimulation with either IFNα or IFNγ greatly increased expression of IRF9 over time (Figure 4.5A and 4.5B).

To validate our observation and test the ability of OspD3 to cleave IRF9, we transfected Flag-OspD3 and Flag-OspD3$_{C64S}$ and HA-IRF9 into HEK 293T cells. Flag-OspD2, Flag-OspD2$_{C79S}$, Flag-EspL and Flag-EspL$_{C47S}$ were also tested, and p3xFlag-*Myc*-CMV-24 was used as a control. We then lysed the cells and examined HA-IRF9 expression by immunoblotting (Figure 4.6). The protein levels of IRF9 were not affected in the presence of both wild type and catalytically inactive Flag-OspD2 and Flag-EspL. However, a significant reduction in HA-IRF9 levels was noted in the presence of wild type Flag-OspD3. This was dependent on the catalytic activity of OspD3, as IRF9 was not affected by the presence of Flag-OspD3$_{C64S}$. At the same time, we detected a band smaller in size to IRF9, at around 28 kDa in the sample containing active Flag-OspD3, indicating OspD3-induced cleavage product of HA-IRF9.

Based on the size of the cleaved fragment, we predicted the cleavage site to be in the central region of IRF9. IRF9 comprises of three main domains, including a DNA binding domain from residues 9-116 and a IRF association domain (IAD) from residues 214-393 which are joined by a middle linker or regulatory domain from residues 117-213 [368].

To determine which domains of IRF9 were cleaved by OspD3, we created a truncated version of IRF9 containing DNA and regulatory domains ($IRF9_{9-213}$) and the regulatory and IAD domains ($IRF9_{117-393}$). This truncated IRF9 was then cloned with 4X N terminal HA tag into pCDNA3. We co-transfected Flag-OspD2, Flag-$OspD2_{C79S}$, Flag-OspD3, Flag-$OspD3_{C64S}$, Flag-EspL or Flag-$EspL_{C47S}$ with HA-$IRF9_{9-213}$ and HA- $IRF9_{117-393}$ and examined whether OspD3 cleaved HA-$IRF9_{117-393}$ by immunoblotting. Levels of $IRF9_{9-213}$ were somewhat reduced upon expression of FLAG-OspD3 (Figure 4.7A). However, we did not detect a cleaved fragment of HA-IRF9 at around 28 kDa as seen previously (Figure 4.6), but instead we saw a larger cleaved fragment of IRF9 at around 32 kDa. Levels of $IRF9_{117-393}$ were also somewhat reduced upon expression of Flag-OspD3 (Figure 4.7B) and a fragment around 28 kDa was detected in this sample, possibly indicating cleaved IRF9. We concluded that the middle regulatory domain was indeed necessary for the cleavage of IRF9 by OspD3, however the DNA binding domain was also important for IRF9 to be completely recognised by OspD3.

4.4 Ectopic co-expression of OspD2, OspD3 and EspL with human IRFs in HEK 293T cells.

The IRF protein family includes 9 members, that play important roles in the regulation and activation of immune response genes involved in both the innate and adaptive immune response [369, 370]. All 9 IRFs exhibit a similar architecture and are highly conserved in their N-terminal DNA binding domain which contains 5 tryptophan repeats (Figure 4.8A). The IRFs have a more variable C-terminal domain which includes the IRF association domain (IAD) that is required for either hetero- or homo-dimerisation with other IRFs as well as with transcription factors [371, 372] (Figure 4.8B). Amongst the IRFs, IRF3 and IRF7 are involved upstream in the production of IFNα/β in response to signalling with different TLRs such as TLR3,4,7 and 9 [373]. IRF3 is constitutively expressed in all cell types whereas IRF7 is expressed in high levels in plasmacytoid DCs (pDCs) [374]. Expression of IRF7 can be enhanced by type I IFNs, resulting in a positive feedback loop to maximise the type I IFN response [375].

Given that the IRFs contain protein domains with significant sequence similarity, we wanted to investigate if OspD2, OspD3 or EspL cleaved any of the other IRFs. For this, we co-

expressed each of the IRFs with an N-terminal 4X HA tag with either p3xFlag-*Myc*-CMV-24, or Flag-tagged OspD2, OspD3, EspL or their catalytic mutants. We then lysed the cells and examined cleavage of the IRFs by immunoblotting (Figure 4.8C-J).

We detected reduced levels of IRF1 in the presence of Flag-OspD3 (Figure 4.8C). A band smaller than the size of HA-IRF1 was also detected at around 40 kDa, which could represent a cleaved fragment of IRF1. This smaller sized IRF1 fragment was also seen in the presence of Flag-OspD2 (Figure 4.8C). However, the levels of full-length HA-IRF1 were unaffected in this sample. No changes in HA-IRF1 levels were detected in the presence of Flag-EspL and the catalytically inactive mutants (Figure 4.8C).

No decrease in HA-IRF2 was detected in the presence of the wild type and catalytically inactive OspD2, OspD3 or EspL (Figure 4.8D). However, several weak bands smaller than the size of HA-IRF2 were observed in the presence of Flag-OspD2. We presumed that these smaller fragments may be due to HA-IRF2 being weakly targeted by Flag-OspD2 at multiple sites.

Levels of full length HA-IRF3 were reduced in the presence of Flag-OspD3, but there was no cleavage product detected (Figure 4.8E). However, in the presence of both Flag-OspD2 and Flag-EspL, the opposite was observed. No changes in levels of full length HA-IRF3 were detected in these samples, but we saw bands smaller than the size of HA-IRF3 at around 38 kDa and 28 kDa, which could represent cleavage products (Figure 4.8E).

Similar to HA-IRF2, we did not observe a decrease in the levels of full-length HA-IRF4 in the presence of any of wild type and catalytically inactive OspD2. OspD3 and EspL (Figure 4.8F). However, weak bands smaller than full length HA-IRF4 at around 28 kDa were seen in the presence of Flag-OspD3 and Flag-EspL (Figure 4.8F).

OspD3, but not OspD2 or EspL decreased the levels of full-length HA-IRF5 (Figure 4.8G), although several bands smaller than full length HA-IRF5 were detected upon expression with Flag-OspD2 at around 38 kDa and 28 kDa (Figure 4.8G).

Subsequently we also saw that levels of HA-IRF6 were significantly reduced upon expression of OspD3 or EspL (Figure 4.8H). In addition, we observed cleavage products smaller than the size of full-length HA-IRF6 at around 28 kDa in the presence of all three of the active cysteine proteases (Figure 4.8H). Flag-OspD3 and Flag-EspL both reduced full-length HA-IRF6 and generated a strong HA-IRF6 cleavage product. Flag-OspD2 gave rise to several weaker cleaved fragments of HA-IRF6 between 38 kDa to 28 kDa.

For HA-IRF7, we saw a decrease of the full-length protein in the presence of Flag-OspD2 and Flag-OspD3, with both proteases producing cleavage fragments of HA-IRF7 (Figure 4.8I). Flag-OspD2 also cleaved HA-IRF7 efficiently leading to significant loss of the full-length protein and a strong cleavage product of around 28 kDa.

Lastly, we co-expressed HA-IRF8 with OspD2, OspD3 and EspL and saw that levels of full length HA-IRF8 were decreased in the presence of Flag-OspD3 and Flag-EspL with possible cleavage products detected in the presence of Flag-OspD2 and Flag-OspD3 (Figure 4.8J).

The results from the co-expression studies are summarised in a table (Figure 4.8K). It is clear that OspD2, OspD3 and EspL targeted IRFs with varying specificities. In addition to IRF9, IRF1, IRF6 and IRF8 were cleaved efficiently by OspD3. Of these, the role of IRF6 in interferon signalling is not well understood but some reports suggest that IRF6 regulates TLR2 and TLR4 signalling. However, beyond these reports, the role IRF6 in IFN signalling is still unclear [376, 377]. The near complete cleavages of IRF1, IRF6, IRF8 and IRF9 by OspD3 could suggest these IRFs share similar residues for recognition and degradation by OspD3.

We observed that Flag-OspD2 cleaved both IRF3 and IRF7, which are involved in the production of type I IFN, IFNα/β. We therefore hypothesized that OspD2 may cleave IRF3 and IRF7 to inhibit type I IFN production and OspD3 may cleave IRF9 to inhibit type I IFN signalling transduction. Hence, both these cysteine proteases could be functioning cooperatively to inhibit the type I IFN response during *Shigella* infection. However, the over-expression studies performed here were a quick method for determining if further IRFs were cleaved by the cysteine proteases, and it is important to determine if the cleavage also occurs in an endogenous setting during infection. This is also important in the case of EspL, and it is crucial to determine if cleavage of IRFs occur during EPEC infection.

4.5 Cleavage of endogenous IRF3 and IRF9 in doxycycline inducible HT-29 cells expressing OspD2, OspD3 and EspL.

To further examine the roles of OspD2 and OspD3 in cleaving the IRFs, we investigated the cleavage of endogenous IRF3 and IRF9 by Flag-OspD2 and Flag-OspD3. These two IRFs in particular were chosen as IRF3 is necessary for the initial wave of type I IFN signalling and IRF9, detected in the mass spectrometry screen, is involved in type I IFN signalling transduction [365]. As IRF7 is only produced in high abundance in specific cell types such as pDCs, we carried out our further validation experiments focusing on IRF3 and IRF9 [207].

HT-29 cells were stimulated with IFNα at the same time as doxycycline induction in order to induce the production of IRF9, which has only low levels of constitutive expression (Figure 4.4). In contrast, IRF3 is constitutively expressed in cells as an inactive monomer in the cytoplasm [378]. We did not detect a reduction in the levels of either IRF3 or IRF9 upon Flag-EspL or Flag-EspL$_{C47S}$ expression (Figure 4.9A). Flag-EspL$_{C47S}$ however exhibited an increase in expression of IRF9 even without doxycycline induction, suggesting that the interferon response is already primed in these cells. More work is required to understand this particular observation (Figure 4.9A).

Next, upon doxycycline induction of Flag-OspD3 following IFNα stimulation, we detected several bands smaller than IRF3 at 24 hr, although we saw no difference in levels of full-length IRF3 (Figure 4.9B), suggesting that this may also be cleavage of IRF3 by OspD3. We also saw bands smaller than the full length IRF9 upon induction of active OspD3 (Figure 4.9B), which presumably were cleaved fragments of IRF9. The size of the cleaved fragments at around 28 kDa was consistent with the cleavage products observed in the co-expression studies with HA-IRF9 and Flag-OspD3 (Figure 4.6). As expected, we did not detect any cleaved fragments of IRF3 or IRF9 in the presence of Flag-OspD3$_{C64S}$.

When the expression of Flag-OspD2 was induced, we detected cleaved fragments of IRF3 with and without IFNα induction (Figure 4.9C). However, we did not detect any decrease in the level of full length IRF3 and we did not detect a decrease in levels of full length IRF9 or the presence of any potential IRF9 cleaved fragments in these cells (Figure 4.9C). Likewise, as seen in the other cell lines, Flag-OspD2$_{C79S}$ did not affect the levels of IRF3 or IRF9.

In conclusion, we observed that OspD2 and OspD3 cleaved endogenous IRF3 and IRF9 respectively and produced cleavage fragments of these IRFs. We therefore postulated that OspD2 and OspD3 working in concert to inhibit both arms of type IFN signalling during *Shigella* infection.

4.6 Cleavage of IRF3 and IRF9 during *Shigella* infection of HeLa 229 cells

In order to investigate the cleavage of IRF3 and IRF9 during *Shigella* infection, we carried out infections on HeLa 229 cells using wild type *S. flexneri* 2a, Δ*mxiD*, Δ*ospD2*, Δ*ospD3* and Δ*ospD2ospD3* mutants of *Shigella*. The cells were harvested for immunoblotting at 2, 8 and 24 hours post infection to include early, middle and late timepoints. The expression of IRF3 and IRF9 were detected using anti-IRF3 and anti IRF9 antibodies.

Levels of IRF3 were not reduced at 2 hours or 24 hours post infection (Figure 4.10). However, at 8 hours post infection, we observed that full length IRF3 was somewhat reduced in cells infected with Δ*ospD3* (Figure 4.10). We also saw cleaved fragments of IRF3 at around 28 kDa in the wild type and Δ*ospD3* infected cells (Figure 4.10). This cleavage of IRF3 was consistent in all the replicates performed. As expected, this cleavage and reduction of full length IRF3 was seen only when OspD2 was present, supporting our hypothesis that OspD2 cleaves IRF3.

In the case of IRF9, we saw that levels of IRF9 were induced 24-hour post infection (Figure 4.10). Increased IRF9 expression may be detectable at this later time point because *Shigella* may inhibit the interferon response in the cells at earlier timepoints, in order to facilitate replication in the cells. It is known that the type I IFN response is activated upon bacterial infection by the cGAS-STING pathway [379, 380] as bacterial components or PAMPs from *Shigella* such as LPS or cytoplasmic DNA are recognised by STING, resulting in the activation of TBK1 and IRF3 [381, 382]. Hence, delayed activation of the type I IFN response during *Shigella* infection may reflect the time required for the accumulation of cytoplasmic *Shigella* DNA in the cells, to activate the cGAS-STING pathway or reflect inhibition of the response at early timepoints. Unfortunately, however, we were unable to attribute IRF9 cleavage to OspD3 during *Shigella* infection.

4.7 IP-10 production upon stimulation with ISD in doxycycline inducible HT-29 cells expressing wild type OspD2, OspD3 and EspL, and during *Shigella* infection

One of the main features of type I IFN signalling is to prevent the spread of infection by creating a cell-intrinsic antimicrobial state in both the infected and neighbouring cells. Upon signalling, transcription of ISGs is initiated to combat infections via several mechanisms including altering cellular lipid metabolism and preventing the replication of the pathogen [383, 384]. Therefore, we wanted to investigate whether the activity of OspD2 and OspD3 resulted in a decrease in the production of ISGs, in particular by examining IP-10. IP-10 functions as a chemoattractant and plays a role in mediating immune responses by activating and recruiting immune cells such as leukocytes [385]. IP-10 secretion and expression were measured upon immune-stimulatory DNA (ISD)-stimulation of HT-29 cell lines which stably express 3xFlag-tagged OspD2, OspD3 or their catalytic mutants. ISD was added for 24 hours in order to stimulate an immune response in these cells [386]. Upon stimulation with ISD in the absence of doxycycline to induce effector expression, robust production of IP-10 was detected in all the cells, as expected (Figure 4.11A). However, we saw that the ISD-induced production of IP-10 was inhibited upon

the expression of the OspD2 and OspD3 (Figure 4.11A). This suggested that OspD2 and OspD3 could dampen the production of ISG, by inducing cleavage of IRF3 and IRF9 respectively.

We also measured IP-10 production during *Shigella* infection of HeLa 229 cells using the WT *S. flexneri 2a* strain, 2457T, Δ*mxiD*, Δ*ospD2*, Δ*ospD3* and Δ*ospD2*Δ*ospD3* strains (Figure 4.10B). Supernatant was collected at 2, 8 and 24 hours post infection and the amount of IP-10 secreted in these supernatants was measured by ELISA (Figure 4.11B). However, no differences in IP-10 production was seen at 2 or 8 hours post infection with any *Shigella* derivatives. IP-10 secretion was induced at 24 hours post infection, apart from the non-invasive *Shigella* strain Δ*mxiD*. However, no major differences in IP-10 secretion was noted amongst the other derivatives of *Shigella*. We presumed the induction of IP-10 at 24 hr post infection was due to *Shigella* replication inducing a type I IFN response at this later time point. As mentioned earlier, *Shigella* DNA in the cytoplasm of cells may activate the cGAS-STING pathway, resulting in a type I IFN response within the cells. Unfortunately, we could not attribute any inhibition of IP-10 expression to OspD2 or OspD3.

4.3 Discussion

Shigella effector proteins remodel the host cell to facilitate internalisation of the bacteria into the cell, promote bacterial replication and evasion of the host immune system [97, 129, 387]. However, the exact roles of many of these effectors are still largely enigmatic. In the previous chapter we identified OspD2 and OspD3 as cysteine proteases due to their similarity with EspL. OspD3 also cleaved the host RHIM family of proteins, similar to EspL [296]. However, cleavage of RIPK1 by OspD3 was not seen during *Shigella* infections of HeLa 229 cells. As such, we wanted to utilise a non-biased approach to determine the proteolytic targets of OspD2 and OspD3.

Recently, many innovative techniques have emerged to decipher proteins functions [351]. Some examples include *in vitro* specificity profiling approaches such as phage, peptide and bacterial display and yeast two hybrid screening [388-390]. Likewise, the functions and interacting partners of bacterial effector proteins may also be determined using these approaches. For instance, the effectors can be used to screen to a library of potential host protein targets to determine if any interactions exist between them. An example of this is the yeast two hybrid system, where commercially available cDNA libraries of host cells are used as prey against effectors which function as bait. This approach has also previously identified cross-talk in cells between proteins which have not been predicted to interact [391]. However, yeast two hybrid screens are known to yield false positive and false negative results especially if there is a lack of post translational modification present in the yeast system which is being used to determine the interaction between proteins [391, 392]. Interaction studies also have limitations in screening with enzymes that may interact only transiently with their substrate.

Two-dimensional gel electrophoresis (2-DGE) has been used for determining cleavage of proteins by example changes in the rate of migration of cleaved proteins upon exposure to a putative protease (or effector proteins in this case). This approach also provides the benefit of determining the interaction in an endogenous setting [393-396]. However, there are also several limitations with this technique such as being relatively low throughput, labor intensive, and having a narrow dynamic range. Furthermore separation of extremely acidic or basic proteins as well as hydrophobic proteins can be difficult [397].

The technique we used in this study to determine potential host cell targets of OspD2 and OspD3 was a SILAC-based PROTOMAP screen [352]. In this approach, we took advantage of the fact that there is a change is the molecular weight of proteolytically cleaved proteins as compared to their intact precursors. This change can be reflected after SDS-PAGE where the

cleaved proteins generally have lower molecular weight and can be separated by electrophoresis. Furthermore, by incorporating SILAC labelling, we were able to directly compare the effect of the proteases with their catalytic mutants when expressed in HT-29 cells in a single experiment. By combining an equal quantity of cell lysates expressing wild type and catalytically inactive proteases at an early stage of the experiment, we were also able overcome any errors which may have arisen due to sample processing or reproducibility. In addition, we were able to achieve high molecular weight resolution by processing the SDS-PAGE in 25 evenly sized bands.

The information obtained from the PROTOMAP screen was three dimensional. After in-gel digestion was carried out, each of the gel slices consisted of peptides from proteins of a molecular weight which corresponded to that particular position in the gel. The data analysis therefore provided information on the protein sequence and the location of the peptide identified as well as an estimate of the molecular weight of proteins in that particular region of the gel. Upon cleavage of host proteins by the cysteine proteases, the full-length host proteins will decrease in abundance. In addition to this, cleaved fragments of the host proteins may be detected in a gel slice containing proteins with a lower predicted molecular weight. Finally, the SILAC labelling allowed us to determine if this cleavage arose within cells expressing the wildtype or catalytically inactive proteases [314].

From our PROTOMAP screens we identified a series of related host proteins in both the OspD2 and OspD3-expressing cells that were decreased in comparison to cells expressing the catalytically inactive mutants. The host cell proteins identified in both screens were predominantly associated with antiviral defence and innate immune pathways. It is known that some *Shigella* effectors function by modulating the host cell response including the innate and adaptive immune responses and cell death [336, 398]. However, it was surprising that “anti-viral defense” was the most enriched keyword term for both the bacterial effectors OspD2 and OspD3. In the OspD2 screen, we identified several host cell proteins which were significantly decreased in the presence of the active protease. These proteins have various functions and include JAKMIP3, MX2, APOB and MAP4. Interestingly, MAP4 is a microtubule associated protein which has been previously shown to play a role with a *Shigella* T3SS effector, VirA [118], although however the subsequent reports suggest that VirA does not target microtubule degradation and depolymerisation [119].

APOB was also identified as a hit in the OspD2 screen. APO (apolipoprotein) are proteins which interact with cholesterol to form a complex called lipoprotein [399]. Lipoproteins contain a membrane of phospholipids, apolipoproteins and free cholesterol surrounding a core region consisting of cholesterol esters. Apolipoproteins in particular have four main roles. They serve as ligands for lipoprotein receptors, have a structural function, aid in lipoprotein formation and regulate lipoprotein metabolism [399]. Lipoproteins in particular have a key role in the absorption and transport of lipids [400]. Lipoproteins have also been shown to inhibit host tissue invasion by bacteria through blocking the adhesion of bacteria to host cells [401]. In addition to this, lipoproteins block cell to cell communication in bacteria which is necessary for the initiation of virulence factors [402]. Peterson *et al.* reported that APOB is a crucial innate defence effector against *Staphylococcus aureus* infections [403]. During infection, *S. aureus* generates an autoinducing peptide which interacts with bacterial surface receptors to allow invasive enzymes and toxin production. APOB binds to these autoinducing peptides to inhibit them and decrease the infectivity of the bacteria [402, 403]. Although the role of APOB during *Shigella* infection has not been studied, it is possible that APOB may also block *Shigella* from adhering to host cell receptors and that OspD2 may cleave APOB to inactivate it. However, this remains to be determined as APOB cleavage was not confirmed in this study.

MX2 (MX dynamin like GTPase 2) is an antiviral protein involved in both type I and type III IFN signalling processes, and was also identified as a potential target of OspD2 and OspD3. MX2 is a member of the small family of dynamin-like large guanosine triphosphatases (GTPases) and is also closely linked to the dynamin GTPase family [404]. MX2 has been extensively studied for its role in inhibiting the early stages of viral replication *[405, 406]*. Although MX2 has not been previously reported to be involved in *Shigella* infections, other interferon-induced GTPases have been shown to inhibit the motility of *Shigella*. It was previously demonstrated that GBPs (GTPase family of guanylate-binding proteins) coat Shigella to prevent actin-based mobility and cell to cell spread. *Shigella* coated by GBP1 can replicate but are not able to form actin tails, resulting in their aggregation in the cytoplasm [407]. However, the *Shigella* ubiquitin ligase effector IpaH9.8 is able to ubiquitylate GBP1, resulting in proteosomal degradation of the GBP coat. This in turn allows the bacteria to continue to spread from cell to cell during infection *[273]*. Since MX2 belongs to the family of interferon inducible GTPases, there is a possibility that OspD2 and OspD3 may also be inhibiting *Shigella* mediated actin tail mobility and OspD2 may be involved in inhibiting the action of MX2. Again, this requires experimental confirmation.

From the OspD3 PROTOMAP screen, we identified RIPK1 as a significant host target. This was in line with our findings from the previous chapter where we showed that OspD3 cleaved the RHIM proteins RIPK1 and RIPK3. Further analysis of the raw SILAC data, revealed that RIPK3 was indeed identified in one of the replicates of the experiment with a fold change of -4.42. However, this result was only in one replicate and was not significant and was not validated as a hit. Even though from our previous work, we found that OspD2 and OspD3 did not target RHIM proteins during infection of HeLa 229 cells, we assumed that overexpression of OspD3 in the lentiviral cell line resulted in more broadened substrate cleavage.

From the OspD3 screen, one protein, IRF9 was of particular interest, as plays a central role in type I IFN signalling [408]. Another important observation from both screens was the identification of many ISGs that were less abundant in cells expressing the active proteases. Some of the common ISGs identified were OAS2, PARP14, MX2, IFIT3, OASL, ISG15, PSMB9, CCL2, OAS1, DDX58, PARP, IFIH1 and IFIT1 from the OspD2 screen and OAS2, MX2, IFIH1, DDX58, OASL, IFIT1 and ISG15 from the OspD3 screen [409]. This led us to the hypothesis that OspD3 and OspD2 may inhibit type I IFN signalling pathways. In support of our hypothesis, we found that both OspD2 and OspD3 inhibited IFNα-induced expression of an ISRE-dependent luciferase reporter. Interestingly, we observed that EspL also inhibited IFNα signalling. We think EspL may indirectly target proteins upstream of the type I IFN pathway. For example, EspL cleaves the RHIM protein such as TRIF and this could inhibit downstream type I IFN signalling [296]. However, further investigation is required to determine precisely how EspL inhibits type I IFN signalling and whether this occurs during EPEC infection.

Inhibition of ISRE-dependent signalling by OspD3 was consistent with cleavage of IRF9, which was indicated in the PROTOMAP screen. We also detected OspD3 cleavage of IRF9 which produced a cleavage fragment of IRF9 around 28 kDa in size (Figure 4.6). IRF9 is made up of 2 distinct domains, the DNA binding domain (DBD) and the IRF association domain (IAD) which are then joined by a linker or regulatory domain [368]. Based on the size of the cleaved fragment, we predicted that OspD3 cleaved IRF9 mid-way in the regulatory/linker domain.

We also investigated whether OspD2, OspD3 and EspL were able to cleave other IRFs. There are a total of 9 different IRFs, which share highly conserved N-terminus but differ in the C-terminus [365]. Upon co-transfection with the IRFs, we saw that OspD2, OspD3 and EspL

cleaved the IRFs with differing specificities. OspD3 predominately targeted IRF9 but was involved in both the reduction of full-length and generation of cleaved fragments upon interaction with most of the IRFs. OspD2 on the other hand mostly generated cleaved fragments of the IRFs without affecting full-length protein levels, with predominately targeting of IRF3 and IRF7. The minimal change in levels of full-length protein may explain why these were not detected in the PROTOMAP screen. Furthermore, Odendall *et al* have also shown by infections of cell lines such as BDMCs, THP1s and T48 cells that *Shigella* infection is able to induce IFNβ expression and hence trigger a type I IFN response, following infection [410]. This therefore may explain the cleavage of the IRFs by OspD2 and OspD3.

From the PROTOMAP screen and co-transfection studies we hypothesised that, OspD2 and OspD3 may be working together to inhibit type I IFN signalling, where OspD2 cleaves IRFs involved upstream in type I IFN production, such as IRF3 and IRF7 and OspD3 cleaves IRF9, which is downstream of type I IFN signalling. In line with this hypothesis, enterovirus 71 3C cleaves IRF7 and IRF9, targets both production of and signalling induced by type I IFN through the activity of the 3C protease [411, 412]. Similarly, the *Shigella* effectors OspD2 and OspD3 may be functioning cooperatively to facilitate bacterial pathogenicity.

When focusing on the cleavage of endogenous IRF3 and IRF9 by OspD2 and OspD3, we observed cleaved fragments of endogenous IRF3 in the presence of OspD2 and cleaved fragments of endogenous IRF9 in the presence of OspD3. We decided to initially test IRF3 instead of IRF7, as IRF3 is constitutively expressed in all cell types whereas IRF7 is only constitutively expressed in pDCs.

Our results suggested that OspD2 and OspD3 may be functioning cooperatively in inhibiting the type I IFN signalling pathway. Although these *in vitro*, functional investigations may be instrumental in elucidating effector protein functions, these methods do not necessarily reveal how OspD2 and OspD3 function during infection. As such, the role of OspD2 and OspD3 in targeting the type I IFN signalling pathways and cleaving the IRF proteins during infection was determined. As expected, we did observe cleavage of IRF3 in the presence of *Shigella* strains expressing OspD2 (wild type and Δ*ospD3* strains) at 8 hours post infection. We also detected a cleaved fragment of IRF3 at around 28 kDa in these samples. In contrast, levels of IRF9 were induced 24 hours post infection, possibly due to the activation of a type I IFN response during *Shigella* infection at this later timepoint. Previous reports have suggested that the cGAS-STING pathway is activated in infected cells after accumulation of cytoplasmic *Shigella* DNA

[283]. We did not detect any cleavage of IRF9 at the time when IRF3 cleavage was observed perhaps, due to low levels of IRF9 in induced cells. However, after 24 hours of infection, we also did not detect cleavage product of IRF9. Potentially this may be due to IRF9 being induced and cleaved at a similar rate and rapid degradation of a cleavage product. Nevertheless, we were unable to validate IRF9 cleavage during infection.

One outcome of IFN signalling is the production of ISGs. We demonstrated that OspD2 and OspD3 were able to inhibit the production of an ISG, IP-10 upon stimulation of the cGAS-STING pathway, when stably expressed in HT-29 cells. The cGAS-STING pathway is activated in response to cytosolic DNA from invading pathogens, and this can result in high expression of IP-10 [413, 414]. Upon stimulation, cGAS induces the formation of cGMP-AMP (cGAMP), a messenger molecule which then dimerises with and activates STING [415]. STING then associates with TBK1 which in turn results in the recruitment of IRF3. IRF3 becomes phosphorylated and translocates into the nucleus to activate expression of ISGs, particularly IP-10 [416]. We used synthetically available short fragments of DNA or ISD (interferon stimulatory DNA) to induce a similar immune response in the HT-29 stable cell lines. We found that all of OspD2, OspD3 and EspL were able to inhibit the production of IP-10 in these cell lines. We also tested IP-10 production from HeLa 229 cells during *Shigella* infection. We saw that at 24 h post infection, all strains of *Shigella* induced IP-10 production except for the T3SS defective mutant Δ*mxiD*. The Δ*mxiD* mutants are non-invasive strains of *Shigella* and therefore would not induce IP-10 production at late time points of infection. However, we did not see any major differences in IP-10 production between the other strains of *Shigella* tested. Production of IP-10 after extended infection indicates that *Shigella* induced a type I IFN response presumably due to the accumulation of *Shigella* cytoplasmic DNA as reported previously. One reason why we did not observe inhibition of IP-10 production during wild type *Shigella* infection compared to OspD2 and OspD3 mutants could be the presence of other T3SS effectors targeting this pathway.

In summary, our work has revealed several potential host protein targets for OspD2 and OspD3 via PROTOMAP and co-transfection assays. We confirmed that OspD3 cleaves IRF9 and OspD2 cleaves IRF3 which is an integral part of type I IFN signalling. We also suggested that *Shigella* actively interferes with Type I IFN signalling. IFNα has previously been reported to inhibit actin tail rearrangements during *Shigella* infection, which is crucial for *Shigella* cell-cell spread [417]. Another group also reported that host RIG-1 and MAVS play an important role in the restriction of cytosolic replication [418]. In addition, type I IFN inducible ISGs such

as viperin and GBPs have been reported to inhibit *Shigella* intracellular replication [273, 419]. These findings will be discussed in more detail in the following chapter.

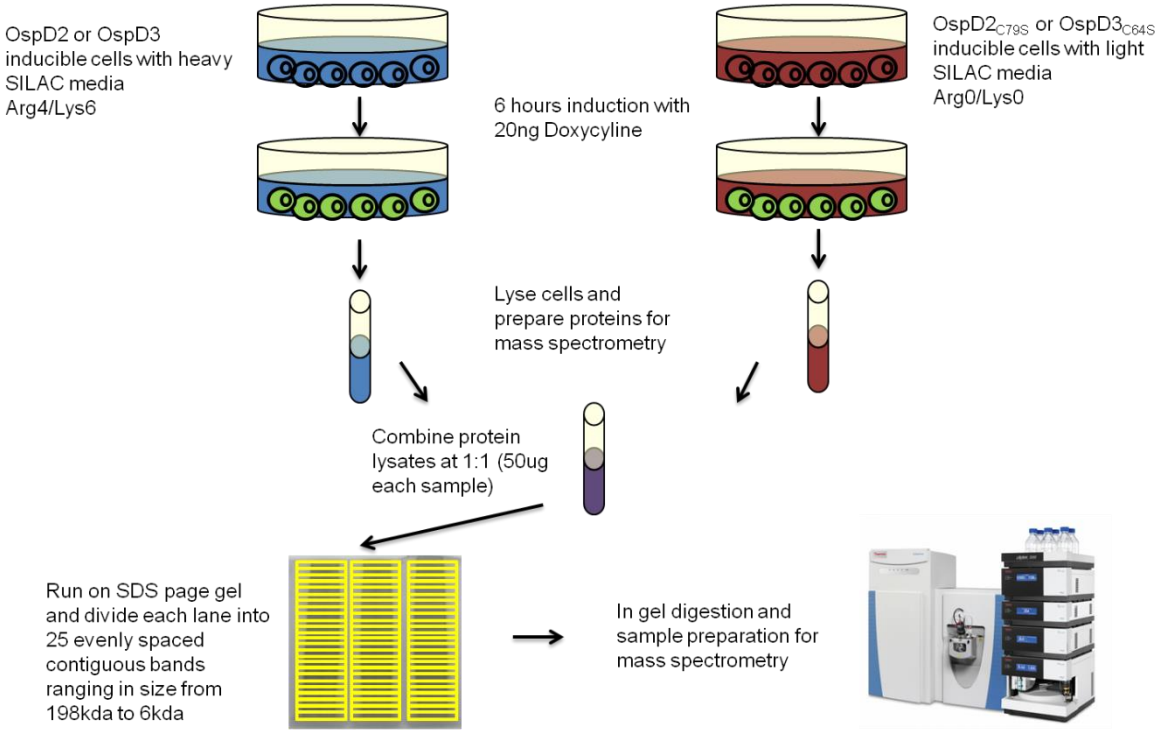

Figure 4. 1: SILAC-based PROTOMAP workflow

SILAC–based PROTOMAP was carried out to identify host cell targets cleaved in the presence of OspD2 and OspD3. Briefly, doxycycline inducible HT-29 cell lines expressing Flag-OspD3 and Flag-OspD3$_{C64S}$ or Flag-OspD2 and Flag-OspD2$_{C79S}$ were treated with media containing either heavy SILAC amino acids (Arg4/Lys6) or light SILAC amino acids (Arg0/Lys0) for 3 passages. HT-29 cell lines expressing the active cysteine proteases were treated with heavy SILAC amino acids whereas HT-29 cell lines expressing the catalytically inactive cysteine proteases were treated with the light SILAC amino acids. After 6-hours of induction with doxycycline, these cells were lysed and protein concentrations were quantified by a BCA assay, before the heavy and light samples were mixed in a 1:1 ratio. The mixed sample was then separated by SDS-page. The resultant gel was cut into 25 evenly spaced contiguous bands ranging in size from 198kDa to 6kDa. In gel digestion was then performed on the bands and the samples were prepared for mass spectrometry analysis.

A

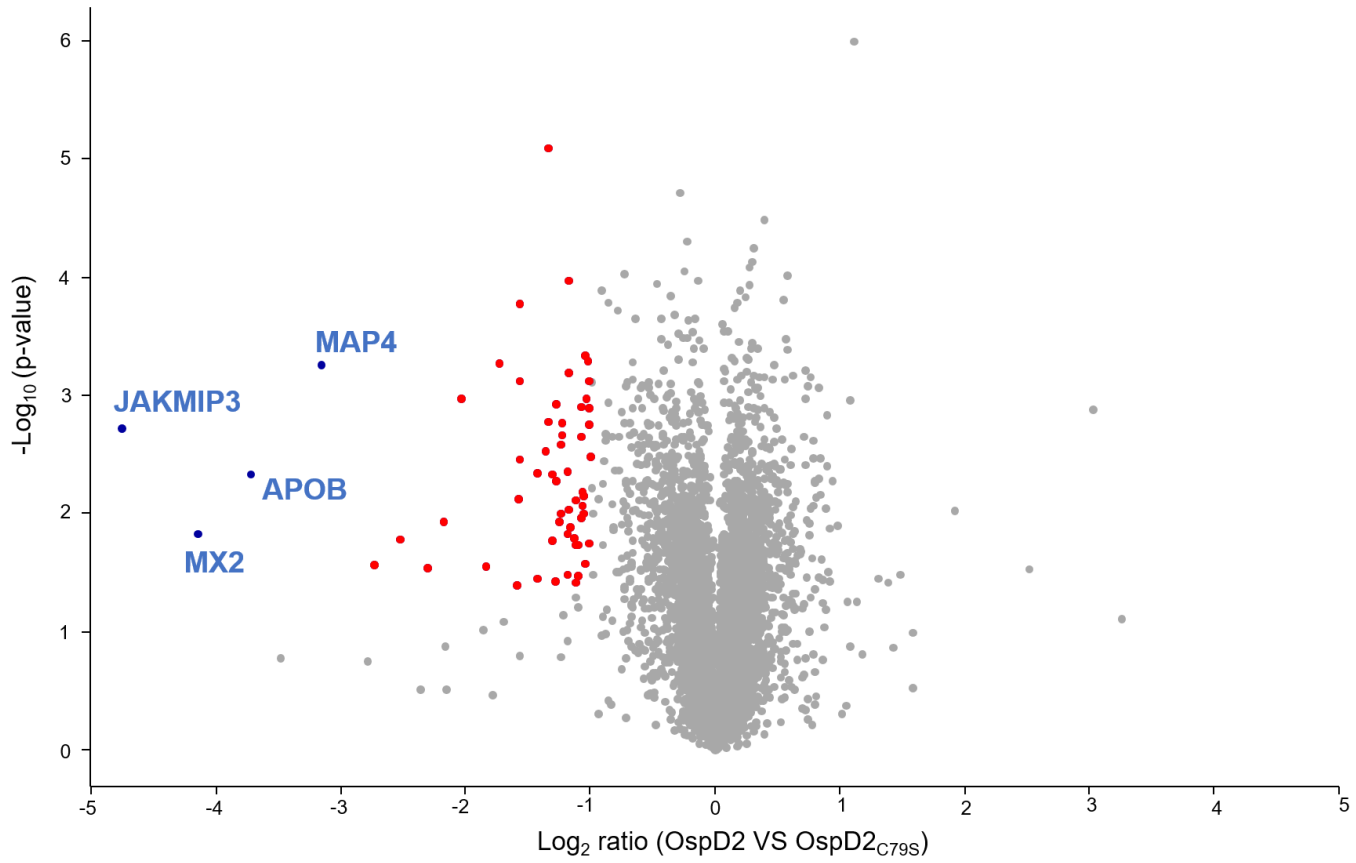
MAP4
JAKMIP3
APOB
MX2
-Log10 (p-value)
Log2 ratio (OspD2 VS OspD2C79S)

B

Gene Name	SILAC Ratio	p-value	Gene Name	SILAC Ratio	p-value	Gene Name	SILAC Ratio	p-value
OAS2	-1.590	0.039878	AGTPBP1	-1.076	0.010618	JAKMIP3	-4.759	0.001899
KIF2C	-1.117	0.038234	PLSCR1	-1.238	0.010004	HLA-C	-1.014	0.001749
CPPED1	-1.289	0.036967	ANLN	-1.056	0.009953	PSMB9	-1.229	0.001701
KIF11	-1.432	0.035571	IFIT3	-1.175	0.009246	S100A2	-1.339	0.001644
DLGAP5	-1.096	0.033829	CD55	-1.071	0.008405	PSAT1	-1.017	0.001266
IDH3G	-1.190	0.032339	KLK10	-1.119	0.007555	ASNS	-1.082	0.001225
FN1	-2.307	0.028595	CCNB1	-1.574	0.007334	UPP1	-1.271	0.001165
FOXK2	-1.836	0.027588	LCN2	-1.055	0.006954	OAS1	-2.034	0.001058
DCD	-2.730	0.027016	SLC7A1	-1.070	0.006448	TGM2	-1.038	0.001053
MKL1	-1.041	0.026373	JUNB	-1.280	0.005271	DDX58	-1.564	0.000741
ZCCHC8	-1.100	0.018211	APOB	-3.724	0.004671	PARP9	-1.017	0.000738
PARP14	-1.118	0.018067	CCNB2	-1.305	0.004622	FAM129A	-1.175	0.000639
ADAM17	-1.017	0.017765	TNS4	-1.426	0.004456	MAP4	-3.160	0.000549
MOCOS	-1.307	0.016735	OASL	-1.192	0.004335	IFIH1	-1.729	0.000532
CMPK2	-2.529	0.016184	TACC3	-1.570	0.003475	NNMT	-1.029	0.000497
TANC1	-1.132	0.016154	ALDH1A3	-1.002	0.003238	CEP192	-1.043	0.000455
MX2	-4.148	0.014912	UBE2S	-1.365	0.002966	NRP1	-1.570	0.000167
DDX60L	-1.188	0.014781	ISG15	-1.237	0.002574	CASC5	-1.174	0.000106
BST2	-1.171	0.012996	SDCBP2	-1.077	0.002229	IFIT1	-1.344	0.000008
HERC6	-2.177	0.011657	DDX60	-1.234	0.002171	-	-	-

C

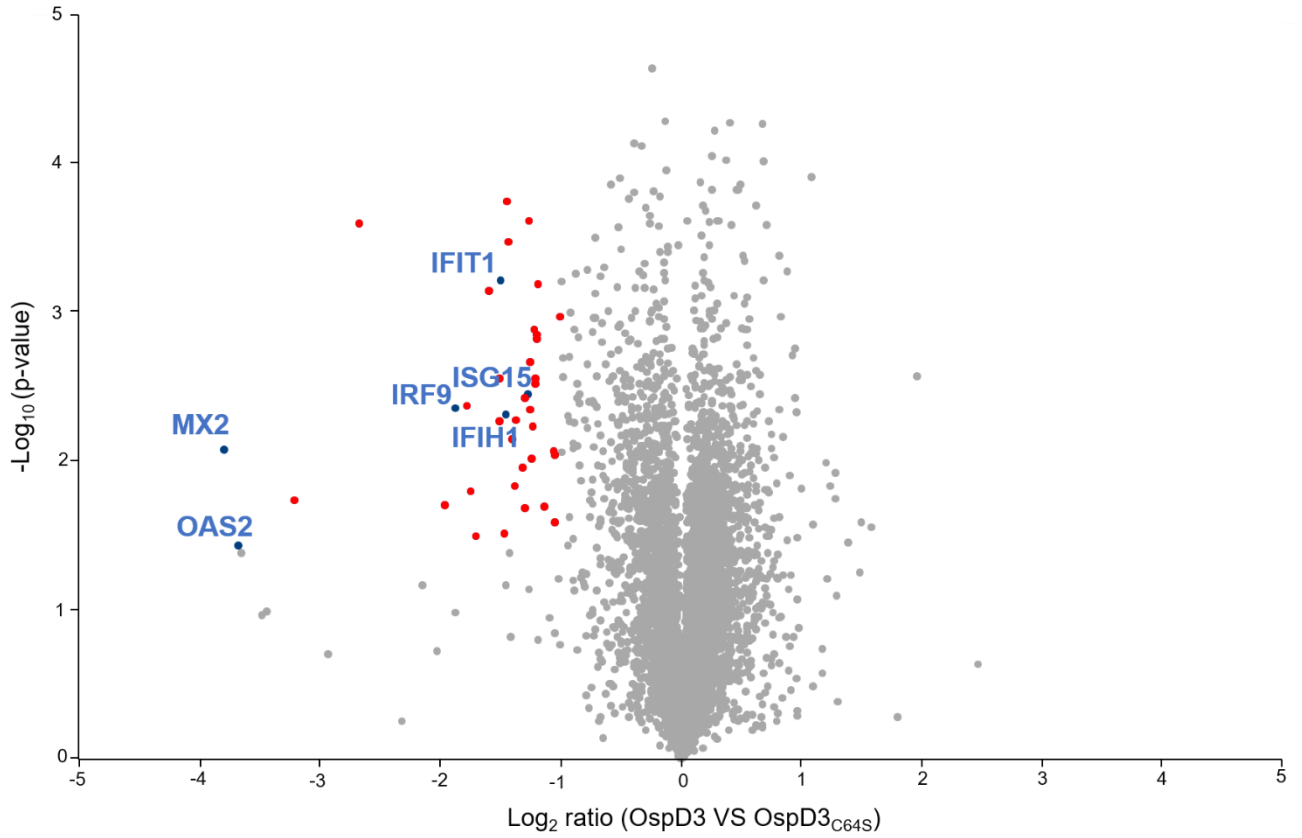
IFIT1
ISG15
IRF9
IFIH1
MX2
OAS2
-Log10 (p-value)
Log2 ratio (OspD3 VS OspD3C64S)

D

Gene Name	SILAC Ratio	p-value	Gene Name	SILAC Ratio	p-value	Gene Name	SILAC Ratio	p-value
RIPK1	-3.215	0.018463	OASL	-1.435	0.000339	FAM129A	-1.245	0.009766
MX2	-3.798	0.00842	IFIT1	-1.507	0.000616	ISG15	-1.280	0.003599
OAS2	-3.689	0.037315	UBE2S	-1.454	0.000183	ITPRIP	-1.210	0.0028
DHRS2	-2.681	0.000256	NRP1	-1.404	0.007152	S100A4	-1.194	0.000654
SH3PXD2B	-1.712	0.032351	PLSCR1	-1.218	0.003042	PSMB9	-1.303	0.003816
IRF9	-1.882	0.004463	CCNB2	-1.376	0.005316	ANLN	-1.261	0.004522
IFIH1	-1.460	0.004905	HAUS6	-1.136	0.020332	HLA-C	-1.055	0.025848
CCNB1	-1.964	0.004294	SLC7A1	-1.202	0.00141	PLIN4	-1.052	0.009067
KIF11	-1.784	0.00072	MB21D1	-1.301	0.020745	SDCBP2	-1.058	0.008579
TBC1D2B	-1.598	0.016086	UPP1	-1.269	0.000247	PSAT1	-1.011	0.001079
DDX60	-1.751	0.014794	NNMT	-1.257	0.002173	IDH3G	-1.231	0.005902
DDX58	-1.382	0.00538	LCN2	-1.225	0.001304	-	-	-
SLC7A11	-1.518	0.002808	KIF2C	-1.198	0.001497	-	-	-

Figure 4. 2: **Volcano plots and tables representing results from SILAC-based PROTOMAP screen for OspD2 and OspD3 in HT-29 stable cell lines**

Volcano plots of OspD2 (A) and OspD3 (C and D) induced proteome changes. Each grey dot represents a host cell protein detected. Proteins observed to consistently change ($p<0.05$) with an average $\log_2$ fold change of over -1 were selected as potential host cell targets as indicated by red dots on the volcano plots. These host targets are listed in tables for the OspD2 (B) and OspD3 (D) screens respectively. Volcano plots and tables are representative of 3 replicates.

A

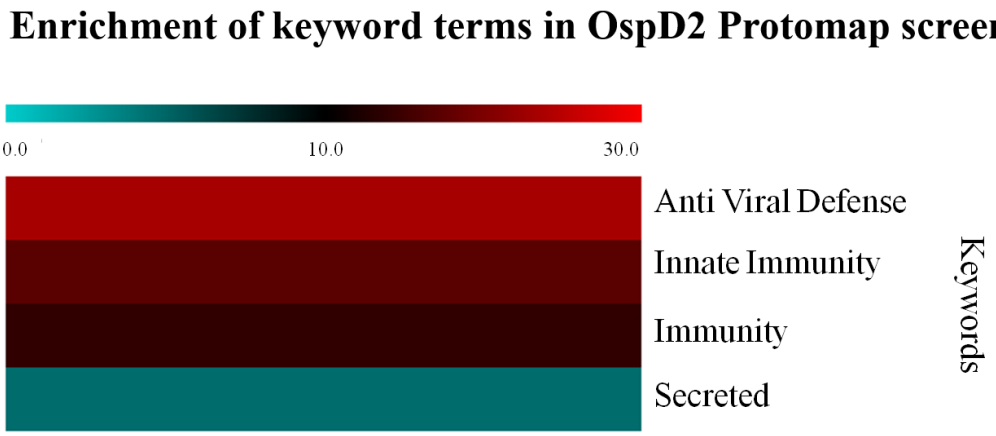

B

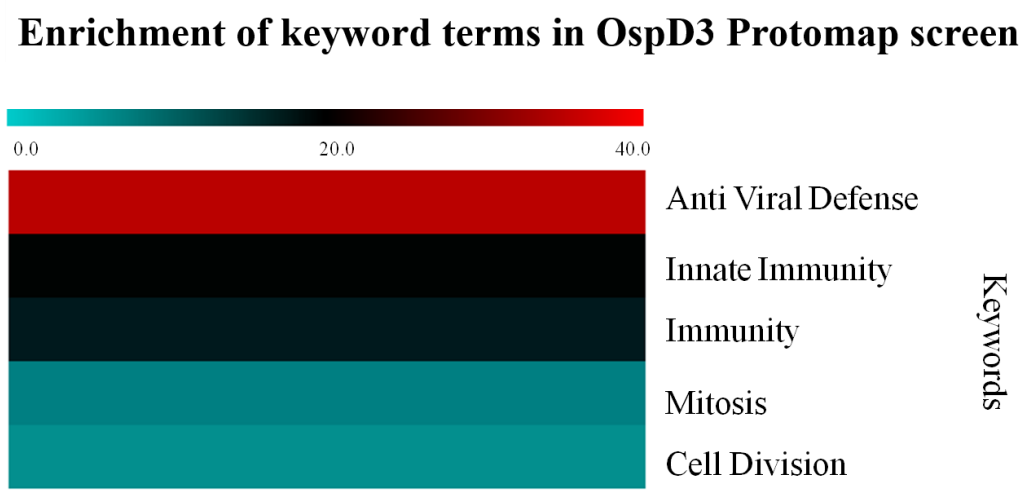

Figure 4. 3: **Enrichment analysis of significant host proteins identified in OspD2 and OspD3 PROTOMAP screens.**

Enrichment analysis was carried out using a Fisher extact test within Perseus. Heat maps were then generated for OspD2 (A) and OspD3 (B) screens using Multiple Experiment Viewer (MEV) where keyword enrichment terms were plotted against the enrichment factor calculated. Significant host proteins identified in both the OspD2 and OspD3 screens were enriched in anti-viral defence and innate immune signalling pathways. Red represents the highest enrichment factor and blue represents the lowest enrichment factor.

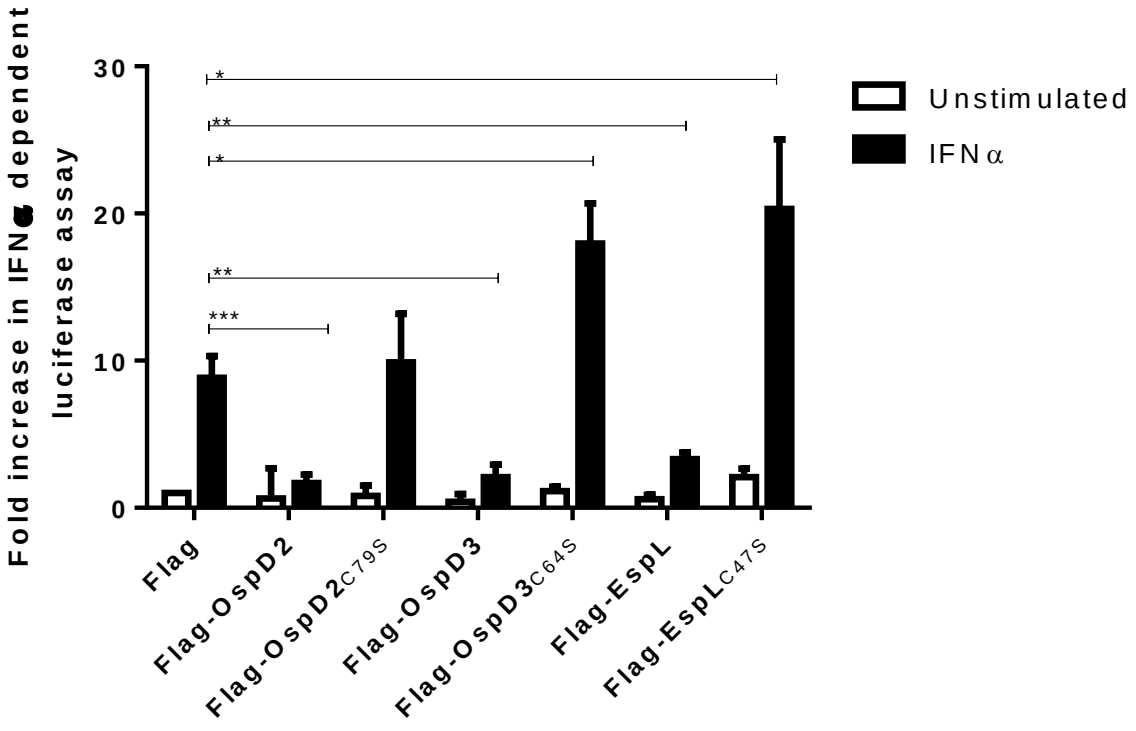

Figure 4. 4: **OspD2, OspD3 and EspL inhibit ISRE-dependent gene transcription of a type I IFN luciferase reporter.**

Fold increase in ISRE-dependent luciferase activity in HEK 293T cells transfected with pISRE-Luc and either p3xFlag-*Myc*-CMV-24, pFlag-OspD2, pFlag-OspD2$_{C79S}$, pFlagOspD3, pFlagOspD3$_{C64S}$, pFlag-EspL or pFlag-EspL$_{C47S.}$ The ISRE plasmid contains 5 copies of the ISRE enhancer elements upstream of the promoter and located downstream of the promoter is the firefly luciferase gene. Cells were left unstimulated or stimulated with IFNα overnight where indicated. ISRE activation was measured as a fold change initially normalised to *Renilla* luciferase and then to unstimulated cells expressing Flag only. Results are the mean ±SEM of three independent experiments carried out in duplicate. *** Significantly different to Flag-transfected HEK 293T cells stimulated with IFNα. (*p< 0.05, **p< 0.01, ***p< 0.001, ****p<0.0001), two-tailed unpaired T test.

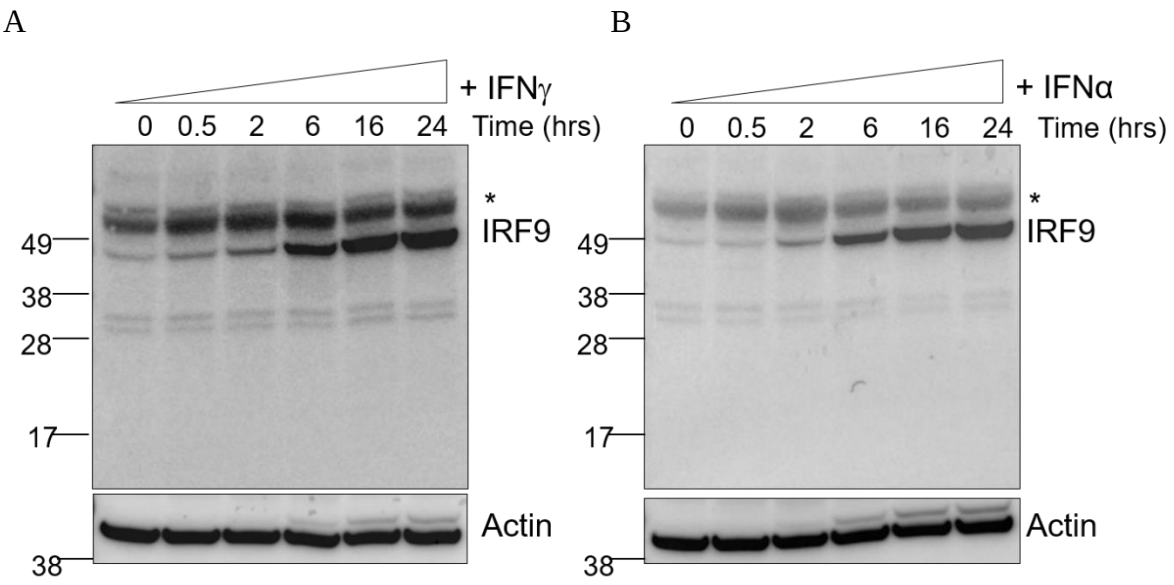

Figure 4. 5: **Expression of IRF9 in HT-29 cells upon IFN stimulation**

Immunoblots of HT29 cells treated with either (A) IFNγ or (B) IFNα for over 24 h. Cells were harvested for immunoblotting and IRF9 expression was detected using human anti-IRF9 antibodies. Antibodies to β-actin were used as a loading control. Immunoblot is representative of at least three independent experiments. * Non-specific bands.

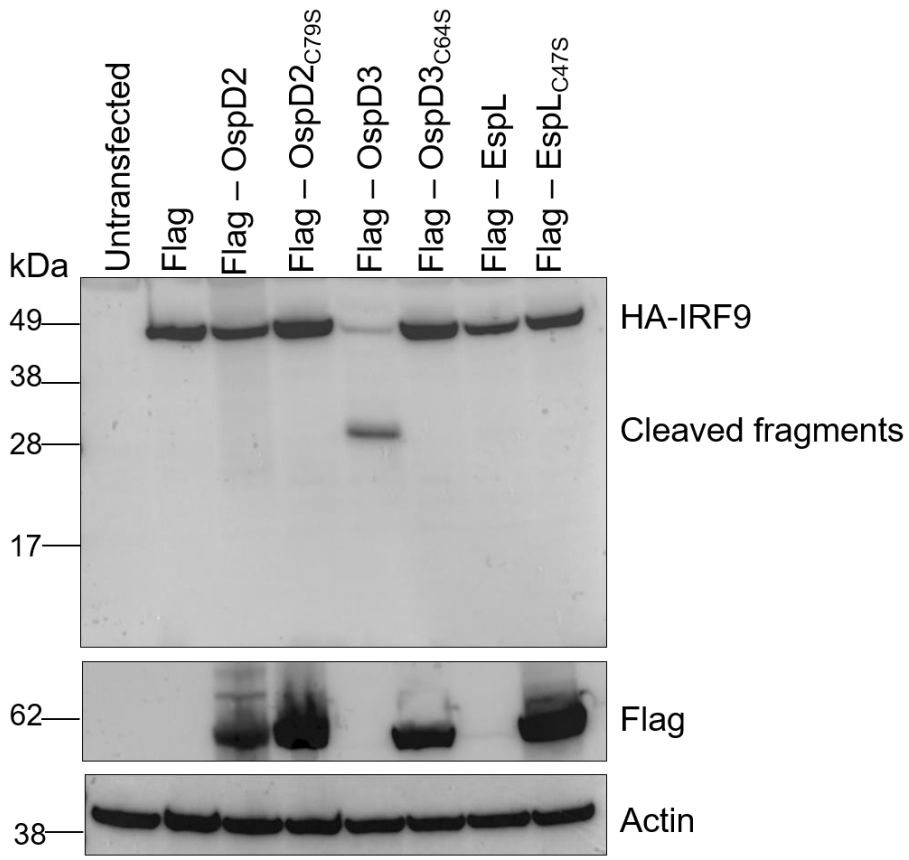

Figure 4. 6: **OspD3 cleaves IRF9 in co-transfected HEK 293T cells**

Immunoblots of HEK 293T cells co-transfected to express wild type and catalytically inactive Flag-tagged OspD2, OspD3 and EspL and HA-IRF9. Transfected cells were harvested for immunoblotting and protein expression was detected using anti-Flag and anti-HA antibodies. Antibodies to β-actin were used as a loading control. Immunoblot is representative of at least three independent experiments.

A

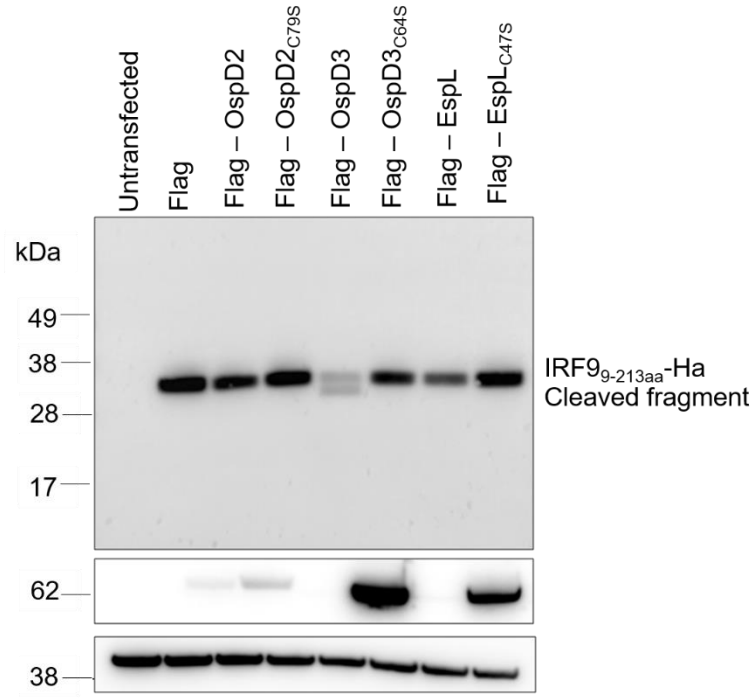
Untransfected
Flag
Flag – OspD2
Flag – OspD2C79S
Flag – OspD3
Flag – OspD3C64S
Flag – EspL
Flag – EspLC47S
kDa
49
38
28
17
62
38
IRF99-213aa-Ha
Cleaved fragment

B

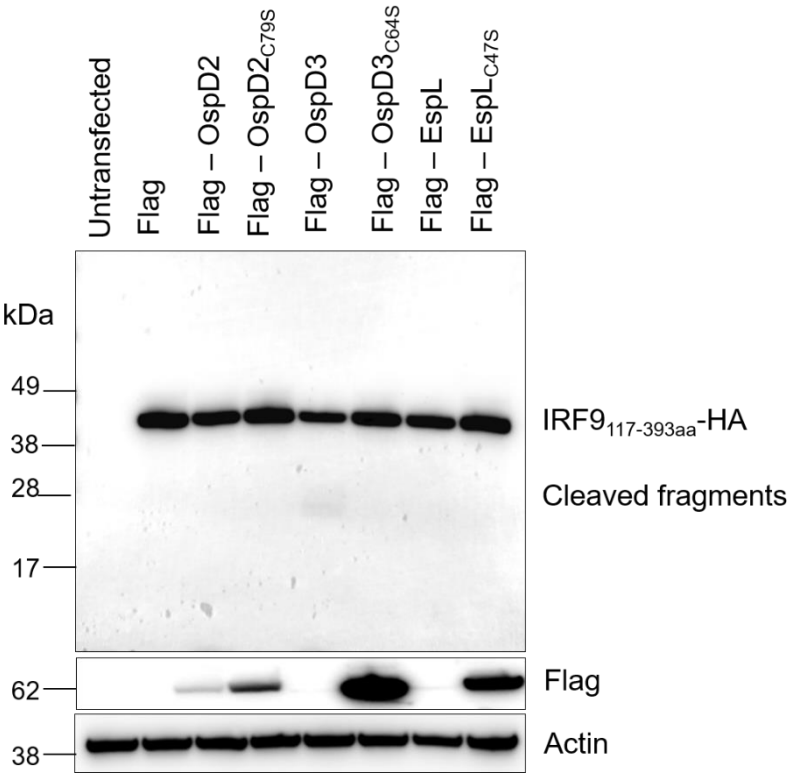
Untransfected
Flag
Flag – OspD2
Flag – OspD2C79S
Flag – OspD3
Flag – OspD3C64S
Flag – EspL
Flag – EspLC47S
kDa
49
38
28
17
62
38
IRF9117-393aa-HA
Cleaved fragments
Flag
Actin

Figure 4. 7: **Ectopic co-expression of wild type and catalytically inactive OspD2, OspD3 and EspL with a truncated domain of IRF9 in HEK 293T cells.**

Immunoblots of HEK 293T cells co-transfected to express wild type and catalytically inactive Flag-tagged OspD2, OspD3 and EspL with truncated $IRF9_{9\text{-}213aa}$-HA (A) and truncated $IRF9_{117\text{-}393aa}$-HA (B). Transfected cells were harvested for immunoblotting and protein expression was detected using anti-Flag and anti-HA antibodies. Antibodies to β-actin were used as a loading control. Immunoblot is representative of at least three independent experiments.

A

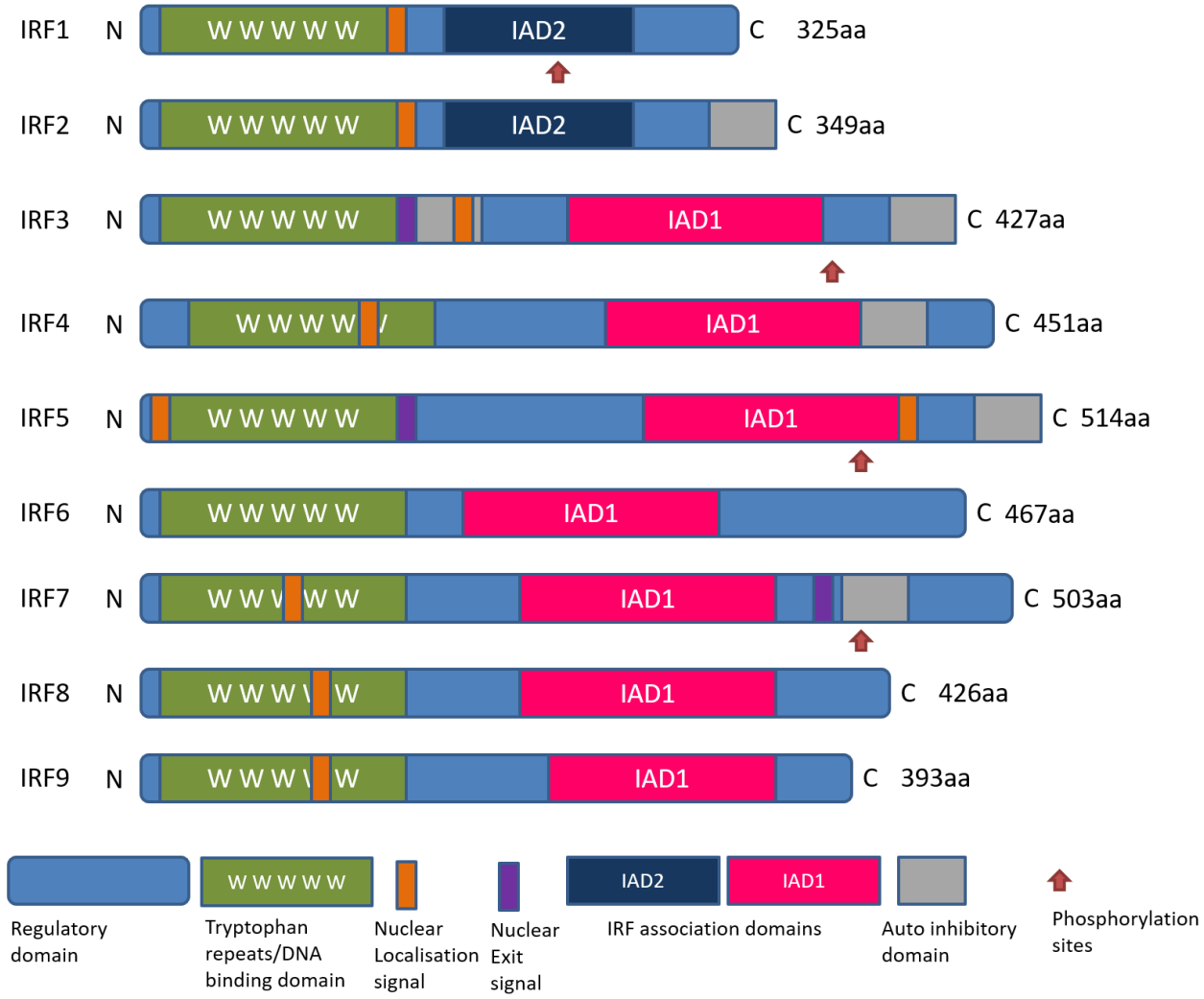
IRF1 N W W W W W IAD2 C 325aa
IRF2 N W W W W W IAD2 C 349aa
IRF3 N W W W W W IAD1 C 427aa
IRF4 N W W W W IAD1 C 451aa
IRF5 N W W W W W IAD1 C 514aa
IRF6 N W W W W W IAD1 C 467aa
IRF7 N W W W W IAD1 C 503aa
IRF8 N W W W W IAD1 C 426aa
IRF9 N W W W W IAD1 C 393aa
Regulatory domain
W W W W W
Tryptophan repeats/DNA binding domain
Nuclear Localisation signal
Nuclear Exit signal
IAD2
IAD1
IRF association domains
Auto inhibitory domain
Phosphorylation sites

B

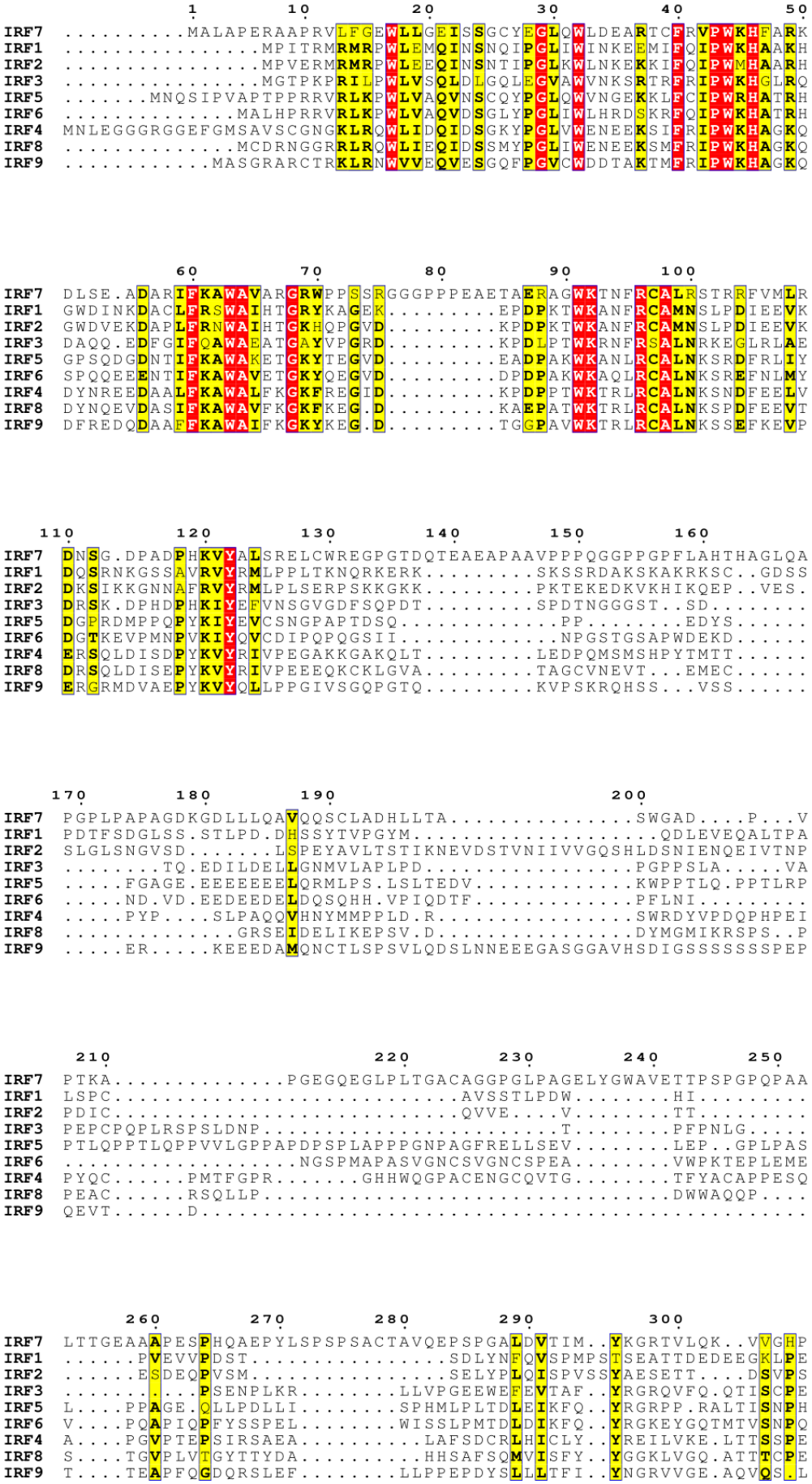
IRF7 .....MALAPERAAPRVLFGEWLLGEISSGCYEGLQWLDEARTCFRVPWKHFARK
IRF1 .....MPITRMRMRPWLEMQINSNQIPGLIWINKEEMIFQIPWKHAAKH
IRF2 .....MPVERMRMRPWLEEQINSNTIPGLKWLNKEKKIFQIPWMHAARH
IRF3 .....MGTPKPRILPWLVSQLDLGQLEGVAWVNKSRTRFRIPWKHGLRQ
IRF5 .....MNQSIPVAPTPPRRVRLKPWLVAQVNSCQYPGLQWVNGEKKLFCIPWRHATRH
IRF6 .....MALHPRRVRLKPWLVAQVDSGLYPGLIWLHRDSKRFQIPWKHATRH
IRF4 MNLEGGGRGGEFGMSAVSCGNGKLRQWLIDQIDSGKYPGLVWENEEKSIFRIPWKHAGKQ
IRF8 .....MCDRNGGRLRQWLIEQIDSSMYPGLIWENEEKSMFRIPWKHAGKQ
IRF9 .....MASGRARCTRKLRNWVVEQVESGQFPGVCWDDTAKTMFRIPWKHAGKQ
IRF7 DLSE.ADARIFKAWAVARGRWPPSSRGGGPPPEAETAERAGWKTNFRCALRSTRRFVMLR
IRF1 GWDINKDACLFRSWAIHTGRYKAGEK.....EPDPKTWKANFRCAMNSLPDIEEVK
IRF2 GWDVEKDAPLFRNWAIHTGKHQPGVD.....KPDPKTWKANFRCAMNSLPDIEEVK
IRF3 DAQQ.EDFGIFQAWAEATGAYVPGRD.....KPDLPTWKRNFRSALNRKEGLRLAE
IRF5 GPSQDGDNTIFKAWAKETGKYTEGVD.....EADPAKWKANLRCALNKSRDFRLIY
IRF6 SPQQEEENTIFKAWAVETGKYQEGVD.....DPDPAKWKAQLRCALNKSREFNLMY
IRF4 DYNREEDAALFKAWALFKGKFREGID.....KPDPPTWKTRLRCALNKSNDFEELV
IRF8 DYNQEVDASIFKAWAVFKGKFKEG.D.....KAEPATWKTRLRCALNKSPDFEEVT
IRF9 DFREDQDAAFFKAWAIFKGKYKEG.D.....TGGPAVWKTRLRCALNKSSEFKEVP
IRF7 DNSG.DPADPHKVYALSRELCWREGPGTDQTEAEAPAAVPPPQGGPPGPFLAHTHAGLQA
IRF1 DQSRNKGSSAVRVYRMLPPLTKNQRKERK.....SKSSRDAKSKAKRKSC..GDSS
IRF2 DKSIKKGNNAFRVYRMLPLSERPSKKGKK.....PKTEKEDKVKHIKQEP..VES.
IRF3 DRSK.DPHDPHKIYEFVNSGVGDFSQPDT.....SPDTNGGGST..SD.....
IRF5 DGPRDMPPQPYKIYEVCSNGPAPTDSQ.....PP.....EDYS.....
IRF6 DGTKEVPMNPVKIYQVCDIPQPQGSII.....NPGSTGSAPWDEKD.....
IRF4 ERSQLDISDPYKVYRIVPEGAKKGAKQLT.....LEDPQMSMSHPYTMTT.....
IRF8 DRSQLDISEPYKVYRIVPEEEQKCKLGVA.....TAGCVNEVT...EMEC.....
IRF9 ERGRMDVAEPYKVYQLLPPGIVSGQPGTQ.....KVPSKRQHSS...VSS.....
IRF7 PGPLPAPAGDKGDLLLQAVQQSCLADHLLTA.....SWGAD....P...V
IRF1 PDTFSDGLSS.STLPD.DHSSYTVPGYM.....QDLEVEQALTPA
IRF2 SLGLSNGVSD.....LSPEYAVLTSTIKNEVDSTVNIIVVGQSHLDSNIENQEIVTNP
IRF3 .....TQ.EDILDELLGNMVLAPLPD.....PGPPSLA.....VA
IRF5 .....FGAGE.EEEEEEELQRMLPS.LSLTEDV.....KWPPTLQ.PPTLRP
IRF6 .....ND.VD.EEDEEDELDQSQHH.VPIQDTF.....PFLNI.....
IRF4 .....PYP....SLPAQQVHNYMMPPLD.R.....SWRDYVPDQPHPEI
IRF8 .....GRSEIDELIKEPSV.D.....DYMGMIKRSPS..P
IRF9 .....ER.....KEEEDAMQNCTLSPSVLQDSLNNEEEGASGGAVHSDIGSSSSSSSPEP
IRF7 PTKA.....PGEGQEGLPLTGACAGGPGLPAGELYGWAVETTPSPGPQPAA
IRF1 LSPC.....AVSSTLPDW.....HI.....
IRF2 PDIC.....QVVE....V.....TT.....
IRF3 PEPCPQPLRSPSLDNP.....T.....PFPNLG.....
IRF5 PTLQPPTLQPPVVLGPPAPDPSPLAPPPGNPAGFRELLSEV.....LEP..GPLPAS
IRF6 .....NGSPMAPASVGNCSVGNCSPEA.....VWPKTEPLEME
IRF4 PYQC.....PMTFGPR.....GHHWQGPACENGCQVTG.....TFYACAPPESQ
IRF8 PEAC.....RSQLLP.....DWWAQQP....
IRF9 QEVT.....D.....
IRF7 LTTGEAAAPESPHQAEPYLSPSPSACTAVQEPSPGALDVTIM..YKGRTVLQK..VVGHP
IRF1 .....PVEVVPDST.....SDLYNFQVSPMPSTSEATTDEDEEGKLLPE
IRF2 .....ESDEQPVSM.....SELYPLQISPVSSYAESETT....DSVPS
IRF3 .....PSENPLKR.....LLVPGEEWEFEVTAF..YRGRQVFQ.QTISCPE
IRF5 L....PPAGE.QLLPDLLI.....SPHMLPLTDLEIKFQ..YRGRPP.RALTISNPH
IRF6 V....PQAPIQPFYSSPEL.....WISSLPMTDLDIKFQ..YRGKEYGQTMTVSNPQ
IRF4 A....PGVPTEPSIRSAEA.....LAFSDCRLHICLY..YREILVKE.LTTSSPE
IRF8 S....TGVPLVTGYTTYDA.....HHSAFSQMVISFY..YGGKLVGQ.ATTTCPE
IRF9 T....TEAPFQGDQRSLEF.....LLPPEPDYSLLLTFI..YNGRVVGE.AQVQS.L

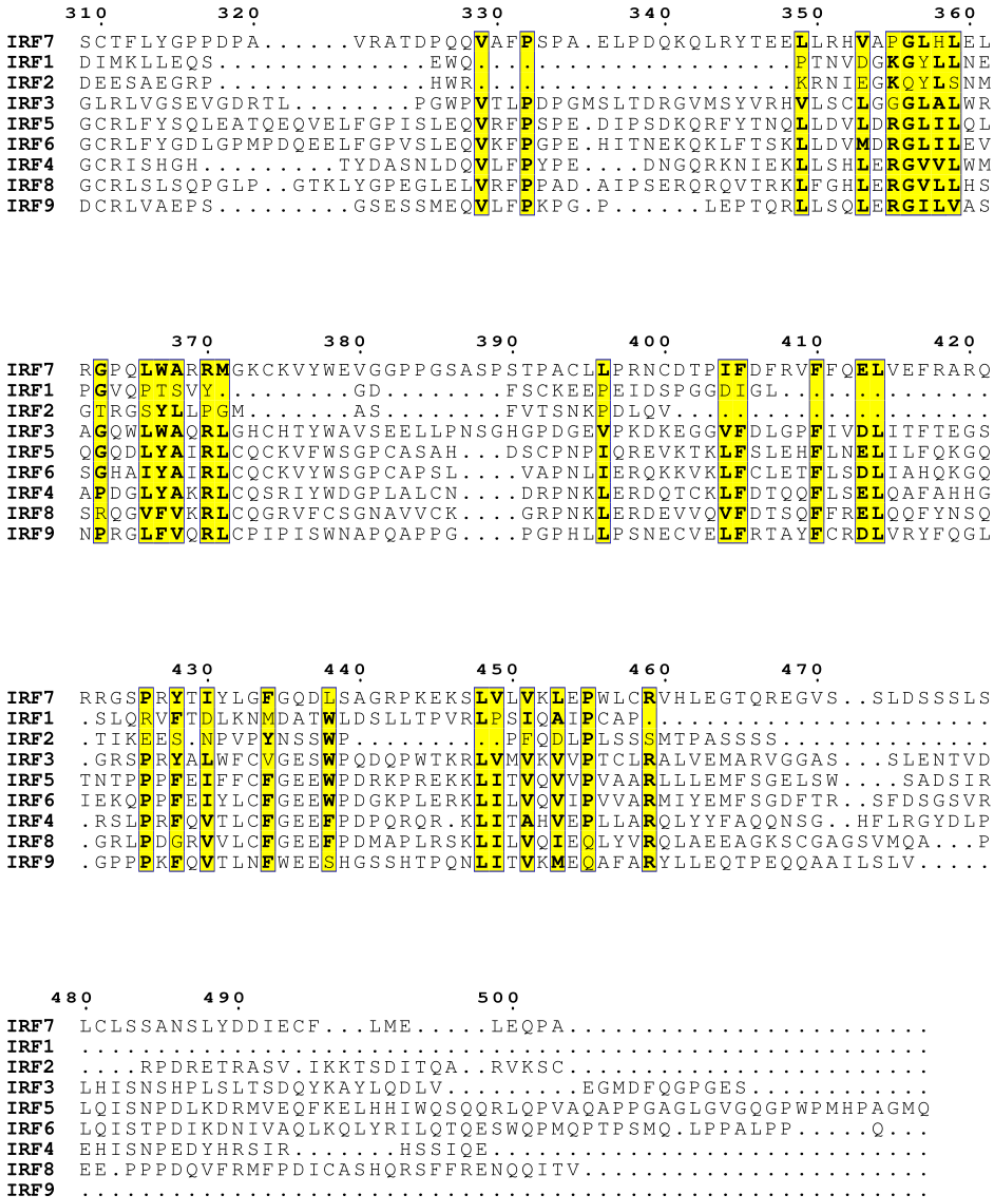

C

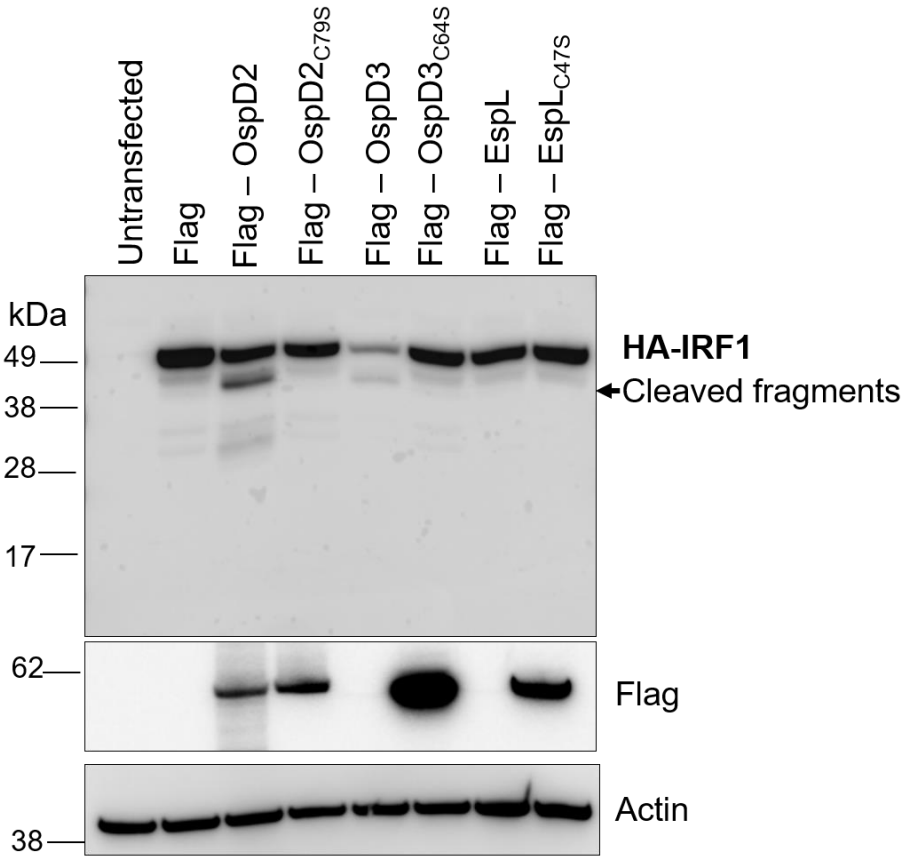
Untransfected
Flag
Flag – OspD2
Flag – OspD2C79S
Flag – OspD3
Flag – OspD3C64S
Flag – EspL
Flag – EsplC47S
kDa
49
38
28
17
HA-IRF1
Cleaved fragments
62
Flag
38
Actin

D

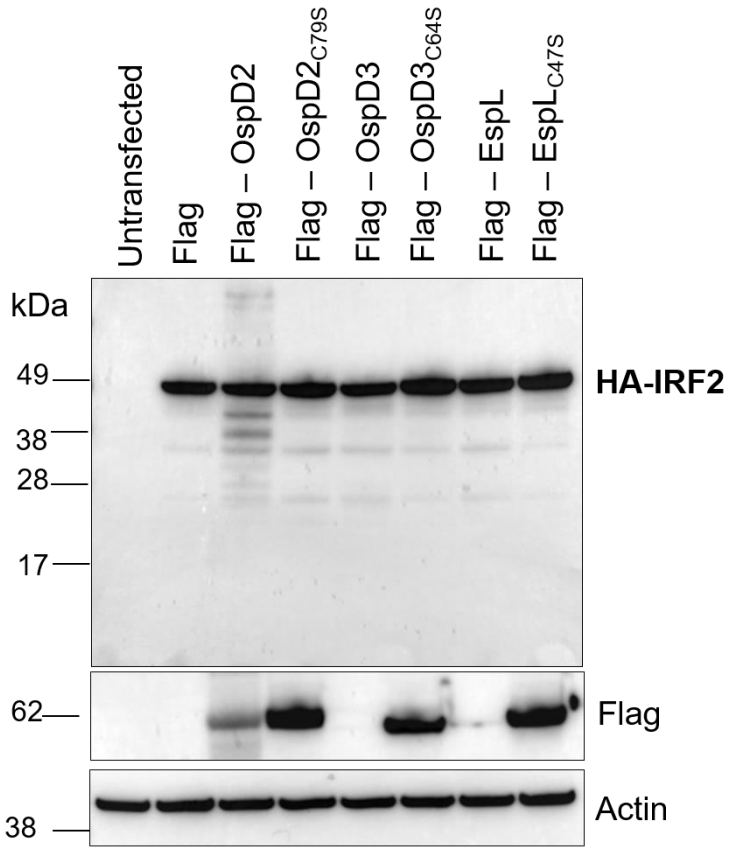
Untransfected
Flag
Flag – OspD2
Flag – OspD2C79S
Flag – OspD3
Flag – OspD3C64S
Flag – EspL
Flag – EsplC47S
kDa
49
38
28
17
HA-IRF2
62
Flag
38
Actin

E

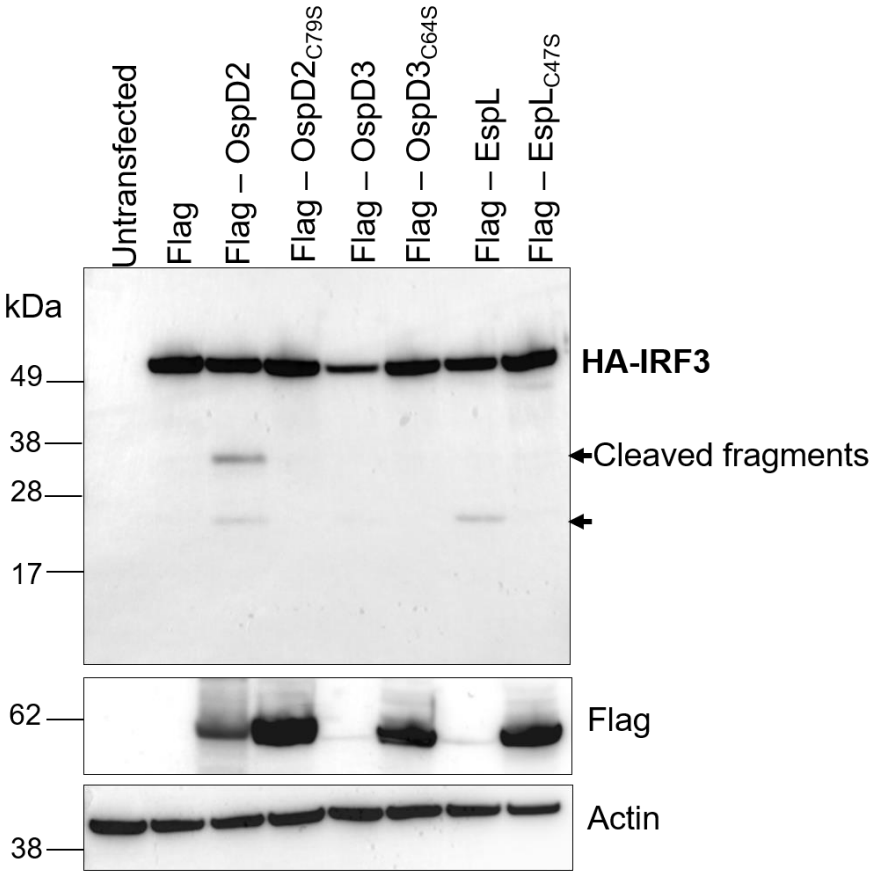
Untransfected
Flag
Flag – OspD2
Flag – OspD2C79S
Flag – OspD3
Flag – OspD3C64S
Flag – EspL
Flag – EspLC47S
kDa
49
38
28
17
HA-IRF3
Cleaved fragments
62
Flag
38
Actin

F

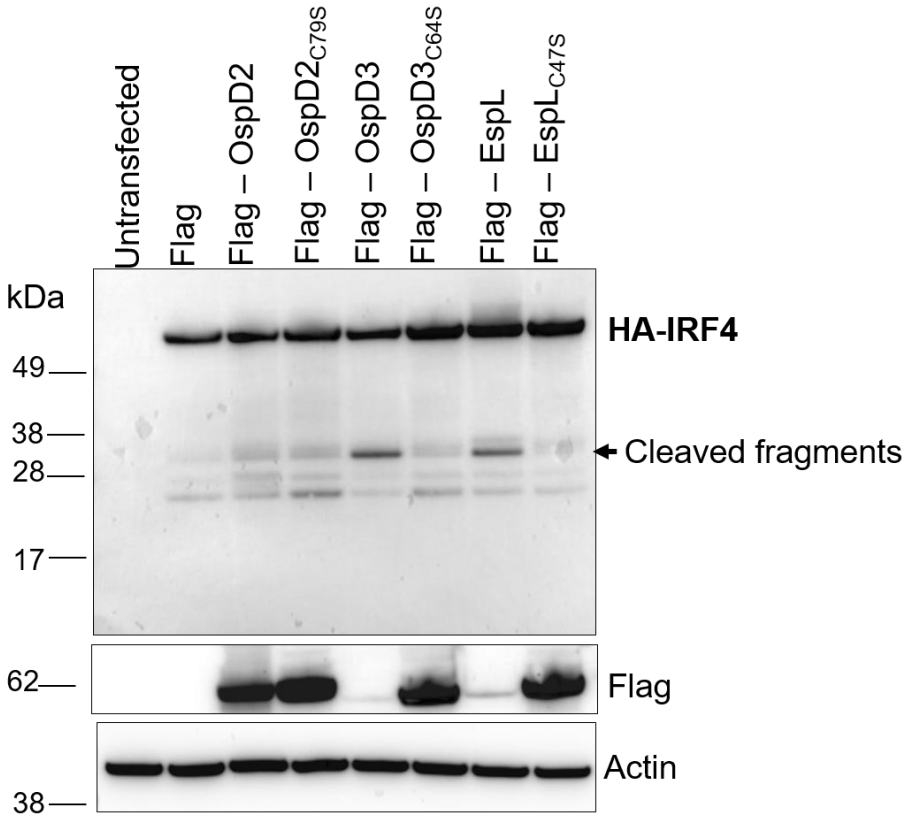
Untransfected
Flag
Flag – OspD2
Flag – OspD2C79S
Flag – OspD3
Flag – OspD3C64S
Flag – EspL
Flag – EspLC47S
kDa
49
38
28
17
HA-IRF4
Cleaved fragments
62
Flag
38
Actin

G

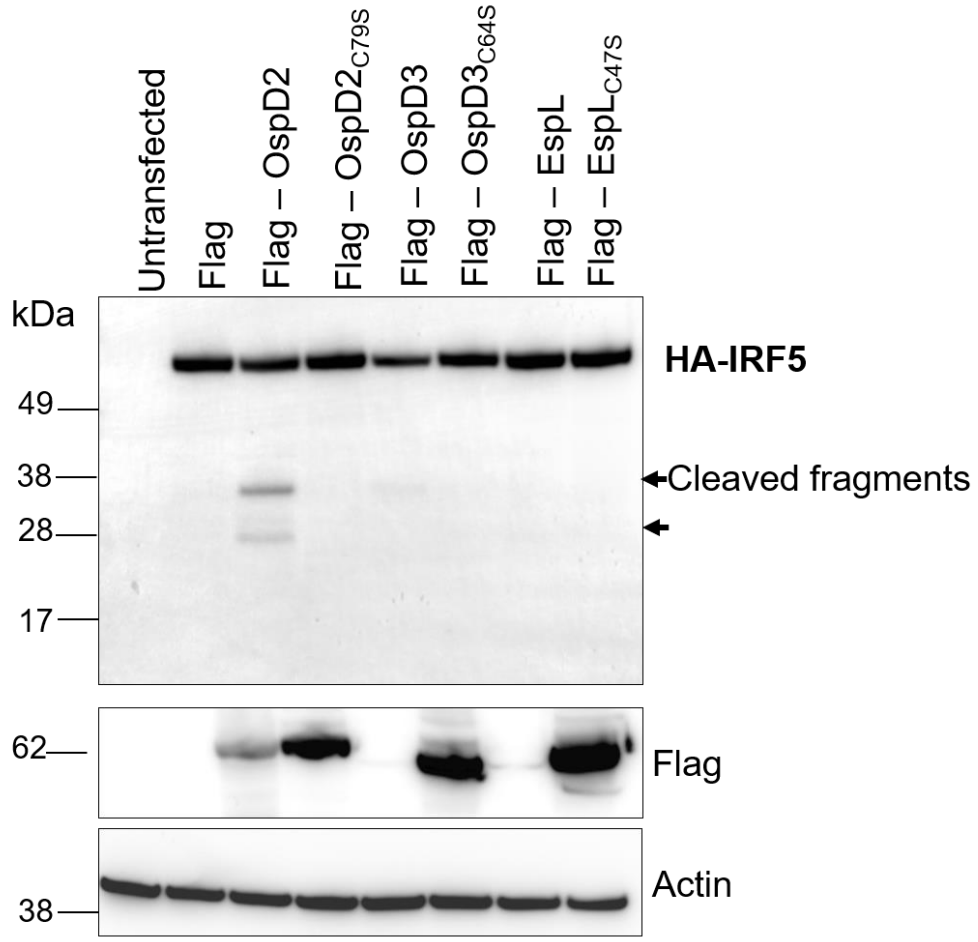
Untransfected
Flag
Flag – OspD2
Flag – OspD2C79S
Flag – OspD3
Flag – OspD3C64S
Flag – EspL
Flag – EspLC47S
kDa
49
38
28
17
HA-IRF5
Cleaved fragments
62
Flag
38
Actin

H

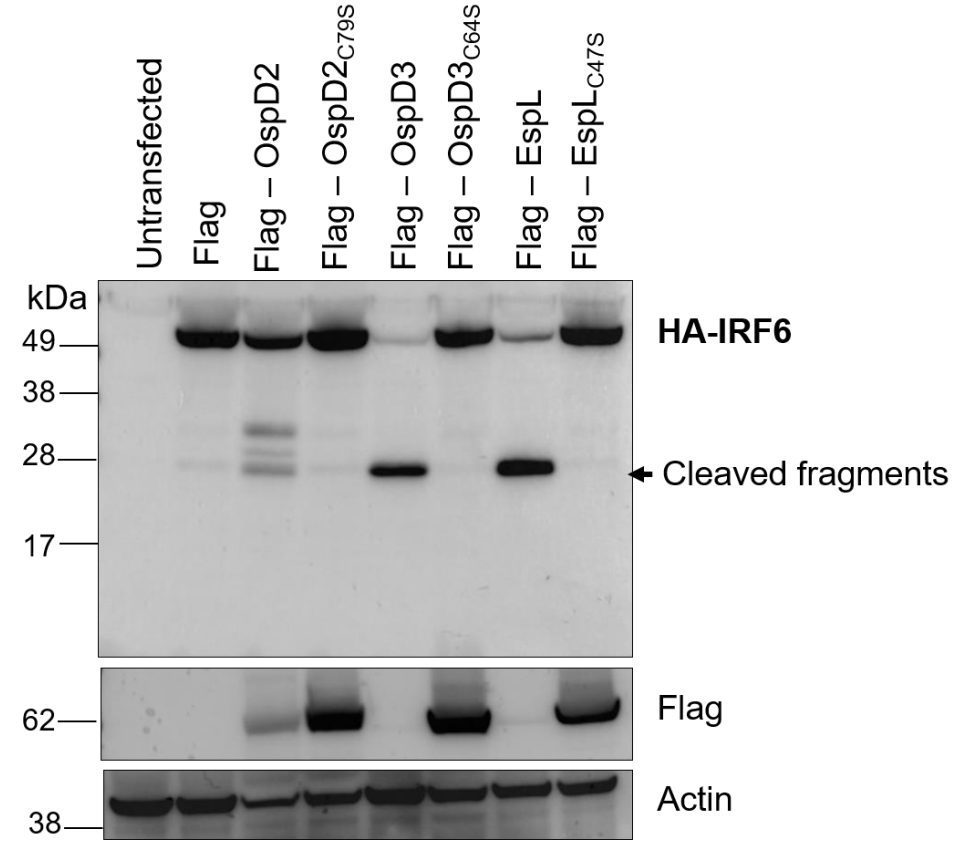
Untransfected
Flag
Flag – OspD2
Flag – OspD2C79S
Flag – OspD3
Flag – OspD3C64S
Flag – EspL
Flag – EspLC47S
kDa
49
38
28
17
HA-IRF6
Cleaved fragments
62
Flag
38
Actin

I

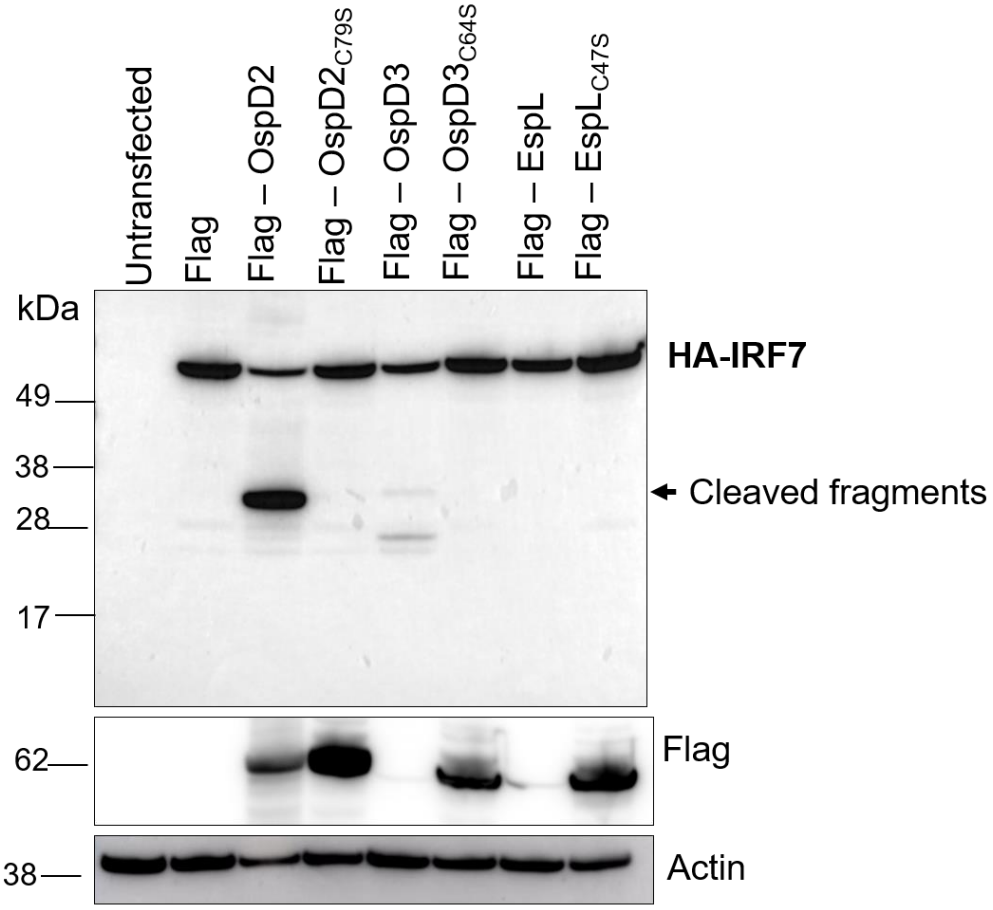
Untransfected
Flag
Flag – OspD2
Flag – OspD2C79S
Flag – OspD3
Flag – OspD3C64S
Flag – EspL
Flag – EspLC47S
kDa
49
38
28
17
HA-IRF7
Cleaved fragments
62
Flag
38
Actin

J

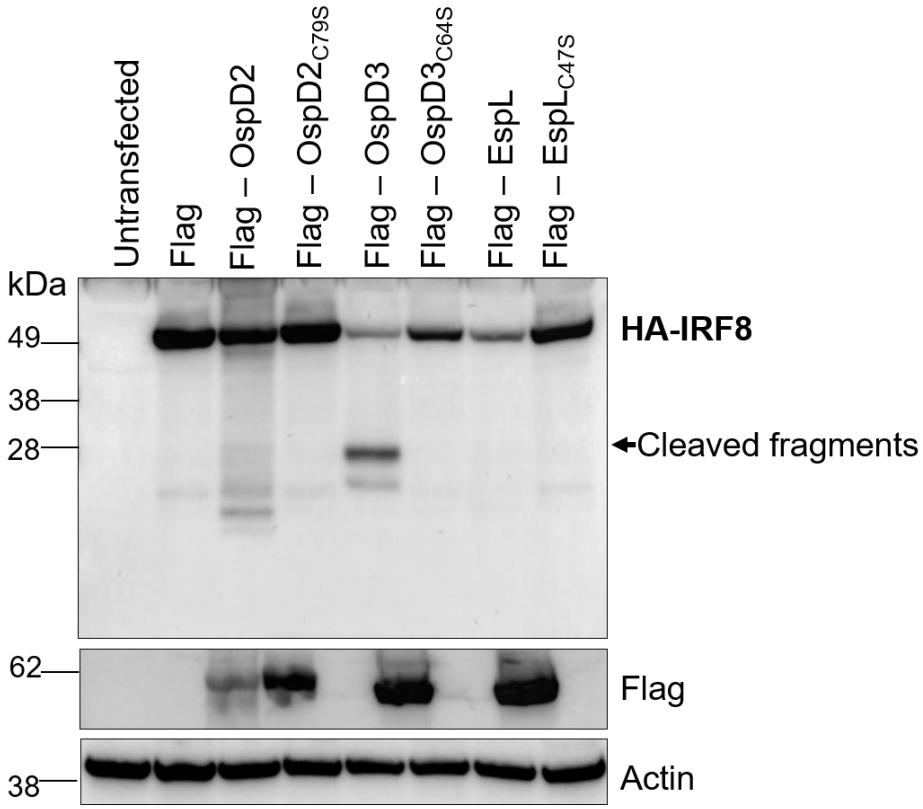
Untransfected
Flag
Flag – OspD2
Flag – OspD2C79S
Flag – OspD3
Flag – OspD3C64S
Flag – EspL
Flag – EspLC47S
kDa
49
38
28
HA-IRF8
Cleaved fragments
62
Flag
38
Actin

K

	OspD2		OspD3		EspL	
	Full length protein decreases	Cleaved fragments	Full length protein decreases	Cleaved fragments	Full length protein decreases	Cleaved fragments
IRF1						
IRF2						
IRF3						
IRF4						
IRF5						
IRF6						
IRF7						
IRF8						
IRF9						

High Medium Low

Figure 4. 8: Ectopic co-expression of wild type and catalytically inactive OspD2, OspD3 and EspL with human IRFs in HEK 293T cells.

(A) Representation of the structure and domains of IRF1-9. (B) Alignments of IRF1-IRF7 which was done using Clustal omega and ESPript3. (C-J) Immunoblots of HEK 293T cells transfected to express wild type and catalytically inactive Flag-tagged OspD2, OspD3 or EspL and either (C) HA-IRF1, (D) HA-IRF2, (E) HA-IRF3, (F) HA-IRF4, (G) HA-IRF5, (H) HA-IRF6, (I) HA-IRF7, (J) HA-IRF8. Cells were harvested for immunoblotting and expression was detected using anti-Flag and anti-HA antibodies. Antibodies to β-actin were used as a loading control. Immunoblot is representative of at least three independent experiments. (J) Table summarising cleavage of the different IRFs by OspD2, OspD3 or EspL. Pink indicates significant reduction in full length IRF or strong cleavage product formed. Green and blue indicate medium to low reduction in full length IRF or cleavage product formed.

A

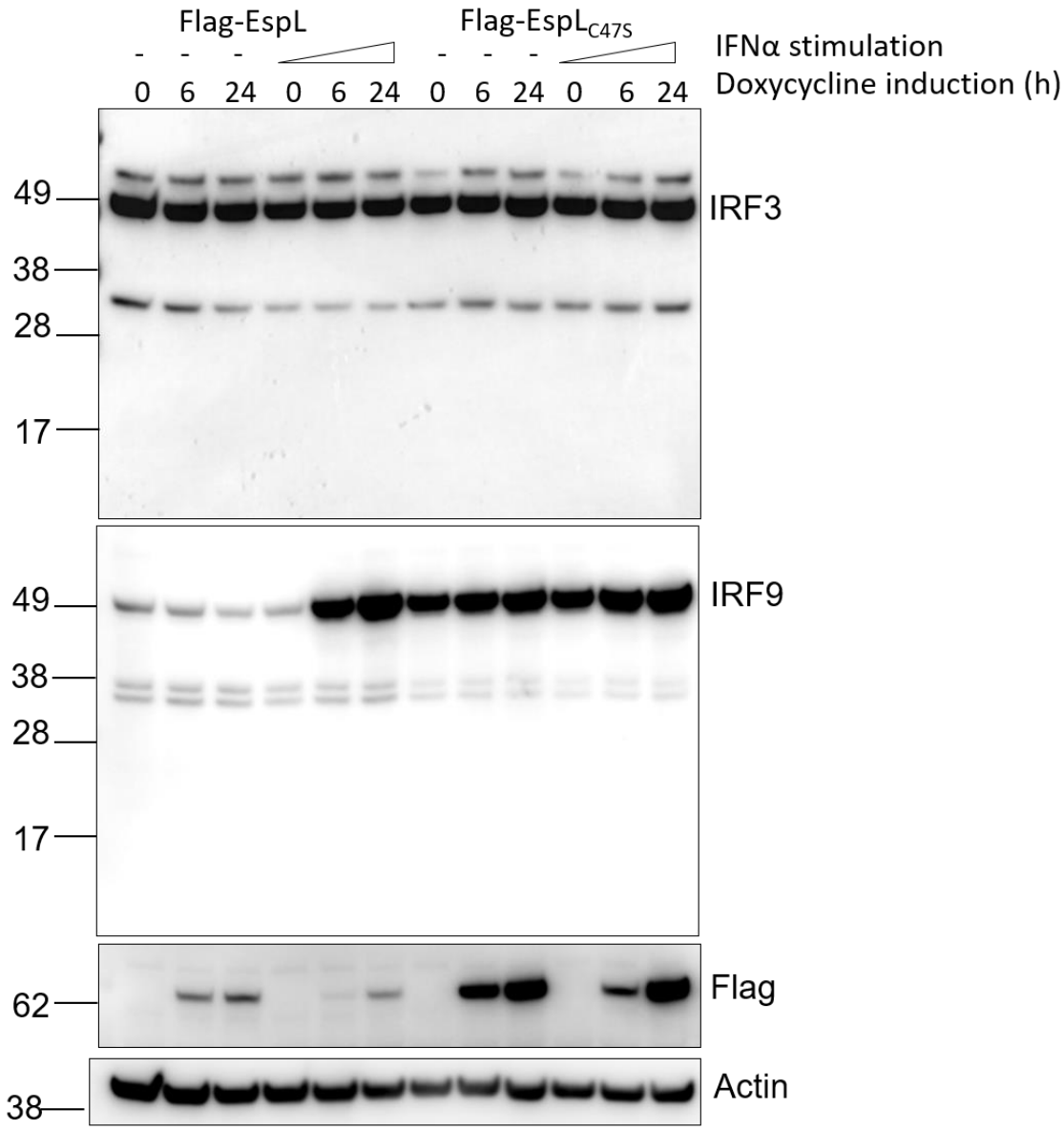
Flag-EspL
Flag-EspL$_{C47S}$
IFNα stimulation
Doxycycline induction (h)
- - - - - -
0 6 24 0 6 24 0 6 24 0 6 24
49
38
28
17
IRF3
49
38
28
17
IRF9
62
Flag
38
Actin

B

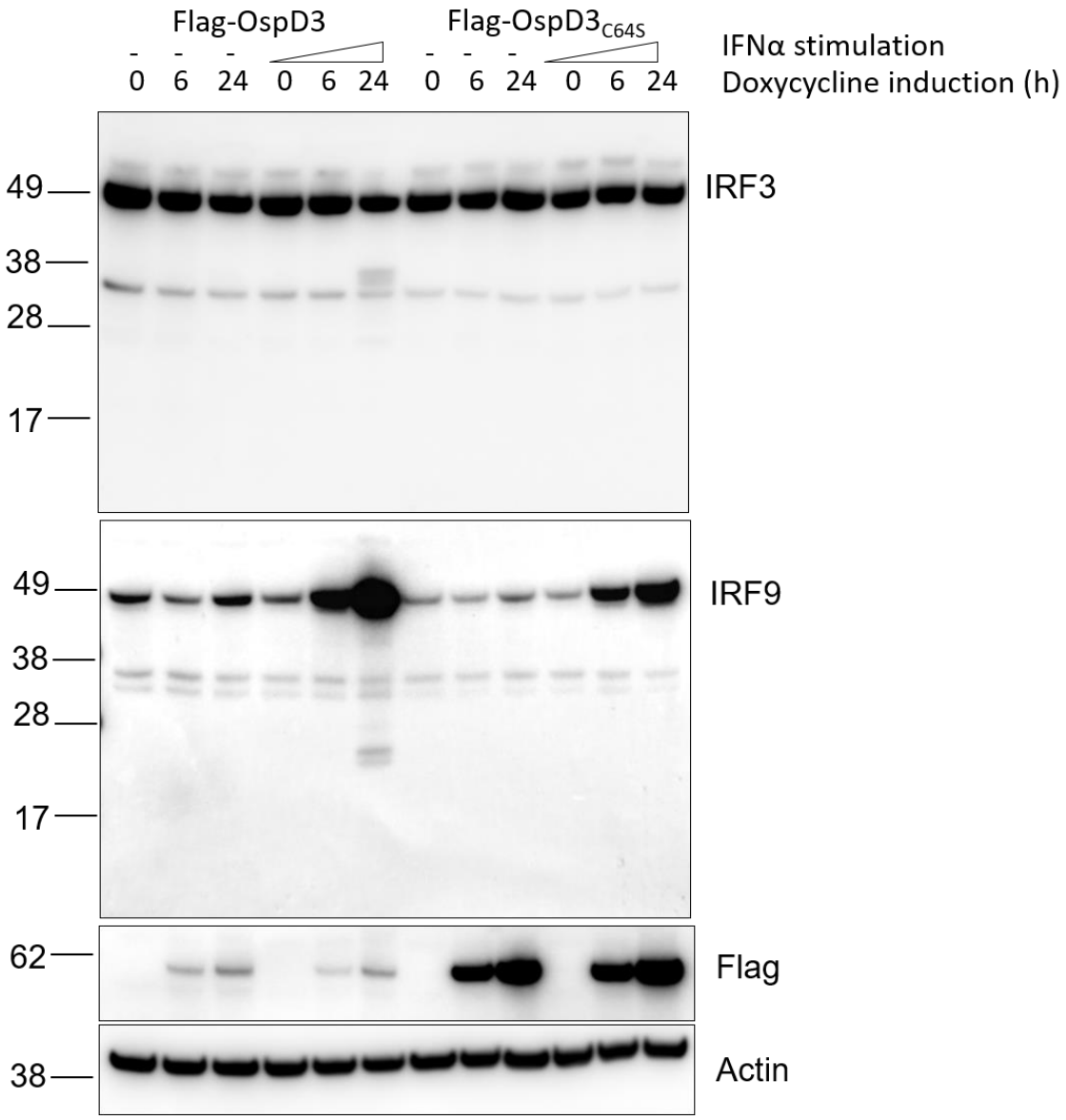
Flag-OspD3
Flag-OspD3C64S
IFNα stimulation
Doxycycline induction (h)
- - - 0 6 24 - - - 0 6 24
0 6 24 0 6 24 0 6 24 0 6 24
49
38
28
17
IRF3
49
38
28
17
IRF9
62
Flag
38
Actin

C

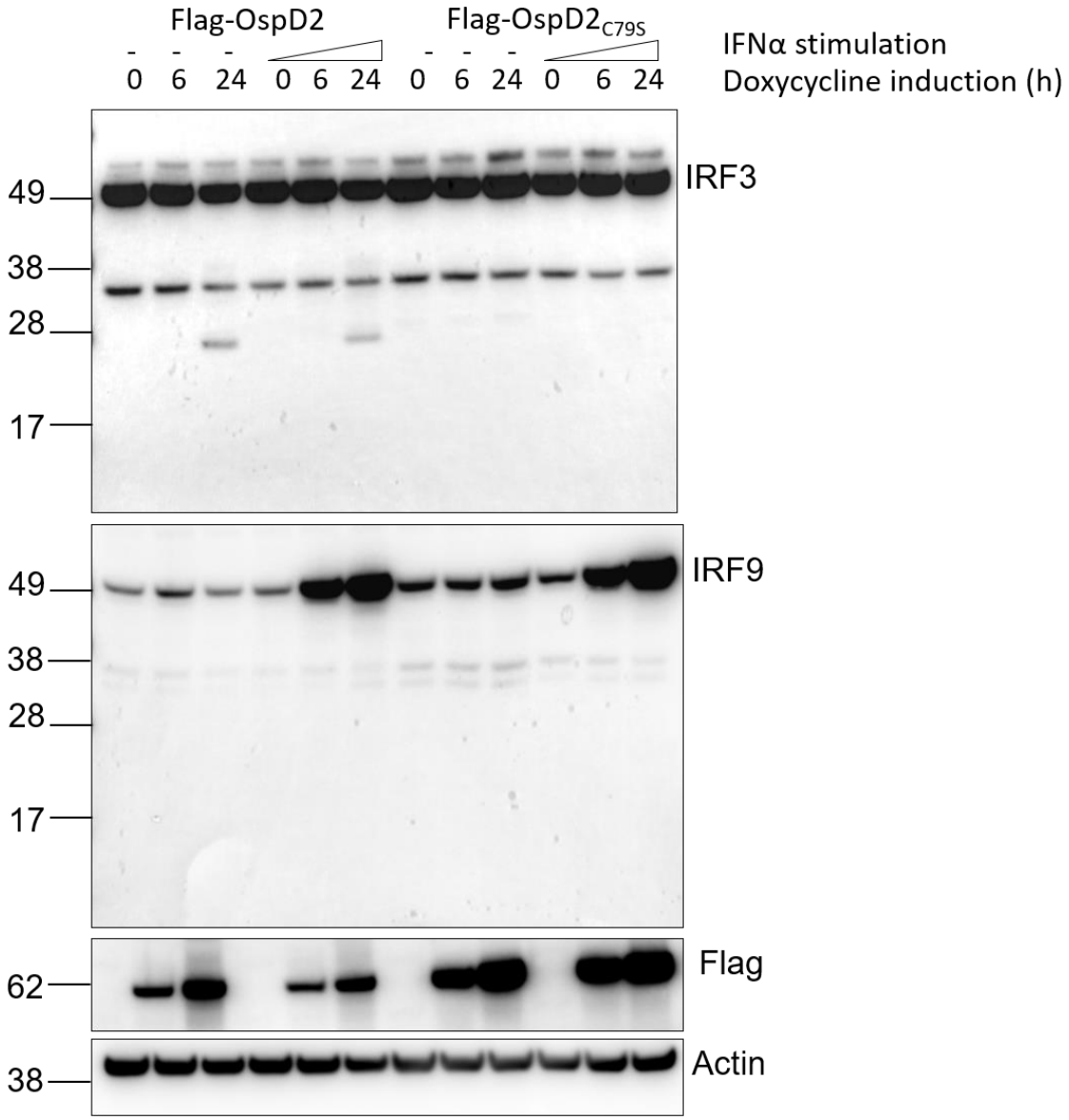

Figure 4. 9: **Cleavage of endogenous IRF3 and IRF9 in doxycycline inducible HT-29 cells expressing wild type and catalytically inactive OspD2, OspD3 and EspL.**

Immunoblots showing levels of IRF3 and IRF9 in doxycycline inducible HT-29 cell lines expressing Flag-EspL or Flag-EspL$_{C47S}$ (A), Flag-OspD3 or Flag-OspD3$_{C64S}$ (B) or Flag-OspD2 or Flag-OspD2$_{C79S}$ (C) which were induced with doxycycline and IFNα for various timepoints as indicated. Expression of endogenous IRF3 and IRF9 were detected using human anti-IRF3 and human anti-IRF9 antibodies. Expression of wild type and catalytically active Flag-OspD2, Flag-OspD3 and Flag-EspL were detected using anti-Flag antibodies. Antibodies to β-actin were used as a loading control. Immunoblots are representative of at least three independent experiments.

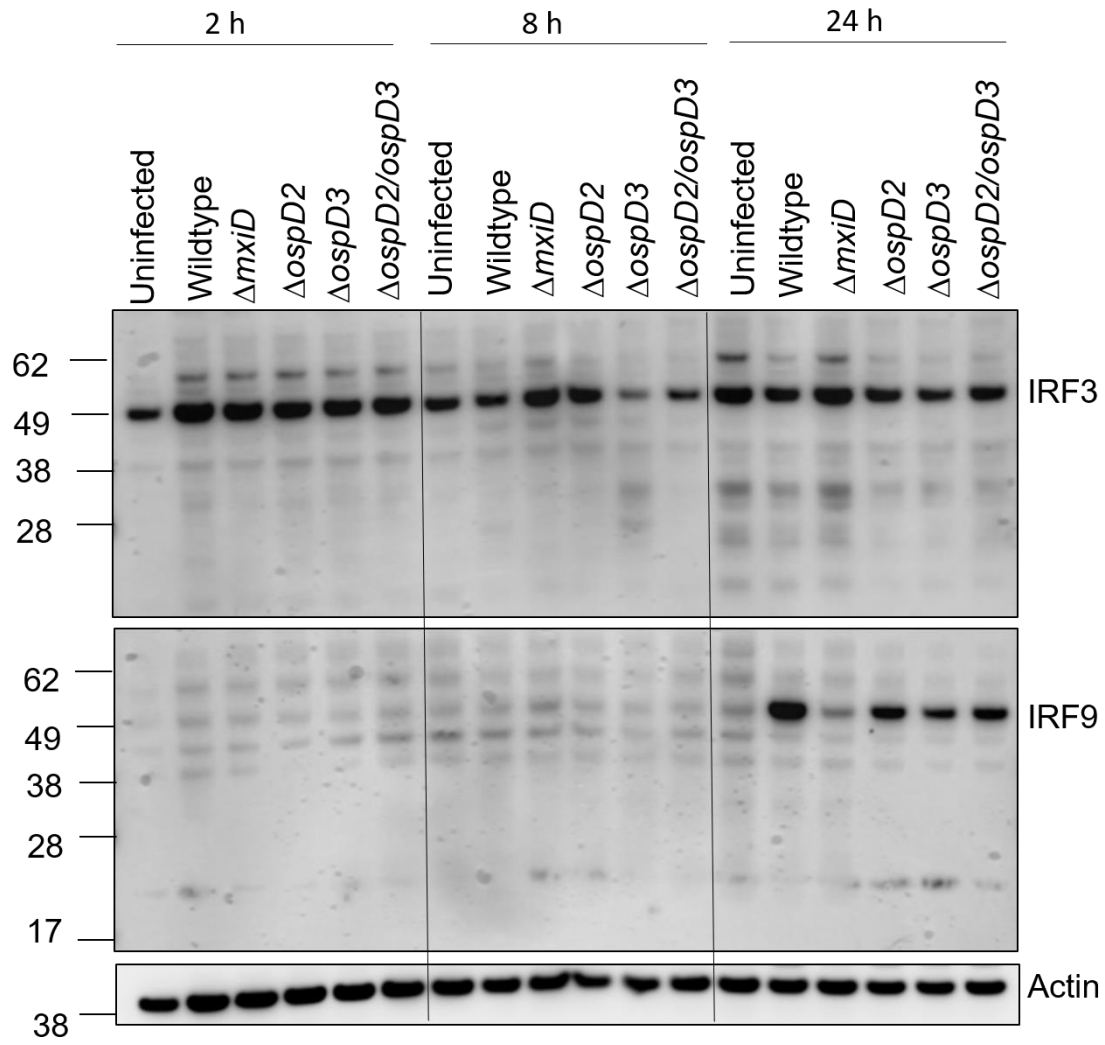

Figure 4. 10: **Immunoblotting IRF3 and IRF9 during *Shigella* infection in HeLa 229 cells**

Immunoblot showing IRF3 and IRF9 expression in HeLa 229 cells either left uninfected, or infected with wild type *S. flexneri* 2a 2457T, or mutants Δ*mxiD*, Δ*ospD2*, Δ*ospD3* or Δ*ospD2ospD3*. Infections were carried out at three timepoints of 2 hours, 8 hours and 24 hours. IRF3 and IRF9 expression was detected using anti-IRF3 and anti-IRF9 antibodies. Antibodies to β-actin were used as a loading control. Representative immunoblots of at least three independent experiments.

A

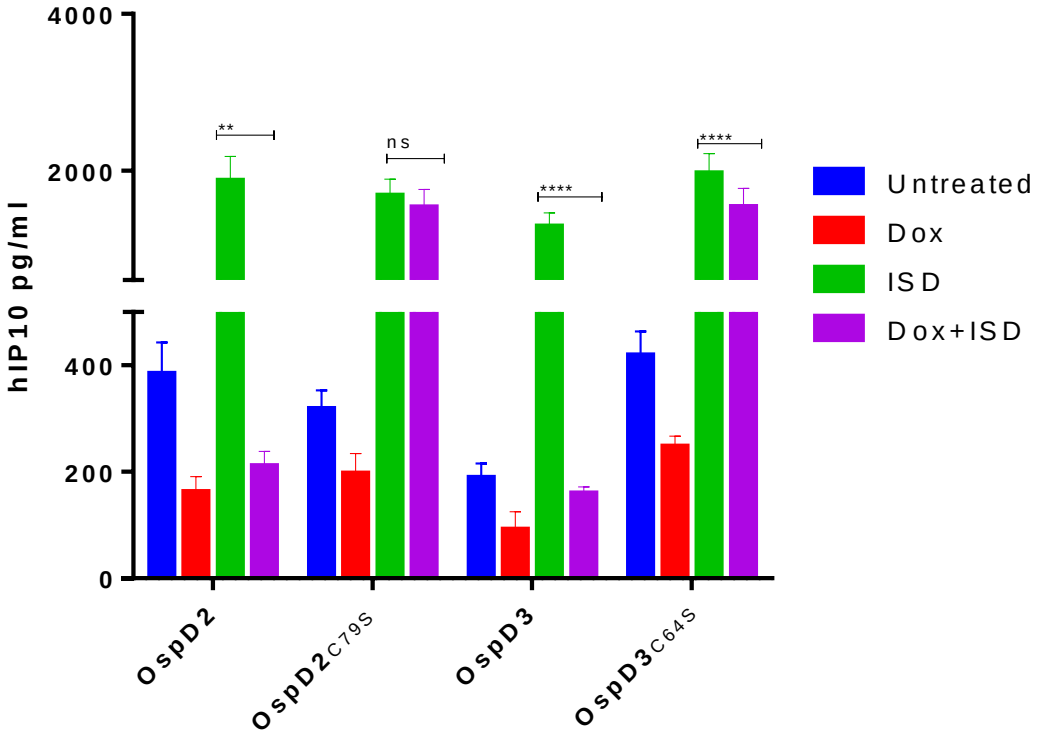
4000
2000
400
200
0
hIP10 pg/ml
**
ns
****
****
Untreated
Dox
ISD
Dox+ISD
OspD2
OspD2C79S
OspD3
OspD3C64S

B

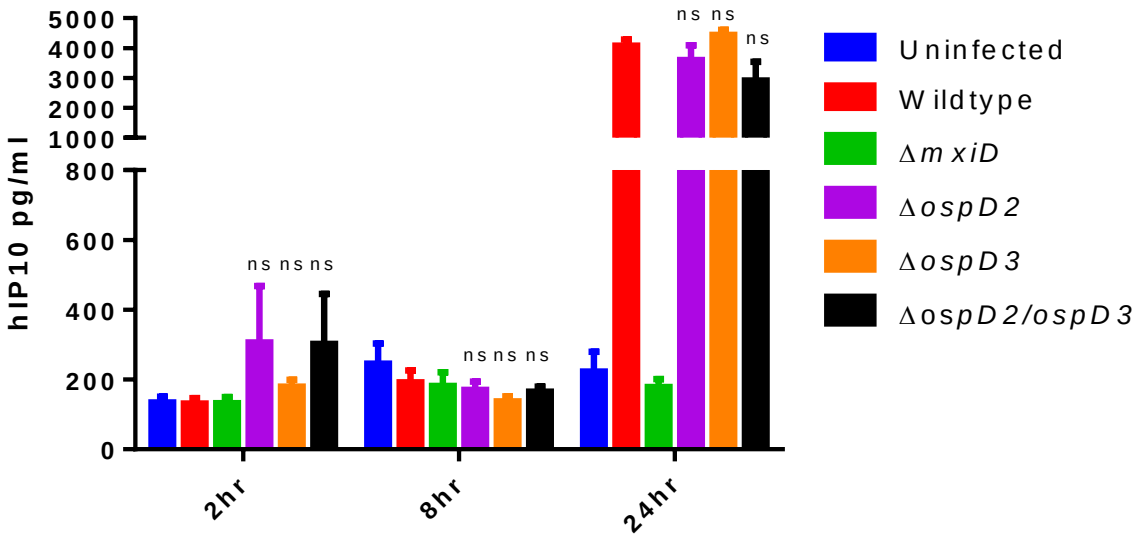
5000
4000
3000
2000
1000
800
600
400
200
0
hIP10 pg/ml
ns ns ns
ns ns ns
ns ns
ns
Uninfected
Wildtype
ΔmxiD
ΔospD2
ΔospD3
ΔospD2/ospD3
2hr
8hr
24hr

Figure 4. 11: **IP-10 production in doxycycline inducible HT-29 cells expressing wild type OspD2, OspD3 and EspL, upon stimulation with ISD and during *Shigella* infection**

(A) Human IP-10 production by doxycycline inducible HT-29 cells, expressing WT and catalytically inactive OspD2, OspD3 or EspL, induced with doxycycline for 24 h. The cells were stimulated with ISD for another 24 hours where indicated. Results are the mean ± s.e.m. of at least three independent experiments carried out in duplicate. (B) Human IP-10 production in HeLa 229 cells infected with WT *S. flexneri 2a* 2457T, or mutants Δ*mxiD*, Δ*ospD2*, Δ*ospD3* or Δ*ospD2ospD3*. Infections were carried out at three timepoints of 2 hours, 8 hours and 24 hours. Results are the mean ± s.e.m. of at least three independent experiments carried out in duplicate. *** Significantly different to ISD and ISD and doxycycline treated samples. (*p< 0.05, **p< 0.01, ***p< 0.001, ****p<0.0001), two-tailed unpaired T test.

Chapter Five:

Perspectives

CHAPTER 5: Perspectives

Diarrhoeal incidences as a result of infection by bacterial pathogens are a major public health concern worldwide. Annually an estimated 1.7 million people, especially in developing countries are vulnerable to diarrhoeal diseases. Amongst these, children below the age of 5 are the most susceptible to such infections [420]. The Global Enteric Multicenter Study (GEMS) reported that enteric bacterial pathogens such as *Shigella* and *E. coli* (EPEC) are amongst the most common causes of diarrhoeal disease in the various locations studied in South Asia and Africa [7]. As such, it essential to understand the pathogenesis and evolution of virulence mechanisms by these bacterial pathogens in order to provide insights into the development of efficient treatments or vaccines against diarrhoeal disease.

One crucial mechanism by which some of these bacterial pathogens mediate infection, is the use of specialised protein secretion systems, which function as molecular syringes that deliver bacterial virulence proteins (effectors) directly into the cytosol of the host cells in order to manipulate host cell processes and establish a replicative niche [421]. These specialised secretion systems in Gram-negative bacteria are designated as Type I to Type VI secretion systems [422]. *Shigella* uses a Type III secretion system (T3SS) to translocate around 30 effectors into the cytoplasm of its target host cell [387]. These T3SS effectors regulate different aspects of the host physiology and cellular processes, including the secretion of surface proteins, rearrangement of cytoskeletal networks, host inflammatory responses as well as cell death and survival signalling pathways.

The T3SS effectors of *Shigella* or encoded on the virulence plasmid. Some of these effectors are shared amongst other enteric pathogens such as EPEC and *Salmonella*. Upon invasion of intestinal epithelium by *Shigella*, PAMPs and DAMPs released by the bacteria such as LPS and bacterial peptidoglycan are recognised by host cell PRRs to activate inflammatory and cell death signalling pathways. Extracellular *Shigella* are mostly recognised by TLR4, located at the plasma membrane of epithelial cells [258, 259]. Intracellular *Shigella* on the other hand, are recognised by NOD-like receptors such as NOD1 and NOD2. Binding to these receptors then activates immune response such as MAPK1 and NF-κB signalling pathways. These pathways will stimulate the production of pro-inflammatory cytokines such as IL-8, resulting in massive inflammation at the intestinal epithelium [423, 424]. To subvert these immune responses, *Shigella* successfully utilises T3SS effectors to inhibit these pathways and prevent the generation of proinflammatory cytokines. The T3SS effectors from *Shigella*, therefore

have a significant role in facilitating *Shigella* replication and spread within the host. Understanding the functions of these effectors has provided many insights to the infection strategy employed by *Shigella*.

As mentioned above, some T3SS effectors from *Shigella* are homologous to those from other bacteria such as EPEC. Recently our laboratory reported that EPEC infection results in cleavage of a group of host cell death signalling proteins which contain a RHIM domain [296]. The T3SS effector from EPEC, EspL, was found to specifically cleave RIPK1, RIPK3, TRIF and ZBP1 within the RHIM domain [296]. RHIM proteins are involved in various inflammatory and cell death signalling pathways. RIPK1 is a key mediator of the NF-κB pathway, is involved in TNF signalling and forms complexes with TRADD, FADD and caspase 8 to induce apoptosis [142]. RIPK1 can also interact with RIPK3 via their RHIM domains, when the activity of caspase 8 is inhibited. This interaction gives rise to necroptosis which is a caspase-independent form of cell death. During necroptosis, activated RIPK3 in turn, phosphorylates MLKL, which then translocates to the plasma membrane and induces membrane rupture [153, 156]. Other RHIM proteins, TRIF and ZBP1can also contribute to necroptosis via RHIM domain interactions with RIPK3 [161, 425]. By cleavage of these RHIM proteins during EPEC infection, EspL blocked inflammation and necroptotic signalling, thus inhibiting a range of host cell defence pathways.

Homologues of EspL are also present in *Shigella* where they are, termed OspD2 and OspD3. The first aim of our study was to determine whether RHIM proteins were also cleaved by OspD2 and OspD3. We demonstrated that OspD3 was indeed a cysteine protease and cleaved the RHIM proteins, RIPK1 and RIPK3 thereby inhibiting downstream RHIM protein signalling such as necroptosis and NF-κB activation. Since OspD3 targets RIPK1, either OspD3 or the kinase structure of RIPK1 could be inactivated by the use of synthetic small molecule inhibitors to prevent cleavage by OspD3. Potentially during clearance of the bacteria by the immune system. However, RIPK1 was not efficiently cleaved by OspD3 during *Shigella* infection.

We therefore investigated other substrates of OspD2 and OspD3. Through this, we demonstrated that OspD2 and OspD3 may be involved in inhibiting type I IFN signalling, thereby affecting the transcription of over 300 ISGs. These ISGs have various roles but mainly are involved in activating an innate and subsequent adaptive response to microbial infections [357, 358].

Jehl *et al* reported that the type II interferon, IFNγ inhibits cytosolic replication of *S. flexneri* in MEF cells. They demonstrated using IRF1 knockout MEFs that IRF1, a main mediator of IFNγ signalling, is crucial for this cytosolic inhibition [418]. Whole genome microarrays then identified retinoic acid-inducible gene I (RIG-1) and mitochondrial antiviral signalling protein (MAVS) to be vital for this IFNγ-dependent growth restriction of *Shigella* [418].

Recently. the *Shigella* T3SS effector IpaH9.8 was reported to inhibit interferon signalling during *Shigella* infection by degrading GPB1. GBP1 Belongs to a GTPase family of guanylate-binding proteins (GBPs) whose expression is induced by interferon. GBP1 can inhibit *Shigella* motility and cell-cell spread [273]. However, *S. flexneri* overcomes this by the secretion of the T3SS effector protein IpaH9.8. IpaH9.8 ubiquitylates GBP1, which results in proteasomal degradation [273]. This then enables *Shigella* to resume actin-based movement and cell to cell spread. Li *et al* also reported that IpaH9.8 targets human GBP1 for proteasomal degradation through lys48-linked ubiquitination [274]. Collectively both these findings highlighted the importance of ISGs such as the GBPs, in inhibiting bacterial replication, in addition this work established the role of the *Shigella* effector IpaH9.8 in degrading GBP1, thereby abolishing its function.

Type I IFN signalling has been well studied during viral infections, where it inhibits viral intracellular replication and the spread of the virus [360]. However, the role of type I interferon signalling during bacterial infection is still largely unexplained. Type I IFN signalling has previously been reported to exacerbate some bacterial infections including *Listeria*, *Francisella tularensis* and *Salmonella* infections. *Listeria*, which causes sepsis and meningitis in immunocompromised people, can trigger a strong type I IFN signalling response which influences host susceptibility. This is evident in mice deficient in IRF3 or IFNAR1 which are protected from infection [426, 427]. A cytolysin termed listeriolysin, produced by *Listeria* can destroy vacuolar integrity to facilitate the escape of the bacteria into the cytoplasm. The presence of bacterial DNA in the cytoplasm triggers signalling via the cGAS-STING pathway to induce type I IFN production [428]. An outcome of type I IFN signalling is production of ISGs such as DAXX and TRAIL, which promote the apoptosis of lymphocytes and macrophages, facilitating the spread of the bacteria [427, 429]. It was therefore reported that *Listeria* infections are resolved more rapidly in the absence of type I IFN response [427, 429, 430].

Francisella tularensis, which causes a life-threatening respiratory illness can also induce a type I IFN response via the c-GAS-STING signalling pathway. Similar to *Listeria*, mice deficient in IFNAR1, IRF3, cGAS or STING exhibited resistance to infection by *F. tularensis* [431, 432]. *Salmonella* Typhimurium is another enteric pathogen which induces diarrhoeal disease in humans. Perkin *et al* reported that mice deficient for IFNAR1 were more resistant to bacterial infection as compared to wild type mice and hence exhibited enhanced survival. This was attributed to the upregulated antimicrobial proinflammatory responses in these mice which did not express IFNAR1 receptors [433].

Paradoxically, the type I IFN response can also promote host protection against bacterial infections. *Legionella* is a bacterial pathogen which causes a pneumonia termed Legionnaires disease. The type I IFN response is activated in macrophages upon *Legionella* infection via the cGAS-STING pathway [434], and prevents the replication of *Legionella* in macrophages, but have no effect in IFNAR1 KO mice [434, 435]. *Helicobacter pylori* is another gram-negative bacterium which causes gastric infections. It has been reported that mice deficient in NOD1 or IFNAR1 were unable to prevent replication of *H. pylori*. It was also noted that the expression of an ISG, CXC110 was significantly reduced in these mice, reflecting the importance of CXC110 production during type I IFN signalling for the control of *H. pylori* replication [436]. *Streptococcus pyogenes* is a gram-positive bacterium which causes deep tissue infections. These bacteria can also induce a type I IFN response in macrophages via the STING pathway. In mouse models of infection, IFNAR1 deficient mice had a significantly lower survival rate compared to wild type mice [437]. The increased survival of wild type mice was attributed to the anti-inflammatory response as a result of type I IFN signalling [438].

From these studies on type I IFN signalling during bacterial infection, it can be clearly seen that unlike during viral infection, type I IFN signalling has disparate functions depending on the bacterial infection. The type I IFN response therefore contributes to a response which can be either detrimental or beneficial to the host defence against bacterial infection. This unpredictable outcome of type I IFN signalling demands a more comprehensive study of the type I IFN response during bacterial infection.

Our study in understanding the role of the type I IFN response during *Shigella* infection will add to the currently limited knowledge in the field. Some early studies found that interferon

can be protective during *Shigella* infection. Dumenil *et al* reported that IFNα is capable of inhibiting *Shigella* cytoskeletal rearrangements required for entry of the bacteria into the host cell [417]. During uptake into host cells, *Shigella* induces excessive cytoskeletal rearrangement at the entry site [439, 440]. Actin polymerisation also contributes to the mechanical force required to form protrusions which eventually engulf the bacteria into the host [441]. Actin associated proteins such as cortactin, actinin and plastin together with focal adhesion proteins such as talin and vinculin are necessary for actin polymerisation and cytoskeleton rearrangement at the entry site [122, 442]. Cortactin recruited to the entry site is a substrate required for the activation of pp60c-src (a tyrosine kinase). *Shigella* then induces a tyrosine cascade which contributes to cortactin phosphorylation [443]. In HeLa cells IFNα can inhibit the Src signalling pathway and prevent both the recruitment of cytoskeletal proteins as well as actin polymerisation during *Shigella* infection [417].

Recently, Helbig *et al* also reported that the ISG viperin, which is primarily produced as consequence of a type I IFN response, can inhibit intracellular *S. flexneri* infection *in vitro* [419]. By infection of cultured epithelial cells (HeLa and Huh-7), they demonstrated that type I IFN hamper bacterial infection due to an upregulation of viperin [419]. Viperin is a radical S-adenosylmethionine (SAM) enzyme, and by using catalytically inactive viperin mutants they showed that this enzymatic activity is necessary for inhibition of intracellular *Shigella* growth. Further deciphering of the mechanism of action of viperin led to the proposal that viperin might alter plasma membrane cholesterol levels and hence inhibit *S. flexneri* entry into epithelial cells [419]. This explanation accounts for the observation that lipid rafts are crucial for *Shigella* entry into epithelial cells and that viperin restricts viral escape by disrupting cholesterol affecting plasma membrane fluidity [444]. However, further investigation is necessary to determine the exact mechanism of action of viperin during *Shigella* infection. Importantly in this study, Helbig *et al* reported that infection of cells *in vitro* induced a type I IFN response and that type I IFN treatment of cells restrict *Shigella* invasion [419]. In their study they assessed if *Shigella* infection of HeLa and HEK 293T cells can induce IRF3 activation and subsequent IFNβ promotor activation. They reported that 5 hours post infection, both these cell lines induced significant activation of IFNβ. In contrast, we only observed induction of a type I IFN response 24 hours post infection. At 8-hour post infection, there was still no induction of either IRF9 or human IP-10. We presume this could be due to using a different line of HeLa cells, HeLa 229, which may have a slower rate of type I IFN activation. Nevertheless, it is clear

that *Shigella* infection activates a type I IFN response and as such it is possible that bacteria have evolved to inhibit such a response.

Odendall *et al* also reported that type III IFNs such as IFNλ play a role in protecting the integrity of host epithelial barrier during *Shigella* infections [410]. Their study used recombinant IFNλ to show that IFNλ induced epithelial barrier repair *in vitro* and inhibit dissemination of transcellular *Shigella* [410]. IFNλ also signals through JAK/ STAT pathway and hence may also be targeted during *Shigella* infection. Together, these studies suggest that interferon signalling inhibits *Shigella* entry and cytosolic replication within the host cell.

Our study supports a possible role for type I IFN signalling in combating *Shigella* infection. In our study, we found the T3SS effectors OspD2 and OspD3 can cleave IRF3 and IRF9 respectively which potentially inhibits both arms of type I IFN signalling. Although this was difficult to observe during infection, further experiments with different cell lines and exogenous stimulation may help to define the role of OspD2 and OspD3 more clearly. For now, IRF3 and IRF9 remain novel targets of these newly described cysteine proteases.

Overall, *Shigella* has evolved numerous mechanisms to prevent being rapidly cleared by the host immune response. *Shigella* subverts these immune signalling pathways through the action of their T3SS effectors. Our study on the T3SS effectors OspD2 and OspD3 therefore provides fresh insight into *Shigella* pathogenesis and the possible role of type I IFN signalling in controlling bacterial replication and spread. This study may also pave the way for future studies on the ability of other T3SS effectors from *Shigella* to inhibit type I IFN signalling. Future investigation on the exact biochemical properties of these T3SS effectors, as well as their host targets will be crucial to understand the multiple ways in which *Shigella* manipulates the host immune response.

REFERENCES

1. Collaborators, G.B.D.D.D., *Estimates of global, regional, and national morbidity, mortality, and aetiologies of diarrhoeal diseases: a systematic analysis for the Global Burden of Disease Study 2015.* Lancet Infect Dis, 2017. **17**(9): p. 909-948.
2. Kotloff, K.L., et al., *Global burden of Shigella infections: implications for vaccine development and implementation of control strategies.* Bull World Health Organ, 1999. **77**(8): p. 651-66.
3. Keusch, G.T., et al., *Diarrheal Diseases*, in *Disease Control Priorities in Developing Countries*, nd, et al., Editors. 2006: Washington (DC).
4. Bennish, M.L., *Potentially lethal complications of shigellosis.* Rev Infect Dis, 1991. **13 Suppl 4**: p. S319-24.
5. Uppal, B., et al., *A comparative study of bacterial and parasitic intestinal infections in India.* J Clin Diagn Res, 2015. **9**(3): p. DC01-4.
6. Liu, J., et al., *Use of quantitative molecular diagnostic methods to identify causes of diarrhoea in children: a reanalysis of the GEMS case-control study.* Lancet, 2016. **388**(10051): p. 1291-301.
7. Kotloff, K.L., et al., *Burden and aetiology of diarrhoeal disease in infants and young children in developing countries (the Global Enteric Multicenter Study, GEMS): a prospective, case-control study.* Lancet, 2013. **382**(9888): p. 209-22.
8. Jennison, A.V. and N.K. Verma, *Shigella flexneri infection: pathogenesis and vaccine development.* FEMS Microbiol Rev, 2004. **28**(1): p. 43-58.
9. Bensted, H.J., *Dysentery bacilli-Shigella; a brief historical review.* Can J Microbiol, 1956. **2**(3): p. 163-74.
10. Trofa, A.F., et al., *Dr. Kiyoshi Shiga: discoverer of the dysentery bacillus.* Clin Infect Dis, 1999. **29**(5): p. 1303-6.
11. Sansonetti, P.J., *Rupture, invasion and inflammatory destruction of the intestinal barrier by Shigella, making sense of prokaryote-eukaryote cross-talks.* FEMS Microbiol Rev, 2001. **25**(1): p. 3-14.
12. Ingersoll, M., E.A. Groisman, and A. Zychlinsky, *Pathogenicity islands of Shigella.* Curr Top Microbiol Immunol, 2002. **264**(1): p. 49-65.
13. Bhagwat, A.A. and M. Bhagwat, *Comparative analysis of transcriptional regulatory elements of glutamate-dependent acid-resistance systems of Shigella flexneri and Escherichia coli O157:H7.* FEMS Microbiol Lett, 2004. **234**(1): p. 139-47.
14. Gorden, J. and P.L. Small, *Acid resistance in enteric bacteria.* Infect Immun, 1993. **61**(1): p. 364-7.
15. Giannella, R.A., S.A. Broitman, and N. Zamcheck, *Gastric acid barrier to ingested microorganisms in man: studies in vivo and in vitro.* Gut, 1972. **13**(4): p. 251-6.
16. Kotloff, K.L., *Shigella infection in children and adults: a formidable foe.* Lancet Glob Health, 2017. **5**(12): p. e1166-e1167.
17. Goren, A., S. Freier, and J.H. Passwell, *Lethal toxic encephalopathy due to childhood shigellosis in a developed country.* Pediatrics, 1992. **89**(6 Pt 2): p. 1189-93.
18. Ashkenazi, S., *Shigella infections in children: new insights.* Semin Pediatr Infect Dis, 2004. **15**(4): p. 246-52.
19. Putnam, S.D., et al., *Self-reported description of diarrhea among military populations in operations Iraqi Freedom and Enduring Freedom.* J Travel Med, 2006. **13**(2): p. 92-9.
20. DuPont, H.L., *Systematic review: the epidemiology and clinical features of travellers' diarrhoea.* Aliment Pharmacol Ther, 2009. **30**(3): p. 187-96.
21. Gupta, A., et al., *Laboratory-confirmed shigellosis in the United States, 1989-2002: epidemiologic trends and patterns.* Clin Infect Dis, 2004. **38**(10): p. 1372-7.
22. Ingle, D.J., et al., *Co-circulation of Multidrug-resistant Shigella Among Men Who Have Sex With Men in Australia.* Clin Infect Dis, 2019. **69**(9): p. 1535-1544.

23. Ashkenazi, S. and D. Cohen, *An update on vaccines against Shigella.* Ther Adv Vaccines, 2013. **1**(3): p. 113-23.
24. Ashkenazi, S., et al., *Growing antimicrobial resistance of Shigella isolates.* J Antimicrob Chemother, 2003. **51**(2): p. 427-9.
25. Barel, L.A. and L.A. Mulard, *Classical and novel strategies to develop a Shigella glycoconjugate vaccine: from concept to efficacy in human.* Hum Vaccin Immunother, 2019. **15**(6): p. 1338-1356.
26. Nataro, J.P. and J.B. Kaper, *Diarrheagenic Escherichia coli.* Clin Microbiol Rev, 1998. **11**(1): p. 142-201.
27. Croxen, M.A. and B.B. Finlay, *Molecular mechanisms of Escherichia coli pathogenicity.* Nat Rev Microbiol, 2010. **8**(1): p. 26-38.
28. Pupo, G.M., R. Lan, and P.R. Reeves, *Multiple independent origins of Shigella clones of Escherichia coli and convergent evolution of many of their characteristics.* Proc Natl Acad Sci U S A, 2000. **97**(19): p. 10567-72.
29. Pettengill, E.A., J.B. Pettengill, and R. Binet, *Phylogenetic Analyses of Shigella and Enteroinvasive Escherichia coli for the Identification of Molecular Epidemiological Markers: Whole-Genome Comparative Analysis Does Not Support Distinct Genera Designation.* Front Microbiol, 2015. **6**: p. 1573.
30. Dodd, C.E. and D. Jones, *A numerical taxonomic study of the genus Shigella.* J Gen Microbiol, 1982. **128**(9): p. 1933-57.
31. Gu, B., et al., *Comparison of the prevalence and changing resistance to nalidixic acid and ciprofloxacin of Shigella between Europe-America and Asia-Africa from 1998 to 2009.* Int J Antimicrob Agents, 2012. **40**(1): p. 9-17.
32. Lan, R. and P.R. Reeves, *Escherichia coli in disguise: molecular origins of Shigella.* Microbes Infect, 2002. **4**(11): p. 1125-32.
33. The, H.C., et al., *The genomic signatures of Shigella evolution, adaptation and geographical spread.* Nat Rev Microbiol, 2016. **14**(4): p. 235-50.
34. Liu, B., et al., *Structure and genetics of Shigella O antigens.* FEMS Microbiol Rev, 2008. **32**(4): p. 627-53.
35. Shepherd, J.G., L. Wang, and P.R. Reeves, *Comparison of O-antigen gene clusters of Escherichia coli (Shigella) sonnei and Plesiomonas shigelloides O17: sonnei gained its current plasmid-borne O-antigen genes from P. shigelloides in a recent event.* Infect Immun, 2000. **68**(10): p. 6056-61.
36. Allison, G.E. and N.K. Verma, *Serotype-converting bacteriophages and O-antigen modification in Shigella flexneri.* Trends Microbiol, 2000. **8**(1): p. 17-23.
37. Slopek, S. and M. Mulczyk, *Concerning the classification of Shigella flexneri 6 bacilli.* Arch Immunol Ther Exp (Warsz), 1967. **15**(4): p. 600-3.
38. Yang, J., et al., *Revisiting the molecular evolutionary history of Shigella spp.* J Mol Evol, 2007. **64**(1): p. 71-9.
39. Connor, T.R., et al., *Species-wide whole genome sequencing reveals historical global spread and recent local persistence in Shigella flexneri.* Elife, 2015. **4**: p. e07335.
40. Killackey, S.A., M.T. Sorbara, and S.E. Girardin, *Cellular Aspects of Shigella Pathogenesis: Focus on the Manipulation of Host Cell Processes.* Front Cell Infect Microbiol, 2016. **6**: p. 38.
41. Martins dos Santos, V., M. Muller, and W.M. de Vos, *Systems biology of the gut: the interplay of food, microbiota and host at the mucosal interface.* Curr Opin Biotechnol, 2010. **21**(4): p. 539-50.
42. Calcuttawala, F., et al., *Activity spectrum of colicins produced by Shigella sonnei and genetic mechanism of colicin resistance in conspecific S. sonnei strains and Escherichia coli.* Antimicrob Agents Chemother, 2015. **59**(1): p. 152-8.
43. Jacob, E., S.J. Baker, and S.P. Swaminathan, *'M' cells in the follicle-associated epithelium of the human colon.* Histopathology, 1987. **11**(9): p. 941-52.

44. Langman, J.M. and R. Rowland, *The number and distribution of lymphoid follicles in the human large intestine.* J Anat, 1986. **149**: p. 189-94.
45. O'Leary, A.D. and E.C. Sweeney, *Lymphoglandular complexes of the colon: structure and distribution.* Histopathology, 1986. **10**(3): p. 267-83.
46. Neutra, M.R., E. Pringault, and J.P. Kraehenbuhl, *Antigen sampling across epithelial barriers and induction of mucosal immune responses.* Annu Rev Immunol, 1996. **14**: p. 275-300.
47. Romero, S., et al., *ATP-mediated Erk1/2 activation stimulates bacterial capture by filopodia, which precedes Shigella invasion of epithelial cells.* Cell Host Microbe, 2011. **9**(6): p. 508-19.
48. Grassart, A., et al., *Bioengineered Human Organ-on-Chip Reveals Intestinal Microenvironment and Mechanical Forces Impacting Shigella Infection.* Cell Host Microbe, 2019. **26**(3): p. 435-444 e4.
49. Wassef, J.S., D.F. Keren, and J.L. Mailloux, *Role of M cells in initial antigen uptake and in ulcer formation in the rabbit intestinal loop model of shigellosis.* Infect Immun, 1989. **57**(3): p. 858-63.
50. Ochman, H., J.G. Lawrence, and E.A. Groisman, *Lateral gene transfer and the nature of bacterial innovation.* Nature, 2000. **405**(6784): p. 299-304.
51. Belotserkovsky, I.a.S., P.J, *Escherichia coli, a Versatile Pathogen*. Current Topics in Microbiology and Immunology ed. Vol. 416. 2018, Switzerland Springer Nature.
52. Dobrindt, U., et al., *Genomic islands in pathogenic and environmental microorganisms.* Nat Rev Microbiol, 2004. **2**(5): p. 414-24.
53. Hacker, J., et al., *Pathogenicity islands of virulent bacteria: structure, function and impact on microbial evolution.* Mol Microbiol, 1997. **23**(6): p. 1089-97.
54. Schmidt, H. and M. Hensel, *Pathogenicity islands in bacterial pathogenesis.* Clin Microbiol Rev, 2004. **17**(1): p. 14-56.
55. Lindberg, A.A., A. Karnell, and A. Weintraub, *The lipopolysaccharide of Shigella bacteria as a virulence factor.* Rev Infect Dis, 1991. **13 Suppl 4**: p. S279-84.
56. Navarro-Garcia, F., et al., *Cytoskeletal effects induced by pet, the serine protease enterotoxin of enteroaggregative Escherichia coli.* Infect Immun, 1999. **67**(5): p. 2184-92.
57. Al-Hasani, K., et al., *The sigA gene which is borne on the she pathogenicity island of Shigella flexneri 2a encodes an exported cytopathic protease involved in intestinal fluid accumulation.* Infect Immun, 2000. **68**(5): p. 2457-63.
58. Al-Hasani, K., et al., *The immunogenic SigA enterotoxin of Shigella flexneri 2a binds to HEp-2 cells and induces fodrin redistribution in intoxicated epithelial cells.* PLoS One, 2009. **4**(12): p. e8223.
59. Henderson, I.R., et al., *Characterization of pic, a secreted protease of Shigella flexneri and enteroaggregative Escherichia coli.* Infect Immun, 1999. **67**(11): p. 5587-96.
60. Fasano, A., et al., *Shigella enterotoxin 1: an enterotoxin of Shigella flexneri 2a active in rabbit small intestine in vivo and in vitro.* J Clin Invest, 1995. **95**(6): p. 2853-61.
61. Gray, M.D., et al., *Clinical isolates of Shiga toxin 1a-producing Shigella flexneri with an epidemiological link to recent travel to Hispaniola.* Emerg Infect Dis, 2014. **20**(10): p. 1669-77.
62. Crosa, J.H., *Genetics and molecular biology of siderophore-mediated iron transport in bacteria.* Microbiol Rev, 1989. **53**(4): p. 517-30.
63. Moss, J.E., et al., *The selC-associated SHI-2 pathogenicity island of Shigella flexneri.* Mol Microbiol, 1999. **33**(1): p. 74-83.
64. Ingersoll, M.A. and A. Zychlinsky, *ShiA abrogates the innate T-cell response to Shigella flexneri infection.* Infect Immun, 2006. **74**(4): p. 2317-27.
65. Maurelli, A.T., et al., *"Black holes" and bacterial pathogenicity: a large genomic deletion that enhances the virulence of Shigella spp. and enteroinvasive Escherichia coli.* Proc Natl Acad Sci U S A, 1998. **95**(7): p. 3943-8.

66. Turner, S.A., et al., *Molecular epidemiology of the SRL pathogenicity island.* Antimicrob Agents Chemother, 2003. **47**(2): p. 727-34.
67. Schroeder, G.N. and H. Hilbi, *Molecular pathogenesis of Shigella spp.: controlling host cell signaling, invasion, and death by type III secretion.* Clin Microbiol Rev, 2008. **21**(1): p. 134-56.
68. Buchrieser, C., et al., *The virulence plasmid pWR100 and the repertoire of proteins secreted by the type III secretion apparatus of Shigella flexneri.* Mol Microbiol, 2000. **38**(4): p. 760-71.
69. Blocker, A., et al., *The tripartite type III secreton of Shigella flexneri inserts IpaB and IpaC into host membranes.* J Cell Biol, 1999. **147**(3): p. 683-93.
70. Buysse, J.M., et al., *Molecular cloning of invasion plasmid antigen (ipa) genes from Shigella flexneri: analysis of ipa gene products and genetic mapping.* J Bacteriol, 1987. **169**(6): p. 2561-9.
71. Menard, R., P. Sansonetti, and C. Parsot, *The secretion of the Shigella flexneri Ipa invasins is activated by epithelial cells and controlled by IpaB and IpaD.* EMBO J, 1994. **13**(22): p. 5293-302.
72. Hromockyj, A.E. and A.T. Maurelli, *Identification of Shigella invasion genes by isolation of temperature-regulated inv::lacZ operon fusions.* Infect Immun, 1989. **57**(10): p. 2963-70.
73. Venkatesan, M.M., J.M. Buysse, and E.V. Oaks, *Surface presentation of Shigella flexneri invasion plasmid antigens requires the products of the spa locus.* J Bacteriol, 1992. **174**(6): p. 1990-2001.
74. Adler, B., et al., *A dual transcriptional activation system for the 230 kb plasmid genes coding for virulence-associated antigens of Shigella flexneri.* Mol Microbiol, 1989. **3**(5): p. 627-35.
75. Dorman, C.J. and M.E. Porter, *The Shigella virulence gene regulatory cascade: a paradigm of bacterial gene control mechanisms.* Mol Microbiol, 1998. **29**(3): p. 677-84.
76. Kane, C.D., et al., *MxiE regulates intracellular expression of factors secreted by the Shigella flexneri 2a type III secretion system.* J Bacteriol, 2002. **184**(16): p. 4409-19.
77. Mavris, M., et al., *Regulation of transcription by the activity of the Shigella flexneri type III secretion apparatus.* Mol Microbiol, 2002. **43**(6): p. 1543-53.
78. Page, A.L., et al., *The secreted IpaB and IpaC invasins and their cytoplasmic chaperone IpgC are required for intercellular dissemination of Shigella flexneri.* Cell Microbiol, 1999. **1**(2): p. 183-93.
79. Parsot, C., C. Hamiaux, and A.L. Page, *The various and varying roles of specific chaperones in type III secretion systems.* Curr Opin Microbiol, 2003. **6**(1): p. 7-14.
80. Arbibe, L., et al., *An injected bacterial effector targets chromatin access for transcription factor NF-kappaB to alter transcription of host genes involved in immune responses.* Nat Immunol, 2007. **8**(1): p. 47-56.
81. Zurawski, D.V., et al., *Shigella flexneri type III secretion system effectors OspB and OspF target the nucleus to downregulate the host inflammatory response via interactions with retinoblastoma protein.* Mol Microbiol, 2009. **71**(2): p. 350-68.
82. Yoshida, S., et al., *Microtubule-severing activity of Shigella is pivotal for intercellular spreading.* Science, 2006. **314**(5801): p. 985-9.
83. Dorman, C.J., S. McKenna, and C. Beloin, *Regulation of virulence gene expression in Shigella flexneri, a facultative intracellular pathogen.* Int J Med Microbiol, 2001. **291**(2): p. 89-96.
84. Nakayama, S. and H. Watanabe, *Involvement of cpxA, a sensor of a two-component regulatory system, in the pH-dependent regulation of expression of Shigella sonnei virF gene.* J Bacteriol, 1995. **177**(17): p. 5062-9.
85. Payne, S.M., et al., *Iron and pathogenesis of Shigella: iron acquisition in the intracellular environment.* Biometals, 2006. **19**(2): p. 173-80.
86. Porter, M.E. and C.J. Dorman, *A role for H-NS in the thermo-osmotic regulation of virulence gene expression in Shigella flexneri.* J Bacteriol, 1994. **176**(13): p. 4187-91.
87. Prosseda, G., et al., *Histone-like proteins and the Shigella invasivity regulon.* Res Microbiol, 2002. **153**(7): p. 461-8.

88. Le Gall, T., et al., *Analysis of virulence plasmid gene expression defines three classes of effectors in the type III secretion system of Shigella flexneri.* Microbiology, 2005. **151**(Pt 3): p. 951-62.
89. Rosqvist, R., K.E. Magnusson, and H. Wolf-Watz, *Target cell contact triggers expression and polarized transfer of Yersinia YopE cytotoxin into mammalian cells.* EMBO J, 1994. **13**(4): p. 964-72.
90. Auvray, F., et al., *Flagellin polymerisation control by a cytosolic export chaperone.* J Mol Biol, 2001. **308**(2): p. 221-9.
91. Evdokimov, A.G., et al., *Unusual molecular architecture of the Yersinia pestis cytotoxin YopM: a leucine-rich repeat protein with the shortest repeating unit.* J Mol Biol, 2001. **312**(4): p. 807-21.
92. Troisfontaines, P. and G.R. Cornelis, *Type III secretion: more systems than you think.* Physiology (Bethesda), 2005. **20**: p. 326-39.
93. Morita-Ishihara, T., et al., *Shigella Spa33 is an essential C-ring component of type III secretion machinery.* J Biol Chem, 2006. **281**(1): p. 599-607.
94. Mota, L.J., et al., *Bacterial injectisomes: needle length does matter.* Science, 2005. **307**(5713): p. 1278.
95. Allaoui, A., et al., *MxiG, a membrane protein required for secretion of Shigella spp. Ipa invasins: involvement in entry into epithelial cells and in intercellular dissemination.* Mol Microbiol, 1995. **17**(3): p. 461-70.
96. Allaoui, A., P.J. Sansonetti, and C. Parsot, *MxiJ, a lipoprotein involved in secretion of Shigella Ipa invasins, is homologous to YscJ, a secretion factor of the Yersinia Yop proteins.* J Bacteriol, 1992. **174**(23): p. 7661-9.
97. Blocker, A., K. Komoriya, and S. Aizawa, *Type III secretion systems and bacterial flagella: insights into their function from structural similarities.* Proc Natl Acad Sci U S A, 2003. **100**(6): p. 3027-30.
98. Cornelis, G.R., *The type III secretion injectisome.* Nat Rev Microbiol, 2006. **4**(11): p. 811-25.
99. Allaoui, A., P.J. Sansonetti, and C. Parsot, *MxiD, an outer membrane protein necessary for the secretion of the Shigella flexneri lpa invasins.* Mol Microbiol, 1993. **7**(1): p. 59-68.
100. Blocker, A., et al., *Structure and composition of the Shigella flexneri "needle complex", a part of its type III secreton.* Mol Microbiol, 2001. **39**(3): p. 652-63.
101. Radtke, A.L. and M.X. O'Riordan, *Intracellular innate resistance to bacterial pathogens.* Cell Microbiol, 2006. **8**(11): p. 1720-9.
102. Jouihri, N., et al., *MxiK and MxiN interact with the Spa47 ATPase and are required for transit of the needle components MxiH and MxiI, but not of Ipa proteins, through the type III secretion apparatus of Shigella flexneri.* Mol Microbiol, 2003. **49**(3): p. 755-67.
103. Magdalena, J., et al., *Spa32 regulates a switch in substrate specificity of the type III secreton of Shigella flexneri from needle components to Ipa proteins.* J Bacteriol, 2002. **184**(13): p. 3433-41.
104. Akeda, Y. and J.E. Galan, *Chaperone release and unfolding of substrates in type III secretion.* Nature, 2005. **437**(7060): p. 911-5.
105. Wilharm, G., et al., *On the role of specific chaperones, the specific ATPase, and the proton motive force in type III secretion.* Int J Med Microbiol, 2007. **297**(1): p. 27-36.
106. Veenendaal, A.K., et al., *The type III secretion system needle tip complex mediates host cell sensing and translocon insertion.* Mol Microbiol, 2007. **63**(6): p. 1719-30.
107. Johnson, S., et al., *Self-chaperoning of the type III secretion system needle tip proteins IpaD and BipD.* J Biol Chem, 2007. **282**(6): p. 4035-44.
108. Menard, R., et al., *Extracellular association and cytoplasmic partitioning of the IpaB and IpaC invasins of S. flexneri.* Cell, 1994. **79**(3): p. 515-25.

109. Watarai, M., S. Funato, and C. Sasakawa, *Interaction of Ipa proteins of Shigella flexneri with alpha5beta1 integrin promotes entry of the bacteria into mammalian cells.* J Exp Med, 1996. **183**(3): p. 991-9.
110. Sani, M., et al., *IpaD is localized at the tip of the Shigella flexneri type III secretion apparatus.* Biochim Biophys Acta, 2007. **1770**(2): p. 307-11.
111. Cordes, F.S., et al., *Helical packing of needles from functionally altered Shigella type III secretion systems.* J Mol Biol, 2005. **354**(2): p. 206-11.
112. Lafont, F., et al., *Initial steps of Shigella infection depend on the cholesterol/sphingolipid raft-mediated CD44-IpaB interaction.* EMBO J, 2002. **21**(17): p. 4449-57.
113. Golub, T., S. Wacha, and P. Caroni, *Spatial and temporal control of signaling through lipid rafts.* Curr Opin Neurobiol, 2004. **14**(5): p. 542-50.
114. Gombos, I., et al., *Cholesterol and sphingolipids as lipid organizers of the immune cells' plasma membrane: their impact on the functions of MHC molecules, effector T-lymphocytes and T-cell death.* Immunol Lett, 2006. **104**(1-2): p. 59-69.
115. Handa, Y., et al., *Shigella IpgB1 promotes bacterial entry through the ELMO-Dock180 machinery.* Nat Cell Biol, 2007. **9**(1): p. 121-8.
116. Garza-Mayers, A.C., et al., *Shigella flexneri regulation of ARF6 activation during bacterial entry via an IpgD-mediated positive feedback loop.* MBio, 2015. **6**(2): p. e02584.
117. Pinaud, L., P.J. Sansonetti, and A. Phalipon, *Host Cell Targeting by Enteropathogenic Bacteria T3SS Effectors.* Trends Microbiol, 2018. **26**(4): p. 266-283.
118. Yoshida, S., et al., *Shigella deliver an effector protein to trigger host microtubule destabilization, which promotes Rac1 activity and efficient bacterial internalization.* EMBO J, 2002. **21**(12): p. 2923-35.
119. Germane, K.L., et al., *Structural and functional studies indicate that Shigella VirA is not a protease and does not directly destabilize microtubules.* Biochemistry, 2008. **47**(39): p. 10241-3.
120. Dong, N., et al., *Structurally distinct bacterial TBC-like GAPs link Arf GTPase to Rab1 inactivation to counteract host defenses.* Cell, 2012. **150**(5): p. 1029-41.
121. Niebuhr, K., et al., *Conversion of PtdIns(4,5)P(2) into PtdIns(5)P by the S.flexneri effector IpgD reorganizes host cell morphology.* EMBO J, 2002. **21**(19): p. 5069-78.
122. Tran Van Nhieu, G., A. Ben-Ze'ev, and P.J. Sansonetti, *Modulation of bacterial entry into epithelial cells by association between vinculin and the Shigella IpaA invasin.* EMBO J, 1997. **16**(10): p. 2717-29.
123. Bourdet-Sicard, R., et al., *Binding of the Shigella protein IpaA to vinculin induces F-actin depolymerization.* EMBO J, 1999. **18**(21): p. 5853-62.
124. Valencia-Gallardo, C., et al., *Shigella IpaA Binding to Talin Stimulates Filopodial Capture and Cell Adhesion.* Cell Rep, 2019. **26**(4): p. 921-932 e6.
125. High, N., et al., *IpaB of Shigella flexneri causes entry into epithelial cells and escape from the phagocytic vacuole.* EMBO J, 1992. **11**(5): p. 1991-9.
126. Barzu, S., et al., *Functional analysis of the Shigella flexneri IpaC invasin by insertional mutagenesis.* Infect Immun, 1997. **65**(5): p. 1599-605.
127. Harrington, A., et al., *Characterization of the interaction of single tryptophan containing mutants of IpaC from Shigella flexneri with phospholipid membranes.* Biochemistry, 2006. **45**(2): p. 626-36.
128. Mellouk, N., et al., *Shigella subverts the host recycling compartment to rupture its vacuole.* Cell Host Microbe, 2014. **16**(4): p. 517-30.
129. Suzuki, T. and C. Sasakawa, *Molecular basis of the intracellular spreading of Shigella.* Infect Immun, 2001. **69**(10): p. 5959-66.
130. Deretic, V., T. Saitoh, and S. Akira, *Autophagy in infection, inflammation and immunity.* Nat Rev Immunol, 2013. **13**(10): p. 722-37.

131. Tattoli, I., et al., *Amino acid starvation induced by invasive bacterial pathogens triggers an innate host defense program.* Cell Host Microbe, 2012. **11**(6): p. 563-75.
132. Dupont, N., et al., *Shigella phagocytic vacuolar membrane remnants participate in the cellular response to pathogen invasion and are regulated by autophagy.* Cell Host Microbe, 2009. **6**(2): p. 137-49.
133. Ogawa, M., et al., *Escape of intracellular Shigella from autophagy.* Science, 2005. **307**(5710): p. 727-31.
134. Medzhitov, R. and C.A. Janeway, Jr., *Innate immune recognition and control of adaptive immune responses.* Semin Immunol, 1998. **10**(5): p. 351-3.
135. Iwasaki, A. and R. Medzhitov, *Regulation of adaptive immunity by the innate immune system.* Science, 2010. **327**(5963): p. 291-5.
136. Chaplin, D.D., *Overview of the immune response.* J Allergy Clin Immunol, 2010. **125**(2 Suppl 2): p. S3-23.
137. Chen, L., et al., *Inflammatory responses and inflammation-associated diseases in organs.* Oncotarget, 2018. **9**(6): p. 7204-7218.
138. Akira, S., *Pathogen recognition by innate immunity and its signaling.* Proc Jpn Acad Ser B Phys Biol Sci, 2009. **85**(4): p. 143-56.
139. Mogensen, T.H., *Pathogen recognition and inflammatory signaling in innate immune defenses.* Clin Microbiol Rev, 2009. **22**(2): p. 240-73, Table of Contents.
140. Ashida, H., et al., *Cell death and infection: a double-edged sword for host and pathogen survival.* J Cell Biol, 2011. **195**(6): p. 931-42.
141. Pasparakis, M. and P. Vandenabeele, *Necroptosis and its role in inflammation.* Nature, 2015. **517**(7534): p. 311-20.
142. Micheau, O. and J. Tschopp, *Induction of TNF receptor I-mediated apoptosis via two sequential signaling complexes.* Cell, 2003. **114**(2): p. 181-90.
143. Bertrand, M.J., et al., *cIAP1 and cIAP2 facilitate cancer cell survival by functioning as E3 ligases that promote RIP1 ubiquitination.* Mol Cell, 2008. **30**(6): p. 689-700.
144. Kovalenko, A., et al., *The tumour suppressor CYLD negatively regulates NF-kappaB signalling by deubiquitination.* Nature, 2003. **424**(6950): p. 801-5.
145. Trompouki, E., et al., *CYLD is a deubiquitinating enzyme that negatively regulates NF-kappaB activation by TNFR family members.* Nature, 2003. **424**(6950): p. 793-6.
146. Draber, P., et al., *LUBAC-Recruited CYLD and A20 Regulate Gene Activation and Cell Death by Exerting Opposing Effects on Linear Ubiquitin in Signaling Complexes.* Cell Rep, 2015. **13**(10): p. 2258-72.
147. Feltham, R., A.I. Webb, and J. Silke, *SPATA2 - Keeping the TNF signal short and sweet.* EMBO J, 2016. **35**(17): p. 1848-50.
148. Newton, K., et al., *Activity of protein kinase RIPK3 determines whether cells die by necroptosis or apoptosis.* Science, 2014. **343**(6177): p. 1357-60.
149. Kreuz, S., et al., *NF-kappaB inducers upregulate cFLIP, a cycloheximide-sensitive inhibitor of death receptor signaling.* Mol Cell Biol, 2001. **21**(12): p. 3964-73.
150. Dondelinger, Y., et al., *NF-kappaB-Independent Role of IKKalpha/IKKbeta in Preventing RIPK1 Kinase-Dependent Apoptotic and Necroptotic Cell Death during TNF Signaling.* Mol Cell, 2015. **60**(1): p. 63-76.
151. Wang, L., F. Du, and X. Wang, *TNF-alpha induces two distinct caspase-8 activation pathways.* Cell, 2008. **133**(4): p. 693-703.
152. McQuade, T., Y. Cho, and F.K. Chan, *Positive and negative phosphorylation regulates RIP1- and RIP3-induced programmed necrosis.* Biochem J, 2013. **456**(3): p. 409-15.
153. He, S., et al., *Receptor interacting protein kinase-3 determines cellular necrotic response to TNF-alpha.* Cell, 2009. **137**(6): p. 1100-11.
154. Cho, Y.S., et al., *Phosphorylation-driven assembly of the RIP1-RIP3 complex regulates programmed necrosis and virus-induced inflammation.* Cell, 2009. **137**(6): p. 1112-23.

155. Zhang, D.W., et al., *RIP3, an energy metabolism regulator that switches TNF-induced cell death from apoptosis to necrosis.* Science, 2009. **325**(5938): p. 332-6.
156. Sun, L., et al., *Mixed lineage kinase domain-like protein mediates necrosis signaling downstream of RIP3 kinase.* Cell, 2012. **148**(1-2): p. 213-27.
157. Liu, X., et al., *Post-translational modifications as key regulators of TNF-induced necroptosis.* Cell Death Dis, 2016. **7**(7): p. e2293.
158. Grootjans, S., T. Vanden Berghe, and P. Vandenabeele, *Initiation and execution mechanisms of necroptosis: an overview.* Cell Death Differ, 2017. **24**(7): p. 1184-1195.
159. Dhuriya, Y.K. and D. Sharma, *Necroptosis: a regulated inflammatory mode of cell death.* J Neuroinflammation, 2018. **15**(1): p. 199.
160. Upton, J.W., W.J. Kaiser, and E.S. Mocarski, *Virus inhibition of RIP3-dependent necrosis.* Cell Host Microbe, 2010. **7**(4): p. 302-13.
161. Kaiser, W.J., et al., *Toll-like receptor 3-mediated necrosis via TRIF, RIP3, and MLKL.* J Biol Chem, 2013. **288**(43): p. 31268-79.
162. Hayden, M.S. and S. Ghosh, *NF-kappaB, the first quarter-century: remarkable progress and outstanding questions.* Genes Dev, 2012. **26**(3): p. 203-34.
163. Li, Q. and I.M. Verma, *NF-kappaB regulation in the immune system.* Nat Rev Immunol, 2002. **2**(10): p. 725-34.
164. Gilmore, T.D., *Introduction to NF-kappaB: players, pathways, perspectives.* Oncogene, 2006. **25**(51): p. 6680-4.
165. Sun, S.C., J.H. Chang, and J. Jin, *Regulation of nuclear factor-kappaB in autoimmunity.* Trends Immunol, 2013. **34**(6): p. 282-9.
166. Hoffmann, A., G. Natoli, and G. Ghosh, *Transcriptional regulation via the NF-kappaB signaling module.* Oncogene, 2006. **25**(51): p. 6706-16.
167. Zhang, H. and S.C. Sun, *NF-kappaB in inflammation and renal diseases.* Cell Biosci, 2015. **5**: p. 63.
168. Karin, M. and M. Delhase, *The I kappa B kinase (IKK) and NF-kappa B: key elements of proinflammatory signalling.* Semin Immunol, 2000. **12**(1): p. 85-98.
169. Karin, M. and Y. Ben-Neriah, *Phosphorylation meets ubiquitination: the control of NF-[kappa]B activity.* Annu Rev Immunol, 2000. **18**: p. 621-63.
170. Chen, L.F. and W.C. Greene, *Shaping the nuclear action of NF-kappaB.* Nat Rev Mol Cell Biol, 2004. **5**(5): p. 392-401.
171. Mukaida, N., Y. Mahe, and K. Matsushima, *Cooperative interaction of nuclear factor-kappa B- and cis-regulatory enhancer binding protein-like factor binding elements in activating the interleukin-8 gene by pro-inflammatory cytokines.* J Biol Chem, 1990. **265**(34): p. 21128-33.
172. Soares-Silva, M., et al., *The Mitogen-Activated Protein Kinase (MAPK) Pathway: Role in Immune Evasion by Trypanosomatids.* Front Microbiol, 2016. **7**: p. 183.
173. Roy, C.R. and E.S. Mocarski, *Pathogen subversion of cell-intrinsic innate immunity.* Nat Immunol, 2007. **8**(11): p. 1179-87.
174. Dong, C., R.J. Davis, and R.A. Flavell, *MAP kinases in the immune response.* Annu Rev Immunol, 2002. **20**: p. 55-72.
175. Arthur, J.S. and S.C. Ley, *Mitogen-activated protein kinases in innate immunity.* Nat Rev Immunol, 2013. **13**(9): p. 679-92.
176. Romagnani, S., *Regulation of the T cell response.* Clin Exp Allergy, 2006. **36**(11): p. 1357-66.
177. Bosschaerts, T., et al., *Tip-DC development during parasitic infection is regulated by IL-10 and requires CCL2/CCR2, IFN-gamma and MyD88 signaling.* PLoS Pathog, 2010. **6**(8): p. e1001045.
178. Jackson, A.M., et al., *Role of mitogen-activated protein kinase and PI3K pathways in the regulation of IL-12-family cytokines in dendritic cells and the generation of T H-responses.* Eur Cytokine Netw, 2010. **21**(4): p. 319-28.

179. Anderson, K.V., L. Bokla, and C. Nusslein-Volhard, *Establishment of dorsal-ventral polarity in the Drosophila embryo: the induction of polarity by the Toll gene product.* Cell, 1985. **42**(3): p. 791-8.
180. Akira, S., S. Uematsu, and O. Takeuchi, *Pathogen recognition and innate immunity.* Cell, 2006. **124**(4): p. 783-801.
181. Takeda, K., T. Kaisho, and S. Akira, *Toll-like receptors.* Annu Rev Immunol, 2003. **21**: p. 335-76.
182. Celhar, T., R. Magalhaes, and A.M. Fairhurst, *TLR7 and TLR9 in SLE: when sensing self goes wrong.* Immunol Res, 2012. **53**(1-3): p. 58-77.
183. Kawai, T. and S. Akira, *The role of pattern-recognition receptors in innate immunity: update on Toll-like receptors.* Nat Immunol, 2010. **11**(5): p. 373-84.
184. Takeuchi, O., et al., *Differential roles of TLR2 and TLR4 in recognition of gram-negative and gram-positive bacterial cell wall components.* Immunity, 1999. **11**(4): p. 443-51.
185. Takeda, K. and S. Akira, *Toll-like receptors in innate immunity.* Int Immunol, 2005. **17**(1): p. 1-14.
186. Shimazu, R., et al., *MD-2, a molecule that confers lipopolysaccharide responsiveness on Toll-like receptor 4.* J Exp Med, 1999. **189**(11): p. 1777-82.
187. Hayashi, F., et al., *The innate immune response to bacterial flagellin is mediated by Toll-like receptor 5.* Nature, 2001. **410**(6832): p. 1099-103.
188. Gewirtz, A.T., et al., *Cutting edge: bacterial flagellin activates basolaterally expressed TLR5 to induce epithelial proinflammatory gene expression.* J Immunol, 2001. **167**(4): p. 1882-5.
189. Hacker, G., V. Redecke, and H. Hacker, *Activation of the immune system by bacterial CpG-DNA.* Immunology, 2002. **105**(3): p. 245-51.
190. Hemmi, H., et al., *A Toll-like receptor recognizes bacterial DNA.* Nature, 2000. **408**(6813): p. 740-5.
191. Lund, J., et al., *Toll-like receptor 9-mediated recognition of Herpes simplex virus-2 by plasmacytoid dendritic cells.* J Exp Med, 2003. **198**(3): p. 513-20.
192. Zhang, D., et al., *A toll-like receptor that prevents infection by uropathogenic bacteria.* Science, 2004. **303**(5663): p. 1522-6.
193. Rassa, J.C., et al., *Murine retroviruses activate B cells via interaction with toll-like receptor 4.* Proc Natl Acad Sci U S A, 2002. **99**(4): p. 2281-6.
194. Kurt-Jones, E.A., et al., *Pattern recognition receptors TLR4 and CD14 mediate response to respiratory syncytial virus.* Nat Immunol, 2000. **1**(5): p. 398-401.
195. Bieback, K., et al., *Hemagglutinin protein of wild-type measles virus activates toll-like receptor 2 signaling.* J Virol, 2002. **76**(17): p. 8729-36.
196. Compton, T., et al., *Human cytomegalovirus activates inflammatory cytokine responses via CD14 and Toll-like receptor 2.* J Virol, 2003. **77**(8): p. 4588-96.
197. Alexopoulou, L., et al., *Recognition of double-stranded RNA and activation of NF-kappaB by Toll-like receptor 3.* Nature, 2001. **413**(6857): p. 732-8.
198. Wang, T., et al., *Toll-like receptor 3 mediates West Nile virus entry into the brain causing lethal encephalitis.* Nat Med, 2004. **10**(12): p. 1366-73.
199. Kato, H., et al., *Cell type-specific involvement of RIG-I in antiviral response.* Immunity, 2005. **23**(1): p. 19-28.
200. Hochrein, H., et al., *Herpes simplex virus type-1 induces IFN-alpha production via Toll-like receptor 9-dependent and -independent pathways.* Proc Natl Acad Sci U S A, 2004. **101**(31): p. 11416-21.
201. O'Neill, L.A. and A.G. Bowie, *The family of five: TIR-domain-containing adaptors in Toll-like receptor signalling.* Nat Rev Immunol, 2007. **7**(5): p. 353-64.
202. Meylan, E., et al., *RIP1 is an essential mediator of Toll-like receptor 3-induced NF-kappa B activation.* Nat Immunol, 2004. **5**(5): p. 503-7.

203. Kaiser, W.J. and M.K. Offermann, *Apoptosis induced by the toll-like receptor adaptor TRIF is dependent on its receptor interacting protein homotypic interaction motif.* J Immunol, 2005. **174**(8): p. 4942-52.
204. Ullah, M.O., et al., *TRIF-dependent TLR signaling, its functions in host defense and inflammation, and its potential as a therapeutic target.* J Leukoc Biol, 2016. **100**(1): p. 27-45.
205. Sato, S., et al., *Toll/IL-1 receptor domain-containing adaptor inducing IFN-beta (TRIF) associates with TNF receptor-associated factor 6 and TANK-binding kinase 1, and activates two distinct transcription factors, NF-kappa B and IFN-regulatory factor-3, in the Toll-like receptor signaling.* J Immunol, 2003. **171**(8): p. 4304-10.
206. Tatematsu, M., et al., *A molecular mechanism for Toll-IL-1 receptor domain-containing adaptor molecule-1-mediated IRF-3 activation.* J Biol Chem, 2010. **285**(26): p. 20128-36.
207. Boxx, G.M. and G. Cheng, *The Roles of Type I Interferon in Bacterial Infection.* Cell Host Microbe, 2016. **19**(6): p. 760-9.
208. Platanias, L.C., *Mechanisms of type-I- and type-II-interferon-mediated signalling.* Nat Rev Immunol, 2005. **5**(5): p. 375-86.
209. Chow, K.T. and M. Gale, Jr., *SnapShot: Interferon Signaling.* Cell, 2015. **163**(7): p. 1808-1808 e1.
210. Fensterl, V. and G.C. Sen, *Interferons and viral infections.* Biofactors, 2009. **35**(1): p. 14-20.
211. Schindler, C., D.E. Levy, and T. Decker, *JAK-STAT signaling: from interferons to cytokines.* J Biol Chem, 2007. **282**(28): p. 20059-63.
212. Prokunina-Olsson, L., et al., *A variant upstream of IFNL3 (IL28B) creating a new interferon gene IFNL4 is associated with impaired clearance of hepatitis C virus.* Nat Genet, 2013. **45**(2): p. 164-71.
213. Liu, Y.J., *IPC: professional type 1 interferon-producing cells and plasmacytoid dendritic cell precursors.* Annu Rev Immunol, 2005. **23**: p. 275-306.
214. Koyama, S., et al., *Innate immune response to viral infection.* Cytokine, 2008. **43**(3): p. 336-41.
215. Darnell, J.E., Jr., I.M. Kerr, and G.R. Stark, *Jak-STAT pathways and transcriptional activation in response to IFNs and other extracellular signaling proteins.* Science, 1994. **264**(5164): p. 1415-21.
216. Kisseleva, T., et al., *Signaling through the JAK/STAT pathway, recent advances and future challenges.* Gene, 2002. **285**(1-2): p. 1-24.
217. Haque, S.J. and B.R. Williams, *Identification and characterization of an interferon (IFN)-stimulated response element-IFN-stimulated gene factor 3-independent signaling pathway for IFN-alpha.* J Biol Chem, 1994. **269**(30): p. 19523-9.
218. Blaszczyk, K., et al., *The unique role of STAT2 in constitutive and IFN-induced transcription and antiviral responses.* Cytokine Growth Factor Rev, 2016. **29**: p. 71-81.
219. Martinez-Moczygemba, M., et al., *Distinct STAT structure promotes interaction of STAT2 with the p48 subunit of the interferon-alpha-stimulated transcription factor ISGF3.* J Biol Chem, 1997. **272**(32): p. 20070-6.
220. Li, X., et al., *Functional subdomains of STAT2 required for preassociation with the alpha interferon receptor and for signaling.* Mol Cell Biol, 1997. **17**(4): p. 2048-56.
221. Qureshi, S.A., et al., *Function of Stat2 protein in transcriptional activation by alpha interferon.* Mol Cell Biol, 1996. **16**(1): p. 288-93.
222. Kessler, D.S., et al., *Interferon-alpha regulates nuclear translocation and DNA-binding affinity of ISGF3, a multimeric transcriptional activator.* Genes Dev, 1990. **4**(10): p. 1753-65.
223. Qureshi, S.A., M. Salditt-Georgieff, and J.E. Darnell, Jr., *Tyrosine-phosphorylated Stat1 and Stat2 plus a 48-kDa protein all contact DNA in forming interferon-stimulated-gene factor 3.* Proc Natl Acad Sci U S A, 1995. **92**(9): p. 3829-33.
224. Bluyssen, A.R., J.E. Durbin, and D.E. Levy, *ISGF3 gamma p48, a specificity switch for interferon activated transcription factors.* Cytokine Growth Factor Rev, 1996. **7**(1): p. 11-7.

225. Veals, S.A., T. Santa Maria, and D.E. Levy, *Two domains of ISGF3 gamma that mediate protein-DNA and protein-protein interactions during transcription factor assembly contribute to DNA-binding specificity.* Mol Cell Biol, 1993. **13**(1): p. 196-206.
226. Kessler, D.S., D.E. Levy, and J.E. Darnell, Jr., *Two interferon-induced nuclear factors bind a single promoter element in interferon-stimulated genes.* Proc Natl Acad Sci U S A, 1988. **85**(22): p. 8521-5.
227. Banninger, G. and N.C. Reich, *STAT2 nuclear trafficking.* J Biol Chem, 2004. **279**(38): p. 39199-206.
228. Brierley, M.M. and E.N. Fish, *Functional relevance of the conserved DNA-binding domain of STAT2.* J Biol Chem, 2005. **280**(13): p. 13029-36.
229. Ghislain, J.J., et al., *The interferon-inducible Stat2:Stat1 heterodimer preferentially binds in vitro to a consensus element found in the promoters of a subset of interferon-stimulated genes.* J Interferon Cytokine Res, 2001. **21**(6): p. 379-88.
230. Gupta, S., M. Jiang, and A.B. Pernis, *IFN-alpha activates Stat6 and leads to the formation of Stat2:Stat6 complexes in B cells.* J Immunol, 1999. **163**(7): p. 3834-41.
231. Bluyssen, H.A. and D.E. Levy, *Stat2 is a transcriptional activator that requires sequence-specific contacts provided by stat1 and p48 for stable interaction with DNA.* J Biol Chem, 1997. **272**(7): p. 4600-5.
232. Lou, Y.J., et al., *IRF-9/STAT2 [corrected] functional interaction drives retinoic acid-induced gene G expression independently of STAT1.* Cancer Res, 2009. **69**(8): p. 3673-80.
233. Sarkis, P.T., et al., *STAT1-independent cell type-specific regulation of antiviral APOBEC3G by IFN-alpha.* J Immunol, 2006. **177**(7): p. 4530-40.
234. Perry, S.T., et al., *STAT2 mediates innate immunity to Dengue virus in the absence of STAT1 via the type I interferon receptor.* PLoS Pathog, 2011. **7**(2): p. e1001297.
235. Ting, J.P., et al., *The NLR gene family: a standard nomenclature.* Immunity, 2008. **28**(3): p. 285-7.
236. Kim, Y.K., J.S. Shin, and M.H. Nahm, *NOD-Like Receptors in Infection, Immunity, and Diseases.* Yonsei Med J, 2016. **57**(1): p. 5-14.
237. Motta, V., et al., *NOD-like receptors: versatile cytosolic sentinels.* Physiol Rev, 2015. **95**(1): p. 149-78.
238. Zhong, Y., A. Kinio, and M. Saleh, *Functions of NOD-Like Receptors in Human Diseases.* Front Immunol, 2013. **4**: p. 333.
239. Said-Sadier, N. and D.M. Ojcius, *Alarmins, inflammasomes and immunity.* Biomed J, 2012. **35**(6): p. 437-49.
240. Shi, J., et al., *Cleavage of GSDMD by inflammatory caspases determines pyroptotic cell death.* Nature, 2015. **526**(7575): p. 660-5.
241. Kayagaki, N., et al., *Caspase-11 cleaves gasdermin D for non-canonical inflammasome signalling.* Nature, 2015. **526**(7575): p. 666-71.
242. Lamkanfi, M. and V.M. Dixit, *Mechanisms and functions of inflammasomes.* Cell, 2014. **157**(5): p. 1013-22.
243. Platnich, J.M. and D.A. Muruve, *NOD-like receptors and inflammasomes: A review of their canonical and non-canonical signaling pathways.* Arch Biochem Biophys, 2019. **670**: p. 4-14.
244. Neiman-Zenevich, J., et al., *Listeria monocytogenes and Shigella flexneri Activate the NLRP1B Inflammasome.* Infect Immun, 2017. **85**(11).
245. Reyes Ruiz, V.M., et al., *Broad detection of bacterial type III secretion system and flagellin proteins by the human NAIP/NLRC4 inflammasome.* Proc Natl Acad Sci U S A, 2017. **114**(50): p. 13242-13247.
246. Platnich, J.M., et al., *Shiga Toxin/Lipopolysaccharide Activates Caspase-4 and Gasdermin D to Trigger Mitochondrial Reactive Oxygen Species Upstream of the NLRP3 Inflammasome.* Cell Rep, 2018. **25**(6): p. 1525-1536 e7.

247. Schnappauf, O., et al., *The Pyrin Inflammasome in Health and Disease.* Front Immunol, 2019. **10**: p. 1745.
248. Hancock, R.E. and G. Diamond, *The role of cationic antimicrobial peptides in innate host defences.* Trends Microbiol, 2000. **8**(9): p. 402-10.
249. Sansonetti, P.J., *War and peace at mucosal surfaces.* Nat Rev Immunol, 2004. **4**(12): p. 953-64.
250. Islam, D., et al., *Downregulation of bactericidal peptides in enteric infections: a novel immune escape mechanism with bacterial DNA as a potential regulator.* Nat Med, 2001. **7**(2): p. 180-5.
251. Sperandio, B., et al., *Virulent Shigella flexneri subverts the host innate immune response through manipulation of antimicrobial peptide gene expression.* J Exp Med, 2008. **205**(5): p. 1121-32.
252. Sperandio, B., et al., *Virulent Shigella flexneri affects secretion, expression, and glycosylation of gel-forming mucins in mucus-producing cells.* Infect Immun, 2013. **81**(10): p. 3632-43.
253. Lucchini, S., et al., *Transcriptional adaptation of Shigella flexneri during infection of macrophages and epithelial cells: insights into the strategies of a cytosolic bacterial pathogen.* Infect Immun, 2005. **73**(1): p. 88-102.
254. Kuwae, A., et al., *Shigella invasion of macrophage requires the insertion of IpaC into the host plasma membrane. Functional analysis of IpaC.* J Biol Chem, 2001. **276**(34): p. 32230-9.
255. Skoudy, A., et al., *CD44 binds to the Shigella IpaB protein and participates in bacterial invasion of epithelial cells.* Cell Microbiol, 2000. **2**(1): p. 19-33.
256. Sansonetti, P.J., et al., *Caspase-1 activation of IL-1beta and IL-18 are essential for Shigella flexneri-induced inflammation.* Immunity, 2000. **12**(5): p. 581-90.
257. Masuda, N. and G.M. Church, *Escherichia coli gene expression responsive to levels of the response regulator EvgA.* J Bacteriol, 2002. **184**(22): p. 6225-34.
258. Poltorak, A., et al., *Defective LPS signaling in C3H/HeJ and C57BL/10ScCr mice: mutations in Tlr4 gene.* Science, 1998. **282**(5396): p. 2085-8.
259. Hoshino, K., et al., *Cutting edge: Toll-like receptor 4 (TLR4)-deficient mice are hyporesponsive to lipopolysaccharide: evidence for TLR4 as the Lps gene product.* J Immunol, 1999. **162**(7): p. 3749-52.
260. Bergsbaken, T., S.L. Fink, and B.T. Cookson, *Pyroptosis: host cell death and inflammation.* Nat Rev Microbiol, 2009. **7**(2): p. 99-109.
261. Senerovic, L., et al., *Spontaneous formation of IpaB ion channels in host cell membranes reveals how Shigella induces pyroptosis in macrophages.* Cell Death Dis, 2012. **3**: p. e384.
262. Suzuki, S., et al., *Shigella IpaH7.8 E3 ubiquitin ligase targets glomulin and activates inflammasomes to demolish macrophages.* Proc Natl Acad Sci U S A, 2014. **111**(40): p. E4254-63.
263. Ingersoll, M.A., et al., *The ShiA protein encoded by the Shigella flexneri SHI-2 pathogenicity island attenuates inflammation.* Cell Microbiol, 2003. **5**(11): p. 797-807.
264. Paciello, I., et al., *Intracellular Shigella remodels its LPS to dampen the innate immune recognition and evade inflammasome activation.* Proc Natl Acad Sci U S A, 2013. **110**(46): p. E4345-54.
265. Sansonetti, P.J., G. Tran Van Nhieu, and C. Egile, *Rupture of the intestinal epithelial barrier and mucosal invasion by Shigella flexneri.* Clin Infect Dis, 1999. **28**(3): p. 466-75.
266. Francois, M., et al., *Induction of necrosis in human neutrophils by Shigella flexneri requires type III secretion, IpaB and IpaC invasins, and actin polymerization.* Infect Immun, 2000. **68**(3): p. 1289-96.
267. Sanada, T., et al., *The Shigella flexneri effector OspI deamidates UBC13 to dampen the inflammatory response.* Nature, 2012. **483**(7391): p. 623-6.

268. Fu, P., et al., *Complex structure of OspI and Ubc13: the molecular basis of Ubc13 deamidation and convergence of bacterial and host E2 recognition.* PLoS Pathog, 2013. **9**(4): p. e1003322.
269. Kim, D.W., et al., *The Shigella flexneri effector OspG interferes with innate immune responses by targeting ubiquitin-conjugating enzymes.* Proc Natl Acad Sci U S A, 2005. **102**(39): p. 14046-51.
270. Li, H., et al., *The phosphothreonine lyase activity of a bacterial type III effector family.* Science, 2007. **315**(5814): p. 1000-3.
271. Zhu, Y., et al., *Structural insights into the enzymatic mechanism of the pathogenic MAPK phosphothreonine lyase.* Mol Cell, 2007. **28**(5): p. 899-913.
272. Rohde, J.R., et al., *Type III secretion effectors of the IpaH family are E3 ubiquitin ligases.* Cell Host Microbe, 2007. **1**(1): p. 77-83.
273. Wandel, M.P., et al., *GBPs Inhibit Motility of Shigella flexneri but Are Targeted for Degradation by the Bacterial Ubiquitin Ligase IpaH9.8.* Cell Host Microbe, 2017. **22**(4): p. 507-518 e5.
274. Li, P., et al., *Ubiquitination and degradation of GBPs by a Shigella effector to suppress host defence.* Nature, 2017. **551**(7680): p. 378-383.
275. Wang, F., et al., *Shigella flexneri T3SS effector IpaH4.5 modulates the host inflammatory response via interaction with NF-kappaB p65 protein.* Cell Microbiol, 2013. **15**(3): p. 474-85.
276. Zheng, Z., et al., *Bacterial E3 Ubiquitin Ligase IpaH4.5 of Shigella flexneri Targets TBK1 To Dampen the Host Antibacterial Response.* J Immunol, 2016. **196**(3): p. 1199-208.
277. Noad, J., et al., *LUBAC-synthesized linear ubiquitin chains restrict cytosol-invading bacteria by activating autophagy and NF-kappaB.* Nat Microbiol, 2017. **2**: p. 17063.
278. de Jong, M.F., et al., *Shigella flexneri suppresses NF-kappaB activation by inhibiting linear ubiquitin chain ligation.* Nat Microbiol, 2016. **1**(7): p. 16084.
279. Tokunaga, F. and K. Iwai, *LUBAC, a novel ubiquitin ligase for linear ubiquitination, is crucial for inflammation and immune responses.* Microbes Infect, 2012. **14**(7-8): p. 563-72.
280. Kobayashi, T., et al., *The Shigella OspC3 effector inhibits caspase-4, antagonizes inflammatory cell death, and promotes epithelial infection.* Cell Host Microbe, 2013. **13**(5): p. 570-583.
281. Burnaevskiy, N., et al., *Proteolytic elimination of N-myristoyl modifications by the Shigella virulence factor IpaJ.* Nature, 2013. **496**(7443): p. 106-9.
282. Burnaevskiy, N., et al., *Myristoylome profiling reveals a concerted mechanism of ARF GTPase deacylation by the bacterial protease IpaJ.* Mol Cell, 2015. **58**(1): p. 110-22.
283. Dobbs, N., et al., *STING Activation by Translocation from the ER Is Associated with Infection and Autoinflammatory Disease.* Cell Host Microbe, 2015. **18**(2): p. 157-68.
284. Mounier, J., et al., *Shigella effector IpaB-induced cholesterol relocation disrupts the Golgi complex and recycling network to inhibit host cell secretion.* Cell Host Microbe, 2012. **12**(3): p. 381-9.
285. Puhar, A., et al., *A Shigella effector dampens inflammation by regulating epithelial release of danger signal ATP through production of the lipid mediator PtdIns5P.* Immunity, 2013. **39**(6): p. 1121-31.
286. Bonnet, M. and G. Tran Van Nhieu, *How Shigella Utilizes Ca(2+) Jagged Edge Signals during Invasion of Epithelial Cells.* Front Cell Infect Microbiol, 2016. **6**: p. 16.
287. Ochoa, T.J. and C.A. Contreras, *Enteropathogenic escherichia coli infection in children.* Curr Opin Infect Dis, 2011. **24**(5): p. 478-83.
288. Cole, M.F., *Unifying Microbial Mechanisms: Shared Strategies of Pathogenesis.* Garland Science, 2019.
289. Clements, A., et al., *EspG of enteropathogenic and enterohemorrhagic E. coli binds the Golgi matrix protein GM130 and disrupts the Golgi structure and function.* Cell Microbiol, 2011. **13**(9): p. 1429-39.

290. Litvak, Y., et al., *Epithelial cells detect functional type III secretion system of enteropathogenic Escherichia coli through a novel NF-kappaB signaling pathway.* PLoS Pathog, 2017. **13**(7): p. e1006472.
291. Zhang, Y., et al., *Identification of a Distinct Substrate-binding Domain in the Bacterial Cysteine Methyltransferase Effectors NleE and OspZ.* J Biol Chem, 2016. **291**(38): p. 20149-62.
292. Zhang, L., et al., *Cysteine methylation disrupts ubiquitin-chain sensing in NF-kappaB activation.* Nature, 2011. **481**(7380): p. 204-8.
293. Hemrajani, C., et al., *NleH effectors interact with Bax inhibitor-1 to block apoptosis during enteropathogenic Escherichia coli infection.* Proc Natl Acad Sci U S A, 2010. **107**(7): p. 3129-34.
294. Royan, S.V., et al., *Enteropathogenic E. coli non-LEE encoded effectors NleH1 and NleH2 attenuate NF-kappaB activation.* Mol Microbiol, 2010. **78**(5): p. 1232-45.
295. Xu, Q. and J.C. Reed, *Bax inhibitor-1, a mammalian apoptosis suppressor identified by functional screening in yeast.* Mol Cell, 1998. **1**(3): p. 337-46.
296. Pearson, J.S., et al., *EspL is a bacterial cysteine protease effector that cleaves RHIM proteins to block necroptosis and inflammation.* Nat Microbiol, 2017. **2**: p. 16258.
297. Farfan, M.J., et al., *Shigella enterotoxin-2 is a type III effector that participates in Shigella-induced interleukin 8 secretion by epithelial cells.* FEMS Immunol Med Microbiol, 2011. **61**(3): p. 332-9.
298. Nataro, J.P., et al., *Identification and cloning of a novel plasmid-encoded enterotoxin of enteroinvasive Escherichia coli and Shigella strains.* Infect Immun, 1995. **63**(12): p. 4721-8.
299. Faherty, C.S., et al., *The synthesis of OspD3 (ShET2) in Shigella flexneri is independent of OspC1.* Gut Microbes, 2016. **7**(6): p. 486-502.
300. Venkatesan, M.M., et al., *Complete DNA sequence and analysis of the large virulence plasmid of Shigella flexneri.* Infect Immun, 2001. **69**(5): p. 3271-85.
301. Mou, X., et al., *Synthetic bottom-up approach reveals the complex interplay of Shigella effectors in regulation of epithelial cell death.* Proc Natl Acad Sci U S A, 2018. **115**(25): p. 6452-6457.
302. Reeves, A.Z., et al., *Engineering Escherichia coli into a protein delivery system for mammalian cells.* ACS Synth Biol, 2015. **4**(5): p. 644-54.
303. Du, J., et al., *The type III secretion system apparatus determines the intracellular niche of bacterial pathogens.* Proc Natl Acad Sci U S A, 2016. **113**(17): p. 4794-9.
304. Tobe, T., et al., *Transcriptional control of the invasion regulatory gene virB of Shigella flexneri: activation by virF and repression by H-NS.* J Bacteriol, 1993. **175**(19): p. 6142-9.
305. Gall, T.L., et al., *Analysis of virulence plasmid gene expression defines three classes of effectors in the type III secretion system of Shigella flexneri.* Microbiology, 2005. **151**(Pt 3): p. 951-962.
306. Mattock, E. and A.J. Blocker, *How Do the Virulence Factors of Shigella Work Together to Cause Disease?* Front Cell Infect Microbiol, 2017. **7**: p. 64.
307. Kang, D., et al., *Highly Sensitive and Fast Protein Detection with Coomassie Brilliant Blue in Sodium Dodecyl Sulfate-Polyacrylamide Gel Electrophoresis.* Bull. Korean Chem. Soc., 2002. **23**(11): p. 2.
308. Ishihama, Y., J. Rappsilber, and M. Mann, *Modular stop and go extraction tips with stacked disks for parallel and multidimensional Peptide fractionation in proteomics.* J Proteome Res, 2006. **5**(4): p. 988-94.
309. Rappsilber, J., M. Mann, and Y. Ishihama, *Protocol for micro-purification, enrichment, pre-fractionation and storage of peptides for proteomics using StageTips.* Nat Protoc, 2007. **2**(8): p. 1896-906.
310. Vizcaino, J.A., et al., *ProteomeXchange provides globally coordinated proteomics data submission and dissemination.* Nat Biotechnol, 2014. **32**(3): p. 223-6.

311. Cox, J. and M. Mann, *MaxQuant enables high peptide identification rates, individualized p.p.b.-range mass accuracies and proteome-wide protein quantification.* Nat Biotechnol, 2008. **26**(12): p. 1367-72.
312. Schaab, C., et al., *Analysis of high accuracy, quantitative proteomics data in the MaxQB database.* Mol Cell Proteomics, 2012. **11**(3): p. M111 014068.
313. Tyanova, S., et al., *The Perseus computational platform for comprehensive analysis of (prote)omics data.* Nat Methods, 2016. **13**(9): p. 731-40.
314. Stoehr, G., et al., *A SILAC-based approach identifies substrates of caspase-dependent cleavage upon TRAIL-induced apoptosis.* Mol Cell Proteomics, 2013. **12**(5): p. 1436-50.
315. Wolf, M.K., *Occurrence, distribution, and associations of O and H serogroups, colonization factor antigens, and toxins of enterotoxigenic Escherichia coli.* Clin Microbiol Rev, 1997. **10**(4): p. 569-84.
316. Van den Bosch, L., P.A. Manning, and R. Morona, *Regulation of O-antigen chain length is required for Shigella flexneri virulence.* Mol Microbiol, 1997. **23**(4): p. 765-75.
317. Barrett, A.J. and J.K. McDonald, *Nomenclature: protease, proteinase and peptidase.* Biochem J, 1986. **237**(3): p. 935.
318. Lopez-Otin, C. and J.S. Bond, *Proteases: multifunctional enzymes in life and disease.* J Biol Chem, 2008. **283**(45): p. 30433-7.
319. Puente, X.S., et al., *Human and mouse proteases: a comparative genomic approach.* Nat Rev Genet, 2003. **4**(7): p. 544-58.
320. Turk, B., *Targeting proteases: successes, failures and future prospects.* Nat Rev Drug Discov, 2006. **5**(9): p. 785-99.
321. Verma, S., R. Dixit, and K.C. Pandey, *Cysteine Proteases: Modes of Activation and Future Prospects as Pharmacological Targets.* Front Pharmacol, 2016. **7**: p. 107.
322. Hueck, C.J., *Type III protein secretion systems in bacterial pathogens of animals and plants.* Microbiol Mol Biol Rev, 1998. **62**(2): p. 379-433.
323. Figaj, D., et al., *The Role of Proteases in the Virulence of Plant Pathogenic Bacteria.* Int J Mol Sci, 2019. **20**(3).
324. Chang, J.H., et al., *A high-throughput, near-saturating screen for type III effector genes from Pseudomonas syringae.* Proc Natl Acad Sci U S A, 2005. **102**(7): p. 2549-54.
325. Day, B., et al., *Molecular basis for the RIN4 negative regulation of RPS2 disease resistance.* Plant Cell, 2005. **17**(4): p. 1292-305.
326. Axtell, M.J. and B.J. Staskawicz, *Initiation of RPS2-specified disease resistance in Arabidopsis is coupled to the AvrRpt2-directed elimination of RIN4.* Cell, 2003. **112**(3): p. 369-77.
327. Coaker, G., A. Falick, and B. Staskawicz, *Activation of a phytopathogenic bacterial effector protein by a eukaryotic cyclophilin.* Science, 2005. **308**(5721): p. 548-50.
328. Shao, F., et al., *A Yersinia effector and a Pseudomonas avirulence protein define a family of cysteine proteases functioning in bacterial pathogenesis.* Cell, 2002. **109**(5): p. 575-88.
329. Wachtel, R., et al., *The protease GtgE from Salmonella exclusively targets inactive Rab GTPases.* Nat Commun, 2018. **9**(1): p. 44.
330. Jennings, E., et al., *Structure-function analyses of the bacterial zinc metalloprotease effector protein GtgA uncover key residues required for deactivating NF-kappaB.* J Biol Chem, 2018. **293**(39): p. 15316-15329.
331. Sun, H., et al., *A Family of Salmonella Type III Secretion Effector Proteins Selectively Targets the NF-kappaB Signaling Pathway to Preserve Host Homeostasis.* PLoS Pathog, 2016. **12**(3): p. e1005484.
332. He, S. and X. Wang, *RIP kinases as modulators of inflammation and immunity.* Nat Immunol, 2018. **19**(9): p. 912-922.
333. Hayden, M.S. and S. Ghosh, *Shared principles in NF-kappaB signaling.* Cell, 2008. **132**(3): p. 344-62.

334. Hildebrand, J.M., et al., *Activation of the pseudokinase MLKL unleashes the four-helix bundle domain to induce membrane localization and necroptotic cell death.* Proc Natl Acad Sci U S A, 2014. **111**(42): p. 15072-7.
335. Schmidt, S.V., et al., *Correction: RIPK3 expression in cervical cancer cells is required for PolyIC-induced necroptosis, IL-1alpha release, and efficient paracrine dendritic cell activation.* Oncotarget, 2019. **10**(43): p. 4503-4504.
336. Ashida, H., H. Mimuro, and C. Sasakawa, *Shigella manipulates host immune responses by delivering effector proteins with specific roles.* Front Immunol, 2015. **6**: p. 219.
337. Faherty, C.S., et al., *Chromosomal and plasmid-encoded factors of Shigella flexneri induce secretogenic activity ex vivo.* PLoS One, 2012. **7**(11): p. e49980.
338. Philpott, D.J., et al., *Invasive Shigella flexneri activates NF-kappa B through a lipopolysaccharide-dependent innate intracellular response and leads to IL-8 expression in epithelial cells.* J Immunol, 2000. **165**(2): p. 903-14.
339. Perdomo, J.J., P. Gounon, and P.J. Sansonetti, *Polymorphonuclear leukocyte transmigration promotes invasion of colonic epithelial monolayer by Shigella flexneri.* J Clin Invest, 1994. **93**(2): p. 633-43.
340. Menard, R., et al., *Autocatalytic processing of recombinant human procathepsin L. Contribution of both intermolecular and unimolecular events in the processing of procathepsin L in vitro.* J Biol Chem, 1998. **273**(8): p. 4478-84.
341. Lowther, J., et al., *The importance of pH in regulating the function of the Fasciola hepatica cathepsin L1 cysteine protease.* PLoS Negl Trop Dis, 2009. **3**(1): p. e369.
342. Wagner, R.N., J.C. Reed, and S.K. Chanda, *HIV-1 protease cleaves the serine-threonine kinases RIPK1 and RIPK2.* Retrovirology, 2015. **12**: p. 74.
343. Croft, S.N., E.J. Walker, and R. Ghildyal, *Human Rhinovirus 3C protease cleaves RIPK1, concurrent with caspase 8 activation.* Sci Rep, 2018. **8**(1): p. 1569.
344. Harris, K.G., et al., *RIP3 Regulates Autophagy and Promotes Coxsackievirus B3 Infection of Intestinal Epithelial Cells.* Cell Host Microbe, 2015. **18**(2): p. 221-32.
345. Shan, B., et al., *Necroptosis in development and diseases.* Genes Dev, 2018. **32**(5-6): p. 327-340.
346. Srivastava, A.K., et al., *Effect of a Smac Mimetic (TL32711, Birinapant) on the Apoptotic Program and Apoptosis Biomarkers Examined with Validated Multiplex Immunoassays Fit for Clinical Use.* Clin Cancer Res, 2016. **22**(4): p. 1000-10.
347. Krepler, C., et al., *The novel SMAC mimetic birinapant exhibits potent activity against human melanoma cells.* Clin Cancer Res, 2013. **19**(7): p. 1784-94.
348. Allensworth, J.L., et al., *Smac mimetic Birinapant induces apoptosis and enhances TRAIL potency in inflammatory breast cancer cells in an IAP-dependent and TNF-alpha-independent mechanism.* Breast Cancer Res Treat, 2013. **137**(2): p. 359-71.
349. Benetatos, C.A., et al., *Birinapant (TL32711), a bivalent SMAC mimetic, targets TRAF2-associated cIAPs, abrogates TNF-induced NF-kappaB activation, and is active in patient-derived xenograft models.* Mol Cancer Ther, 2014. **13**(4): p. 867-79.
350. Slee, E.A., et al., *Benzyloxycarbonyl-Val-Ala-Asp (OMe) fluoromethylketone (Z-VAD.FMK) inhibits apoptosis by blocking the processing of CPP32.* Biochem J, 1996. **315 (Pt 1)**: p. 21-4.
351. auf dem Keller, U., A. Doucet, and C.M. Overall, *Protease research in the era of systems biology.* Biol Chem, 2007. **388**(11): p. 1159-62.
352. Dix, M.M., G.M. Simon, and B.F. Cravatt, *Global mapping of the topography and magnitude of proteolytic events in apoptosis.* Cell, 2008. **134**(4): p. 679-91.
353. Ong, S.E. and M. Mann, *Mass spectrometry-based proteomics turns quantitative.* Nat Chem Biol, 2005. **1**(5): p. 252-62.
354. Schulze, W.X. and B. Usadel, *Quantitation in mass-spectrometry-based proteomics.* Annu Rev Plant Biol, 2010. **61**: p. 491-516.

355. Lanucara, F. and C.E. Eyers, *Mass spectrometric-based quantitative proteomics using SILAC.* Methods Enzymol, 2011. **500**: p. 133-50.
356. Lopez de Padilla, C.M. and T.B. Niewold, *The type I interferons: Basic concepts and clinical relevance in immune-mediated inflammatory diseases.* Gene, 2016. **576**(1 Pt 1): p. 14-21.
357. Yan, N. and Z.J. Chen, *Intrinsic antiviral immunity.* Nat Immunol, 2012. **13**(3): p. 214-22.
358. Crouse, J., U. Kalinke, and A. Oxenius, *Regulation of antiviral T cell responses by type I interferons.* Nat Rev Immunol, 2015. **15**(4): p. 231-42.
359. Isaacs, A. and J. Lindenmann, *Virus interference. I. The interferon.* Proc R Soc Lond B Biol Sci, 1957. **147**(927): p. 258-67.
360. Perry, A.K., et al., *The host type I interferon response to viral and bacterial infections.* Cell Res, 2005. **15**(6): p. 407-22.
361. Teijaro, J.R., *Type I interferons in viral control and immune regulation.* Curr Opin Virol, 2016. **16**: p. 31-40.
362. Muller, U., et al., *Functional role of type I and type II interferons in antiviral defense.* Science, 1994. **264**(5167): p. 1918-21.
363. Cervantes-Barragan, L., et al., *Control of coronavirus infection through plasmacytoid dendritic-cell-derived type I interferon.* Blood, 2007. **109**(3): p. 1131-7.
364. Kim, H.Y., *Statistical notes for clinical researchers: Chi-squared test and Fisher's exact test.* Restor Dent Endod, 2017. **42**(2): p. 152-155.
365. Zhao, G.N., D.S. Jiang, and H. Li, *Interferon regulatory factors: at the crossroads of immunity, metabolism, and disease.* Biochim Biophys Acta, 2015. **1852**(2): p. 365-78.
366. Fink, K. and N. Grandvaux, *STAT2 and IRF9: Beyond ISGF3.* JAKSTAT, 2013. **2**(4): p. e27521.
367. Platanitis, E., et al., *A molecular switch from STAT2-IRF9 to ISGF3 underlies interferon-induced gene transcription.* Nat Commun, 2019. **10**(1): p. 2921.
368. Paul, A., T.H. Tang, and S.K. Ng, *Interferon Regulatory Factor 9 Structure and Regulation.* Front Immunol, 2018. **9**: p. 1831.
369. Nguyen, H., J. Hiscott, and P.M. Pitha, *The growing family of interferon regulatory factors.* Cytokine Growth Factor Rev, 1997. **8**(4): p. 293-312.
370. Mamane, Y., et al., *Interferon regulatory factors: the next generation.* Gene, 1999. **237**(1): p. 1-14.
371. Taniguchi, T., et al., *IRF family of transcription factors as regulators of host defense.* Annu Rev Immunol, 2001. **19**: p. 623-55.
372. Lin, R., et al., *Selective DNA binding and association with the CREB binding protein coactivator contribute to differential activation of alpha/beta interferon genes by interferon regulatory factors 3 and 7.* Mol Cell Biol, 2000. **20**(17): p. 6342-53.
373. Wu, J. and Z.J. Chen, *Innate immune sensing and signaling of cytosolic nucleic acids.* Annu Rev Immunol, 2014. **32**: p. 461-88.
374. Au, W.C., et al., *Characterization of the interferon regulatory factor-7 and its potential role in the transcription activation of interferon A genes.* J Biol Chem, 1998. **273**(44): p. 29210-7.
375. Marie, I., J.E. Durbin, and D.E. Levy, *Differential viral induction of distinct interferon-alpha genes by positive feedback through interferon regulatory factor-7.* EMBO J, 1998. **17**(22): p. 6660-9.
376. Joly, S., et al., *Interferon Regulatory Factor 6 Has a Protective Role in the Host Response to Endotoxic Shock.* PLoS One, 2016. **11**(4): p. e0152385.
377. Kwa, M.Q., et al., *Interferon regulatory factor 6 differentially regulates Toll-like receptor 2-dependent chemokine gene expression in epithelial cells.* J Biol Chem, 2014. **289**(28): p. 19758-68.
378. Yanai, H., et al., *Revisiting the role of IRF3 in inflammation and immunity by conditional and specifically targeted gene ablation in mice.* Proc Natl Acad Sci U S A, 2018. **115**(20): p. 5253-5258.

379. Marinho, F.V., et al., *The Emerging Roles of STING in Bacterial Infections.* Trends Microbiol, 2017. **25**(11): p. 906-918.
380. Zhang, Y., et al., *The DNA sensor, cyclic GMP-AMP synthase, is essential for induction of IFN-beta during Chlamydia trachomatis infection.* J Immunol, 2014. **193**(5): p. 2394-404.
381. McWhirter, S.M., et al., *A host type I interferon response is induced by cytosolic sensing of the bacterial second messenger cyclic-di-GMP.* J Exp Med, 2009. **206**(9): p. 1899-911.
382. Woodward, J.J., A.T. Iavarone, and D.A. Portnoy, *c-di-AMP secreted by intracellular Listeria monocytogenes activates a host type I interferon response.* Science, 2010. **328**(5986): p. 1703-5.
383. MacMicking, J.D., *Interferon-inducible effector mechanisms in cell-autonomous immunity.* Nat Rev Immunol, 2012. **12**(5): p. 367-82.
384. Saka, H.A. and R. Valdivia, *Emerging roles for lipid droplets in immunity and host-pathogen interactions.* Annu Rev Cell Dev Biol, 2012. **28**: p. 411-37.
385. Vazirinejad, R., et al., *The biological functions, structure and sources of CXCL10 and its outstanding part in the pathophysiology of multiple sclerosis.* Neuroimmunomodulation, 2014. **21**(6): p. 322-30.
386. Ku, C.H. and B.J. Ferguson, *Stimulation of cytoplasmic DNA sensing pathways in vitro and in vivo.* J Vis Exp, 2014(91): p. 51593.
387. Parsot, C., *Shigella type III secretion effectors: how, where, when, for what purposes?* Curr Opin Microbiol, 2009. **12**(1): p. 110-6.
388. Harris, J.L., et al., *Rapid and general profiling of protease specificity by using combinatorial fluorogenic substrate libraries.* Proc Natl Acad Sci U S A, 2000. **97**(14): p. 7754-9.
389. Kridel, S.J., et al., *Substrate hydrolysis by matrix metalloproteinase-9.* J Biol Chem, 2001. **276**(23): p. 20572-8.
390. Matthews, D.J. and J.A. Wells, *Substrate phage: selection of protease substrates by monovalent phage display.* Science, 1993. **260**(5111): p. 1113-7.
391. Bruckner, A., et al., *Yeast two-hybrid, a powerful tool for systems biology.* Int J Mol Sci, 2009. **10**(6): p. 2763-88.
392. Stynen, B., et al., *Diversity in genetic in vivo methods for protein-protein interaction studies: from the yeast two-hybrid system to the mammalian split-luciferase system.* Microbiol Mol Biol Rev, 2012. **76**(2): p. 331-82.
393. Bredemeyer, A.J., et al., *A proteomic approach for the discovery of protease substrates.* Proc Natl Acad Sci U S A, 2004. **101**(32): p. 11785-90.
394. Brockstedt, E., et al., *Identification of apoptosis-associated proteins in a human Burkitt lymphoma cell line. Cleavage of heterogeneous nuclear ribonucleoprotein A1 by caspase 3.* J Biol Chem, 1998. **273**(43): p. 28057-64.
395. Gerner, C., et al., *The Fas-induced apoptosis analyzed by high throughput proteome analysis.* J Biol Chem, 2000. **275**(50): p. 39018-26.
396. Lee, A.Y., et al., *Identification of caspase-3 degradome by two-dimensional gel electrophoresis and matrix-assisted laser desorption/ionization-time of flight analysis.* Proteomics, 2004. **4**(11): p. 3429-36.
397. Magdeldin, S., et al., *Basics and recent advances of two dimensional- polyacrylamide gel electrophoresis.* Clin Proteomics, 2014. **11**(1): p. 16.
398. Ashida, H., M. Kim, and C. Sasakawa, *Manipulation of the host cell death pathway by Shigella.* Cell Microbiol, 2014. **16**(12): p. 1757-66.
399. Mahley, R.W., et al., *Plasma lipoproteins: apolipoprotein structure and function.* J Lipid Res, 1984. **25**(12): p. 1277-94.
400. Feingold, K.R. and C. Grunfeld, *Lipids: a key player in the battle between the host and microorganisms.* J Lipid Res, 2012. **53**(12): p. 2487-9.
401. Netea, M.G., et al., *Circulating lipoproteins are a crucial component of host defense against invasive Salmonella typhimurium infection.* PLoS One, 2009. **4**(1): p. e4237.

402. Horswill, A.R. and W.M. Nauseef, *Host interception of bacterial communication signals.* Cell Host Microbe, 2008. **4**(6): p. 507-9.
403. Peterson, M.M., et al., *Apolipoprotein B Is an innate barrier against invasive Staphylococcus aureus infection.* Cell Host Microbe, 2008. **4**(6): p. 555-66.
404. Schneider, W.M., M.D. Chevillotte, and C.M. Rice, *Interferon-stimulated genes: a complex web of host defenses.* Annu Rev Immunol, 2014. **32**: p. 513-45.
405. Haller, O., et al., *Dynamin-like MxA GTPase: structural insights into oligomerization and implications for antiviral activity.* J Biol Chem, 2010. **285**(37): p. 28419-24.
406. Haller, O. and G. Kochs, *Human MxA protein: an interferon-induced dynamin-like GTPase with broad antiviral activity.* J Interferon Cytokine Res, 2011. **31**(1): p. 79-87.
407. Piro, A.S., et al., *Detection of Cytosolic Shigella flexneri via a C-Terminal Triple-Arginine Motif of GBP1 Inhibits Actin-Based Motility.* MBio, 2017. **8**(6).
408. Schreiber, G., *The molecular basis for differential type I interferon signaling.* J Biol Chem, 2017. **292**(18): p. 7285-7294.
409. Liu, S.Y., et al., *Systematic identification of type I and type II interferon-induced antiviral factors.* Proc Natl Acad Sci U S A, 2012. **109**(11): p. 4239-44.
410. Odendall, C., A.A. Voak, and J.C. Kagan, *Type III IFNs Are Commonly Induced by Bacteria-Sensing TLRs and Reinforce Epithelial Barriers during Infection.* J Immunol, 2017. **199**(9): p. 3270-3279.
411. Lei, X., et al., *Cleavage of interferon regulatory factor 7 by enterovirus 71 3C suppresses cellular responses.* J Virol, 2013. **87**(3): p. 1690-8.
412. Hung, H.C., et al., *Synergistic inhibition of enterovirus 71 replication by interferon and rupintrivir.* J Infect Dis, 2011. **203**(12): p. 1784-90.
413. Gao, D., et al., *Cyclic GMP-AMP synthase is an innate immune sensor of HIV and other retroviruses.* Science, 2013. **341**(6148): p. 903-6.
414. Motani, K., S. Ito, and S. Nagata, *DNA-Mediated Cyclic GMP-AMP Synthase-Dependent and -Independent Regulation of Innate Immune Responses.* J Immunol, 2015. **194**(10): p. 4914-23.
415. Xia, P., et al., *DNA sensor cGAS-mediated immune recognition.* Protein Cell, 2016. **7**(11): p. 777-791.
416. Tao, J., X. Zhou, and Z. Jiang, *cGAS-cGAMP-STING: The three musketeers of cytosolic DNA sensing and signaling.* IUBMB Life, 2016. **68**(11): p. 858-870.
417. Dumenil, G., et al., *Interferon alpha inhibits a Src-mediated pathway necessary for Shigella-induced cytoskeletal rearrangements in epithelial cells.* J Cell Biol, 1998. **143**(4): p. 1003-12.
418. Jehl, S.P., et al., *IFNgamma inhibits the cytosolic replication of Shigella flexneri via the cytoplasmic RNA sensor RIG-I.* PLoS Pathog, 2012. **8**(8): p. e1002809.
419. Helbig, K.J., et al., *The interferon stimulated gene viperin, restricts Shigella. flexneri in vitro.* Sci Rep, 2019. **9**(1): p. 15598.
420. Walker, R.I., *An assessment of enterotoxigenic Escherichia coli and Shigella vaccine candidates for infants and children.* Vaccine, 2015. **33**(8): p. 954-65.
421. Bhavsar, A.P., J.A. Guttman, and B.B. Finlay, *Manipulation of host-cell pathways by bacterial pathogens.* Nature, 2007. **449**(7164): p. 827-34.
422. Green, E.R. and J. Mecsas, *Bacterial Secretion Systems: An Overview.* Microbiol Spectr, 2016. **4**(1).
423. Girardin, S.E., et al., *CARD4/Nod1 mediates NF-kappaB and JNK activation by invasive Shigella flexneri.* EMBO Rep, 2001. **2**(8): p. 736-42.
424. Girardin, S.E., et al., *Nod1 detects a unique muropeptide from gram-negative bacterial peptidoglycan.* Science, 2003. **300**(5625): p. 1584-7.
425. Upton, J.W., W.J. Kaiser, and E.S. Mocarski, *DAI/ZBP1/DLM-1 complexes with RIP3 to mediate virus-induced programmed necrosis that is targeted by murine cytomegalovirus vIRA.* Cell Host Microbe, 2012. **11**(3): p. 290-7.

426. O'Connell, R.M., et al., *Immune activation of type I IFNs by Listeria monocytogenes occurs independently of TLR4, TLR2, and receptor interacting protein 2 but involves TNFR-associated NF kappa B kinase-binding kinase 1.* J Immunol, 2005. **174**(3): p. 1602-7.
427. O'Connell, R.M., et al., *Type I interferon production enhances susceptibility to Listeria monocytogenes infection.* J Exp Med, 2004. **200**(4): p. 437-45.
428. Hansen, K., et al., *Listeria monocytogenes induces IFNbeta expression through an IFI16-, cGAS- and STING-dependent pathway.* EMBO J, 2014. **33**(15): p. 1654-66.
429. Carrero, J.A., B. Calderon, and E.R. Unanue, *Type I interferon sensitizes lymphocytes to apoptosis and reduces resistance to Listeria infection.* J Exp Med, 2004. **200**(4): p. 535-40.
430. Auerbuch, V., et al., *Mice lacking the type I interferon receptor are resistant to Listeria monocytogenes.* J Exp Med, 2004. **200**(4): p. 527-33.
431. Henry, T., et al., *Type I interferon signaling is required for activation of the inflammasome during Francisella infection.* J Exp Med, 2007. **204**(5): p. 987-94.
432. Storek, K.M., et al., *cGAS and Ifi204 cooperate to produce type I IFNs in response to Francisella infection.* J Immunol, 2015. **194**(7): p. 3236-45.
433. Perkins, D.J., et al., *Salmonella Typhimurium Co-Opts the Host Type I IFN System To Restrict Macrophage Innate Immune Transcriptional Responses Selectively.* J Immunol, 2015. **195**(5): p. 2461-71.
434. Lippmann, J., et al., *Dissection of a type I interferon pathway in controlling bacterial intracellular infection in mice.* Cell Microbiol, 2011. **13**(11): p. 1668-82.
435. Plumlee, C.R., et al., *Interferons direct an effective innate response to Legionella pneumophila infection.* J Biol Chem, 2009. **284**(44): p. 30058-66.
436. Watanabe, T., et al., *NOD1 contributes to mouse host defense against Helicobacter pylori via induction of type I IFN and activation of the ISGF3 signaling pathway.* J Clin Invest, 2010. **120**(5): p. 1645-62.
437. Gratz, N., et al., *Type I interferon production induced by Streptococcus pyogenes-derived nucleic acids is required for host protection.* PLoS Pathog, 2011. **7**(5): p. e1001345.
438. Castiglia, V., et al., *Type I Interferon Signaling Prevents IL-1beta-Driven Lethal Systemic Hyperinflammation during Invasive Bacterial Infection of Soft Tissue.* Cell Host Microbe, 2016. **19**(3): p. 375-87.
439. Sasakawa, C., et al., *Virulence-associated genetic regions comprising 31 kilobases of the 230-kilobase plasmid in Shigella flexneri 2a.* J Bacteriol, 1988. **170**(6): p. 2480-4.
440. Menard, R., P.J. Sansonetti, and C. Parsot, *Nonpolar mutagenesis of the ipa genes defines IpaB, IpaC, and IpaD as effectors of Shigella flexneri entry into epithelial cells.* J Bacteriol, 1993. **175**(18): p. 5899-906.
441. Adam, T., et al., *Cytoskeletal rearrangements and the functional role of T-plastin during entry of Shigella flexneri into HeLa cells.* J Cell Biol, 1995. **129**(2): p. 367-81.
442. Jockusch, B.M., et al., *The molecular architecture of focal adhesions.* Annu Rev Cell Dev Biol, 1995. **11**: p. 379-416.
443. Dehio, C., M.C. Prevost, and P.J. Sansonetti, *Invasion of epithelial cells by Shigella flexneri induces tyrosine phosphorylation of cortactin by a pp60c-src-mediated signalling pathway.* EMBO J, 1995. **14**(11): p. 2471-82.
444. Wang, X., E.R. Hinson, and P. Cresswell, *The interferon-inducible protein viperin inhibits influenza virus release by perturbing lipid rafts.* Cell Host Microbe, 2007. **2**(2): p. 96-105.